THE UNIVERSITY OF QUEENSLAND

AUSTRALIA

The role of E2F7 and E2F8 in squamous differentiation, UV- and chemotherapy-induced responses in keratinocytes

Mehlika Hazar Rethinam

MScBiotech (Hons)

A thesis submitted for the degree of Doctor of Philosophy at

The University of Queensland in 2014

UQ Diamantina Institute

Abstract

Among keratinocyte-derived squamous cell carcinoma (SCC), cutaneous SCC (CSCC) is the second most common cutaneous cancer type and the most common of the potentially fatal skin cancers. Approximately 90% of head and neck cancers are SCC (HNSCC) and HNSCC worldwide is the sixth most common cancer type afflicting mankind. While resectable disease may be treated by surgery with radiation or chemoradiation, there are still no curative options for advanced, unresectable disease. However, chemotherapy alone may offer a hope for unresectable, disseminated SCC, where 50-60% of patients have disease recurrence within 2 years and approximately 30% of these develop metastatic disease. The mainstay of chemotherapeutic treatment in SCC is the platinum-based drug, cisplatin, 5-fluorouracil (5-FU), taxanes, and anti-EGFR monoclonal antibody such as Cetuximab. Nonetheless, despite advances in treatment techniques, the 5-year survival rate still remains at around 55%. Therefore, there remains a lack of options for recurrent or metastatic disease.

The E2F family of transcription factors has emerged as key regulators of proliferation, differentiation and response to stress and apoptotic stimuli in keratinocytes. Consistent with these roles, dysregulation of E2F expression/activity is a common occurrence in cancer and SCC in particular. Thus, better understanding of the E2F family of proteins is essential to establish how these processes are disrupted during SCC genesis. The E2F network exists as a complex map of interacting pathways, and the complete understanding of the E2F family will not be possible until physiological functions of newly identified inhibitory E2F proteins, E2F7 and E2F8, are fully revealed. I provide strong evidence, from *in vitro* experiments, that E2F7 plays a unique and non-redundant role in modulating UV- or chemotherapy-induced cytotoxicity whereas E2F8 has a unique and non-redundant capacity to regulate squamous differentiation. In addition, I report on a unique feedback loop between E2F1, E2F7 and E2F8 that highlights a previously unreported interdependent axis.

With respect to E2F7-specific functions, my work characterised two previously unidentified pathways as therapeutic targets, E2F7/Sphk1/S1P/AKT and E2F7/RacGAP1/AKT, by which the transcription factor E2F7 suppresses doxorubicin specific sensitivity in SCC cells. Targeting these pathways has the potential to expand the clinical activity of existing chemotherapeutics. I provide, *in vitro, in vivo* and patient data in this study that shows that E2F7-dependent repression of doxorubicin sensitivity is mediated *via* the induction of Sphingosine kinase 1 (Sphk1) and Rac GTPase activating protein 1 (RacGAP1). These are

both novel findings and have significant implications for drug resistant SCC. Specifically, I showed that (i) E2F7 is overexpressed in patient SCCs and inhibits sensitivity to doxorubicin, (ii) that E2F7-dependent doxorubicin resistance is mediated *via* E2F-dependent induction of Sphk1 leading to overproduction of Sphingosine-1-phosphate (S1P) which in turn activates AKT, (iii) that pharmacological inhibition of Sphk1 or AKT sensitizes SCC cells to the cytotoxic actions of doxorubicin in *in vivo* models of SCC resulting in profound tumour regression, iv) that induction RacGAP1 in SCC cells increases their sensitivity to doxorubicin and overexpression of RacGAP1 is linked to poor outcomes in SCC patients and v) that E2F7-dependent doxorubicin resistance is mediated *via* induction of RacGAP1 which in turn activates AKT-dependent pathways *in vitro* and *in vivo*. Since dysregulation of the E2F family of transcription factors is one of the most frequent targets in oncogenesis, it is likely that our findings will be relevant to many other cancer types. Moreover, our findings provide proof of concept for immediate translation to initiate a clinical trial using combinations of clinically available agents such as doxorubicin + AKT inhibitor or doxorubicin + an SK1 inhibitor.

Declaration by author

This thesis is composed of my original work, and contains no material previously published or written by another person except where due reference has been made in the text. I have clearly stated the contribution by others to jointly-authored works that I have included in my thesis.

I have clearly stated the contribution of others to my thesis as a whole, including statistical assistance, survey design, data analysis, significant technical procedures, professional editorial advice, and any other original research work used or reported in my thesis. The content of my thesis is the result of work I have carried out since the commencement of my research higher degree candidature and does not include a substantial part of work that has been submitted to qualify for the award of any other degree or diploma in any university or other tertiary institution. I have clearly stated which parts of my thesis, if any, have been submitted to qualify for another award.

I acknowledge that an electronic copy of my thesis must be lodged with the University Library and, subject to the policy and procedures of The University of Queensland, the thesis be made available for research and study in accordance with the Copyright Act 1968 unless a period of embargo has been approved by the Dean of the Graduate School.

I acknowledge that copyright of all material contained in my thesis resides with the copyright holder(s) of that material. Where appropriate I have obtained copyright permission from the copyright holder to reproduce material in this thesis.

Publications during candidature

1. **Hazar-Rethinam M**, Endo-Munoz L, Gannon O and Saunders N. ***Int J Mol Sci.*** 2011; 12(12): 8947-8960. Review.

2. **Hazar-Rethinam M**, Merida de Long L, Gannon OM, Topkas E, Boros S, Vargas AC, Dzienis M, Mukhopadhyay P, Simpson F, Endo-Munoz L, Saunders NA. ***Clin Cancer Res*** Published Online First November 19, 2014; doi: 10.1158/1078-0432.CCR-14-1962.

3. **Hazar-Rethinam M**, Merida de Long L, Gannon OM, Boros S, Vargas AC, Dzienis M, Mukhopadhyay P, Simpson F and Saunders NA. ***Oncogene*** [Submitted; December 2014]

Poster Presentations

Australian Society for Medical Research Postgraduate Student Conference, Brisbane, Queensland 2014

"Sphingosine kinase 1 is a novel E2F7-dependent effector that regulates chemotherapeutic sensitivity in squamous cell carcinoma"

American Association for Cancer Research Annual Meeting, Washington DC, US 2013

"E2F7 regulates sensitivity to the cytotoxic actions of anthracyclines in squamous cell carcinoma"

Lorne Cancer Conference, Lorne, Victoria 2013

"E2F7 regulates sensitivity to the cytotoxic actions of anthracyclines in squamous cell carcinoma"

Australian Society for Medical Research Postgraduate Student Conference, Brisbane, Queensland 2012

"E2F7 regulates sensitivity to the cytotoxic actions of anthracyclines in squamous cell carcinoma"

Princess Alexandra Hospital Health Symposium, Brisbane, Queensland 2012

"E2F7 regulates sensitivity to the cytotoxic actions of anthracyclines in squamous cell carcinoma"

Molecular and Experimental Pathology Society of Australasia Conference, Adelaide, South Australia 2012

"E2F7 regulates sensitivity to the cytotoxic actions of anthracyclines in squamous cell carcinoma"

Publications included in this thesis

1. **Hazar-Rethinam M**, Endo-Munoz L, Gannon O and Saunders N. ***Int J Mol Sci.*** 2011; 12(12): 8947-8960. Review.

   Partially incorporated as paragraphs in Chapter 1. A PDF version of the paper is included as an appendix (Appendix II) to this thesis.

   The preparation of the manuscript was the work of the candidate, with helpful suggestions on the manuscript contributed by all authors.

2. **Hazar-Rethinam M**, Merida de Long L, Gannon OM, Topkas E, Boros S, Vargas AC, Dzienis M, Mukhopadhyay P, Simpson F, Endo-Munoz L, Saunders NA. ***Clin Cancer Res*** Published Online First November 19, 2014; doi: 10.1158/1078-0432.CCR-14-1962.

   Incorporated as Chapter 5

   The preparation of the manuscript was the work of the candidate (MHR). LEM, FS and NAS contributed intellectual input to the project and edited the manuscript. SB, ACV and MD assisted with acquisition of data presented in Figure 2F. LMdL performed some of the animal work resulted in Figure 4, Figure 5E and F, Figure 6F and Figure S6B. PM and OMG provided technical support with analysis of the raw microarray data. ET assisted with the analysis of Figure 6G. All other experimental work was the work of the candidature (MHR).

3. **Hazar-Rethinam M**, Merida de Long L, Gannon OM, Boros S, Vargas AC, Dzienis M, Mukhopadhyay P, Saenz-Ponce N, Simpson F and Saunders NA. ***Oncogene*** [Submitted; December 2014]

   Incorporated as Chapter 6

   The candidate (MHR) designed all experiments, produced all figures and wrote the manuscript. LMdL performed some of the animal work resulted in Figure 7a and b. SB, ACV, MD and NSP assisted with acquisition of data presented in Figure 3a-e. PM and OMG provided technical support with analysis of the raw microarray data explained in Figure 2a. FS critically reviewed the manuscript. NAS provided intellectual input to the project and edited the manuscript.

Contributions by others to the thesis

This thesis is the product of work primarily performed by myself with contributions from many people listed below and in the contributions to jointly authored works above. All the intellectual reasoning behind this project was initiated and guided by A/Prof Nicholas Saunders. A/Prof Nicholas Saunders assisted with the editing of this thesis. Dr Fiona Simpson provided intellectual input and assisted with the editing of this thesis. Ms Karena Pryce, University of Queensland Diamantina Institute, processed the RNA samples for the microarray analysis. Dr Pamela Mukhopadhyay, University of Queensland Diamantina Institute, performed the bioinformatics analysis of the raw microarray data. Mrs Lilia Merida de Long, University of Queensland Diamantina Institute, performed some of the animal work presented in this thesis with the assistance of the University of Queensland Biological Research Facility staff, Michelle Kappler and Corinne Alberthsen. All other experimental work described in the thesis was performed solely by the candidate. The thesis was written solely by the candidate.

Statement of parts of the thesis submitted to qualify for the award of another degree

None

Acknowledgements

I would like to acknowledge first and foremost my boss, supervisor and mentor A/Prof Nicholas Saunders for all his support and encouragement throughout my time in his laboratory. You have definitely made a difference in my career by teaching me how to be a better scientist and a positive person and for that, I am grateful. Thank you for being there for me and for all of your students. I would also like to thank Fiona Simpson for being a supportive co-supervisor and for her guidance.

Orla, my partner in crime, you have definitely been a big part of my life and will continue to be one for years to come. I would also like to thank all the members of the Saunders laboratory, past and present, for their continual intellectual and scientific support, for the friendship and camaraderie of the past 7 years. A special mention must go to Sarina, Alison, Melinda and Eleni; I was extremely lucky to have your friendship, support and wisdom.

I would like to acknowledge the financial support I received throughout my PhD. I am grateful to the Australian Postgraduate award committee and UQ Diamantina Institute for providing the stipend and funding for my project.

I must thank my parents Ayse and Nejdet Hazar, my sister Ceren and rest of my family, who have supported me throughout my life and gave me the opportunity to pursue my dream of going abroad for a higher education. I am honoured to be your daughter. And most importantly, thank you to my wonderful husband Shiva. Your immense understanding, patience, support and faith has been invaluable; I couldn't have completed this thesis without you. Finally, the biggest achievement of my life, my little boy Uday Taylan, I dedicate this thesis to you…….

Keywords

Keratinocytes, E2F7, E2F8, differentiation, UVB, chemosensitivity, Sphingosine kinase 1, Rac GTPase activating protein 1, squamous cell carcinoma

Australian and New Zealand Standard Research Classifications (ANZSRC)

ANZSRC code: 060103, Cell Development, Proliferation and Death, 20%,

ANZSRC code: 111201, Cancer Cell Biology, 40%

ANZSRC code: 111207, Molecular Targets, 40%

Fields of Research (FoR) Classification

FoR code: 0601, Biochemistry and Cell Biology, 50%

FoR code: 1112, Oncology and Carcinogenesis, 50%

Table of Contents

List of Figures

List of Tables

List of Commonly Used Abbreviations

ºC	degrees Celsius
Ad	adenovirus
AE1/3	pan epithelial marker
APS	ammonium persulphate
BCC	basal cell carcinoma
bp	base pair
BPE	bovine pituitary extract
BrdU	5'-Bromo-2'-deoxyuridine
BSA	bovine serum albumin
$CaCl_2$	calcium chloride
cDNA	complementary DNA
CFE	colony forming efficiency
ChIP	chromatin immunoprecipitation
cm	centimetres
CMV	cytomegalovirus
CO_2	carbon dioxide
cRNA	complementary RNA
CSCC	cutaneous squamous cell carcinoma
DAB	3,3' Diaminobenzidine
DAPI	4',6-diamino-2-phenylindole
DBD	DNA binding domain
DMEM	Dulbecco's Modified Eagle Medium
DMSO	dimethyl sulfoxide
DNA	Deoxyribonucleic Acid
dNTP	deoxyribonucleoside triphosphate
DP	dimerisation partner
E2F	E2 factor
EDTA	ethylene diamine tetra acetic acid
e.g.	for example
EGFR	epidermal growth factor receptor
EGF	epidermal growth factor

ELISA	enzyme-linked immunosorbent assay
FBS	foetal bovine serum
g	grams
g	relative centrifugal force
GDP	guanosine diphosphate
GFP	green fluorescent protein
GTP	guanosine triphosphate
H&E	hematoxylin and eosin
HDAC	histone deacetylase
HIF1α	hypoxia-inducible factor 1-alpha
HEK	human epidermal keratinocyte
HNSCC	head and neck squamous cell carcinoma
HPV	human papilloma virus
HRP	horseradish peroxidase
i.e.	that is
IF	immunofluorescence
IgG	immunoglobulin G
IP	immunoprecipitation
i.p.	intraperitoneal
J	joule
kDa	kilo Dalton
KC	keratinocyte
KC-SFM	Keratinocyte Serum-Free Medium
KD	knockdown
KO	knockout
L	litre
M	molar
MAPK	mitogen activated protein kinase
MEK	mouse epidermal keratinocyte
mg	milligrams
$MgCI_2$	magnesium chloride
mL	millilitre
mm	millimetre
mM	millimolar

MOI	multiplicity of infection
mRNA	messenger RNA
mTOR	mammalian target of rapamycin
NaOH	sodium hydroxide
ng	nanogram
nM	nanomolar
NMSC	non-melanoma skin cancer
NOD/SCID	nonobese diabetic/severe combined immunodeficiency
PARP	poly ADP ribose polymerase
PBS	phosphate-buffered saline
PCNA	proliferating cell nuclear antigen
PCR	polymerase chain reaction
Pen/Strep	penicillin streptomycin
PFU	plaque-forming unit
PI3K	phosphatidylinositol 3 kinase
pmol	picomol
PVDF	polyvinylidene fluoride
qRT-PCR	quantitative real time polymerase chain reaction
RacGAP1	Rac GTPase activating protein 1
Rb	retinoblastoma
RIN	RNA integrity number
RIPA	radio immunoprecipitation assay
RNA	ribonucleic acid
RNAi	RNA interference
S1P	sphingosine-1-phosphate
s.c.	subcutaneous
SCC	squamous cell carcinoma
SDS	sodium dodecyl sulphate
SEM	standard error of the mean
shRNA	small hairpin RNA
siRNA	short interfering RNA
SK1-I	Sphingosine kinase 1 inhibitor
Sp1	specificity protein 1
Sphk1	sphingosine kinase 1

TBE	Tris-borate-EDTA
TBP	TATA-box-binding protein
TBS	tris-buffered saline
TBS-T	tris-buffered saline with tween
TMA	tissue microarray
UV	ultraviolet
VEGFA	vascular endothelial growth factor A
µg	micrograms
µL	microlitre
µM	micromolar
v	volume
w	weight

CHAPTER ONE

1 Introduction

Excerpts of this introductory chapter were published as an invited review in the International Journal of Molecular Sciences in a specialist volume entitled UV Induced Cell Death. "The role of the E2F Transcription factor family in UV-induced apoptosis" (Hazar-Rethinam, Endo-Munoz et al. 2011).

1.1 Foreword

Squamous cell carcinoma (SCC) is a common life threatening malignancy in humans and is associated with significant mortality in the advanced disease setting (Clayman, Lee et al. 2005). Among SCC, approximately, 95% of head and neck cancers are SCC and in the developed world approximately 40% of patients with head and neck squamous cell carcinoma will die because of their disease (Clayman, Lee et al. 2005). Whilst surgery and radiation therapy are curative in early or localised disease, advanced disseminated disease is generally considered incurable and current systemic therapies are palliative in nature (Cranmer, Engelhardt et al. 2010). For this reason there is considerable need for new and selective agents to treat SCCs. However, development of new treatment strategies for SCC will require knowledge of keratinocyte (KC) biology and the underlying pathology of how SCCs form.

Although epigenetics and post-translational processes play a role in KC functions, the major regulators remain the transcription factors. Many transcription factors have been reported to play a role in the control of squamous differentiation and carcinogenesis. Of these, the E2F family of transcription factors has emerged as key regulators of many functions of KCs (Endo-Munoz, Dahler et al. 2009). This family of master proteins are key regulators of proliferation, differentiation and responses to stressors such as ultra violet (UV) radiation, oxidative stress and cytotoxic agents.

We, and others, have previously shown that SCC of the skin and mucosae are characterised by the overexpression and dysregulation of the transcription factor, E2F1 (Jones, Dicker et al. 1997; Dicker, Popa et al. 2000; Wong, Barnes et al. 2003). This results in the deregulation of proliferation, suppression of differentiation and deregulation of apoptotic responses in human KCs (Jones, Dicker et al. 1997; Pierce, Gimenez-Conti et al. 1998; Pierce, Schneider-Broussard et al. 1999; Dicker, Popa et al. 2000). Furthermore, my laboratory has recently shown that the E2F inhibitor, E2F7, is also overexpressed in human SCC (Endo-Munoz,

Dahler et al. 2009). Thus, E2F7, and presumably other inhibitory E2Fs such as E2F8, are able to antagonize the pro-apoptotic effects of E2F1 (Endo-Munoz, Dahler et al. 2009). Moreover, it was previously shown that inhibiting E2F1 or E2F7 is able to reinstate many properties relating to differentiation and growth inhibition (Wong, Barnes et al. 2003). The opposing action of E2F members is predicted to determine proliferation, differentiation and apoptosis in KCs in response to normal endogenous and exogenous stimuli (eg: mitogens or UV).

I will now introduce some of the concepts and molecular data relating to the control of squamous differentiation and the mediation of responses to various cytotoxic stimuli such as UV and chemotherapeutics. Finally, I will focus on the role and contribution of newly identified, inhibitory E2F proteins, E2F7 and E2F8 in modulating many of these functions in KCs.

1.2 Skin in general

The skin is the largest organ in the body and provides a protective barrier against environmental insults (Eckert 1989). The structure of skin can broadly be divided into two compartments: an epidermal layer of keratinising stratified squamous epithelial cells and the dermal layer which provides nutrients, insulation and structural support for the epidermis (Eckert 1989). The epidermis is a self-renewing tissue consisting of many different cell types including Langerhan's cells, Merkel's cells, melanocytes and KCs. KCs are the predominant cells in keratinising stratified squamous epithelium (Fuchs and Raghavan 2002; Gambardella and Barrandon 2003). Therefore, understanding KC biology will provide knowledge about the key mechanisms controlling the integrity of the skin, and events that lead to cutaneous neoplasia.

1.3 Neoplastic development of the skin and squamous cell carcinoma

Skin cancers are frequently divided into melanoma and non-melanoma skin cancers (NMSC). Melanoma is a common and aggressive tumour type derived from melanocytes. NMSC are neoplasms of epithelial origin and include basal cell carcinoma (BCC) and squamous cell carcinoma (SCC) (Conney, Kramata et al. 2008). In a recent study, Trakatelli *et al*. (Trakatelli, C et al. 2007) showed that NMSC had significantly increased in incidence in Caucasians in the last decade. The frequency of NMSC in Europe is 300 out of 100,000 per year for BCC, and 150 out of 100,000 per year for SCC. In fact, KC-derived skin cancers are the most common neoplasm in Caucasian populations with a risk of 70% in a 70 years old Australian male (Staples, Elwood et al. 2006). Common risk factors for NMSC are UV radiation, compromised immune system, age, tobacco use and arsenic. Accordingly, NMSC are commonly found on sun-exposed areas such as the face, head and neck, and the dorsum of hands (Erb, Ji et al. 2005). Human papillomavirus infection has also been associated with NMSCC and virally-associated NMSC often has an earlier onset than NMSC caused by ultraviolet radiation, tobacco and alcohol use (Harwood, Surentheran et al. 2000; Nindl, Gottschling et al. 2007). Inherited factors such as polymorphism in glutathione S-transferases are also considered as risk factors (Copper, Jovanovic et al. 1995; Ramsay, Harden et al. 2001).

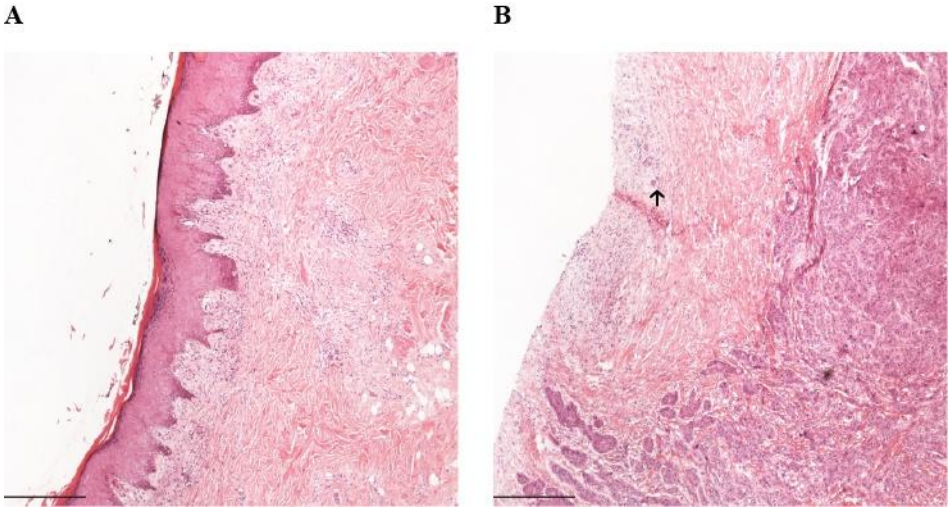

Figure 1.1 Hematoxylin and Eosin stained sections of normal (A) and neoplastic skin (B). The arrow indicates keratin pearls.

Among SCC, cutaneous squamous cell carcinoma (CSCC) is the second most common cutaneous cancer type and the most common of the potentially fatal skin cancers. Excessive UV exposure is the most common causative agent for CSCCs (Walshe, Serewko-Auret et al. 2007). Approximately 90% of head and neck cancers are squamous cell carcinomas (HNSCC) (Sankaranarayanan, Masuyer et al. 1998; Chin, Boyle et al. 2006), and HNSCC worldwide is the sixth most common cancer type afflicting mankind (Chin, Boyle et al. 2006). SCCs most frequently arise from stratified squamous epithelia such as the epidermis or the mucosae of the head and neck, oesophagus or cervix. SCC generally arises due to malignant transformation of the predominant cells in keratinising stratified squamous epithelium. Histological examination of SCC demonstrates the presence of distinctive keratin pearls which are bundles of keratin filaments (*Figure 1.1*). SCCs have the ability of metastasize locally, regionally and to distant sites (Erb, Ji et al. 2005). SCC is staged according to the Tumour Nodes Metastases (TNM) classification system developed by the American Joint Committee on Cancer (AJCC) (Edge and Compton 2010). In the TNM classification, T refers to size of the primary tumour, N refers to the levels of nodal involvement and M describes whether distant metastasis is detectable. By the use of this classification, four stages of disease were defined, from I to IV. These numbers reflect increasing disease progression; the more advanced the disease stage, the poorer the prognosis for the SCC patient. SCC follows a pattern of lymph node metastasis dependent on tumour location, such as the tongue and floor of the mouth having greater tendency for lymphatic spread because of the volume of lymphatics in these areas (Chin, Boyle et al. 2006).

Advanced disease that has spread regionally or to distant sites is associated with a poor survival rate of 50% (Veness, Porceddu et al. 2007; Marur and Forastiere 2008).

Generally surgery and/or radiation therapy are the principle treatment option in early stages of SCC (Stage I and II) and for local disease control. While resectable stage III and IV disease may be treated by surgery with radiation or chemoradiation (Chin, Boyle et al. 2006), there are still no curative options for advanced, unresectable Stage III and IV disease (Watt, Pourreyron et al. 2011). However, chemotherapy alone may offer a hope palliatively for unresectable, disseminated SCC, where 50-60% of patients have disease recurrence within 2 years and approximately 30% of these develop metastatic disease (Posner 2005). The mainstay of chemotherapeutic treatment in SCC is the platinum-based drug, cisplatin, 5-fluorouracil (5-FU), taxanes, and anti-EGFR monoclonal antibody such as Cetuximab (Posner 2005; Bernier and Vrieling 2008; Panikkar, Astsaturov et al. 2008; Specenier and Vermorken 2009). Nonetheless, despite advances in treatment techniques, the 5-year survival rate still remains at around 55%. Therefore, treatment is always required for SCC with a lack of options for recurrent or metastatic disease.

CSCCs are typically thought to originate from premalignant precursor lesions such as actinic keratoses and Bowen's Diseases (Diepgen and Mahler 2002) whilst premalignant forms of HNSCC are referred to as leukoplakias or erythroplasias. Multi-step accumulation of genetic alterations including inactivation of tumour suppressor genes such as p16 and p53 and activation of oncogenes such as Cyclin D1 and Epidermal Growth Factor Receptor (EGFR) in these premalignant progenitor cells contributes to neoplastic transformation. In fact, EGFR signalling promotes survival of SCC cells *via* activation of several downstream signalling molecules such as ERK, AKT and STAT3 and STAT5 (Kalyankrishna and Grandis 2006). Almost 50% of genes that are altered in neoplastic epithelial cells are already altered in these precursor lesions (Serewko, Popa et al. 2002; Perez-Ordoñez, Beauchemin et al. 2006). As a consequence, SCC cells exhibit defects in cell cycle regulatory machinery (Shintani, Mihara et al. 2002; Le and Giaccia 2003), differentiation markers (Sugiyama, Speight et al. 1993; Gasparoni, Fonzi et al. 2004), and many other regulatory molecular pathways including apoptotic machinery (Serewko, Popa et al. 2002; Ye, Yu et al. 2008). One of the hallmarks of squamous cell carcinoma is aberrant/dysregulated control of differentiation and response to DNA damage mediated by UV radiation.

1.3.1 Dysregulated Differentiation Program

One well documented cause of SCC transformation is dysregulated differentiation. As mentioned above, SCCs arise from precursor lesions (e.g.: actinic keratoses for CSCC or leukoplakia or erythroplasia for HNSCC). Early lesional events transform normal cells into premalignant cells with greater proliferation potential and defects in their differentiation program. This is evidenced by their compromised ability to commit to an irreversible terminal differentiation program compared to non-malignant KCs (Dicker, Serewko et al. 2000). There is a need to elucidate the mechanisms at a molecular and cellular level, which regulate these early transforming events. Notably, our earlier studies have shown that these early transformed cells retain an ability to respond to a normal differentiation stimuli and initiate a squamous differentiation program, but there is a block in the pathways that prevents them from doing so (Wong, Barnes et al. 2003; Wong, Barnes et al. 2004). Thus, identifying the nature of this block may provide a mechanism by which we could intervene to reinstate differentiation in early or advanced SCC.

1.3.2 UV in skin malignancies

Regardless of classification, the main contributory factor in the development of cutaneous malignancies, in humans, is ultraviolet (UV) exposure (Black, deGruijl et al. 1997). Although this link was first reported in 1875, it took over one hundred years to accumulate evidence for the causative nature of UV in CSCC formation (Boukamp 2005). For example, i) epidemiological studies have shown a strong link between UV exposure and SCC incidence (Young 2009), ii) use of UV-blocking sunscreens reduces SCC incidence (Ulrich, Jürgensen et al. 2009), iii) UV radiation causes SCC in experimental animal systems (Holmberg, Helin et al. 1998; Pierce, Schneider-Broussard et al. 1999), iv) SCCs acquire a mutation signature that is diagnostic of UV exposure (Nishigori 2006) and v) various molecules such as p53 have been shown to be mutated and causative in the formation of UV-induced SCC (Boukamp 2005). As mentioned in the above section, the incidence rates of skin cancers are rising and their incidence reflects the potent carcinogenic activity of UV radiation (Clayman, Lee et al. 2005). UV-induced SCC formation is associated with dysregulation of the control of proliferation, differentiation and apoptosis (de Gruijl, van Kranen et al. 2001; Ichihashi, Ueda et al. 2003; Erb, Ji et al. 2005; Walshe, Serewko-Auret et al. 2007; Endo-Munoz, Dahler et al. 2009). In particular, apoptotic controls related to sensitivity and response to UV-induced damage are a key target during SCC transformation (Qin, Chaturvedi et al. 2002). Consequently, the major safeguard mechanism, sunburn cell formation, is compromised in

KCs following mutational/carcinogenic doses of UV (Wrone-Smith, Bergstrom et al. 1999). However, the exact mechanisms by which UV-induced mutational damage contributes to the biological events controlling KC transformation and SCC progression remain unclear.

After addressing the above two dysregulated processes during neoplastic transformation, now I will focus on these programs in the context of the epidermis.

1.4 The Epidermis and Squamous Differentiation

The integrity of the epidermis is maintained by the KCs undergoing a tightly regulated program of squamous differentiation. The differentiated KCs establish and maintain a tight barrier to serve as a defence against environmental insults and to prevent the loss of fluids (Fuchs and Raghavan 2002). Complete differentiation is a slow and coordinated program which usually takes 2 weeks to complete. It occurs sequentially through the different layers of the epidermis (Fuchs and Raghavan 2002). The KCs undergo morphological, nuclear, cytoskeletal and biochemical alterations, eventually giving rise to specialized and distinct layers of epidermis. These layers include the basal layer, spinous layer, granular layer, transition zone and cornified layer (*Figure 1.2*).

The basal layer of the epidermis comprises mitotically active and undifferentiated KCs that are attached to the basement membrane of the epidermis (Lippens, Denecker et al. 2005) (*Figure 1.2*). This layer also contains the stem cell population (Alonso and Fuchs 2003). The stem cells give rise to a continuous supply of transit amplifying cells (TA) that eventually undergo terminal differentiation and renew the epidermis (Li, Simmons et al. 1998). Upon receiving the growth arrest signal, TA cells irreversibly withdraw from the cell cycle, detach and move into the spinous layer. This is the layer where differentiation starts to take place. As a result the cells become larger and flatter in appearance. Thus, orchestrated cytoskeletal reorganization takes place by the replacement of cytokeratin types present in this layer (Eckert 1989; Lippens, Denecker et al. 2005). The functional consequence of this rearrangement of keratins is the formation of cytoskelatal filaments that contribute to the integrity and rigidity of the epidermis. Cells of the spinous layer continue to move to the external surface of the epidermis and differentiate forming the granular layer (*Figure 1.2*). The granular layer is characterised by the presence of keratohyalin granules (Eckert 1989). The cells in this layer are still alive and metabolically active (Wolff-Schreiner 1977). The

outermost layer of the epidermis is the cornified layer where generation of corneocytes takes place. Corneocytes are characterised by a network of keratin filaments accounting for 80% of the cornified cell (Eckert 1989). Cells of the granular layer lose their organelles and nucleic acids by enzymatic digestion, and final assembly of the cornified envelope takes place (Fuchs 1990). The corneocytes are embedded in, and integrated within, a tough horny layer of crosslinked proteins known as the cross linked envelope. Cross linking of proteins *via* γ-glutamyl ε-lysine bonds is catalysed by the actions of transglutaminase type I (Byrne, Tainsky et al. 1994; Eckert, Sturniolo et al. 2005).

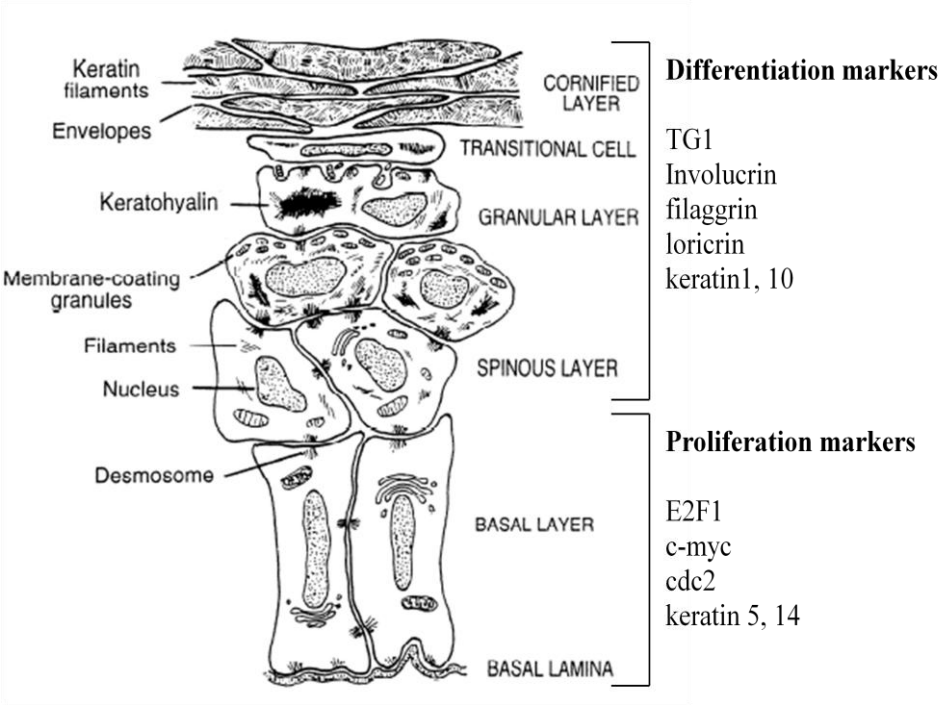

Figure 1.2 The morphology of epidermis during squamous differentiation. Adapted from Eckert et al., 1997 (Eckert, Crish et al. 1997).

The progress through the differentiation program is controlled primarily by transcription factors and hence differentiation status is marked by the expression/downregulation of specific suites of genes (Harvat, Wang et al. 1998; Sark, Fischer et al. 1998; Ito, Udaka et al. 2000; D'Souza, Pajak et al. 2001). Significantly, the differentiation program *in vitro* and *in vivo* is almost identical and consequently the culture of KCs represents an excellent model to study KC differentiation and responses (Jones, Dicker et al. 1997; Dahler, Jones et al. 1998; Dicker, Serewko et al. 2000; Serewko, Popa et al. 2002). The primary keratins expressed in the basal layer are keratin 5 and keratin 14 (Alonso and Fuchs 2003). Besides the expression of these specific keratins, cells of this layer also express genes involved in proliferation, such as cdc2 (or cdk1) and E2F1 (Dahler, Jones et al. 1998; Dicker, Popa et al. 2000). When the cells are stimulated to differentiate the expression of these proliferation specific genes, including keratin 5 and 14, is terminated and the expression of differentiation-specific genes is induced. These early differentiation specific genes include glutamine-lysine rich proteins such as, involucrin and the calcium dependent enzyme, transglutaminase type 1 (TG1) (Banks-Schlegel and Green 1981; Watt and Green 1982; Simon and Green 1984). Involucrin is expressed early in the transition into the spinous layer. It is an important protein for squamous differentiation as involucrin with TG1 protein will form the primary component of the cross linked cornified envelope. The other characteristic proteins expressed from the cells

of spinous layer are keratin 1 and keratin 10, where they contribute to the cytoskeletal network for KCs (Eichner, Sun et al. 1986; Eckert 1989). The transcription of these cytokeratins is terminated as cells pass into the granular layer. Their transcription is superceded by the transcription of precursors of the cornified envelope including: loricrin, filaggrin and cornifin (Fleckman, Dale et al. 1985; Magnaldo, Pommes et al. 1990; Marvin, George et al. 1992). Many of these proteins are included in the formation of the cross-linked envelope and their crosslinking is catalysed by TG1 (Dlugosz and Yuspa 1993). Once cells are incorporated into the cornified layer they will ultimately be shed and replaced by cells beneath them (Eckert 1989). Thus, the differentiation program involves proliferation, growth arrest, differentiation, apoptosis and shedding of KCs. All these processes are tightly co-ordinated by a combination of key regulatory transcription factors.

1.5 Molecular Regulation of Squamous Differentiation

The regulation of gene expression that accompanies, and drives, the differentiation process is complex and involves transcriptional regulation, mRNA stability, microRNA and epigenetic regulation. However, transcription factor-mediated regulation of gene expression is by far the most important of these mechanisms.

1.5.1 Transcriptional Control of Squamous Differentiation

Transcription, the synthesis of RNA from a DNA template, is governed by several regulators that either modulate the basal transcription rate or modulate transcription in response to stimuli (Eckert, Crish et al. 1997). One of the major groups of regulators consists of transcription factors. Transcription factors regulate the transcription of genes in a tissue-specific manner in response to physiological and/or environmental stimuli (Martinez 2002). They bind to *cis*-acting DNA sequences in the promoter or enhancer region of genes and determine the function of those genes, allowing for either the activation of suppression of transcription (Kadonaga, Carner et al. 1987; Kornberg 1999).

The squamous differentiation program is primarily managed at the transcriptional level by several well characterized regulatory transcription factors as described above. Some of the well characterized differentiation specific genes and the transcription factors that have been shown to regulate them are summarized in *Table 1.1*. Sp1 also known as specificity protein 1 was the first mammalian transcription factor cloned (Kadonaga, Carner et al. 1987). It is

involved in tissue-specific transcriptional control as evidenced from the presence of functional Sp1 sites in several tissue-specific promoters (Blake, Jambou et al. 1990). Functional Sp1 sites are present in the promoters of squamous differentiation-specific genes where Sp1 is responsible for the differentiation-specific induction of gene expression (Won, Yim et al. 2002). Sp1 acts cooperatively with other transcription factors in the regulation of the differentiation program. One example of this partnership is the cooperative role of Sp1 and the activator protein-1 (AP1) which is another important transcription factor that plays a role in the activation of keratin 1 and profilaggrin (Huff, Yuspa et al. 1993; Jang, Steinert et al. 1996). Sp1 and AP1 act together to co-ordinate the induction of differentiation genes such as involucrin, which is required for cornified envelope formation (Jang and Steinert 2002). AP1 regulates the expression of most of the keratins such as keratin 1, 5 and 14 and comprises functional hetero and homodimers of jun and fos family of proteins (Ohtsuki, Tomic-Canic et al. 1992; Sinha, Degenstein et al. 2000). AP1 has also been shown to modulate the protein kinase C pathway which gets activated during differentiation (Karin 1995). Moreover, AP1 also regulates the activation of late differentiation genes such as TG1, loricrin and involucrin (Saunders, Bernacki et al. 1993; Welter, Gali et al. 1996; Jang and Steinert 2002). POU domain proteins have been shown to negatively regulate differentiation specific genes like keratin 5, keratin 14 and involucrin (Welter, Gali et al. 1996; Sugihara, Kudryavtseva et al. 2001). Ets group of proteins plays a role in differentiation through the interactions with other key transcription factors like Sp1 (Eckert, Crish et al. 1997).

Table 1.1 Summary of transcription factors involved in the regulation of differentiation specific genes.

Genes	*Transcription Factor*	*Refs*
cdc2	E2F1	**(Dicker, Popa et al. 2000)**
E2F1	E2F7, E2F8	**(de Bruin, Maiti et al. 2003; Di Stefano, Jensen et al. 2003; Logan, Delavaine et al. 2004; Hallstrom, Mori et al. 2008; Panagiotis Zalmas, Zhao et al. 2008; Endo-Munoz, Dahler et al. 2009)**
Keratin 5	NF-$_{K}$B, Sp1, AP1, POU factor	**(Ohtsuki, Tomic-Canic et al. 1992; Sugihara, Kudryavtseva et al. 2001)**
Keratin 14	NF-$_{K}$B, POU factor, AP1, AP2, Ets, CBP/p300, E2F1	**(Rossi, Jang et al. 1998; Dicker, Popa et al. 2000; Sugihara, Kudryavtseva et al. 2001; Paramio and Blumenberg 2006)**
Involucrin	p63, AP1, Sp1, POU factor, Whn, RBP-J	**(Welter, Crish et al. 1995; Welter, Gali et al. 1996; Rangarajan, Talora et al. 2001; Baxter and Brissette 2002; Jang and Steinert 2002)**
TG-1	AP1, p63, E2F1	**(Saunders, Bernacki et al. 1993; Dicker, Popa et al. 2000)**
Keratin 1	AP1, p63, C/EBP, RBP-J, Whn	**(Huff, Yuspa et al. 1993; Zhu, Oh et al. 1999; Rangarajan, Talora et al. 2001; Baxter and Brissette 2002)**
Keratin 10	C/EBP, RBP-J, AP2, E2F1	**(Maytin, Lin et al. 1999; Zhu, Oh et al. 1999; Dicker, Popa et al. 2000; Rangarajan, Talora et al. 2001)**
Loricrin	Sp1, c-jun, p300/CREB, AP1, RBP-J, Whn	**(Zhu, Oh et al. 1999; Rangarajan, Talora et al. 2001; Baxter and Brissette 2002; Jang and Steinert 2002)**

filaggrin	AP1, RBP-J, Whn	**(Jang, Steinert et al. 1996; Rangarajan, Talora et al. 2001; Baxter and Brissette 2002)**
TG-3	Sp1, Ets	**(Lee, Jang et al. 1996)**
Sp1	E2F7	**(Hazar-Rethinam, Cameron et al. 2011)**

RBP-J is highly expressed in the skin, and its role is implicated in the regulation of early differentiation markers, whilst repressing the late differentiation ones (Rangarajan, Talora et al. 2001). C/EBP proteins get activated upon the initiation of differentiation and regulate the expression of keratin 1 and 10 (Zhu, Oh et al. 1999). Nuclear factor kappa-light-chain-enhancer of activated B cells (NF-$_K$B) negatively regulates the promoters of keratin 4 and 15. Moreover, they interact with AP1 proteins and contribute to the regulation of differentiation specific genes (Rossi, Jang et al. 1998; Paramio and Blumenberg 2006). Opposing action of p63 was proposed, and it was reported that p63 is required for both the proliferative and differentiation potential of developmentally mature KCs (Truong, Kretz et al. 2006; Senoo, Pinto et al. 2007). The pleiotropic E2F family of proteins is also considered to be an important family of transcription factors to regulate squamous differentiation (Dicker, Popa et al. 2000). Their role is complex and will be discussed later in this review. However, as seen from the above discussion, multiple transcription factors are involved in the regulation of differentiation genes and the co-ordination of the complete differentiation program undoubtedly involves the co-ordinated action of multiple transcription factors acting together.

1.6 The Epidermis and UV (Sunburn Cells)

One of the major insults that challenges the skin is UV. The UV radiation spectrum is grouped into three bands based on wavelength including UVA, UVB and UVC. Although only 10% of UVB (280-320 nm) radiation penetrates the atmosphere, the ability of UVB radiation to damage DNA, to disrupt pro-apoptotic signalling pathways and to suppress immune responses makes it the most carcinogenic wavelength in the terrestrial environment (Nickoloff, Qin et al. 2002). Despite the more potent carcinogenic activity of UVB, it is only capable of penetrating the more superficial epidermal layers whereas UVA can penetrate deeper into the dermis (Maverakis, Miyamura et al. 2010). Following UVB exposure, KCs of the epidermis will follow one of two fates. They either undergo growth arrest accompanied

by the mobilisation and activation of the nucleotide excision repair system (NER) to repair the damaged DNA (mutations/DNA lesions). Alternatively, if the DNA damage is perceived to be too great and the cells lack the capacity to repair the damage then the cells will be induced to apoptose (Chaturvedi, Qin et al. 1999; Qin, Chaturvedi et al. 2002). Apoptosis is a safeguard mechanism that prevents cells from passing on mutated DNA to their progeny. Thus, the apoptotic machinery provides a means by which mutated, potentially premalignant cells, are able to be eliminated (Rodust, Stockfleth et al. 2009). UV-induced apoptosis results in the formation of so-called "sunburn cells" or apoptotic KCs. Sunburn cells are easily identified by the presence of photo lesions, pyknotic nuclei and cytoplasmic shrinkage characteristic of apoptotic cells (Laethem, Claerhout et al. 2005).

1.7 Transcriptional Control of UV-induced Responses

When KCs are exposed to UV, especially UVB radiation, specific transcription factors get activated. This results in the expression of "UV response genes". Two well characterized transcription factors activated upon UV exposure are AP1 and NF-$_K$B (López-Camarillo, Aréchaga Ocampo et al. 2011). NF-$_K$B has also been shown to play important role in the transcriptional response to cytotoxic agents like chemotherapeutic drugs (López-Camarillo, Aréchaga Ocampo et al. 2011). Crosstalk between these two transcription factors and signalling pathways exists and has been studied extensively (Zenz and Wagner 2006; Cooper and Bowden 2007). MAPK pathway is one of these pathways, which includes JNKs, ERKs and p38 MAP kinases (Assefa, Garmyn et al. 1997; Muthusamy and Piva 2010). Other transcription factors characteristic of the UV response are JUNB, JUND, c-FOS, ETR101, EGR1, HRY and XBP-1 and E2F family of transcription factors (Li, Turi et al. 2001; Hazar-Rethinam, Endo-Munoz et al. 2011; López-Camarillo, Aréchaga Ocampo et al. 2011). Exposure to UV radiation is thought to activate the Retinoblastoma/E2F axis (Rb/E2F). Moreover, the disruption of the Rb/E2F axis, caused by UV exposure, results in elevated levels of E2F proteins (Endo-Munoz, Dahler et al. 2009). This indicates that E2F proteins are involved in the cellular response to UV irradiation.

1.8 The E2F Family of Transcription Factors

The E2F transcription factor family plays a major role in a number of KC functions such as proliferation, differentiation and response to stress or apoptotic signals. Consistent with these roles, dysregulation of E2F is a common occurrence in human cancer and SCC in particular

(Jones, Dicker et al. 1997; Dicker, Popa et al. 2000; Wong, Barnes et al. 2003). Specifically, the E2F family of transcription factors has emerged as pleiotropic regulators, directly controlling i) cell proliferation, ii) apoptosis, iii) differentiation, iv) DNA-damage response and DNA repair, v) development, vi) senescence, vii) autophagy, viii) mammalian endocycle, ix) mammalian polyploidisation and x) tumour angiogenesis and metastasis (Helin, Lees et al. 1992; Trimarchi and Lees 2002; Ichihashi, Ueda et al. 2003; Stevens and La Thangue 2004; Erb, Ji et al. 2005; Moon and Dyson 2008; Panagiotis Zalmas, Zhao et al. 2008; Polager, Ofir et al. 2008; Chen, Ouseph et al. 2012; Pandit, Westendorp et al. 2012; Schaal, Pillai et al. 2014), despite the fact that E2F target genes were initially implicated in the regulation of the G_1/S phase transition of the cell cycle and in DNA replication (Rowland and Bernards 2006). Moreover, E2Fs are also indirectly involved in modulating the activity of important cellular signalling pathways such as MAPK, p38 and PI3K/AKT through transcriptional regulation of upstream pathway components (Chaussepied and Ginsberg 2005; Bashari, Hacohen et al. 2011).

E2F was first discovered as a cellular factor required for the activation of the E2 viral promoter (Nevins 1998; Erb, Ji et al. 2005), and then identified as the essential downstream target of Rb (Rowland and Bernards 2006). This factor was later cloned and named E2F1 (Helin, Lees et al. 1992; Kaelin, Krek et al. 1992; Shan, Zhu et al. 1992). However, it was quickly recognised that E2F1 was just one member of, what is now a family of 8 members. E2Fs 1-8 code for 10 different E2F forms (Dimova and Dyson 2005) (*Figure 1.3*).

The E2F family can be broadly classified as typical E2Fs (E2F1-6) and atypical E2Fs (E2F7-E2F8). All typical E2Fs carry one N-terminally located, evolutionary conserved, DNA-binding domain (DBD) (*Figure 1.3*). The DBD is followed by a dimerisation partner (DP) binding domain (Lammens, Li et al. 2009) (*Figure 1.3*). There are two members of DP family proteins, DP1 and DP2 that interact with E2F isoforms through the conserved DP binding domain (Ichihashi, Ueda et al. 2003) (*Figure 1.3*). In mammalian cells, most E2F DNA-binding takes place once E2F-DP heterodimers form to exert their function (Stevens and La Thangue 2003).

E2Fs are most frequently classified based on their transcriptional activity (*Figure 1.3*). For example, the E2F family is generally divided into three subclasses: activator E2Fs (E2F1-

E2F3a), repressor E2Fs (E2F3b-6) and inhibitory E2Fs (E2F7, E2F8). The activator subclass of E2Fs can drive quiescent cells into S phase of the cell cycle by binding to their target genes and inducing gene expression. The combined deletion of the three activator E2Fs in mouse embryo fibroblast results in the complete inhibition of proliferation (Wu, Timmers et al. 2001). The expression of activator E2Fs varies during the cell cycle reaching a peak of activity, bound to target gene promoters *via* E2F response elements, during late G_1/S phase. In this context, they are key factors controlling the expression of genes and activities required for DNA synthesis (Cam and Dynlacht 2003; Dimova and Dyson 2005; Li, Ran et al. 2008). The expression and activity of the repressor E2Fs (E2F3b, E2F4, E2F5 and E2F6) remain relatively constant throughout the cell cycle (Dimova and Dyson 2005). E2F4 and E2F5 bind target gene promoters during G_0 with E2F inhibitory pocket proteins coupled with repressive histone deacetylases (HDACs) (Takahashi, Rayman et al. 2000; Sherr and McCormick 2002) and prevent promiscuous transcription of proliferation genes (Attwooll, Denchi et al. 2004; Berton, Mitchell et al. 2005; Dimova and Dyson 2005). The so-called repressor E2Fs get their name due to their ability to actively recruit transcriptional inhibitors such as HDAC1 (e.g. E2F4 and E2F5) or PRC2 (E2F6) to the E2F sites resulting in transcriptional repression (Leone, DeGregori et al. 1998; Berton, Mitchell et al. 2005). Indeed, Gaubatz and his colleagues showed that ablation of two repressor E2Fs together, E2F4 and E2F5, in mouse embryonic fibroblasts (MEFs), causes reduction in their responsiveness to growth inhibitory signals and fail to repress G_0-specific genes (Gaubatz, Lees et al. 2001). E2F6 forms a multimeric protein complex containing Mga and Max proteins in order to repress target gene transcription during G_1/S phase in a Rb independent manner (Ogawa, Ishiguro et al. 2002; Giangrande, Zhu et al. 2004).

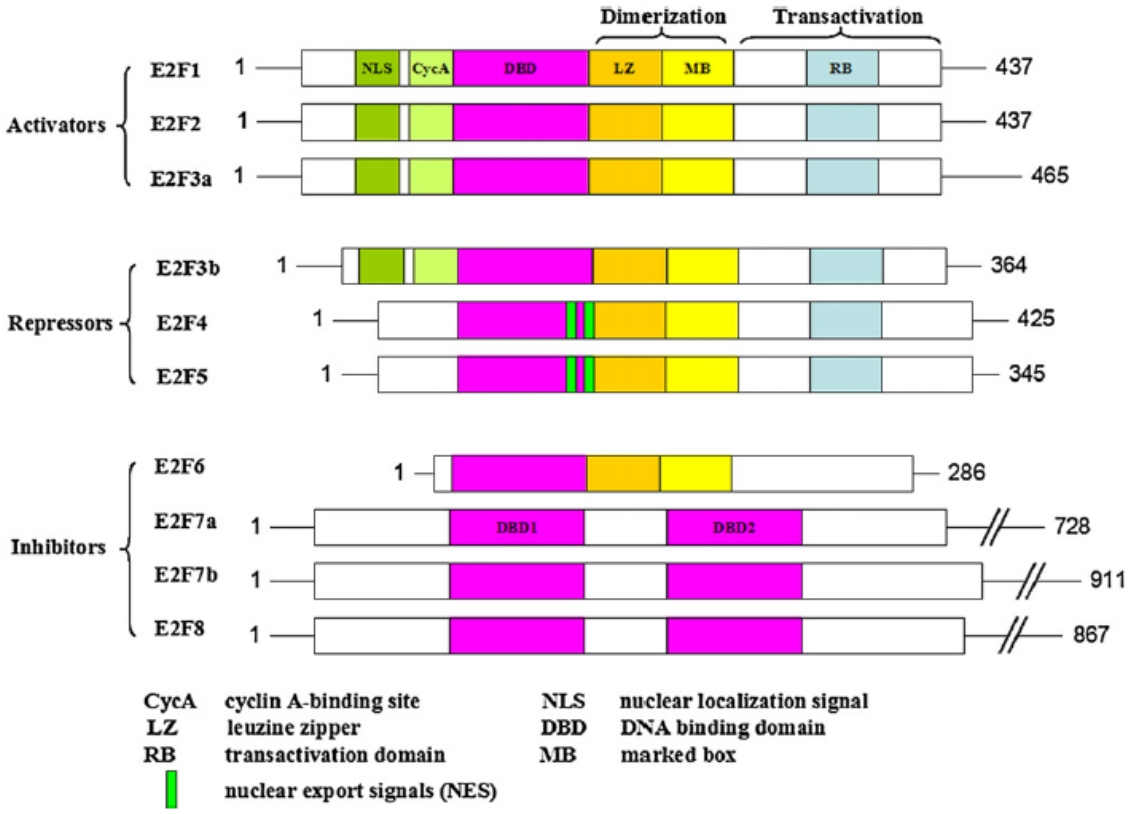

Figure 1.3 Domain organisation of activating, repressive or inhibitory E2Fs. Number of amino acid is indicated on the right. Same colour boxes indicate homologues regions. There are two known E2F7 isoforms; E2F7a and E2F7b which differ only in their C termini. Both isoforms of E2F7 are expressed in all cell lines analysed (Zhan, Huang et al. 2014).

Several studies demonstrate that E2Fs serve critical functions beyond cell-cycle regulation (Chen, Tsai et al. 2009; Chong, Wenzel et al. 2009; Wenzel, Chong et al. 2011). Hence, the role of the E2Fs is complex. Individual E2F family members can be involved in multiple cellular activities. For example, E2F1 is directly involved in the G_1/S transition of the cell cycle (Johnson, Ohtani et al. 1994), stimulating apoptosis (Trimarchi and Lees 2002; Iaquinta and Lees 2007), suppressing differentiation (Wong, Barnes et al. 2003; Wong, Barnes et al. 2004; DeGregori and Johnson 2006) and acting as a transducer of the DNA damage response in KCs (Berton, Mitchell et al. 2005). In addition, multiple E2F family members can play a role in the same cellular functions and frequently share the same E2F binding sites in gene promoters (consensus E2F binding site is TTTCGCGC) (de Bruin, Maiti et al. 2003; Di Stefano, Jensen et al. 2003). For example E2Fs 1, 2 and 3a are all involved in the transition through the G_1/S phase of the cell cycle (Leone, DeGregori et al. 1998). Finally, there is emerging evidence to indicate that E2F isoform specific-sites and functions may also exist. For example, in KCs we recently showed that E2F7 could selectively suppress differentiation

through the repression of Sp1's transcription mediated *via* a selective and novel E2F7-specific response element (5'-CTCCTTTCCCCCTCCCTCAT-3') (Hazar-Rethinam, Cameron et al. 2011). Finally, it is important to note that activating and repressive or inhibitory E2Fs exist that antagonise one another function either through direct competition for binding sites (eg: E2F1 and E2F7 in G_1/S phase gene promoters) or indirectly by opposing each other's action (Mariconti, Pellegrini et al. 2002; de Bruin, Maiti et al. 2003; Christensen, Cloos et al. 2005). For example E2F1 can suppress differentiation genes whilst E2F7 can derepress the same genes but through independent DNA response elements (Hazar-Rethinam, Cameron et al. 2011). Thus, understanding E2F function requires an understanding of the opposing actions of the E2F family members.

1.9 Atypical E2Fs: new players in the E2F family

Despite around 3500 publications focusing on E2Fs, our knowledge about these master regulators is very limited especially when it comes to two most recently identified members of the family. These novel, evolutionary conserved, members form a distinct arm of E2F family and were first discovered in *Arabidopsis thaliana*, and named as DP-E2F-Like (DEL1 to DEL3) through a genome survey in order to find genes containing sequences homologues to E2F-DBD (Kosugi and Ohashi 2002; Mariconti, Pellegrini et al. 2002). They have been found in numerous organisms so far, and named as EF27 and E2F8 following their discovery in mice and human (de Bruin, Maiti et al. 2003; Di Stefano, Jensen et al. 2003; Logan, Delavaine et al. 2004; Christensen, Cloos et al. 2005; Logan, Graham et al. 2005; Maiti, Li et al. 2005). Their unique structural properties distinguish them from the rest of the family. Therefore, they were also termed as "atypical" E2Fs.

1.9.1 Molecular features of atypical E2F proteins

One of the atypical E2Fs, E2F7, exists as an alternatively spliced form (*Figure 1.3*). The shorter isoform, E2F7a, is 728 amino acid-long. The longer isoform of E2F7, E2F7b, carries 13 exons, and encodes a protein of 911 amino acids (de Bruin, Maiti et al. 2003). The only difference between these two isoforms is the extra exon of E2F7b located in the C-terminal tail from amino acid 7143 (Di Stefano, Jensen et al. 2003). Our previous experiments showed that E2F7a expression is negligible compared to E2F7b in KCs. Therefore, the future reference to E2F7 refers to E2F7b.

Although there are numerous structural differences between atypical and canonical E2F proteins, DBD is the most notable feature that separates them from each other. In contrast to canonical E2Fs, the DBD is duplicated in atypical E2Fs and the integrity between these two DBDs is essential for their function (*Figure 1.3*). It was previously shown that the mutation in either of the DBD is able to completely diminish the DNA binding function of these proteins (Kosugi and Ohashi 2002; Di Stefano, Jensen et al. 2003; Logan, Delavaine et al. 2004; Christensen, Cloos et al. 2005; Logan, Graham et al. 2005; Maiti, Li et al. 2005). Three-dimensional modelling of E2F7 and E2F8 further demonstrated that duplicated DBD of atypical E2Fs is able to mimic the binding between canonical E2F protein and their partner protein (Li, Ran et al. 2008).

Atypical E2Fs bind target gene promoters in a DP-independent fashion due to the lack of a DP-binding domain (*Figure 1.3*) (de Bruin, Maiti et al. 2003; Di Stefano, Jensen et al. 2003; Ichihashi, Ueda et al. 2003; Logan, Delavaine et al. 2004; Logan, Graham et al. 2005; Maiti, Li et al. 2005). Instead, they utilize two tandem DBDs to recognise and bind target sequences (Ouseph, Li et al. 2012). Moreover, coimmunoprecipitation studies have shown that the atypical E2Fs are able to form homodimers and heterodimers with each other (Di Stefano, Jensen et al. 2003; Maiti, Li et al. 2005; Li, Ran et al. 2008). One other important feature of atypical E2Fs is the lack of a recognisable *trans*activation domain (*Figure 1.3*) (Iaquinta and Lees 2007). The lack of functional domains on E2F7 and E2F8 has led to the hypothesis that their main mode of action is to compete with canonical E2Fs binding and subsequent modulation of response elements. Indeed, studies have shown that ablation of atypical E2Fs can induce the expression of defined subsets of E2F-regulated genes (Li, Ran et al. 2008; Panagiotis Zalmas, Zhao et al. 2008). Finally, atypical E2Fs possess motifs known to be responsible for ubiquitin-mediated degradation, which is absent in canonical E2Fs (Christensen, Cloos et al. 2005). This ties in with the observed instability of atypical E2Fs (Christensen, Cloos et al. 2005).

1.9.2 Transcriptional regulation of atypical E2F expression

The expression of E2F7 and E2F8 is cell-cycle regulated, which distinguishes them from repressor E2Fs. Transcription of E2F7 and E2F8 increases towards G_1/S transition reaching its peak during mid to late S phase as targets of E2F1 (Berton, Mitchell et al. 2005; Christensen, Cloos et al. 2005; Lammens, Li et al. 2009; Hazar-Rethinam, Cameron et al. 2011). Sequence analysis of atypical E2Fs resulted in the identification of consensus E2F-

binding sites on their promoters. In particular, the direct association of E2F1, E2F3, E2F4 and E2F7 proteins with promoter elements of atypical E2Fs was shown previously (Di Stefano, Jensen et al. 2003; Christensen, Cloos et al. 2005). In a separate study, this relationship between atypical promoters and other family members was also confirmed demonstrating that E2F1 and, to a lesser extent, E2F4 and E2F7 bind the E2F8 promoter (Christensen, Cloos et al. 2005), and E2F7 occupies the promoters of E2F1, E2F2, E2F3 and E2F8 as well as its own promoter (Westendorp, Mokry et al. 2011). Clearly, atypical E2Fs are targets of E2Fs. Indeed, screening for genes regulated by E2F1 independently identified E2F7 as an E2F1-regulated gene (Di Stefano, Jensen et al. 2003). Of interest, in addition to canonical E2Fs, recent work has shown that E2F7 is a direct p53 target gene and is upregulated by p53 in mediating response to DNA damage and cellular senescence (Aksoy, Chicas et al. 2012; Carvajal, Hamard et al. 2012). E2F7 has a p53-binding site in its promoter, and, interestingly, no specific p53 binding sites were detected in any of the other E2F promoters (Aksoy, Chicas et al. 2012).

Once expressed, E2F7 and E2F8 bind to the E2F1 promoter *via* an E2F response element and inhibit its expression (de Bruin, Maiti et al. 2003; Di Stefano, Jensen et al. 2003; Logan, Delavaine et al. 2004). Hence, there is clear evidence that E2F1 and E2F7 exist in a negative feedback loop that modulate both their activity and transcription. Thus, the role of E2F7 and E2F8 in cell cycle control appears to tie in with the direct inhibition of the E2F1 activities related to cell cycle traverse (Di Stefano, Jensen et al. 2003; Raj, Brash et al. 2006). To date, the participation of E2F8 in this feedback loop has not been elucidated. Besides E2F1, E2F2 and E2F3a have been also reported to induce E2F7 and E2F8 transcription at G_1/S phase of cell cycle (de Bruin, Maiti et al. 2003; Di Stefano, Jensen et al. 2003; Logan, Delavaine et al. 2004; Christensen, Cloos et al. 2005; Logan, Graham et al. 2005; Maiti, Li et al. 2005). Furthermore, expression profiling and biochemical approaches identified one of the canonical E2F activators, E2F3a, as a key E2F family member that antagonizes E2F7/8 functions in coordinating cell cycle progression and subsequent placental development (Ouseph, Li et al. 2012). This suggests that they are required for the balanced and timely regulation of genes involved in S-phase *via* a feed-forward loop, where an activator induces a target gene but at the same time also induces a repressor of the very same target limiting the extent of the induction, between two arms of the E2F family (Westendorp, Mokry et al. 2011; Aksoy, Chicas et al. 2012). In addition to canonical E2Fs, Westendorp *et al* performed a genome-wide promoter occupancy analysis and reported that E2F7 binds to multiple G_1/S-regulated

gene promoters and inhibits their transcription in cell cycle phase-specific context (Westendorp, Mokry et al. 2011).

When it comes to the expression patterns of atypical E2Fs, our knowledge is limited as not much is known about the tissue-specific expression profiles of these proteins. From the little that has been published there appears to be considerable overlap in expression (Maiti, Li et al. 2005). However, there are observed differences between atypical E2Fs' expression profiles in cell lines. The observation that E2F7 and E2F8 can be expressed in the same tissue begs the question of whether they share similar gene targets or whether they perform independent roles in these cells. At present there is no data available on this matter.

1.9.3 Regulation of transcription by atypical E2Fs

Till now how atypical E2Fs act to repress gene transcription remains to be determined. One possibility could be ruled out based on structural differences between canonical and atypical E2Fs. It is unlikely that atypical E2Fs act through co-recruitment of Rb family members to target promoters which repress gene expression by sequestering activated E2Fs and recruiting histone-modifying activities (Morris and Dyson 2001; Nijwening, Geutjes et al. 2011), since atypical E2Fs lack pocket protein binding domain. Instead, several studies suggest that atypical E2Fs compete with the activating E2Fs for promoter occupancy of E2F target genes to prevent transcriptional activation (Li, Ran et al. 2008; Westendorp, Mokry et al. 2011; Aksoy, Chicas et al. 2012). Recently, Liu *et al* unveiled the mechanism by which E2F7 repress E2F1 gene transcription (Liu, Shats et al. 2013). The authors showed that E2F7 (and E2F8) forms an E2F1-E2F7 complex and an E2F7-E2F7 homodimer on adjacent E2F-binding sites. Upon forming these complexes, E2F7 recruits the co-repressor C-terminal-binding protein (CtBP), and, significantly, CtBP2 is essential for E2F7-mediated repression of E2F1 transcription (Liu, Shats et al. 2013). In the very same paper, the authors also hypothesized based on their results that the direct interaction between E2F1 and E2F7 could direct E2F7 to the E2F target promoters which are activated by E2F1 (Liu, Shats et al. 2013). A recent unbiased proteomics analysis of CtBP2-associated proteins confirmed the findings from Liu's paper and showed that CtBP proteome contains components of the Nucleosome Remodelling Deacetylase (NuRD) and E2F7 (Zhao, Subramanian et al. 2014). This study further provides insight into binding kinetics between CtBP2 and E2F7, and demonstrates that E2F7 interacts with CtBP2 though a canonical CtBP binding motif with the hydrophobic cleft region of CtBP2 (Zhao, Subramanian et al. 2014)

Despite their classification as transcriptional repressors, intriguingly, several recent studies highlighted an unanticipated functional interaction between E2F7/8 and their target genes (Deng, Wang et al. 2010; Sirma, Kumar et al. 2011; Weijts, Bakker et al. 2012). E2F7 was shown to bind and activate human telomerase reverse transcriptase (TERT) promoter in hepatocytes in response to proliferation (Sirma, Kumar et al. 2011), and Collagen and Calcium Binding EGF domains 1 protein promoters (Ccbe1) in HeLa cells (Weijts, van Impel et al. 2013). However, a molecular mechanism through which E2F7 activates the transcription of these promoters was not provided. In the liver, E2F8 was found to bind and enhance promoter activity of Cyclin D1 promoter. In the same study, a possible model was proposed where E2F8 acts in a dominant negative manner by relocating some E2F transrepressors (Deng, Wang et al. 2010). On the other hand, Weijts and his colleagues elegantly provided evidence for a molecular mechanism as to how atypical E2Fs enhance promoter activity (Weijts, Bakker et al. 2012). This study showed a novel function for E2F7 and E2F8 in activating the transcription of the vascular endothelial growth factor A (VEGFA) and subsequently contributing to proper formation of blood vessels (Weijts, Bakker et al. 2012). E2F7/8 directly binds and stimulates VEGFA promoter activity independent of canonical E2F binding sites; instead they bind to non-canonical E2F binding sites and form a transcriptional complex with an transcriptional activator the hypoxia inducible factor 1 alpha (HIF1α) for full activation of the VEGFA promoter (Weijts, Bakker et al. 2012).

1.9.4 Atypical E2F proteins and differentiation

As mentioned previously, squamous differentiation is primarily controlled at the transcriptional level by key transcription factors such as the E2F family of proteins. The participation of E2Fs in differentiation was first observed in myogenic differentiation where ectopic expression of one of the typical E2Fs, E2F1, suppressed terminal differentiation (Wang, Helin et al. 1995). Similarly, an essential prerequisite to initiate differentiation is the downregulation of activating E2Fs, such as E2F1 (*Figure 1.4*). Our laboratory recently showed that one of the inhibitory E2Fs, E2F7, was highly expressed in proliferating KCs and could inhibit proliferation-specific markers and sensitise KCs to differentiation stimuli (Endo-Munoz, Dahler et al. 2009). It was shown that E2F7 was capable of repressing the activity of one of the established differentiation activators, Sp1 (*Figure 1.4*) (Hazar-Rethinam, Cameron et al. 2011). The loss of E2F7 leads to derepression of Sp1 protein, and subsequent transcription of differentiation specific genes, such as TG-1. Furthermore, we

recently showed that E2F7 could selectively suppress differentiation through the repression of Sp1 transcription mediated *via* a selective and novel E2F7-specific response element (Hazar-Rethinam, Cameron et al. 2011). In agreement with these studies, E2F7 as a novel target of miR-26a was shown to play an important role in monocytic differentiation of acute myeloid leukemia cells where ablation of E2F7 was sufficient to commit monocytic/macrophage cells to differentiate and increased E2F7 levels counteracted monocytic differentiation (Salvatori, Iosue et al. 2012).

The published data clearly shows the involvement of E2F1 and E2F7 in the regulation of squamous differentiation. However, E2F7 cannot be considered a global regulator of differentiation since it interacts with only selective genes in the differentiation program. Although E2F8 has previously been shown to promote erythroid terminal differentiation by collaborating with Rb protein where Rb binds and sequesters E2F2 and E2F8 competes with E2F2 for E2F2-binding sites on target gene promoters (Ghazaryan, Sy et al. 2014), to our knowledge, there is no reported data showing the participation of E2F8 in the differentiation program in KCs. Dysregulation of squamous differentiation is a key event in malignant conversion of KCs and is evident in early forms of SCC (Sugiyama, Speight et al. 1993; Watanabe, Ichikawa et al. 1995; Gasparoni, Fonzi et al. 2004). Significantly, E2Fs are also known to be dysregulated in SCC and to contribute to the dysregulation of differentiation (Wong, Barnes et al. 2003; Wong, Barnes et al. 2004). Therefore, understanding both the role of individual E2Fs and the interactions between those individual E2Fs is of interest.

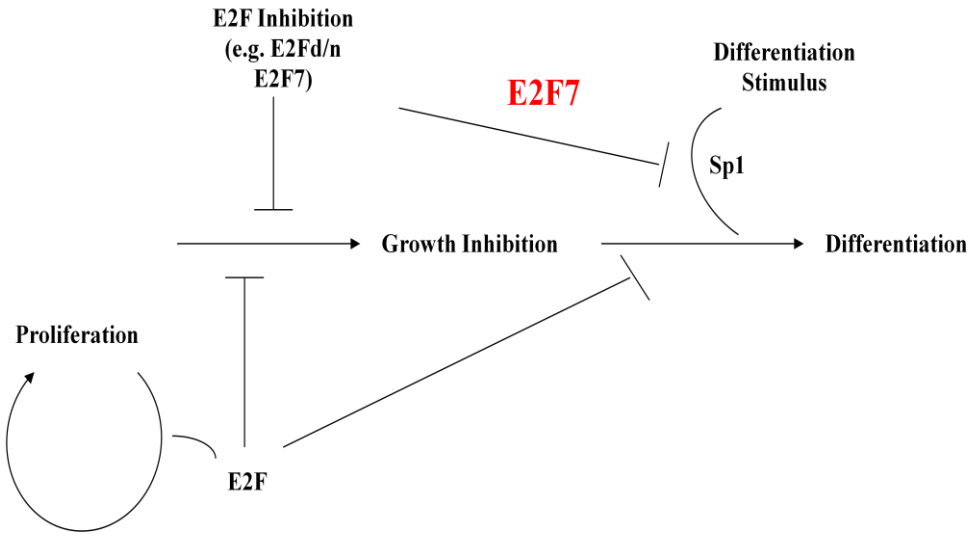

Figure 1.4 Model of E2F7's role in squamous differentiation. E2F inhibition and Sp1 activation *via* downregulation of E2F7 is sufficient to induce markers of squamous

differentiation in normal KCs and SCC cells. Figure courtesy of Associate Professor Nicholas Saunders and used with permission.

1.9.5 Atypical E2F proteins and DNA damage response

In vitro and *in vivo* knockout studies have provided information about atypical E2Fs and their biological contribution to DNA damage including UV and chemotherapy mediated responses. Reassuringly, E2F7 has been recently identified as a *bona fide* p53 target gene that is activated during DNA damage response and executes its role through transcriptional regulation of a subset of indirect p53 target genes (Aksoy, Chicas et al. 2012; Carvajal, Hamard et al. 2012). Curiously, only E2F7 expression (in a p53-dependent manner) was affected upon DNA damage since the levels of E2F8 remained unchanged (Carvajal, Hamard et al. 2012). In addition, in an effort to identify novel E2F7 binding sites in promoters of target genes, ChIP-Seq and the global gene expression experiments resulted in a list of E2F7 target genes (Westendorp, Mokry et al. 2011). DNA repair genes are overrepresented in this list, confirming previously publishes studies and providing evidence for an important role for E2F7 in DNA damage responses (Westendorp, Mokry et al. 2011).

E2F7 has been shown to bind directly and repress target genes which are important in the DNA damage responses such as Rad51, Check1, BRCA1 and BRCA2 by Westendorp and his colleagues (Westendorp, Mokry et al. 2011). They further reported that E2F7 overexpression alone is sufficient to induce DNA damage by increasing DNA double-strand breaks (Westendorp, Mokry et al. 2011). Interestingly, Zalmas and his colleagues examined the biological role of E2F7 in DNA damage response and demonstrated that E2F7 contributes to DNA damage response not only by regulating transcription of target genes involved in DNA damage response, but also by altering the local chromatin environment of the DNA lesion (Zalmas, Coutts et al. 2013). Upon DNA damage, E2F7 recognises and binds to damaged DNA, recruits CtBP and HDAC to the damaged DNA (Zalmas, Coutts et al. 2013), contributing to the DNA damage response through both transcriptional and non-transcriptional mechanisms.

1.9.5.1 UV-induced responses

The ability of the different E2Fs to contribute to apoptosis, especially to UVB-mediated apoptosis, is contentious. Much of this controversy arises from some seemingly paradoxical data relating to the action of E2F1. In response to UVB, E2F1 transcript and protein levels

increase in an ATM/ATR dependent manner and triggers a series of events required for apoptosis (Carcagno, Ogara et al. 2009). This suggested that UVB-induced E2F1 mediated apoptosis in skin may have tumour suppressive effects. However, studies from Dimova and Dyson reported otherwise (Helin, Lees et al. 1992; Dimova and Dyson 2005). Collectively, the studies so far suggest that the role of E2F1 in regulating apoptosis may be context-specific. Moreover, the dose of UVB and the level E2F1 should also be considered in terms of apoptotic responses.

Atypical E2Fs bind to, and repress, E2F1-mediated apoptosis via direct inhibition of E2F1 (Li, Ran et al. 2008; Panagiotis Zalmas, Zhao et al. 2008; Endo-Munoz, Dahler et al. 2009). Both E2F7 and E2F8 are expressed in skin (Stevens and La Thangue 2003; Berton, Mitchell et al. 2005) and are able to influence the cellular DNA damage response (Panagiotis Zalmas, Zhao et al. 2008). In fact, microarray analysis of cells subjected to DNA damage revealed that E2F7 and E2F8 could be considered *bona fide* DNA damage response genes (Li, Ran et al. 2008). These studies seem to be relevant to UV responses in skin since we recently reported that E2F7 plays a role in regulating proliferation, differentiation and UV-induced cytotoxicity in human KCs *in vitro* (Endo-Munoz, Dahler et al. 2009). Moreover, we reported that E2F1 and E2F7 were overexpressed in human SCCs approximately 50-fold and 200-fold (Endo-Munoz, Dahler et al. 2009). Such elevations in E2F1 and E2F7 are clearly pathologic and the consequences on UV-induced tumour development and progression remain unknown. However, given that E2F1 and E2F7 are said to autoregulate the expression of one another and given that E2F7 antagonises E2F1-induced apoptosis and UV-induced apoptosis in human KCs, it would seem reasonable to speculate that E2F7 may also play a role in UV responses in human KCs (*Figure 1.5*). Thus, apoptotic responses of KCs to UV are likely to be dictated by the relative levels of E2F1 and E2F7.

Although the direct relationship between E2F7 proteins and UV-mediated responses has been published, the role of E2F8 in UV-mediated DNA damage has not been investigated. Therefore, our knowledge about E2F8 is limited in relation to its biological contribution to cytotoxic responses caused by UV.

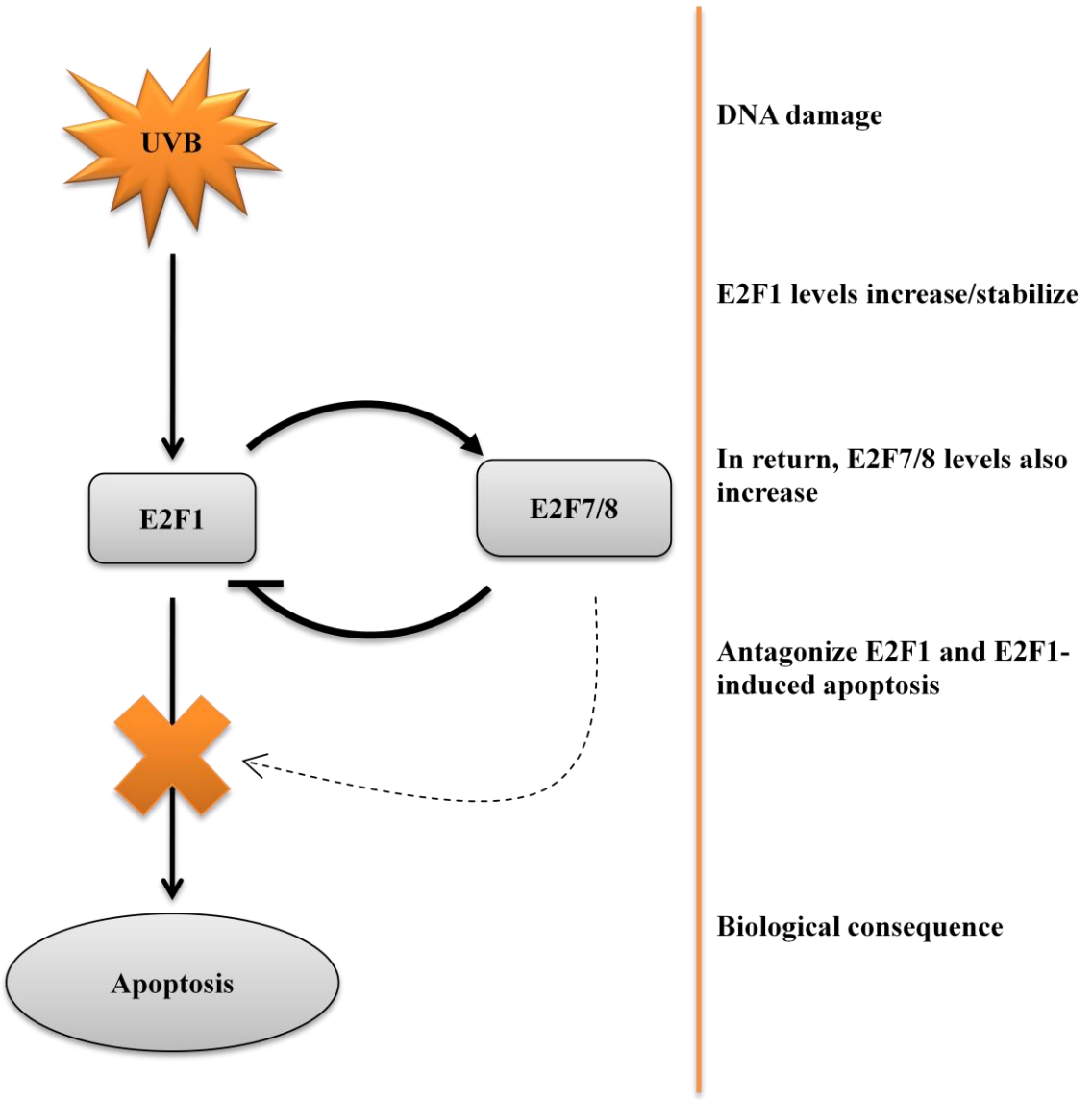

Figure 1.5 Schematic showing of how E2F1 and E2F7 contribute to formation of cutaneous malignancies due to dysregulated apoptotic control. (Hazar-Rethinam, Endo-Munoz et al. 2011).

1.9.5.2 Chemotherapy-induced responses

DNA damage and subsequent stress responses can also be triggered by chemotherapeutic agents. Several cell death pathways have been implicated in cisplatin induced cytotoxicity, one of which is an E2F1-dependent death pathway (Gordon and Gattone 1986; Ramesh and Reeves 2003; Liu and Baliga 2005). Upon cisplatin exposure, E2F1 levels increase and E2F1 gets stabilized. In this context, E2F1 induction is downstream of cdk2 (Yu, Megyesi et al. 2007; Yu, Megyesi et al. 2008). This, in turn, induces death signalling *via* TopBP1 protein expression (Liu, Lin et al. 2003). Supporting this, the involvement of E2F1 in cisplatin-mediated cytotoxicty has been reported *in vivo* and *in vitro* (Yu, Megyesi et al. 2007). In

addition, to cisplatin-induced cytotoxicity, there are reports on the involvement of E2F1 in doxorubicin-mediated stress responses (Dong, Yang et al. 2002; Han, Park et al. 2003; Ianari, Gallo et al. 2004). A recent study demonstrated that E2F1 is stabilized following exposure to doxorubicin even in the absence of either ATM-dependent phosphorylation or p53 and cAbl, which are the two major elements in DNA damage signalling (Ianari, Gallo et al. 2004). Moreover, adenovirus mediated E2F1 gene delivery/therapy was able to sensitize melanoma cells towards Topoisomerase II inhibitors such as doxorubicin and etoposide *in vitro* and *in vivo* (Dong, Yang et al. 2002).

Although E2F1 has been shown to play a vital role in the induction of apoptosis caused by DNA-damage inducing agents, the fine tuning of E2F1 is required in order to prevent aberrant accumulation of E2F1. Accordingly, elevated levels of E2F1 and E2F7 in human SCCs have an impact on apoptotic responses and result in chemotherapeutic insensitivity in SCC.

As mentioned previously, analysis of cells following DNA damage revealed that E2F7 and E2F8 could be considered *bona fide* DNA damage response genes (Li, Ran et al. 2008). Zalmas *et al* (Panagiotis Zalmas, Zhao et al. 2008) recently showed that DNA damage induced by etoposide increased E2F7 and E2F8 expression. Moreover, they demonstrated that DNA damage invoked an increase in E2F7 and E2F8 binding to E2F-responsive genes such as E2F1 resulting in an inhibition of E2F1-mediated apoptosis (Panagiotis Zalmas, Zhao et al. 2008). Li and his group also demonstrated that cells lacking E2F7 and E2F8 were hypersensitive to DNA-damage induced apoptosis when treated with camptothecin and cisplatin (Li, Ran et al. 2008). Collectively, these findings provide tantalising clues as to the relationship between E2Fs and chemotherapeutic responses. Interestingly, in a recent study where the authors demonstrated that E2F7 mediates DNA damage-dependent transcriptional repression after genotoxic stress, treatment of U2OS cells with a single dose of doxorubicin and increasing amounts of etoposide resulted in a time-dependent increase in only E2F7 mRNA and protein levels whilst E2F8 levels were downregulated (Carvajal, Hamard et al. 2012). DNA damage-induced transcriptional repression of E2F7 target genes such as E2F1 was also confirmed in this study demonstrating that E2F7 is recruited to E2F1 promoters after treatment with the genotoxic drugs (Carvajal, Hamard et al. 2012). Similar differences in E2F8 expression levels were also reported in a recent study where the effects of the proteasome inhibitor bortezomib (BZB) on atypical E2Fs was evaluated in hepatocellular

carcinoma cells (Baiz, Dapas et al. 2014). BZB treatment of the hepatocyte-like hepatocellular carcinoma cells had a significant impact on E2F8 by reducing its levels (Baiz, Dapas et al. 2014). Interestingly, BZB treatment had an effect only on E2F8 levels but E2F7 mRNA levels remained unchanged (Baiz, Dapas et al. 2014), suggesting a chemotherapeutic agent-dependent mechanism of action.

1.10 Project aims and hypothesis

KC-derived SCC of the skin and mucosae are amongst the most common malignancies afflicting humans. SCC is characterized by dysregulated proliferation, apoptosis and dysregulated differentiation control. Collectively, there is a significant amount of data about the importance of E2F family of transcription factors in KC biology. Thus, our previous studies with E2F family of transcription factors in the context of KCs have provided considerable insight into squamous differentiation and squamous neoplasia. The key findings from the work were i) that E2F1, E2F7 and E2F8 are preferentially expressed in proliferating human KCs (HEK), ii) that E2F1 is pro-proliferative, a differentiation suppressive and proapoptotic, iii) that in contrast, E2F7, and presumably E2F8, are able to antagonize E2F1 including E2F1-induced apoptosis, iv) that E2F7 is anti-proliferative, a differentiation initiator and anti-apoptotic, v) that Sp1 is one of the E2F7-specific genes within KCs playing a crucial role in the initiation of differentiation, vi) that E2F8 is anti-proliferative and anti-apoptotic, however, its contribution toward differentiation has not been elucidated to date and vii) that E2F1 and E2F7 are both overexpressed in SCCs by greater than 100-folds. Thus, better understanding of the E2F family of proteins is essential to understand how these processes are disrupted during SCCgenesis. The E2F network exists as a complex map of cross-talking pathways, and the complete understanding of the E2F family will not be possible until physiological functions of E2F7/E2F8 and E2F isoform-specific activities and gene targets in KCs are fully revealed. Moreover, the knowledge on how E2Fs interact with each other will produce a shift in our understanding of the defects underlying SCC formation and also provide clear evidence of a potential therapeutic strategy that is SCC-specific. Hence, the hypotheses of this project are:

i. That E2F7 and/or E2F8 are key regulators of squamous differentiation.
ii. That E2F7 and/or E2F8 modulate cytotoxic responses to UV radiation and chemotherapeutic agents.

iii. That disruption of the E2F1/E2F7/E2F8 axis during SCC formation contributes to the development of SCC.

In order to explore these hypotheses, a number of aims were addressed:

1. Characterise the biological activity of E2F1, E2F7 and E2F8 in murine KC models of squamous differentiation, with particular emphasis on E2F8.
2. Define the molecular basis for E2F1- and E2F7-dependent modulation of chemotherapeutic agents including cisplatin, etoposide and anthracyclines sensitivity in SCC *in vitro* and *in vivo.*

CHAPTER TWO

2 Material and Methods

This Chapter will detail general experimental procedures which will be referred to throughout the Results Chapters of this thesis. General buffers and media used in this project are described in Appendix I.

2.1 Mice

2.1.1 Mouse strains

Five different groups of mice were used in this study so far. Control mice were from mix background, C57/BL6 and FVB, and did not carry any genetic alterations. Flox mice**;** E2F7 and E2F8, were kindly provided by Gustavo Leone (Li, Ran et al. 2008). Specifically, exon 4 was flanked by LoxP sequences for E2F7 $^{Flox/Flox}$ mice, whereas exon 3 and 4 both were flanked for E2F8 $^{Flox/Flox}$ littermates. E2F7/8$^{Flox/Flox\ mice}$ were generated in house by crossing E2F7 $^{Flox/Flox}$ mice with E2F8 $^{Flox/Flox}$ mice. Littermates of floxed mice were from C57/BL6 background. E2F1 KO mice were generated by inserting a PGK-neo cassette in the DNA binding and dimerisation domains of a 7.4 kb fragment of the E2F1 gene, which resulted in mutated E2F1 locus that does not encode a functional protein (Field, Tsai et al. 1996). E2F1KO mice were also from mixed background. Floxed mice were maintained as homozygous population for the E2F floxed allele as well as E2F1KO mice.

2.1.2 Genotyping

Genotypic analysis of offspring on tail tip DNA was performed by PCR using locus-specific primers described in *Table 2.2*.

2.1.2.1 DNA extraction

DNA was extracted using the Qiagen DNeasy Blood and Tissue Kit (Qiagen, Chadstone Centre, Australia) in accordance with the manufacturer's instructions. All reagents in this section are provided with the DNeasy Blood and Tissue Kit unless otherwise indicated.

2.1.2.2 PCR

Where E2F7 and E2F8 genotyping was to performed, 2 µL of extracted DNA was used in a PCR reaction consisting of 5µL reaction buffer (Platinum *Taq* DNA Polymerase Kit, Invitrogen, Mt Waverly Australia), 10 µM forward and reverse primers, 40 mM dNTP, 1.5 µL magnesium chloride ($MgCI_2$), 2.5 µL (5%) dimethyl sulfoxide (DMSO), 34.8 µL water

and 0.2 µL Platinum *Taq* (Invitrogen). E2F7 and E2F8 PCR were run using the same cycling conditions:

Temperature and Time	Number of Cycles
94°C for 2 minutes	1
94°C for 30 seconds 55°C for 30 seconds 72°C for 30 seconds	40
4°C	Hold

Where E2F1 genotyping was to be performed, two reaction mixes were prepared for each DNA sample: Mix "A" and Mix "B". Mix "A" consisted of 5µL reaction buffer (Platinum *Taq* DNA Polymerase Kit, Invitrogen), 10 µM forward (WT#2) and reverse primers (COM#3), 40 mM dNTP, 1.5 µL $MgCI_2$, 38.3 µL water and 0.2 µL Platinum *Taq* (Invitrogen). Mix "B" contained the same ingredients as Mix "A" except the forward primer (NEO#1). E2F1 PCR was run using the following conditions:

Temperature and Time	Number of Cycles
94°C for 2 minutes	1
94°C for 30 seconds 56°C for 30 seconds 72°C for 30 seconds	40
4°C	Hold

PCR reactions were run in an Eppendorf Gradient Thermal Cycler (Eppendorf, North Ryde, Australia). The E2F7 PCR product was electrophoresed on a 3% agarose (Bioline, Alexandria, Australia) gel made in TBE (Appendix I) buffer with 0.001% w/v ethidium bromide and a DNA ladder (New England Biolabs) to ensure that the PCR product was the correct size and visualised under UV light whereas the percentage of agarose/TBE gel for E2F8 was 2.5%. E2F1 PCR products from both Mix A and Mix B reactions per sample were electrophoresed on a 2% agarose/TBE gel and visualised under UV light.

2.2 Tissue culture methods

2.2.1 Mouse epidermal keratinocyte isolation

Mouse epidermal keratinocytes (MEK) were isolated from newborn mouse pups, 0 to 3 days old, in accordance with Institutional Ethics Approval. All procedures were carried out under aseptic techniques in a laminar flow hood. Upon transferring pups from animal house (UQ Biological Research Facility) to laminar flow hood, pups were sacrificed by decapitation with scissors. The body was washed in 70% ethanol for 15 seconds to decontaminate the skin and then soaked in phosphate-buffered saline (PBS). Tail tip sample was taken for PCR screening. A single incision was made through the skin along the underside of the pup, from the neck to the base of the tail. The skin was peeled from the body wall and the carcass was discarded. The skin was washed in PBS. The peeled skin was cut into approximately four even pieces and tissue pieces were then submerged and incubated overnight at 4°C in filter sterilized 5 mg/mL Dispase II (Roche Diagnostics, Castle Hill, Australia) in PBS. The Dispase solution was supplemented with 0.1% v/v penicillin/streptomycin (Invitrogen, Mt Waverly, Australia), 10 µg/mL gentamycin (Pfizer, West Ryde, Australia) and 0.2 µg/mL amphotericin B (Fungizone) (Gibco, Mulgrave, Australia).

Next day, the epidermis (white) was separated from the dermis (jelly) and washed twice in PBS to reduce fungal contamination. The epidermal sheet was placed into a 15 mL Falcon tube (BD Biosciences, North Ryde, Australia) containing 2 mL of 0.25% w/v trypsin with 1mM ethylene diamine tetra acetic acid (EDTA) (Invitrogen) and pipetted vigorously for 20 seconds. 1 mL of 10% v/v foetal bovine serum (FBS) (Bovogen Biologicals, Essendon, Australia) in PBS and 5 mL of PBS were added and mixed gently by gentle inversion. Most of the skin chunks were removed, and the tube was spun at 200 *g* for 2 minutes and supernatant discarded. The pellet was resuspended in 5 mL of keratinocyte serum-free media (KC-SFM) without calcium (Invitrogen) supplemented with 5 µg/mL epidermal growth factor (EGF) (Invitrogen), 50 µg bovine pituitary extract per mL (BPE) (Invitrogen), 0.1% v/v penicillin/streptomycin (Invitrogen), 1 µg/mL gentamycin (Pfizer) and 0.05 mM calcium chloride ($CaCl_2$) (Invitrogen). The resuspended MEKs were seeded in a 25 cm^2 tissue culture flask (Corning Life Sciences, Mount Martha, Australia). MEKs were maintained in culture for four to seven days at 37°C, 5% carbon dioxide (CO_2) until the keratinocyes approached 70% confluence and ready to be serially passed.

2.2.2 Serial cultivation of mouse epidermal keratinocytes

When MEKs were ready to passage, media was aspirated and cells were washed twice with PBS. 1mL of 0.25% trypsin (Sigma Aldrich, Castle Hill, Australia) supplemented with 1 mM EDTA was added to the flask and incubated at 37°C for five minutes in a 5% CO_2 incubator. Following microscopic observation, when cells had detached from the flask, an equivalent volume of 10% v/v FBS (Bovogen Biologicals) in PBS was added to the flask to halt trypsinisation. The cells and trypsin solution were transferred into a 15 mL Falcon tube (BD Biosciences). The culture vessel was washed with 5 mL of PBS and the PBS wash was added to the Falcon tube containing the cells. The tube was centrifuged at 200 *g* for three minutes. The supernatant was discarded and the cell pellet was resuspended in KC-SFM without calcium (Invitrogen). MEKs were used at different seeding densities described in the relevant materials and method section for the downstream experiments. MEKs were passaged at a maximum of three times.

2.2.3 Induction of differentiation

MEK differentiation was induced *in vitro* by increasing the concentration of calcium from 0.05 mM to 1.2 mM in the KC-SFM media. MEKs were cultured with KC-SFK media without calcium supplemented with 1.2 mM calcium for the duration of 48 hours. Calcium treated MEKs were visualised in a tissue culture vessel on an Olympus CKX41 inverted microscope (Olympus), using the Nikon DS-Fi1 camera. Differentiation was also induced by growth of cells to confluence.

2.2.4 Human epidermal keratinocytes isolation

Human epidermal keratinocytes (HEK) were isolated from neonatal foreskins, obtained from Dr Terry Russell (Russell Medical Clinic, Mount Gravatt), in accordance with Institutional Ethics Approval. All procedures were carried out under aseptic techniques in a laminar flow hood. The foreskin was washed twice with 70% ethanol and PBS before removing the excess subcutaneous fat layer. The foreskin was cut into small segments and incubated overnight at 4°C in Dispase II solution as per *Section 2.2.1 mouse epidermal keratinocyte isolation*.

Next day, the epidermis (white) was separated from the dermis (jelly) and washed twice in PBS. The epidermal sheet was placed into a 15 mL Falcon tube (BD Biosciences) containing 1 mL of 0.25% w/v trypsin with 1mM ethylene diamine tetra acetic acid (EDTA) (Invitrogen) and pipetted vigorously for 3 minutes. 1 mL of 10% v/v FBS (Bovogen Biologicals) in PBS and 5 mL of PBS were added and mixed gently by gentle inversion. Most of the skin chunks

were removed, and the tube was spun at 200 *g* for 3 minutes and supernatant discarded. The pellet was resuspended in 5 mL of keratinocyte serum-free media (KC-SFM) (Invitrogen) supplemented with 5 µg/mL epidermal growth factor (EGF) (Invitrogen), 50 µg bovine pituitary extract per mL (BPE) (Invitrogen), 0.1% v/v penicillin/streptomycin (Invitrogen) and 1 µg/mL gentamycin (Pfizer). The resuspended HEKs was seeded in a 25 cm^2 tissue culture flask (Corning Life Sciences) and maintained in culture for five to seven days at 37°C, 5% carbon dioxide (CO_2) until the keratinocyes approached 70% confluence and ready to be serially passed.

2.2.5 Serial cultivation of human epidermal keratinocytes

Culturing of human epidermal keratinocytes was carried out as per *Section 2.2.2 serial cultivation of mouse epidermal keratinocytes*. The cell pellet was resuspended in KC-SFM media. HEKs were used at different seeding densities described in the relevant materials and method section for the downstream experiments. HEKs were passaged at a maximum of four times.

2.2.6 Serial cultivation of squamous cell carcinoma (SCC) cell lines

Several different SCC cell lines were described in the thesis. SCC25 and Detroit562 cell lines were obtained from ATCC (ATCC, Cryosite, South Granville, Australia). SCC9, SCC15, Cal27, Colo16 and FaDu cell lines were a kind gift from the laboratory of Dr Elizabeth Musgrove (Garvan Institute, Sydney, Australia). Short tandem repeats (STR) Genotyping was carried out on SCC9, SCC15, Cal27, Colo16 and FaDu cell lines to confirm the genetic make-up of these cells. All cells lines were maintained in mycoplasma free conditions and routinely tested fro mycoplasma contamination. SCC cells were maintained in SCC media (Appendix I) and incubated at 37°C, 5% CO_2. Cells were passaged by dissociation as for serial cultivation of human epidermal keratinocytes (*Section 2.2.5*).

2.2.7 Generation of stable cell lines

In order to generate stable shRNA-expressing SCC cell line (SCC25), SCC cells were transfected using Lipofectamine 2000 Transfection Reagent (Invitrogen) as per *Section 2.5.2 SCC cell line transfection*. Cells were incubated overnight at 37°C/5% CO_2 post transfection and the following day cells were trypsinised as per *Section 2.2.6 Serial cultivation of squamous cell carcinoma* cells and plated at a 1:10 dilution into fresh SCC media. Cells were allowed to grow overnight and then selection was commenced using 200 µg/mL geneticin

selective antibiotic (G418 sulfate) (Gibco), an analog of neomycin sulphate, since shRNA plasmids encodes neomycin selection. SCC media supplemented with neomycin were replaced every two to three days. Cells were continued to grow under selection for 21 days.

2.2.8 Cryopreservation of cells

HEKs, MEKs and SCC cell lines were stored in freeze-down media containing specific growth media supplemented with 20% FBS (Bovogen Biologicals) and 10% v/v DMSO (Sigma Aldrich) in a 1 mL Cryo Vial (Greiner BioOne). A cooling rate of 1°C/minute was achieved by using a 5100 Cryo 1° Freezing Container (Nalgene) for minimum of four hours. Following this, the cells were transferred to liquid nitrogen for long term storage. To bring and repassage cells, the vial was quickly thawed at 37°C and transferred into warmed specific media. Following centrifugation (200 *g* for two minutes), the cell pellet was resuspended in media and transferred to a tissue culture vessel.

2.3 Adenovirus protocols

2.3.1 Pre-packaged adenoviruses

The following pre-packaged, replication-deficient (E1 and E3 region deleted), human serotype 5 adenovirus (Ad) supernatants were obtained from Vector Biolabs (Vector Biolabs, Philadelphia, PA, USA): Ad-Cre-GFP which expresses both Cre recombinase and green fluorescent protein (GFP) as marker which are driven by two separate promoters, Ad-GFP which expresses enhanced GFP (eGFP) transgene under the control of a CMV promoter and Ad-CMV-Null which does not contain any transgene and only carries an empty CMV promoter. Viral supernatants were supplied at a titer of $1x10^{10}$ PFU/mL in a storage buffer Dulbecco's Modified Eagle Medium (DMEM) with 2% bovine serum albumin (BSA), 2.5% Glycerol, and upon receipt the supernatants were aliquoted and stored at -80°C.

2.3.2 Adenovirus infection of mouse epidermal keratinocytes

To infect the isolated MEKs with adenoviruses, 5000 cells/cm^2 cells were plated in tissue culture vessels and grown overnight to be about 50% confluent the next day. The following day, the virus supernatant was thawed on ice and a specific multiplicity of Infection (MOI) of virus was prepared. MOI refers to the number of virions that are added per cell during infection. To figure out the amount of virus needed to add for a certain MOI, the following formulas were used:

number of cells X desired MOI = total PFU (Plaque Forming Units)

(total PFU needed) / (PFU/mL) = total mL of virus needed to reach desired dose

Fluorescent images of Ad-GFP infected keratinocytes were visualised on a Widefield Fluorescence microscope, using the Zen Software (Carl Zeiss, North Ryde, Australia). The required number of virus supernatant was freshly prepared in 150 µL/cm^2 using the same media that the cells are grown in at a various MOI of virus. The media was aspirated and the infection media containing virus particles was added to cells. Specific MOI of virus is described in the relevant result section, and ranged from MOI of 10 to MOI of 2500. After around 16 hours of incubation with virus supernatant at 37ºC/5% CO_2, the media was replaced with fresh media. Cells were then cultured and harvested after 2 days for analysis and/or further treatments.

2.4 General tissue culture methods

2.4.1 *In vitro* UVB exposure

Cells were seeded into a 96-well plate in triplicate at a density of 5000 cells per well and allowed to adhere overnight. The following day, media was removed from each well and cells were washed once with warmed PBS. Excess PBS was aspirated and 40 µL of warmed PBS was added to each well. Cells were exposed to varying doses of UVB radiation (home-made irradiator) at various J/cm^2 delivered as a single exposure while the plate lid removed for the indicated doses. UV panel is equipped with two Phillips UVB bulbs (Fisher Biotec, Wembley, Australia), which are TL 20W/01RS UV-B Medical bulbs and have the only output in the UVB range (280-320 nm). Immediately after UVB exposure, PBS was aspirated and 100µL warmed growth media was added to each well. Cells were then cultured further 24 hours before determining the cell viability.

2.4.2 *In vitro* drug treatments

Cells were seeded into a 96-well plate in triplicate at a density of 5000 cells per well and allowed to adhere overnight. The following day, cells were treated with doxorubicin (Sigma Aldrich), epirubicin (Sigma Aldrich), etoposide (Sigma Aldrich), cisplatin (InterPharma, Australia), ZVAD-fmk (Alexis Biochemicals, Sapphire Bioscience, Waterloo, Australia), Sphingosine kinase 1 inhibitor (SK1-I) (BML-EI411) (Enzo Life Sciences, Sapphire

Bioscience), Sphingosine-1-phosphate (S1P) (Cayman Chemicals, Sapphire Bioscience) and BGT226 (Novartis, Basel, Switzerland) at various concentrations delivered as a continuous exposure. SK1-I was solubilised in sterile water for *in vitro* and *in vivo* experiments. S1P was dissolved in 0.3 M NaOH for *in vitro* experiments. Stocks of BGT226 were prepared in N-methyl-2-pyrrolidone (NMP) (Fluka Analytical, Sigma Aldrich, Castle Hill, Australia). All drugs were diluted in growth media to the indicated doses, and cells were subjected to drug/inhibitors for the duration of two days before determining the cell viability. In co-treatment assay, ZVAD-fmk was added 30 minutes before other treatment.

2.4.3 Colony forming efficiency assay

For colony forming efficiency (CFE) assay cells were dissociated by trypsinisation and counted using a haemocytometer (Bright-line). Known number of cells, typically, ranging from 100 to 30 000 per well were seeded into a 6-well tissue culture plates and allowed to grow for 10 to 15 days or until colonies formed. Then, media was removed and cells were fixed and stained with 0.1% w/v Coomassie Blue (MP Biomedicals, Seven Hills, Australia), 40% methanol, 10% acetic acid solution. Plates were incubated at room temperature for 30 to 60 minutes. Cells were then destained with a 40% methanol and 10% acetic acid solution and rinsed with water and air-dried. Colonies were counted and CFE was expressed as the total number of colonies / total number of cells plated x 100.

2.4.4 DNA synthesis

A colorimetric enzyme linked immunosorbet assay (ELISA) (Roche Diagnostics) was used to determine the DNA synthesis by measuring incorporation of the thymidine analogue 5-bromo-2-deoxyuridine (BrdU) in accordance with the manufacturers' instructions. All reagents in this section are provided with the ELISA Kit unless otherwise indicated. The assay was performed with a density of 5000 cells per well in a 96-well plate in triplicate following cells to adhere overnight. The colorimetric reaction was stopped by adding 25 µL of a 1 M sulphuric acid solution to each well. The absorbance was read first at 490 nm as a reference reading and then at 405 nm on a Multiskan FC Microplate Photometer (Thermo Scientific) after 30 seconds of mixing. BrdU incorporation was calculated by subtracting the reference value from the absorbance value. The background absorbance (no BrdU) and a media only control absorbance were also determined, and the background absorbance was subtracted from each absorbance value.

2.4.5 Cell viability

2.4.5.1 Proliferation assay

The effect of infection with virus, UVB exposure and drugs or specific inhibitor treatments on cell viability was determined using the Cell Titer 96 Aquous One Solution Cell Proliferation assay (Promega, Alexandria, Australia) in accordance with the manufacturers' instructions. The assay was performed with a density of 5000 cells per well in a 96-well plate in triplicate in a final volume of 100 µL. When cell viability was to be determined, cells were incubated with 20 µL of the reagent in the dark at 37°C/5% CO_2 for 2 hours prior to absorbance reading at 490 nm using the MultiSkan FC Microplate Photometer (Thermo Scientific). The background absorbance was determined from a media only control and subtracted from each absorbance value.

2.4.5.2 Trypan blue exclusion

Cell viability was determined using Trypan Blue Solution, 0.4% (Gibco) and expressed as number of viable cell counts relative to initial plating counts or normalised to untreated cells. Cells were seeded and allowed to adhere overnight. The following day, cells were subjected to specific treatments. When cell viability was to be determined, 100 µL of 0.4% Trypan Blue solution was added to 1 mL of cell suspension. Cells were counted using a haemocytometer, and the number of blue stained and the number of total cells was determined. The number of viable cells per mL was expressed as the number of viable cells x 10^4 x 1.1.

2.4.6 Sphingosine kinase activity assay

Sphingosine kinase (Sphk1) activity was measured using an absorbance assay (Echelon Biosciences, Sapphire Bioscience, Waterloo, Australia) in accordance with the manufacturer's instructions. All reagents in this section are provided with the Sphingosine Kinase Activity Assay Kit unless otherwise indicated. Total protein was extracted from cultured cells in which sphingosine activity was to be determined by lysis in radio immunoprecipitation assay buffer (RIPA buffer) (Appendix I). The sample reaction was consisted of 10 µL of sphingosine, 20 µL ATP and 10 µL of samples. ATP standards were consisted of 5 µL sample buffer, 5 µL complete reaction buffer, 10 µL sphingosine and 20 µL ATP standard dilution. 2-fold series ATP standards ranging from 0-10 µM were prepared. The assay was performed in a 96-well plate supplied in duplicate, and the reaction was incubated at room temperature for two hours prior to luminescence reading using FLUOstar

OPTIMA microplate reader (BMG LABTECH, Mornington, Australia). Sample buffer was included as a buffer only background control and the background absorbance was subtracted from each absorbance value. Sphk1 concentration was estimated using Graph Pad Prism v6 (Graph Pad Software, LA Jolla, USA). The linear regression function in Graph Pad Prism was used to generate a standard curve from the absorbance reading obtained from the standards. The standard curve was used to extrapolate relative sample values.

2.4.7 Sphingosine-1-phosphate assay

Quantification of sphingosine-1-phosphate was conducted using a Sphingosine-1-Phosphate (S1P) ELISA Kit (Echelon Biosciences, Sapphire Bioscience, Waterloo, Australia) in cell culture lysate in accordance with the manufacturer's instructions. All reagents in this section are provided with the Sphingosine-1-Phosphate Assay Kit unless otherwise indicated. Cell culture lysate was prepared as per manufacturers' instructions. Briefly, cells in which S1P levels to be determined were lysed in RIPA buffer. Protein concentration was measured using the Bradford protein assay as per *Section 2.7.2 Protein Quantification*. Cell lysate was diluted in 1:10 in delipidised human sera and analysed. The assay was performed in a 96-well microtiter plate supplied in duplicate and absorbance at 450 nm was then calculated using the MultiSkan FC Microplate Photometer (Thermo Scientific). Diluted streptavidin HRP solution only was included as the blank control and the absorbance was subtracted from each absorbance value. S1P concentration was estimated using Graph Pad Prism v6 (Graph Pad Software, LA Jolla, USA). A best fit curve for the standards was generated using non-linear regression analysis with Graph Pad Prism Software. The standard curve was used to extrapolate relative sample values, using the absorbance reading obtained. A dilution factor of 10 was included in the calculated protein concentration of S1P.

2.4.8 RhoA/Rac1/Cdc42 Activation Assays

Rho family activation was monitored using a RhoA/Rac1/Cdc42 Activation Assay Combo Biochem Kit (Cytoskeleton, Jomar Bioscience, Kensington, Australia) in whole cell lysate in accordance with the manufacturer's instructions. All reagents in this section are provided with the RhoA/Rac1/Cdc42 Activation Assay Combo Biochem Kit unless otherwise indicated. Cells were not serum-starved or treated with Rho family activators prior to the assay. 300 µg total cell protein was added to a 50 µg of rhotekin-RBD (RhoA activation) or 10 µg of PAK-PBD (Rac1 and Cdc42 activation) per assay and analysed by sodium dodecyl sulphate polyacrylamide gel electrophoresis (SDS-PAGE) through a 12% SDS-PAGE gel.

Samples of 25 µg of total cell lysate per sample were also separated with SDS-PAGE through a 12% SDS-PAGE gel to detect total RhoA and Rac1. The amount of activated and total RhoA and Rac1 were determined by an immunoblot analysis as per *Section 2.7.4 Immunoblot analysis* using a RhoA and Rac1 specific antibodies. The RhoA and Rac1 antibodies were incubated with the PVDF membrane at 4°C overnight.

2.5 Transfection

2.5.1 Mouse primary keratinocytes

Primary keratinocytes were transfected using Mirus Keratinocyte Transfection Reagent (Mirus, Geneworks, Adelaide, Australia) according to the manufacturers' guidelines. Briefly, 2.5 x 10^4/cm^2 cells were plated in a 6-well plate and grown overnight. The following day, cells were washed twice with PBS and the media was replaced with minimal KC-SFM medium (Invitrogen) containing no antibiotics, EGF or BPE. A 2.5 µg aliquot of plasmid DNA was diluted in 100 µL of Optimem Serum-Free Medium (Invitrogen). Then, 7.5 µL of Mirus Keratinocyte Transfection Reagent was added to the diluted plasmid DNA and the plasmid/tranfection reagent complex was incubated at room temperature for 15 minutes. Post incubation, the complex was added to the cells by dropwise fashion and gently rocking. The cells were washed twice with PBS following five to six hours transfection and the media was replaced with KC-SFM. Cells expressing the plasmid DNA were then analysed for expression 48 hours post transfection.

2.5.2 SCC cell line

SCC cell lines were transfected with expression plasmids and expression plasmids coding for four different shRNAs directed against Sphk1 and RacGAP1. Myc-DDK-tagged ORF clone of Sphk1 and Myc-DDK-tagged ORF clone of RacGAP1 plasmids were purchased from OriGene Technologies (Australian Biosearch, Karrinyup, Australia). The DDK epitope is also known as Flag tag epitope. Sphk1 and RacGAP1 shRNAs as well as control shRNA which does not contain any transgene were purchased from SuperArray Bioscience (SA Biosciences, Qiagen, Chadstone Centre, Australia). SCC cells were transfected using Lipofectamine 2000 Transfection Reagent (Invitrogen) according to the manufacturers' guidelines. Briefly, 2 x 10^4/cm^2 cells were plated in a 6-well plate and grown overnight. The following day, cells were washed twice with PBS and the media was replaced with Optimem Serum-Free Medium (Invitrogen). An aliquot of 1.3 µg aliquot of plasmid DNA was diluted

in 250 µL of Optimem media (Invitrogen). 3.9 µL of Lipofectamine 2000 (Invitrogen) was diluted in 250 µL of Optimem media and incubated for five minutes. The diluted plasmid DNA and the diluted tranfection reagent complex were combined and incubated at room temperature for 20 minutes. Post incubation, the siRNA/Lipofectamine 2000 complex was added to the cells by dropwise fashion and gentle rocking. The cells were washed twice with PBS following five to six hours transfection and the media was replaced with SCC media. Cells expressing the plasmid DNA were then analysed for expression 48 hours post transfection.

SCC cell lines were also transfected with siRNAs which the sequences are described in *Table 2.1*. E2F7 siRNA and control siRNA directed against GFP and show no homology to other known genes were purchased from Sigma Aldrich. The E2F7 siRNA sequence was previously published (Panagiotis Zalmas, Zhao et al. 2008). Single stranded siRNAs were re-constituted into solution using UltraPure DEPC-treated water (Ambion, Life Technologies) to a concentration of 100 µM upon receipt. An equal volume of sense and antisense strands were added to a 1.5 mL tube (Eppendorf) and heated at 99°C in a heating block (Eppendorf) for 10 minutes. Duplexed siRNAs were then left to cool down to room temperature for 30 minutes. For siRNA transfection, SCC cells were transfected using Lipofectamine 2000 Transfection Reagent (Invitrogen) according to the manufacturers' guidelines. Briefly, 2 x $10^4/cm^2$ cells were plated in a 6-well plate and grown overnight. The following day, cells were washed twice with PBS and the media was replaced with Optimem Serum-Free Medium (Invitrogen). siRNAs (pmol) were diluted in 100 µL Optimem media (Invitrogen) to obtain a final concentration of 40 nM in the tissue culture vessel. 5 µL of Lipofectamine 2000 (Invitrogen) was diluted in 250 µL of Optimem and incubated for five minutes. The diluted siRNA and the diluted tranfection reagent complex were combined and incubated at room temperature for 20 minutes. Post incubation, the siRNA/Lipofectamine 2000 complex was added to the cells by dropwise fashion and gentle rocking. The cells were washed twice with PBS following five to six hours transfection and the media was replaced with SCC media. Cells were then analysed for gene knockdown 48 hours post transfection.

Table 2.1 Sequences of siRNAs used in this study. siGFP was used as a non-specific siRNA control. Reference indicates the source of siRNa sequences were not designed by the author.

Gene	Sense 5'-3'	Antisense 5'-3'	Reference
E2F7 siRNA_1	AAAGGUACGACGCCUCUAUGA	UCAUAGAGGCGUCGUACCUUU	(Panagiotis Zalmas, Zhao et al. 2008)
E2F7 siRNA_2	AACAGAAGAGCGAGGUCGUAA	UUACGACCUCGCUCUUCUGUU	(Panagiotis Zalmas, Zhao et al. 2008)
siGFP	GCACGACUUCUUCAAGUCCUU	AAGGACUUGAAGAAGUCGUGC	

2.6 Expression analysis

2.6.1 RNA isolation

Total RNA was isolated from cultured cells, using TRIzol Reagent (Invitrogen). Cells grown in tissue culture vessel were detached using 0.25% trypsin+EDTA as per *Section 2.2.5* and *Section 2.2.6 Serial cultivation of HEKs and SCC cell lines* and pelleted by centrifugation. The cell pellet was then resuspended in 1 mL TRIzol reagent (Invitrogen) by pipetting up and down several times. Where cells were cultured in a 6-well plate for some experiments, TRIzol reagent was directly added to the cells after removing the media and washing the cells twice with PBS. Cells were then harvested by scraping and collected. Up to 3 x 10^6 cells were lysed in 1 mL TRIzol. The TRIzol/cell mixture was lysed for 5 minutes at room temperature. 200 µL chloroform was added and samples were mixed vigorously by hand followed by three minutes incubation at room temperature and centrifugation at 12 000 *g* at 4°C for 15 minutes. The aqueous layer containing the RNA was then removed and transferred to a fresh tube, and an equal volume of isopropanol (500 µL) was added to and mixed well, followed by a 10 minutes incubation at room temperature. The samples were then centrifuged at 12 000 *g* for 10 minutes. The RNA pellet was washed with 1 mL of 75% ethanol, followed by centrifugation at 7500 *g* for 5 minutes. The pellet was allowed to air dry completely at room temperature for approximately 10 minutes. The pellet was then resuspended in UltraPure DEPC-treated water (Ambion, Life Technologies) and the concentration was assessed using a NanoDrop 1000 spectrophotometer (Thermo Scientific). The RNA was stored at -80°C for future use.

2.6.2 cDNA synthesis

For complementary single stranded DNA (cDNA) synthesis, 2 µg total RNA was incubated with 0.5 µg oligo DT_{12-18} primer (Invitrogen) in a total volume of 12 µL at 70° for 5 minutes. The sample was then cooled down on ice. 4 µL of 10 mM dNTP mix (Finnzymes,

Genesearch, Arundel, Australia), 1X reaction buffer (Bioline), 0.25 µL (50units) of BioScript Reverse Transcriptase (BioLine) and 2.75 µL fo H_2O were added to the sample and the reaction was incubated at 42°C for 1 hour. It was followed by an incubation step at 70°C for 10 minutes to stop the reaction. The cDNA was stored at -20°C for future use.

2.6.3 Quantitative real time (qRT) PCR analysis

Quantification of PCR products was evaluated in duplicate using a Rotorgene 6000 Thermal Cycler (Corbett Life Sciences, Qiagen, Doncaster, Australia). The relative quantification of the gene of interest was determined using the standard curve method. Serial dilutions of a control cDNA to generate the standard curve were prepared in UltraPure DEPC-treated water (Ambion, Life Technologies). The dilutions were 1/10, 1/100, 1/1000, 1/10000, 1/100000 and undiluted control cDNA was included in the standard curve. A 20 µL reaction containing 10 µL of Sensifast SYBR Mix (BioLine), 200 nM each of forward and reverse primers and 2 µL of a 1:10 dilution of cDNA or standard curve dilutions was subjected to PCR cycling for each gene to be analysed. Primers were designed to span exon-exon boundaries and to produce an amplicon with length between 75 and 150 nucleotides. Primers were ordered from Geneworks (Geneworks, Adelaide, Australia) or Integrated DNA Technologies (IDT, Skokie, USA). The SYBR Rotorgene profile was 95°C for 2 minutes, 40 cycles of 95°C for 5 seconds, 60°C for 10 seconds and 72°C for 10 seconds, followed by a melt curve analysis where the total RNA product was subjected to temperature ranging from 62°C to 95°C. Data was analysed using Rotorgene Software Version 1.7 (Corbett Life Sciences). TATA box binding protein (TBP) for human and β-actin for murine samples were used as the housekeeping gene for the normalization of results to determine relative quantitation of the gene of interest. *Table 2.2* details the sequence of primers used for qRT PCR.

Table 2.2 Sequence of primers used for genotyping, quantitative real time and chromatin immunoprecipitation PCR analysis.

Gene	Forward Primer	Reverse Primer
Genotyping		
E2f1 (Mix A)	TCCAAGAATCATATCCAGTGGCT	GCTGGAATGGTGTCAGCACAGCG
E2f1 (Mix B)	CTACCCGGTAGAATTGACCTGCA	GCTGGAATGGTGTCAGCACAGCG
E2f7	AGGCAGCACACTTGACACG	ACTTTTGGGACAGAGGTAGGA
		CCAAGATGAAGGCCGAGATGCTAC
E2f8	TAAAAAGCTTTGCGGTCGTT	AAGCCAACCTCGATGAATTG
		CTCGCATCATCGTCTGCTAA
Quantitative RT-PCR		
Actin	GCTACAGCTTCACCACCACA	TCTCCAGGGAGGAAGAGGAT
CD44	AGCAACTGAGACAGCAACCA	AGACGTACCAGCCATTTGTGT
E2f1	GCCCTTGACTATCACTTTGGTCTC	CCTTCCCATTTTGGTCTGCTC
E2f7	GCCAAGCAGGAAACAGAAGA	ACCGTGCCAACCATACTGAT
E2f8	GAGAAATCCCAGCCGAGTC	CATAAATCCGCCGACGTT
E2F1	TGCAGAGCAGATGGTTATGG	CTCAGGGCACAGGAAAACAT
E2F7	GTCAGCCCTCACTAAACCTAAG	TGCGTTGGATGCTCTTGG
E2F8	GTGGATTACCTGAGGCCAAA	CTTCGTCAAGGCAGATGTCA
RACGAP1	GACGTTGAATAGGATGAGTCATGG	GCTCAAACAGATTCCGCACA
RRP8	TACTGAAGCCAGGGGGTCTC	AATGGCTGTTGGTCAGGTCC
SPHK1	AAGACCTCCTGACCAACTGC	GGCTGAGCACAGAGAAGAGG
TBP	TCAAACCCAGAATTGTTCTCCTTAT	CCTGAATCCCTTTAGAATAGGGTAGA
Quantitative ChIP-PCR		
E2F1-promoter	AGGAACCGCCGCCGTTGTTCCCGT	GTTGACAGAAGAGAAAAGC
RACGAP1-promoter	GAAGTGAGTAGTGGGGGTGC	TCCATCTTTCACACGAACACTCT
SPHK1-promoter	GGGACCCTTGGTTTCACCTC	GAATTTCGGGTGGGCTAGGG

2.6.4 Immunohistochemistry

Tissue samples were fixed in 4% formaldehyde (Histopot, Australian Biostain) for 24 hours and then transferred in 100% ethanol for storage. The fixed tissue was embedded in paraffin and sectioned to 5 µm thickness and mounted on Super Frost Plus slides (Menzel-Glaser, HD Scientific Supplies, Willawong, Australia) by Ms Crystal Chang (University of Queensland Diamantina Institute Histology Facility). Tissue sections were first incubated at 60ºC for one hour followed by dewaxing the sections with 100% xylene (Point of Care Diagnostics, Artarmon, Australia) 10 minutes. The sections were then rehydrated in 100% ethanol, 95% ethanol, 75% ethanol, distilled water for 10 minutes each wash. The antigen retrieval was carried out by heat activation method with 10 mM sodium citrate solution (pH 6.0) supplemented with 0.05% v/v Tween 20. For antigen retrieval, sections were microwaved in sodium citrate solution for 5 minutes and then left to cool down. This was repeated and then sections were cooled down under the running tap water for approximately 6 minutes. The sections were washed twice with PBS for 2 minutes, permeabilised of the sections with 0.01% v/v Triton X-100 diluted in PBS for 10 minutes and washed twice with PBS for 5 minutes.

Around the tissue was drawn by a hydrophobic pen (DAKO, Botany, Australia). The tissue was then blocked with 10% BSA in PBS (blocking buffer) for one hour, followed by overnight incubation with the primary antibody diluted in blocking buffer in a humidified chamber at 4ºC. The list of primary antibodies used for immunohistochemistry is summarised in *Table 2.3*. The tissue was also incubated overnight at 4ºC with rabbit IgG serving as a negative control, after diluting rabbit IgG at the same concentration as the primary antibody. The following day, the primary antibody was removed and the sections were washed twice with PBS for 5 minutes. The sections were incubated with 0.3% v/v solution of hydrogen peroxide (Sigma Aldrich) in PBS for 10 minutes to block endogenous peroxidase, followed by washes twice with PBS for 5 minutes. A commercially available secondary antibody Kit, Starr Trek Universal Horseradish Peroxidase (HRP) Detection System (Biocare Medical, Applied medical, Stafford, Australia) secondary antibody Kit or directly conjugated secondary antibody was used on order to develop the immunohistochemistry staining. Where the Starr Trek system was used, the universal linker antibody was applied to the section for 20 minutes at room temperature in a humidified chamber. The section was then washed twice with PBS and a streptavidin-HRP solution was applied to the section and incubated for 15 minutes at room temperature in a humidified chamber. The section was then washed twice

with PBS. Where a directly conjugated secondary antibody was used, the section was incubated with the F(ab')2 fragment of goat anti-rabbit IgG (H+L) HRP conjugate antibody (Invitrogen) for one hour at room temperature in a humidified chamber after diluting it at a half concentration of the primary antibody used. Cardassian DAB Chromogen (3,3' diaminobenzidine) (Biocare Medical) was then diluted according to the manufacturer's instructions and applied to the tissue section until a brown colour had developed. The slides were washed thoroughly in distilled water, followed by a 25 second incubation in filtered acid haematoxylin (Sigma Aldrich). The slides were washed thoroughly in tap water. The slide was then dehydrated through distilled water, 75%, 95%, 100% alcohol and 100% xylene for 2 minutes each. A 22 mm coverslip (ProSciTech) was mounted on the tissue section using DPX Neutral Mounting Medium (Ajax Fine Chemicals, Thermo Scientific, Scoresby, Australia). The section was left to dry at room temperature, visualized and imaged on a Nikon Eclipse 50i light microscope, using the NIS-Elements BR software (version 3.2) (Nikon).

2.6.5 Immunofluorescence: paraffin embedded sections

Paraffin embedded tissue sections were de-waxed as per *Section 2.6.4 Immunohistochemistry*. The sections were de-waxed by two washes with 100% xylene 10 minutes each. The sections were then rehydrated in two washes of 100% ethanol for 5 minutes, 90% ethanol for 1 minute, 80% ethanol for 1 minute, 70% ethanol for 1 minute, 50% ethanol for 1 minute, 30% ethanol for 1 minute and distilled water for 5 minutes. The antigen retrieval was carried out as per *Section 2.6.4 Immunohistochemistry*, with an exception of a cooling step in PBS for 20 minutes. The sections were washed twice with PBS for 5 minutes and blocked in 1% BSA diluted in PBS and supplemented with 4% horse serum (Gibco) (blocking buffer) for 30 minutes at room temperature in a humidified chamber. Excess solution was then removed and the sections were incubated with the primary antibody diluted in blocking buffer and supplemented with 0.1% Triton X-100 for one hour at room temperature in a humidified chamber. The list of primary antibodies used for immunofluorescence is summarised in *Table 2.3*. The primary antibody was removed and the sections were washed with blocking buffer for 5 minutes, followed by a 5 minutes wash with 1% BSA diluted in PBS. The sections were then incubated with the secondary antibody for one hour at room temperature in a humidified chamber. The secondary antibody used was AlexaFluor conjugated antibody and used at a 1:1000 concentration in blocking buffer. *Table 2.3* details the secondary antibody used for immunofluorescence. The sections were washed four times with blocking buffer. The slides

were dipped briefly in distilled water and a 22 mm coverslip (ProSciTech) was mounted on the tissue section with VectaShield, a hard setting aqueous mounting medium containing the DNA stain 4',6-diamidino-2-phenylindole (DAPI) (Vector Labs, Abacus ALS, East Brisbane, Australia). The slides were left to dry for 30 minutes at 37^0C. Immunofluorescent images were visualised and imaged on the Zeiss 510 Meta Confocal Microscope, using the AxioVision software (Carl Zeiss).

Table 2.3 Antibodies used for immunohistochemistry and immunofluorescence. IgG was used as a negative control at the same concentration as the corresponding primary antibody. α is 'anti'.

Antigen	Species	Antibody	Dilution
Immunohistochemistry			
Anti-Keratin 10	Rabbit	Sigma Aldrich *SAB4501656*	1:200
Anti-Proliferating Cell Nuclear Antigen	Mouse	Sigma Aldrich *P8825*	1:3000
Anti-RACGAP1 [EPR9018]	Rabbit	Abcam *ab134972*	1:100
Anti-RACGAP1 [EPR9018] (TMA)	Rabbit	Abcam *ab134972*	1:100
Anti-Sphk1 (TMA)	Rabbit	Sigma Aldrich *HPA022829*	1:75
Cleaved Caspase-3 (Asp175)	Rabbit	Cell Signaling #9661	1:50
cytokeratin 1	Rabbit	Abcam *ab24643*	1:500
cytokeratin 5	Rabbit	Abcam *ab53121*	1:2000
cytokeratin 14	Rabbit	Abcam *ab53115*	1:50
E2F7 (TMA)	Rabbit	Abcam *ab56022*	1:250
IgG	Rabbit	Cell Signaling #2729	Same as corresponding primary antibody
Involucrin	Rabbit	Abcam *ab28057*	1:100
Phospho-Akt (Ser473) (D9E) XP	Rabbit	Cell Signaling #4060	1:50
Immunofluorescence			
Anti-Keratin 10	Rabbit	Sigma Aldrich *SAB4501656*	1:200
cytokeratin 5	Rabbit	Abcam *ab53121*	1:200
IgG	Rabbit	Cell Signaling #2729	Same as corresponding primary antibody
Involucrin	Rabbit	Abcam *ab28057*	1:100
α Rabbit AlexaFluor 488	Goat	Molecular Probes #A11011	1:1000

2.7 Protein methods

2.7.1 Protein extraction

Total protein was extracted from cultured cells by lysis using RIPA buffer or 1x sample buffer supplemented with 1% v/v protease inhibitor cocktail (Sigma Aldrich). Cells grown to the desired confluency were washed twice with ice cold PBS and the PBS was aspirated completely. RIPA buffer or 1x sample buffer was then added to the culture vessel and cells/lysis buffer mix was collected by scraping all the cells from the surface of the culture vessel using a cell scraper (Grenier Bio One). Where protein extracted in RIPA buffer, the sample/lysis buffer mix was incubated on a rotating wheel at 4°C for 15 minutes, followed by a centrifugation at 15 000 *g* for 5 minutes. Post centrifugation, the supernatant representing total proteins was transferred into a new tube. Where protein extracted in 1x sample buffer, the sample/lysis buffer mix was sonicated for 4 seconds at amplitude of 50 with a 3 mm sonicator probe using a Sonic Materials Vibra Cell sonicator (Sonics and Materials). The total protein was stored at -80°C if not used immediately.

2.7.2 Protein quantification

Protein extracted using 1x sample buffer did not undergo protein estimation, rather protein extracted in RIPA buffer was subjected to protein estimation. The protein concentration estimation was carried out using the Bradford protein assay solution (BioRad, Gladesville, Australia). The standard curve was used to extrapolate relative sample values and was generated using serial dilutions of bovine serum albumin (BSA) (Sigma Aldrich). Briefly, to make the standard, BSA stock at a concentration of 10 µg/µL was diluted to 0.1 µg/µL in distilled water. A volume of diluted BSA and 5 µL of RIPA buffer were added to a final volume of 800 µL in distilled water. The concentrations of diluted BSA used for the standard curve were, 0 µg/mL (no protein control), 1 µg/mL, 2 µg/mL, 3 µg/mL, 5 µg/mL, 7 µg/mL, 10 µg/mL, 15 µg/mL. 200 µL of Bradford protein assay solution was then added to each protein standard and mixed by inversion. For the samples for which protein concentration was to be estimated, 5 µL of each sample was diluted in 795 µL of distilled water. 200 µL of Bradford protein assay solution was then added to each protein standard and mixed by inversion. 200 µL of prepared protein standard or protein sample was transferred into a 96-well plate (Corning) in triplicate. The protein reading was then taken at 595 nm using the MultiSkan FC Microplate Photometer (Thermo Scientific).

The protein concentration was estimated using Graph Pad Prism v6 (Graph Pad Software, LA Jolla, USA). The linear regression function in Graph Pad Prism was used to generate a standard curve from the absorbance reading obtained from the standards. The standard curve was used to extrapolate relative sample values. A dilution factor of 200 was applied to the calculated protein concentrations to obtain the concentration of the protein sample in µg/µL.

2.7.3 Polyacrylamide gel electrophoresis

Protein expression was examined by immunoblot of cell lysates. 20 µg of protein was mixed with 4x sample buffer (Appendix I), boiled at 99°C for 5 minutes and centrifuged briefly. Protein was separated with SDS-PAGE using the Protean 3 Mini Gel Apparatus (BioRad) through a 10-12% SDS-PAGE gel (Appendix I). Acrylamide SDS-PAGE gels were cast using 1.5 mm thickness mini gel plates (BioRad). The stacking gel was cast using a 15-well 1.5 mm thick spacing comb (BioRad). Once the gels had polymerised, the gels were placed into the BioRad Protean III mini gel apparatus and submerged in electrophoresis running buffer (Appendix I). The protein samples and pre-stained protein marker (New England Biolabs, Genesearch, Arundel, Australia) were loaded into the wells of the gel and electrophoresed at 100 Volts for approximately 2 hours.

2.7.4 Immunoblot analysis

The polyvinylidene fluoride (PVDF) membrane (Immobilon FL, Millipore, Kilsyth, Australia) was equilibrated by washes in 100% methanol for 15 seconds followed by distilled water for 2 minutes and then transfer buffer for 5 minutes. The SDS-PAGE gel was removed and equilibrated in cold transfer buffer containing 20% v/v methanol (Appendix I) for 5 minutes post electrophoresis. The 'sandwich' was then assembled into a transfer cassette with the gel and PVDF membrane. The protein was transferred from the gel to the PVDF membrane using a transfer cassette (BioRad) for 1 hour at 100 Volts in cold transfer buffer with an ice pack. The membrane was then removed and washed in TBS-T buffer (Appendix I) for 2 minutes post transfer. The membrane was blocked with 5% w/v skim milk powder (Diploma, Fonterra Food Services, Mount Waverly, Australia) in TBS-T for one hour at room temperature. The primary antibody was diluted at the appropriate concentration in 5% w/v skim milk powder in TBS-T and incubated with the PVDF membrane at 4°C overnight. The list of primary antibodies used for immunoblotting is summarised in *Table 2.4*. The following day, the PVDF membrane was washed three times with TBS-T for 5 minutes. Following rinsing in TBS-T, the membrane was incubated with a horseradish peroxidise (HRP)

secondary antibody diluted in 5% w/v skim milk powder in TBS-T at room temperature on a rotating platform for 1 hour. The list of secondary antibodies used for immunoblotting is summarised in *Table 2.4*. The PVDF membrane was washed three times with TBS-T for 5 minutes. Following rinsing, the membrane was incubated for 5 minutes with Super Signal West Pico (Pierce, Thermo Scientific) or Super Signal West Femto Chemiluminescent Substrate (Pierce) in accordance with the manufacturer's instructions. An X-Ray film (Kodak Australia) was then applied to the membrane and the film was kept until a detectable signal was observed. The film was visualised with standard X-Ray developing and fixing techniques using Kodak developer and Kodak fixer solutions. The film was then washed in tap water and allowed to dry. Where protein loading was visualised by staining with Coomassie Blue (R-250) (MP Biomedicals), the PVDF membrane was stained in Coomassie Blue solution prepared as per *Section 2.4.3* for 1 minute, followed by complete destain using a 25% acetic acid and 50% methanol solution and washes with TBS-T to rid background. Films or stained PVDF membranes were scanned with an Epson 7000 Photo Perfection scanner (Epson, North Ryde, Australia). Quantitative analysis of protein concentration was performed using Image J (Wayne Rasband, National Institutes of Health, USA) and results represent relative protein levels normalised to β-actin.

Table 2.4 Antibodies used for immunoblotting.

Antigen	Species	Antibody	Dilution
Immunoblotting			
AE1/AE3	Mouse	ICN Biomedical #69145	1:1000
Anti-Cre	Rabbit	Novagen *69050-3*	1:10000
Anti-Mouse HRP	Donkey	Molecular Probes #G21040	
Anti-RACGAP1 [EPR9018]	Rabbit	Abcam *ab134972*	1:2000
Anti-Rabbit HRP	Donkey	GE Healthcare #NA934V	1:500-1:5000
Anti-Sphk1	Rabbit	Sigma Aldrich *HPA022829*	1:1000
Akt	Rabbit	Cell Signaling #9272	1:2000
cdc2	Rabbit	Upstate *06-141*	1:1000
Cleaved Caspase-3 (Asp 175)	Rabbit	Cell Signaling #9661	1:1000
E2F1 (C-20)	Rabbit	Santa Cruz *sc-193*	1:1000
E2F7	Rabbit	Abcam *ab56022*	1:1000
ERK 1 (C-16)	Rabbit	Santa Cruz *sc-93*	1:2000
Involucrin	Rabbit	Abcam *ab28057*	1:1000
PARP	Rabbit	Cell Signaling #9542	1:1000
Phospho-Akt (Ser473) (D9E) XP	Rabbit	Cell Signaling #4060	1:2000
Phospho-p44/42 MAPK (Erk1/2) (Thr202/Tyr204) (E10)	Mouse	Cell Signaling #9106	1:2000
β-actin	Rabbit	Sigma Aldrich *A2228*	1:10000

2.8 Microarray analysis

2.8.1 RNA preparation

RNA which had been isolated using TRIzol reagent (Invitrogen) was further purified using the RNAeasy Kit (Qiagen) in accordance with the manufacturer's instructions. All reagents in this section are provided with the RNAeasy Kit (Qiagen) unless otherwise indicated. 10 µg of total RNA was purified and eluted in 50 µL sterile nuclease free water. RNA concentration was determined using a NanoDrop 1000 spectrophotometer (Thermo Scientific). The RNA was stored at -80°C for future use.

2.8.2 RNA quality control

RNA was analysed for integrity using a 2100 BioAnalyzer (Agilent, Forest Hill, Australia). Briefly, to prepare a BioAnalyzer chip, 1 µL of Agilent RNA 6000 Nano dye was added to a 65 µL aliquot of filtered gel matrix, mixed by vortexing, and the dye/gel matrix mix was loaded to the Agilent RNA 6000 Nano chip. 1.2 µL aliquots of RNA were then denatured at 70°C for 2 minutes in a thermal cycler, along with a 1.5 µL aliquot of RNA ladder (Agilent). Samples were then cooled on ice. RNA Nano chip was then prepared according to manufacturers' instructions. 1 µL of each denatured RNA sample and ladder were then loaded into wells and the chip was read using the Agilent BioAnalyzer, using the 2100 Expert Software Package (Agilent). A RNA Integrity Number (RIN) score which gives information about the quality of the RNA was assigned to each sample by this software. Samples with a RIN score of greater than 8 were considered suitable for microarray analysis. The integrity of cRNA samples (*Section 2.8.3 generation of biotinylated amplified cRNA for microarray hybridisation*) were also assessed *via* BioAnalyzer prior to microarray hybridisation. Visual inspection of BioAnalyzer traces, A260/280 ratios and cRNA concentrations obtained using a NanoDrop spectrophotometer (Thermo Scientific) were used to determine whether the RNA had amplified appropriately rather than a RIN score for cRNA. High quality cRNA samples had A260/280 ratios of 1.9 – 2, and had s size distribution of 250 to 5000 nucleotides with an average size of 1200 nucleotides.

2.8.3 Generation of biotinylated amplified cRNA for microarray hybridisation

RNA samples which had passed quality control by the Agilent BioAnalyzer (RIN score of 8 or greater) were amplified and biotinylated using the Illumina TotalPrep RNA amplification Kit (Illumina, Scoresby, Australia), in accordance with the manufacturer's instructions. All

reagents in this section are provided with the Illumina TotalPrep RNA amplification Kit (Illumina) unless otherwise indicated. The RNA analysed was i) untreated, KJDSV40 cells, ii) doxorubicin-treated KJDSV40 cells, iii) empty vector transfected, untreated KJDSV40 cells, iv) empty vector transfected, doxorubicin-treated KJDSV40 cells, v) E2F7 expression plasmid transfected, untreated KJDSV40 cells, vi) E2F7 expression plasmid transfected, doxorubicin-treated KJDSV40 cells, vii) untreated, SCC25 cells, viii) doxorubicin-treated SCC25 cells, ix) control siRNA transfected, untreated SCC25 cells, x) control siRNA transfected, doxorubicin-treated SCC25 cells, xi) E2F7siRNA transfected, untreated SCC25 cells, xii) E2F7siRNA transfected, doxorubicin-treated SCC25 cells. Three independent biological replicates were used for each condition. RNA of biological replicates was pooled to account for the minor biological variations expected under standard cell culture conditions. A total of 12 samples were run in duplicate. 11 µL of total RNA at 45 ng/µL (a total of 500 ng) was used for each sample. The biotinylated, amplified and purified cRNA was assessed for the integrity using the Agilent 2000 BioAnalyzer and for quantitation using the NanoDrop spectrophotometer (Thermo Scientific).

2.8.4 Microarray hybridisation

The hybridization of biotinylated cRNA to the microarray chip was carried out by Ms Karena Pryce (University of Queensland Diamantina Institute Genomics Facility). Microarrays were performed using Illumina Human HT-12 Expression BeadChip (Illumina). The BeadChip had a capacity for 12 samples; two chips were acquired in this study. Chips were hybridised with cRNA using the Human HT-12 v4 Expression BeadChips Kit (Illumina) in accordance with the manufacturer's instructions. All reagents in this section are provided with the RNAeasy Kit (Qiagen) unless otherwise indicated. The chips were scanned using an Illumina BeadArray Reader (Illumina). BeadStudio 3.2 Software (Illumina) was used for initial data visualization and export.

2.8.5 Microarray analysis

Microarray analysis was performed by Dr Pamela Mukhopadhyay, University of Queensland Diamantina Institute Bioinformatics Department. Raw signal intensity was calculated using Illumina BeadStudio 3.2 Software. Subsequently data was processed with the R programming language with Bioconductor v2.3 (Fred Hutchinson Cancer Centre, Seattle, USA). The analysis required two freely available, open source packages 'lumi' (Du, Kibbe et al. 2008) and 'limma' (Smyth 2005). Probe intensities were variance stabilized and normalized using

robust spline normalization method with the lumi Bioconductor package. Differential expression analysis between each comparison was performed by fitting linear model to normalized intensities and statistical significance was assigned by a Bayesian approach based on the t test using the limma package. Genes were selected using a B statistic cut off (B>0). P values were adjusted for multiple testing using Benjamini and Hochberg's method. Only genes with a fold change of 1 (in either direction) or greater and a B-value of greater than 3 (exceeding the 95% probability of differential expression) were considered to be differentially expressed and further analysed. The B-value is a parameter that describes the natural log of the odds that a gene was truly differentially expressed. Differentially expressed probe sets were analysed as pair-wise contrasts. Microarray data has been uploaded to Gene Expression Omnibus under the reference: GSE58074.

2.9 Chromatin immunoprecipitation experiments

Chromatin Immunoprecipitation (ChIP) was performed using the SimpleChIP Enzymatic Chromatin IP Kit (Magnetic Beads) (Cell Signaling, Genesearch, Arundel, Australia), in accordance with the manufacturer's instructions with some modifications, summarized below. All reagents in this section are provided with the SimpleChIP Enzymatic Chromatin IP Kit (Magnetic Beads) (Cell Signaling) unless otherwise indicated.

Cell harvesting and crosslinking were carried out according to the Farhman Lab protocol, available online at http://farnham.genomecenter.ucdavis.edu/pdf/FarnhamLabChIP%20Protocol.pdf. SCC cell lines were cultured as per *Section 2.2.6 Serial cultivation of squamous cell carcinoma*. The cells were trypsinised, counted using the Countess Automated Cell Counter (Invitrogen, Life Technlogies), and resuspended in a 50 mL Falcon tube at a final concentration of 4×10^6 cells in 50 mL of SCC media. Formaldehyde (Asia Pacific Specialty Chemicals, Seven Hills, Australia) was added to a final concentration of 1% and the cells were incubated on a rocking platform at room temperature for 8 minutes prior to addition of Glycine (Amresco, Astral Scientific, Sydney, Australia) to a final concentration of 0.125M. The cells were incubated with Glycine at room temperature for 5 minutes, centrifuged at 2000 *g* at 4°C for 10 minutes and washed twice with ice cold PBS. The supernatant was removed and the cell pellet was snap frozen in a dry ice and 100% ethanol bath and stored at -80°C until use. 4×10^6 cells per ChIP were used. To break nuclear membrane and lyse nuclei completely, the samples were

subjected to sonication using a Sonic Materials Vibra Cell sonicator (Sonics and Materials, Newton, CT, USA). The cells nuclei were completely lysed after 4 sets of 20 seconds pulses with 30 seconds incubation on wet ice between pulses at amplitude of 50 with a 3 mm sonicator probe. Prior to immunoprecipitation step, the chromatin was subjected to pre-clearing using Protein G magnetic beads (Cell Signaling). A 10 µL aliquot of Protein G magnetic beads was incubated with the cross-linked and lysed chromatin on a rotating wheel at 4°C for 20 minutes. The Protein G magnetic beads were pelleted by placing the tubes in a magnetic separation rack. The supernatant was then carefully removed after waiting for one to two minutes for solution to clear. A sample corresponding to 2% total chromatin sample was served as 'input'. Two micrograms of E2F7 antibody (*Table 2.3*), 5 µL of Histone H3 (D2B12) XP Rabbit antibody (SimpleChIP Enzymatic Chromatin IP Kit) and 2 µL of normal Rabbit IgG (SimpleChIP Enzymatic Chromatin IP Kit) were added to the corresponding diluted chromatin and the samples were incubated on a rotating wheel at 4°C overnight. Immunoprecipitated chromatin was washed, eluted from antibody/Protein G beads and subjected to reversal of cross-links, following the manufacturer's protocol. The ChIP samples were then subjected to DNA purification using spin columns as per the manufacturer's protocol, and the immunoprecipitated DNA was quantitated by real time PCR.

ChIP analysis was performed using real time quantitative PCR. Cycling conditions and preparation of reaction mix including 1X SYBR and 200 nM forward and reverse primers were as per *Section 2.6.3 Quantitative real time PCR analysis*. Quantitative real time PCR primers were designed for two genes which are downstream effectors of E2F7. To determine ChIP enrichment, the comparative threshold cycle (Ct) method was used rather than the standard curve method, as the quantitation was not relative to a housekeeping gene. The Ct value was calculated for each ChIP and input sample using the following formula:

$$2\% \times 2^{(2\%\ Input\ Ct - ChIP\ Ct)}$$

2.10 Tissue Microarray Analysis

Tissue microarrays (TMAs) were constructed by Dr Marcin Dzienis (Princess Alexandra Hospital Medical Oncology Department) and Dr Ana Cristina Vargas (Princess Alexandra Hospital Pathology Department) following pre-designed maps and according to published guidelines (Avninder, Ylaya et al. 2008; Eckel-Passow, Lohse et al. 2010). A Hematoxylin

and Eosin (H&E) slide with representative primary tumour, its matched normal squamous epithelium (when available) and lymph node metastasis were selected for each patient. Depending on the availability of the tissue, 2 to 4 replicates cores were selected to be arrayed. A Manual Tissue Arrayer (MTA-1) (Beecher Instruments, Estigen Tissue Science) and 0.6 mm punches (Beecher Instruments) was used for TMA construction by the Department of Pathology at the Princess Alexandra Hospital. TMA blocks were placed in a 37°C oven for 2 hours followed by 4°C incubation overnight, and 4 µm tissue sections were then cut for immunohistochemistry by the Department of Pathology at the Princess Alexandra Hospital. Immunohistochemistry was conducted using Dako EnVision+System-HRP (DAB) Kit in accordance with the manufacturer's instructions, with an addition of antigen retrieval step as per *Section 2.6.4 Immunohistochemistry*. TMAs were incubated with the primary antibody overnight at 4ºC in a humidified chamber. The list of primary antibodies used for TMA analysis is summarised in *Table 2.3*.

The staining pattern was determined using a modified quickscore method as previously described (Detre, Saclani Jotti et al. 1995) where the tumour and metastatic epithelial cells were evaluated by two blinded pathologists, Dr Samuel Boros and Dr Ana Cristina Vargas, to determine the percentage of cells stained (0-100%) and the intensity of staining (1+ to 3+). The scoring was performed with no knowledge of the position of the replicates within the TMA block. The value of individual cores was obtained by multiplying percentage by intensity and the final sample score was the result of the average of replicate cores. Missing replicates or those showing artefactual staining (i.e. "edge artefact") were excluded and the final score was obtained from the remaining core/s. To determine the intensity of the stain, tumour or metastatic cells were compared with normal non-neoplastic foreskin and squamous epithelium, which showed lack of staining (0+) or only weak staining (1+). Intervening lymphocytes were identified to express the protein and were used as internal positive control.

2.11 Animal studies

2.11.1 Establishment of tumour xenografts

Animal work was performed in accordance with University of Queensland Ethics Guidelines. Six to ten weeks old female non-obese diabetic/severe combined immunodeficient (NOD/SCID) mice (Animal Resources Centre, Perth, Australia) were used in this study. Establishment of tumour xenografts were uniform, regardless of any cell lines used. 2×10^6

cells were resuspended in 50 µL of PBS per injection with a 100 µL dead volume where solution is entrapped in the syringe and injected with a 23 gauge needle subcutaneously into the flanks of anaesthetised mice.

2.11.2 Treatment with Doxorubicin, Sphingosine kinase Inhibitor (SK1-I) and BGT226

Mice were randomly divided into 2 groups (*n* = 6/group). One group of mice were inoculated with SCC25 cells transfected with control vector as control group. The other group was inoculated with SCC25 cells transfected with Sphk1shRNA construct. When tumours were around 3 mm in diameter (about 3 weeks after injection), each group of mice were further randomised into two groups and received either vehicle only (DMSO) or doxorubicin 0.5 mg/kg, respectively, twice per week with intraperitoneal (i.p.) injections. Injection of an equivalent volume of DMSO in PBS served as a vehicle control.

For studies where the effect of SK1-I was tested, mice were implanted with SCC25 cells. When tumours were around 4 to 5 mm in diameter, animals were randomly assigned to 6 groups (*n* = 5/group) and received the following treatments: (i) vehicle only, (ii) doxorubicin 0.5 mg/kg, (iii) SK1-I 5 mg/kg, (iv) SK1-I 10 mg/kg, (v) SK1-I 5 mg/kg + doxorubicin 0.5 mg/kg or (vi) SK1-I 10 mg/kg + doxorubicin 0.5 mg/kg, respectively, twice per week by i.p. injections. Injection of an equivalent volume of DMSO in PBS served as a vehicle control.

The above experiment where the effectiveness of SK1-I in combination with doxorubicin was assessed was repeated using FaDu cells. When tumours were around 2 mm in diameter, animals were randomised and received treatments (*n* = 2/group). Injection of an equivalent volume of DMSO in PBS served as a vehicle control.

In the experiment testing the effect of BGT226 combined with SK1-I, mice were implanted with SCC25 cells. When tumours were around 4 to 5 mm diameter, animals were randomly assigned to 4 groups (*n* = 4/group) and received the following treatments: (i) vehicle only, (ii) doxorubicin 0.5 mg/kg, (iii) BGT226 10 mg/kg or (iv) BGT226 10 mg/kg + doxorubicin 0.5 mg/kg, respectively, twice per week by i.p. injections. Injection of an equivalent volume of DMSO in PBS served as a vehicle control.

2.11.3 Mouse monitoring

Tumour growth and animal weights were monitored regularly for a period of up to 3 weeks. Tumour diameter was measured using callipers. Experiments terminated when the tumours reached a diameter of 10 mm. Animals were euthanized and tumours were excised, imaged, and subjected to pathologic examination after being fixed in a 4% formaldehyde (Histopot) for 24 hours. Tumour volumes were determined with the following formula: $\pi/6$ x (length in millimeters) x (width in millimeters)^2.

2.11.4 Statistical analysis

Graphs were generated using GraphPad Prism (GraphPad software) version 6.0. Graphs depict mean values ± SEM of triplicate determinations from at least three independent experiments. Statistical differences were determined by Student's *t* test with a 95% confidence level. A *P* value greater than 0.05 was deemed not significant. For *in vivo* experiments, animals were randomly assigned into treatment or control groups. The sample size for animal studies was based on previous studies reported in the literature. Control and treatment cohorts had tight tumor growth curves and were adequately powered with experimental recipient cohorts of average size $n = 4$ to 6. *In vivo* experimental data points represent means ± SEM of the measurements of each mouse tumour.

CHAPTER THREE

3 Identification of Isoform-Specific Functions for E2F7 and E2F8

3.1 Introduction

E2Fs are a family of multifunctional context-specific transcription factors (Field, Tsai et al. 1996; Pierce, Schneider-Broussard et al. 1999; Hazar-Rethinam, Endo-Munoz et al. 2011). Work from my laboratory has previously shown that E2F1 and E2F7 may play important roles in KC proliferation, differentiation and apoptotic responses in human keratinocytes (Dicker, Popa et al. 2000; Endo-Munoz, Dahler et al. 2009; Hazar-Rethinam, Cameron et al. 2011; Hazar-Rethinam, Endo-Munoz et al. 2011). However, these studies relied heavily on overexpression analysis and therefore may be subject to errors associated with high levels of overexpression of specific isoforms. Moreover, the potential role of E2F8 in squamous differentiation or squamous neoplasia has not been addressed at this time. In order to interrogate the roles of E2F1, E2F7 and E2F8 in KC proliferation, differentiation, apoptosis and neoplasia, we needed to establish strategies to knockdown E2F1, 7 and 8 expressions in the context of KCs *in vitro*. Moreover, we needed to establish *in vitro* and *in vivo* assays to measure proliferation, differentiation and apoptosis in murine epidermal keratinocytes (MEK). Previous studies from my laboratory have focused on human KCs and epidermis, so we needed to adapt some of these techniques to the murine system. Thus, in this chapter we have validated *in vitro* assays and *in vivo* markers of MEKs and epidermis. In addition, we have generated E2F7, E2F8 and E2F7/8 deficient KCs *in vitro* using a Cre/lox system with which to characterise the roles of E2F1, 7 and 8 on KC proliferation, differentiation and apoptosis. Specifically, we obtained E2F1 conventional KO mice and E2F7 or E2F8 floxed mice, and then generated KCs deficient in E2F7, E2F8 or both E2F7 and 8 following infection with Cre expressing adenovirus viral construct. These KCs were then assayed for their ability to differentiate in response to calcium or to die in response to UVB radiation, doxorubicin, etoposide or cisplatin. We now have strong evidence, from these *in vitro* experiments, that E2F7 plays a unique and non-redundant role in modulating apoptosis whereas E2F8 has a unique and non-redundant capacity to regulate squamous differentiation. In addition, we report on a unique feedback loop between E2F1, E2F7 and E2F8 that highlights a previously unreported interdependent axis. These findings provide evidence implicating the atypical E2F proteins as potent and biologically relevant modulators of squamous differentiation and cytotoxic responses.

3.1.1 Mouse model

In this study we aim to generate a series of models in which E2F family members are deliberately dysregulated in order to examine their role in normal epithelial maturation as well as sensitivity to cytotoxic stimuli. These studies will identify potential targets for preventing or treating SCC. The *Cre/loxP* system thus provides a powerful means by which we can study the roles of atypical E2Fs, *in vitro*.

Targeting of E2F7 and E2F8 was achieved by flanking exon 4 in E2F7 and exon 3 and 4 in E2F8 with *loxP* sites using homologous recombination techniques (*Figure 3.1*). These mice were a kind gift from Gustavo Leone (Li, Ran et al. 2008). These mice will be used as a source of KCs for *in vitro* studies. These mice are a unique and powerful resource that will help us to elucidate the role of atypical E2Fs in KC biology.

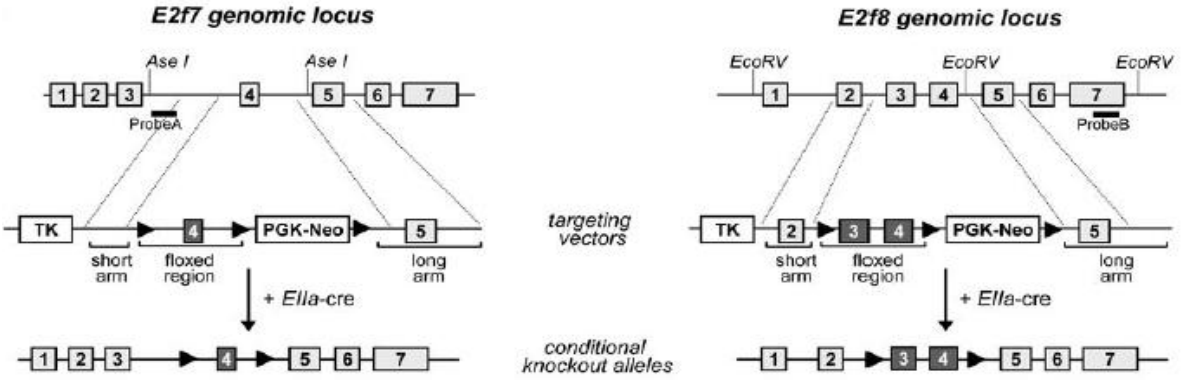

Figure 3.1 Schematic representation of generation of E2F7 and E2F8 conditional knockout alleles. (Li, Ran et al. 2008).

3.1.2 Adenovirus mediated gene delivery

We wanted to employ a method for studying the roles of atypical E2Fs *in vitro*. A strategy was to utilise adenovirus-mediated Cre deletion of floxed sequences in primary cells isolated from floxed mice. In this approach, the isolated primary KCs carrying flanked sequences are infected with Cre expressing adenovirus particles at a low multiplicity of infection for a short period of time in tissue culture flasks in order to achieve successful recombination.

Cre expressing adenoviruses have been successfully used as an alternative to Cre transgenic mice (Anton and Graham 1995; Wang, Krushel et al. 1996). Studies have shown that infection of primary cells is rapid, efficient and less labour intensive (Hunt, Deng et al. 1997;

Rijnkels and Rosen 2001; Deyrieux, Rosas-Acosta et al. 2007). Successful gene delivery can easily be achieved at a low multiplicity of infection avoiding potential toxicity (Prost, Sheahan et al. 2001). There are many advantages of this method including the tissue specificity achieved by the isolation method, the time of recombination and toxicity controlled by the intervals of infection, the reduction to a minimum number of animals used in subsequent *in vivo* work (Prost, Sheahan et al. 2001). Besides, it offers a convenient and flexible study system (Prost, Sheahan et al. 2001). Several papers have demonstrated that many epithelial cell types can easily be infected at a high level by this technology (Ohba, Ishino et al. 1998; Bielefeld, Amini-Nik et al. 2011; Hwang, Kita et al. 2011). The caveat to this approach is the Cre-dependent toxicicty where prolonged exposure to a Cre protein can lead to genetic instability.

3.2 Results

3.2.1 Characterisation of differentiation in MEKs

The morphology of human skin is routinely examined by analysing the expression of proliferation and differentiation markers. Since there are inherent structural differences in skin between humans and mice (Ratushny, Gober et al. 2012), we wanted to characterise the expression of established differentiation markers of differentiation in MEKs. For this study, we used skin derived from C57/BL6 pups. To evaluate the state of differentiation and proliferation, deparaffinised paraffin sections were stained immunohistochemically or by immunofluorescence using various primary antibodies. Consistent with human epidermis, in all basal layer cells, keratins 5 and 14, which are markers of undifferentiated and proliferation-competent KCs, respectively, were found to be expressed (*Figure 3.2*). Once again, consistent with human epidermis, early differentiation markers keratin 1 and 10 were detected in all suprabasal layers of mouse epidermis (*Figure 3.2*). Moreover, among the terminal differentiation marker, involucrin was expressed in the upper spinous and granular layers of mouse epidermis in agreement with the expression profile seen in human skin (*Figure 3.2*)

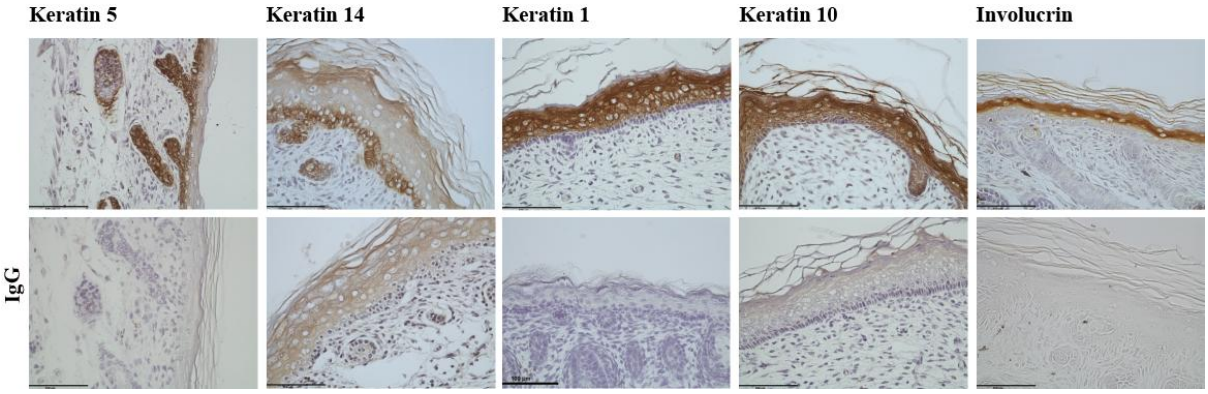

Figure 3.2 Immunostaining of proliferation and differentiation markers in the control mouse epidermis. Postnatal day 3 control mice skin samples were fixed, paraffin embedded, sectioned and mounted on slides. Tissue was stained with an antibody against keratin5, keratin14, keratin 1, keratin 10, Involucrin and IgG. Epidermis proliferation markers, keratin 5 and keratin 14 are localized to the basal layers of the epidermis. Early differentiation markers, keratin 1 and keratin 10 are expressed evenly throughout the suprabasal layers of mouse epidermis. In mouse skin, involucrin is localized only to the suprabasal layer of the epidermis. Antibody staining is specific as an IgG negative control shows no staining. Positive staining is shown by brown staining. IgG control was used as a control. Bar = 100 μm.

We repeated these investigations using immunofluorescent detection rather than immunohistochemistry and found similar results (*Figure 3.3*). Immunofluorescence images demonstrated that, mouse epidermis has the same degree of maturation compared to human skin as reflected by the expression of early differentiation marker, keratin 10 (*Figure 3.3*), in the suprabasal layer and by the expression of terminal differentiation marker, involucrin, in the upper spinous and granular layers of mouse epidermis (*Figure 3.3*). Additionally, the proliferation marker, keratin 5 (*Figure 3.3*) was also expressed in all the basal cells in the mouse epidermis. These immunohistochemistry and immunofluorescence analyses highlight the fact that there are marked similarities between human and mouse epidermis. More importantly, these data indicate that we have excellent markers to interrogate squamous differentiation in both human and murine KCs *in vitro* and *in vivo*.

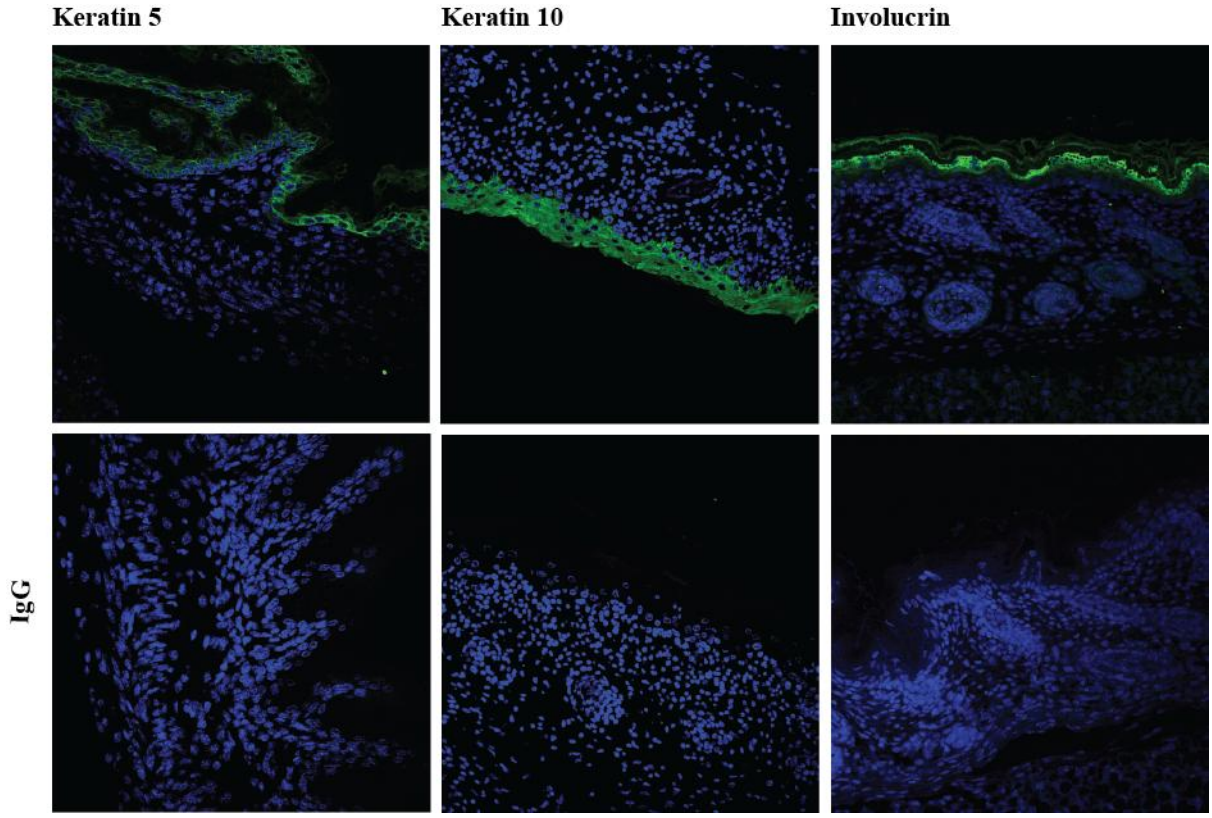

Figure 3.3 Proliferation marker and cytokeratin expression status in the control mice epidermis. Postnatal day 3 control mice skin was subjected to dual colour immunostaining with antibodies to keratin 5, keratin 1 and involucrin and visualised using confocal microscope. Immunostaining with normal rabbit IgG reveals the lack of non-specific staining. Blue represent nuclei stained with DAPI, green represents Alexa Fluor 488 stained keratin 1, 5 and involucrin positive cells. Original magnification, x25.

3.2.2 Adenoviral infection of primary KCs is highly efficient and has no effect on cell viability, mRNA synthesis, protein expression, differentiation and response to stress

To test the hypothesis that E2F7 and E2F8 are important regulators of KC biology, we have initiated a series of *in vitro* experiments in which we engineer E2F7, E2F8 or E2F7 and E2F8 knockdown in MEKs by utilizing adenovirus-mediated Cre deletion of floxed sequences. Cre-expressing adenoviruses have been used successfully in primary cells as an efficient tool for gene deletion *in vitro* (Ohba, Ishino et al. 1998; Prost, Sheahan et al. 2001; Rijnkels and Rosen 2001).

We started with titration experiments using a control adenovirus, Ad-GFP, in order to optimize the conditions of viral infection including the amount of virus particles to be used and the duration of infection. Multiplicity of infection (MOI) of 50 48 hours post-infection with virus showed low toxicity and the highest infection efficiency among all (*Figure 3.4A*).

There was no effect of control Ad-CMV-Null virus, an empty CMV viral construct, on proliferation measured by cell proliferation assay (*Figure 3.4B*). Further, it did not have any effect on E2F7 mRNA expression evidence by qRT-PCR analysis (*Figure 3.4C*). We also looked at the possible effect of viral infection on differentiation. Ad-CMV-Null infected and $CaCl_2$ treated MEKs, isolated from control mice, showed an increase in involucrin protein levels (*Figure 3.4D*) as expected. Moreover, control adenovirus infected cells were able to respond normally to stress such as UVB irradiation (*Figure 3.4E*), doxorubicin (*Figure 3.4F*) and cisplatin (*Figure 3.4G*) treatments compared to uninfected control MEKs. These data demonstrate that differentiation and cytotoxicity responses of KCs are unaltered by infection with an adenovirus.

High gene delivery efficiency (>90%) was achieved with Ad-Cre-GFP, at a MOI of 50 (*Figure 3.5A*), and expression of Cre recombinase was detected by immunoblotting 48 hours post-infection (*Figure 3.5B*). Importantly, we further validated target cell specificity by examining the expression levels of epithelial cell specific marker, AE1/AE3. Immunoblotting results confirmed that we were able to deliver and consequently cause recombination only in the epithelial cells and not other cell populations including fibroblast (*Figure 3.5C*). In agreement with gene delivery efficiency, analysis of recombination and subsequent gene deletion of Ad-Cre-GFP infected KCs isolated from E2F7, 8 and 7/8 floxed mice demonstrated that we were able to efficiently knockdown the cognate transcript with high efficiency (*Figure 3.5D, E and F*). It is noteworthy that the knockdown (KD) efficiency of the E2F7/8 double floxed KCs was less than that for the individually floxed KCs. The recombination rate was around 60% for E2F7 and 70% for E2F8 (*Figure 3.5F*). E2F1 gene expression levels were also examined in KCs isolated from conventional E2F1KO mice. E2F1 levels were only reduced by 70% (*Figure 3.5G*). We confirmed by sequencing that the PCR product in the E2F1 KO experiment was E2F1. In addition to gene recombination analysis, we also evaluated the levels of E2F7 proteins in E2F7 deficient KCs. The results demonstrated that we were able to totally delete E2F7 protein in those cells (*Figure 3.5D*). This analysis could not be possible in E2F8 deficient KCs due to lack of reliable antibody against E2F8. Moreover, E2F1 protein levels were also evaluated and results were in agreement with the qRT-PCR results. Surprisingly, once again, only modest level of reduction in E2F1 protein levels was observed (*Figure 3.5G*).

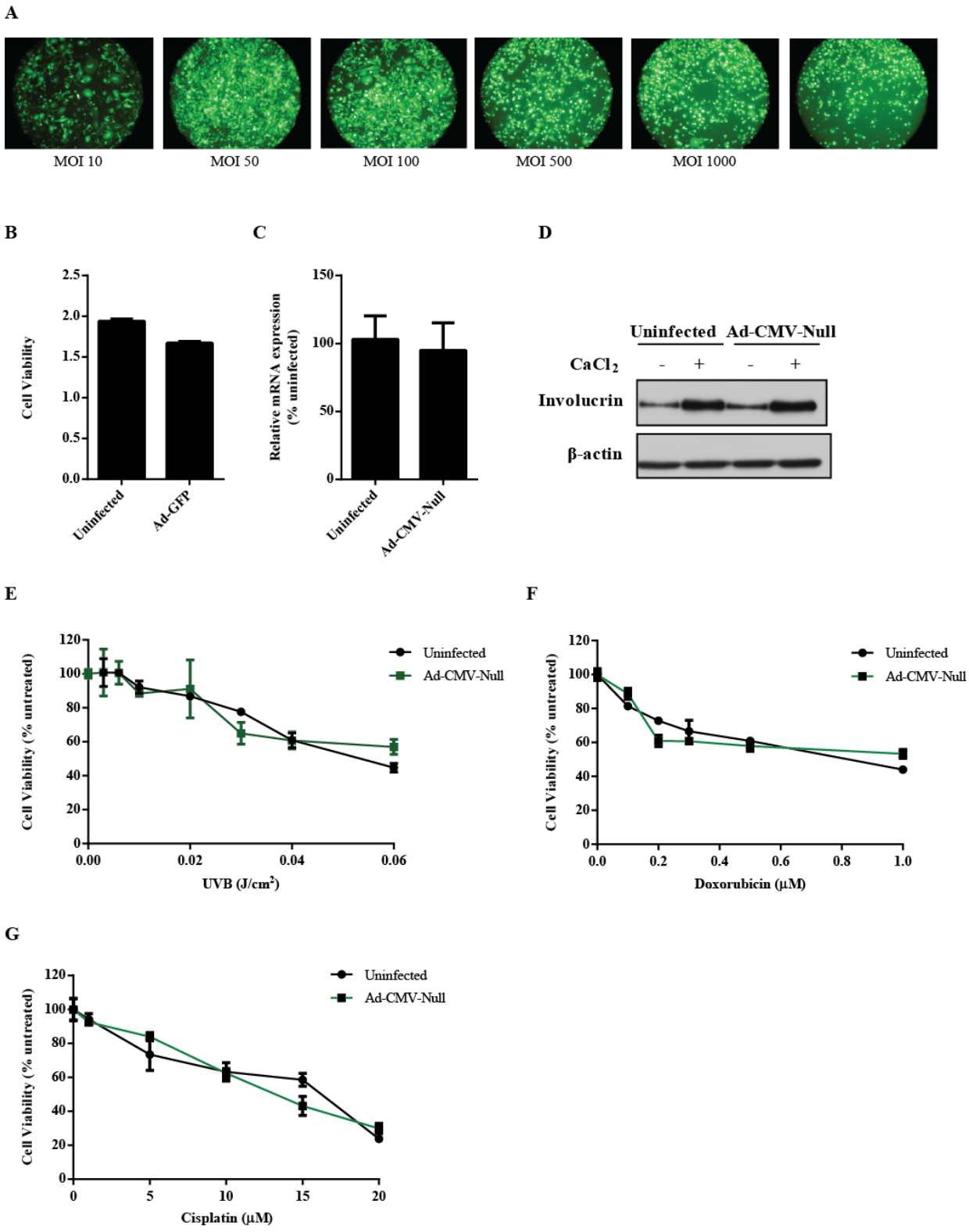

Figure 3.4 Adenovirus infection of MEKs is highly efficient and has no adverse effect on cellular functions. Fluorescence microscopy images of control MEKs infected with differing MOI of control virus, Ad-GFP (A). Images were taken 48 hours post-infection. Cell viability following 48 hours post-infection with Ad-CMV-Null, at a MOI of 50, was measured by cell proliferation assay (B). Quantitative RT-PCR was performed on control (uninfected) MEKs and MEKs which were infected with Ad-CMV-Null virus (C). Ad-CMV-Null control virus infected MEKs were cultured with 1.2 mM $CaCl_2$ for 48 hours to induce differentiation and

differentiation marker, involucrin, levels were detected by immunoblotting (D). β-actin was used as a loading control. Control (uninfected) and Ad-CMV-Null infected MEKs were subjected to variable doses of UVB (E), doxorubicin (F) or cisplatin (G). Cell viability was assessed following 48 hours post-treatment and plotted as percentage of untreated cells. Quantitative data represent the mean ± SEM obtained from triplicate determinations of three independent experiments. Real time PCR data are the mean ± SEM of duplicate determinants normalized for expression of the housekeeping gene β-actin; $n = 3$. Western blot figures are representative of three independent experiments.

Overall, we were able generate KCs that are deficient in E2F7, E2F8, and E2F7/8 following infection with Ad-Cre-GFP viral constructs without any significant effect on the cellular functions that have been studied.

3.2.3 E2F8-deficient MEKs display an abnormal phenotype in response to elevated $CaCl_2$

Although our previously published work clearly showed that E2F7 plays a critical role in differentiation initiation by repressing key regulators of differentiation in proliferating cells, this effect was restricted to a subset of genes and cannot be considered a global regulator of differentiation (Hazar-Rethinam, Cameron et al. 2011). Moreover, given the lack on data on E2F8's contribution to differentiation, we examined the role that E2F8 plays with regards to differentiation. To date, there is no data about E2F8 on squamous differentiation and neoplasia.

There are several physiologically relevant agents that are able to alter growth and differentiation in KCs *in vitro*. These agents are capable of mimicking *in vivo* processes of squamous differentiation when included in KC tissue culture. In this study, we utilised elevated calcium levels to induce differentiation. It was previously shown that supplementation of KC medium with calcium induces the expression of differentiation specific genes (Poumay and Pittelkow 1995). Initial experiments demonstrated that by increasing the calcium concentration from 0.05 mM to 1.2 mM $CaCl_2$ after a 48 hour treatment was sufficient to induce the protein levels of differentiation specific genes such as involucrin (*Figure 3.6A*) and repress the protein levels of proliferation specific genes such as cdc2 (*Figure 3.6B*). This treatment scheme was followed for the differentiation study.

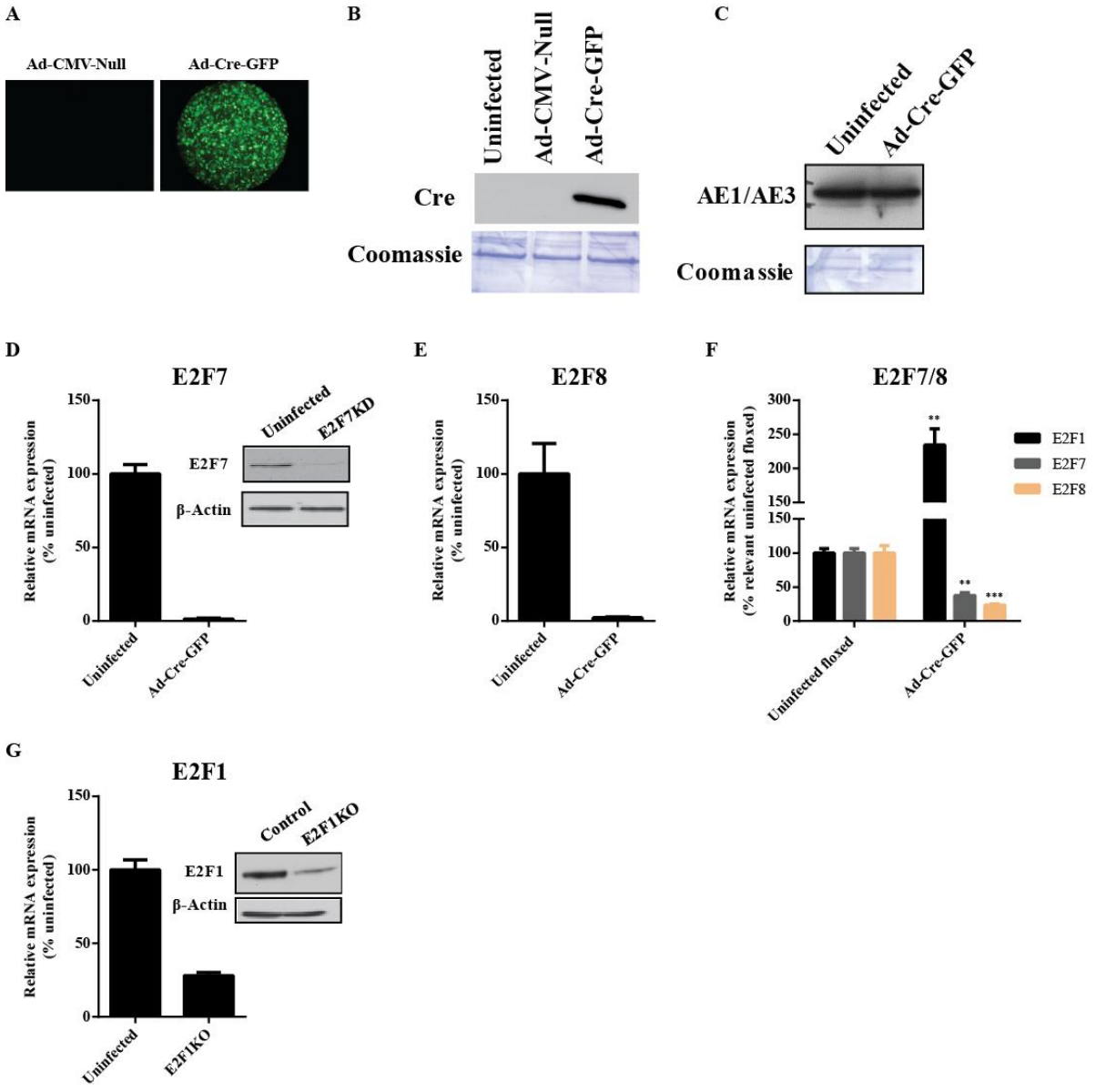

Figure 3.5 Generation of E2F7 and E2F8 deficient MEKs and the validation of E2F1 levels in E2F1KO mice. High level of Cre gene delivery was evident from microscopic analysis of Ad-Cre-GFP infected KCs isolated from E2F8 floxed mice (A). Immunoblotting for Cre recombinase expression post-infection was carried out in uninfected E2F8 floxed MEKs, control Ad infected E2F8 floxed MEKs and Ad-Cre-GFP infected E2F8 floxed MEKs (B). Immunoblotting for AE1/AE3 expression post-infection was carried out in Ad-Cre-GFP infected E2F8 fl/fl MEKs (C). The membrane was stained with Coomassie blue for loading control. Levels of E2F7 mRNA expression and protein levels were measured in E2F7 fl/fl MEKs following infections with Ad-Cre-GFP by qRT-PCR and immunoblotting, respectively (D). E2F8 (E) or E2F7/8 (F) mRNA expression was measured in the relevant fl/fl MEKs following infections with Ad-Cre-GFP and compared to uninfected MEKs. Levels of E2F1 mRNA expression and protein levels were measured in MEKs isolated from E2F1KO mice and compared with uninfected MEKs isolated from control mice by qRT-PCR and immunoblotting, respectively (G). Real time PCR data are the mean ± SEM of duplicate determinants normalized for expression of the housekeeping gene β-actin; $n = 3$. Western blot figures are representative of three independent experiments. β-actin was used as a loading control for (D) and (G). **, $P < 0.01$, ***, $P < 0.001$.

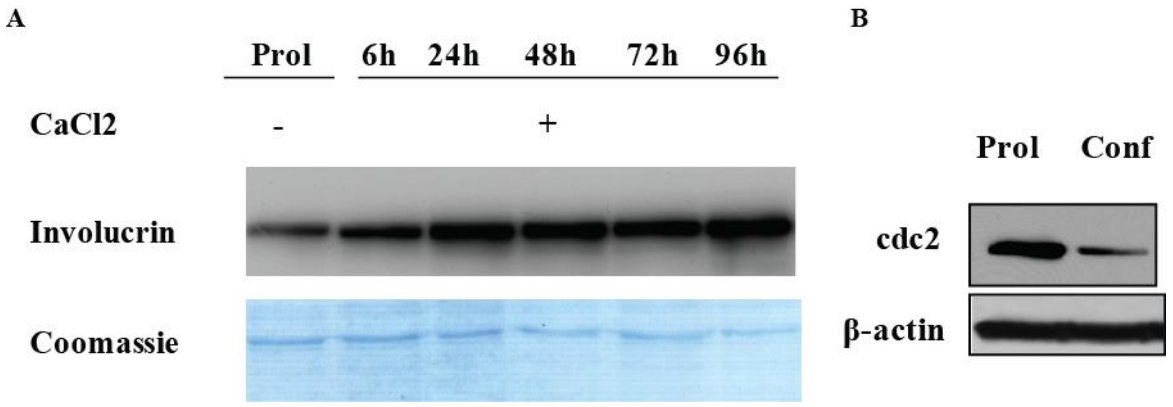

Figure 3.6 Calcium time-course: the elevated levels of calcium in culture medium was sufficient to induce differentiation. Time course analysis of involucrin protein expression in MEKs isolated from control mice which are cultured in KC-SFM supplemented with 1.2 mM $CaCl_2$. The membrane was stained with Coomassie blue for loading control. Immunoblotting for proliferation marker cdc2 expression in differentiated MEKs following 48 hours $CaCl_2$ (1.2 mM) treatment (B). β-actin was used as a loading control. Western blot figures are representative of three independent experiments. Prol is proliferative; Conf is confluent keratinocytes.

Microscopy of Ad-Cre-GFP infected KCs isolated from E2F8 fl/fl mice revealed differences in their phenotype compared to E2F1, E2F7 an E2F7/8 deficient keratinocytes in the presence of calcium (*Figure 3.7A*). Moreover, when these cells were exposed to elevated levels of calcium, they did not induce differentiation markers as measured by immunoblotting, indicating that E2F8 may be required for cells to undergo squamous differentiation (*Figure 3.7B and C*). In contrast, E2F1 and E2F7 deficient MEKs retained their ability to respond to increased levels of calcium (*Figure 3.7B and C*). These results identified a novel non-redundant activity for E2F8 in modulating involucrin expression and suggested that E2F8 may be a key regulator of differentiation.

Given the unexpected and unique role of E2F8 in differentiation, we also looked at the mRNA expression levels of E2F1, E2F7 and E2F8 in differentiated MEKs following calcium treatment. In agreement with our protein results, E2F1 and E2F7 levels were significantly reduced in differentiated MEKs (*Figure 3.7E*). Whereas the mRNA level of E2F8 was downregulated only by 20% (*Figure 3.7E*). This result further confirmed that E2F8 plays a non-redundant and significant role in squamous differentiation and perhaps in squamous cell carcinoma development.

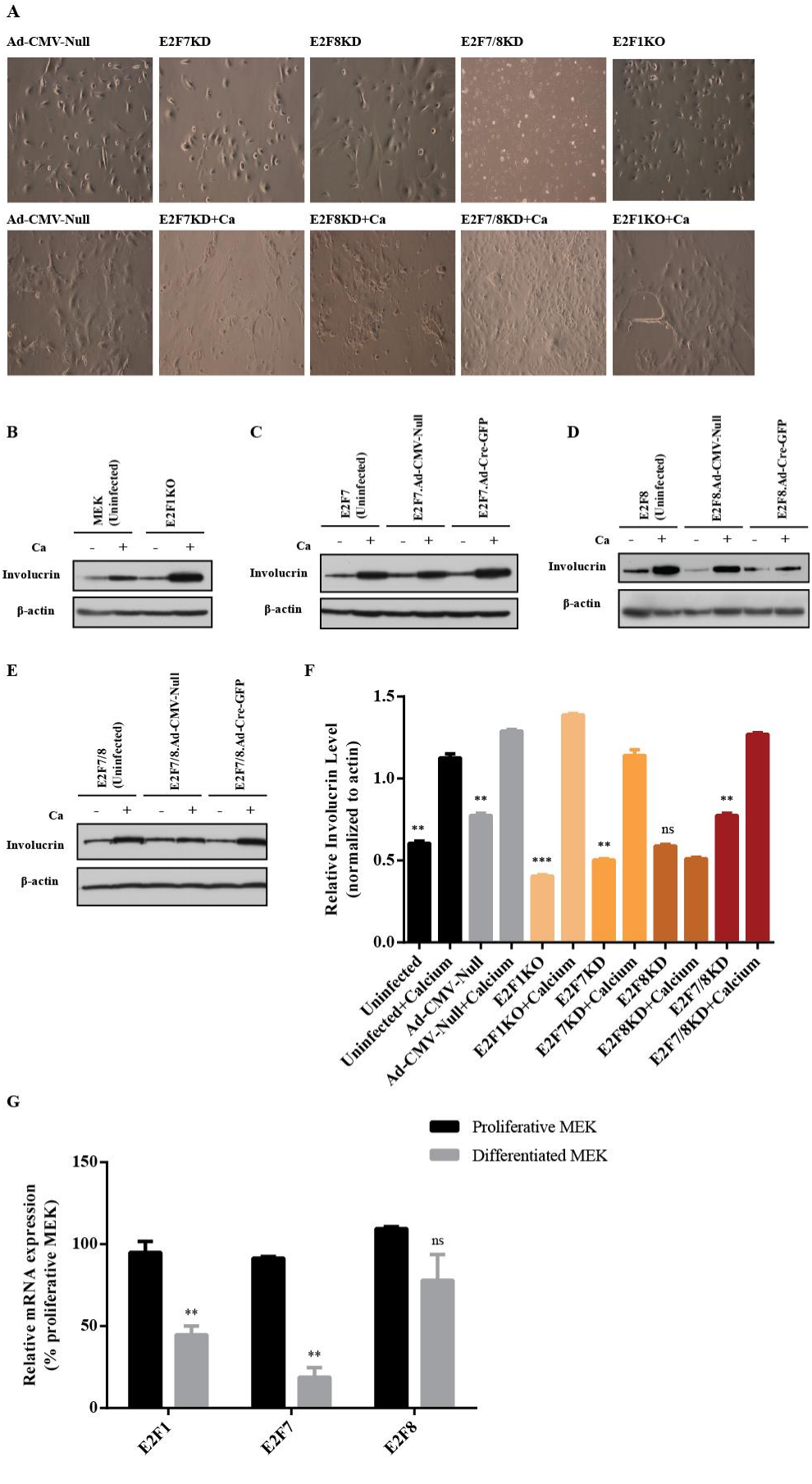
A
Ad-CMV-Null
E2F7KD
E2F8KD
E2F7/8KD
E2F1KO
Ad-CMV-Null
E2F7KD+Ca
E2F8KD+Ca
E2F7/8KD+Ca
E2F1KO+Ca
B
MEK (Uninfected)
E2F1KO
Ca
Involucrin
β-actin
C
E2F7 (Uninfected)
E2F7.Ad-CMV-Null
E2F7.Ad-Cre-GFP
D
E2F8 (Uninfected)
E2F8.Ad-CMV-Null
E2F8.Ad-Cre-GFP
E
E2F7/8 (Uninfected)
E2F7/8.Ad-CMV-Null
E2F7/8.Ad-Cre-GFP
F
Relative Involucrin Level (normalized to actin)
1.5
1.0
0.5
0.0
**
**
***
**
ns
**
Uninfected
Uninfected+Calcium
Ad-CMV-Null
Ad-CMV-Null+Calcium
E2F1KO
E2F1KO+Calcium
E2F7KD
E2F7KD+Calcium
E2F8KD
E2F8KD+Calcium
E2F7/8KD
E2F7/8KD+Calcium
G
Proliferative MEK
Differentiated MEK
Relative mRNA expression (% proliferative MEK)
150
100
50
0
**
**
ns
E2F1
E2F7
E2F8

Figure 3.7 Loss of E2F8 in MEKs inhibits the induction of differentiation. Phase-contrast microscopy images of E2F7, E2F8, E2F7/8 or E2F1 deficient MEKs in the presence and absence of calcium chloride (A). E2F1 deficient MEKs (B) or uninfected, Ad-CMV-Null or Ad-Cre-GFP infected E2F7 (C), E2F8 (D), E2F7/8 (E) or were either left untreated or treated with 1.2 mM $CaCl_2$ for 48 hours following viral infection at which time expression of involucrin protein was visualized by immunoblotting. β-Actin is provided as a loading control. Densitometric analysis of involucrin was quantified using ImageJ. Expression level was normalized against β-Actin and plotted as relative involucrin level (F). Western blot figures are representative of three independent experiments. mRNA expression levels of E2F1, E2F7 and E2F8 in undifferentiated or 1.2 mM $CaCl_2$ treated MEKs were examined by qRT-PCR (G). Real time PCR data are the mean ± SEM of duplicate determinants normalized for expression of the housekeeping gene β-actin; $n = 3$. ns is not significant, **, $P < 0.01$, ***, $P < 0.001$.

3.2.4 Cytotoxic responses to UV are selectively enhanced in E2F7-deficient MEKs

We previously reported that E2F7 overexpression could reduce the E2F1-dependent response of KCs to respond to the major cutaneous carcinogen, UV radiation (Endo-Munoz, Dahler et al. 2009). To confirm our previous findings and extend these findings to include E2F8, we performed UV-induced cytotoxicity experiments on uninfected control and Ad-Cre-GFP infected KCs isolated from cognate floxed mice. When infected MEKs were subjected to varying doses of UVB ranging from 0-0.06 J/cm^2, E2F1-deficient cells had an attenuated response to UV (*Figure 3.8*). This suggests that E2F1 is involved in UV-mediated apoptosis. In contrast, E2F7-deficient (E2F7KD) MEKs became more sensitive to UV (*Figure 3.8*). Finally, E2F8 deficient (E2F8KD) and E2F7/8 deficient (E2F7/8KD) MEKs displayed unaltered responses to UV (*Figure 3.8*). These data indicate that UV-induced cytotoxic responses may involve E2F1 and E2F7-dependent processes. This is more obvious if one compares the E2F1KO dose response curve to that of the E2F7KD data.

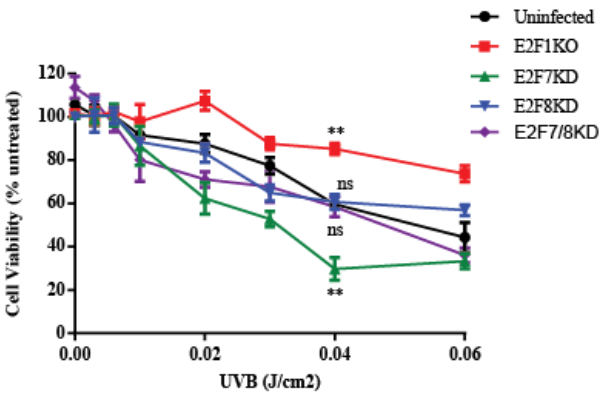

Figure 3.8 Cytotoxic responses to UVB selectively enhanced in E2F7-deficient MEKs. Uninfected and Cre treated proliferative E2F1, E2F7, E2F8 and E2F7/8 MEKs were exposed to varying doses of UVB irradiation and left for 24 hours. Cell viability was then measured. Results are expressed as a percentage of uninfected MEKs, and quantitative data represent the mean ± SEM obtained from triplicate determinations of three independent experiments. Significant differences between Uninfected and E2F1KO or Uninfected and E2F7KD are indicated (ns is not significant, **, $P < 0.01$).

3.2.5 Cytotoxic responses to doxorubicin are selectively enhanced in E2F7-deficient MEKs

In order to find out whether the ability of E2F7 to regulate stress responses is selective for UVB radiation, we also looked at the chemotherapy-induced cytotoxicity. For this, we examined the effects of E2F1, 7, 8 and 7/8 on cytotoxic responses to doxorubicin, cisplatin and etoposide. These experiments indicated that E2F7, but not E2F8, may play a role as a modulator of doxorubicin-induced cytotoxic responses (*Figure 3.9A*). Significantly, E2F7 deficiency only had minimal effect on cisplatin sensitivity (*Figure 3.9B*) and no impact on etoposide sensitivity (*Figure 3.9C*). E2F8 and E2F7/8 had no effect on cytotoxic responses to any of the drugs (*Figure 3.9A, B and C*). E2F1 deficiency had a modest protective role against doxorubicin or cisplatin-induced cytotoxicity (*Figure 3.9A, B and C*). Combined, these data indicate that E2F1 and E2F7 may play opposing roles in the modulation of doxorubicin sensitivity. These results highlight a potentially unique and isoform-specific function of E2F7 in modulating sensitivity to doxorubicin.

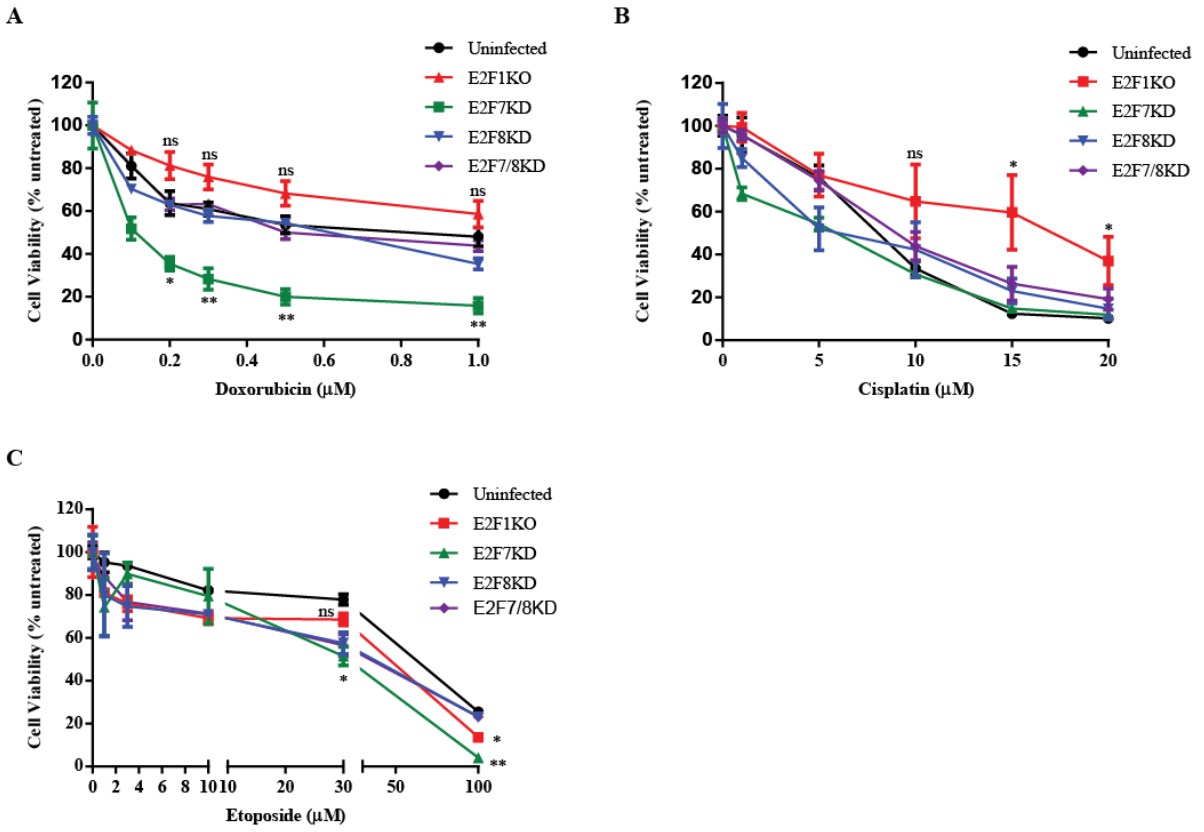

Figure 3.9 Cytotoxic responses to doxorubicin selectively enhanced in E2F7-deficient MEKs. Dose response curve of uninfected, E2F1, E2F7, E2F8 and E2F7/8 deficient proliferative KCs to doxorubicin (A), cisplatin (B) and etoposide (C). Cells were exposed to chemotherapeutic drugs for 2 days. Viability was then assessed and plotted as percentage uninfected KCs. Quantitative data represent the mean ± SEM obtained from triplicate determinations of three independent experiments. Significant differences between Uninfected and E2F1KO or Uninfected and E2F7KD are indicated (ns is not significant, *, $P < 0.05$, **, $P < 0.01$).

3.2.6 E2F1/E2F7/8 exist as an interdependent axis in KCs

We examined the expression levels of E2F1, 7 and 8 in E2F deficient MEKs. Quantitative RT-PCR results confirmed previously published data showing the existence of a negative feedback loop between E2F1 and E2F7 (*Figure 3.10A and B*). Loss of E2F8 resulted in elevation in E2F1 and E2F7 expressions (*Figure 3.10C*), whereas loss of E2F1 caused reductions in E2F7 and E2F8 expressions (*Figure 3.10A*). Unexpectedly, qRT-PCR results demonstrated a unique and unknown transcriptional relationship between E2F7 and E2F8. E2F8 appeared to suppress E2F7 transcription in agreement with it being a transcription inhibitor, whereas E2F7 functioned as an activator and E2F7 deficiency caused an increase in E2F8 expression (*Figure 3.10B and C*). These results clearly demonstrate the existence of a complex and interdependent network between E2F1, E2F7 and E2F8 in KCs.

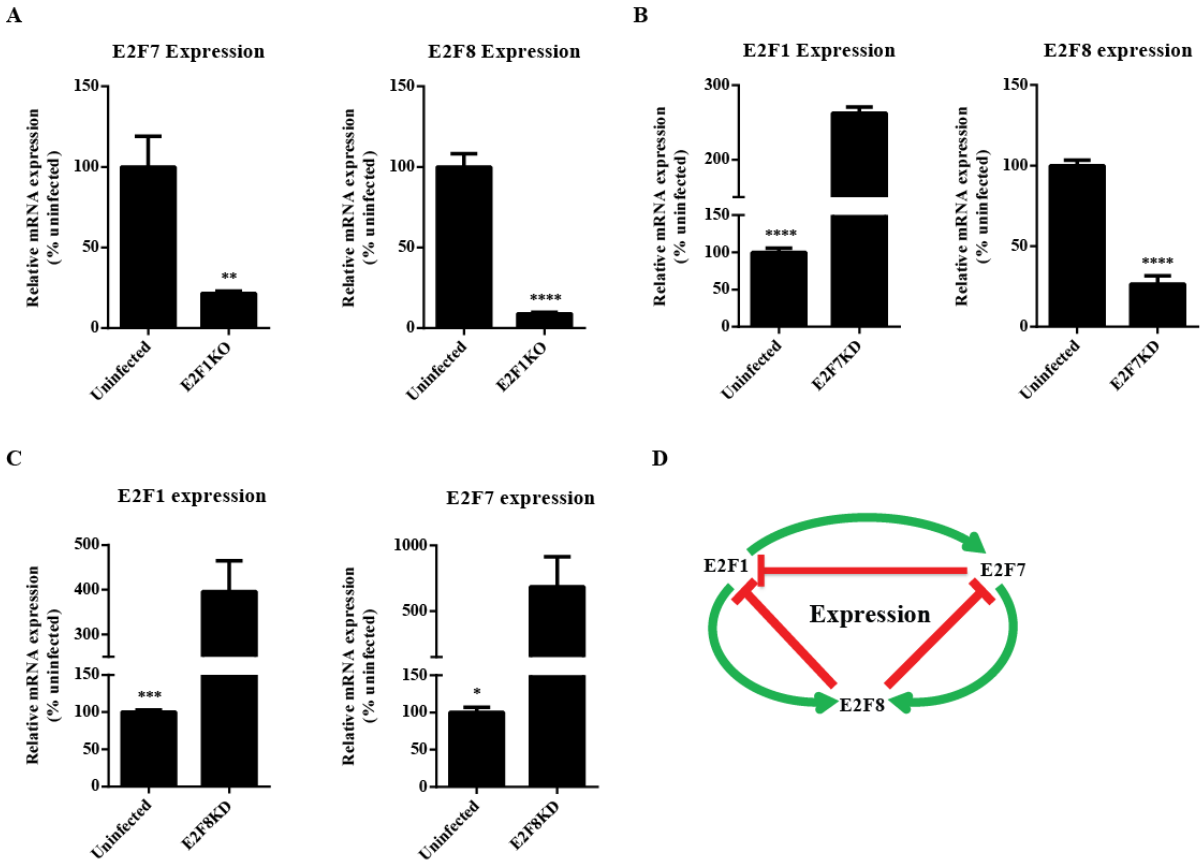

Figure 3.10 E2F1/E2F7/E2F8 exist in an interdependent network. E2F1, E2F7 and E2F8 expression levels were measured by qRT-PCR in E2F1 deficient (A), E2F7 deficient (B) and E2F8 (C) deficient MEKs. Schematic model summarising the interdependent network between E2F1, E2F7 and E2F8 at the transcriptional level (D). Results expressed as percentage of relevant uninfected floxed MEKs. The expression levels are the mean ± SEM of duplicate determinants normalized for expression of the housekeeping gene β-actin by the standard curve method; $n = 3$. *, $P < 0.05$, **, $P < 0.01$, ***, $P < 0.001$, ****, $P < 0.0001$. P value was calculated using Student's t test.

3.3 Discussion

To characterise the actions of E2F7 and E2F8 in KCs of stratified epithelia *in vitro*, we conducted a series of *in vitro* studies on the contribution of E2F1, E2F7 and E2F8 to squamous differentiation using cultured MEKs derived from wildtype, E2F1 KO or E2F7, E2F8, E2F7/8 floxed mice. E2F deficient KCs were generated *in vitro* by utilizing adenovirus-delivered Cre-mediated gene deletion. Our early experiments showed that infection occurred in almost all cells and had little effect on biological processes such as proliferation, differentiation and apoptosis. It should be noted that the recombination rate of the double knockdown KCs was lower than that of the individual ones. Surprisingly, conventional E2F1KO KCs still expressed measurable levels of E2F1 transcript. This residual E2F1 expression was confirmed by sequencing and thus significant reduction of E2F1 occurred but was not absolute. Predictably, significant knockdown of E2F7 mRNA and protein was achieved whilst the lack of commercially useful E2F8 antibodies meant we could only confirm E2F8 knockdown at the mRNA level. These preliminary studies have provided us with the unique resources to assess differentiation and apoptosis i*n vitro* in MEKs that are selectively deficient for specific E2F isoforms.

Dysregulation of apoptosis is common amongst SCC (Pierce, Gimenez-Conti et al. 1998; Hanahan and Weinberg 2000; Wang, Russell et al. 2000; DeGregori and Johnson 2006). Similarly, dysregulation of E2F1 and E2F7 expression is common in SCC (Endo-Munoz, Dahler et al. 2009). It has been shown that some apoptotic responses are regulated by E2F in an E2F isoform-specific manner (Li, Ran et al. 2008; Panagiotis Zalmas, Zhao et al. 2008; Endo-Munoz, Dahler et al. 2009). E2F1 is one of those E2F isoforms. The role of E2F1 in the regulation of apoptosis is well-documented (Bell and Ryan 2003; Jamshidi-Parsian, Dong et al. 2005; Lazzerini Denchi and Helin 2005; Stanelle and Pützer 2006; Hallstrom, Mori et al. 2008; Wu, Zheng et al. 2009). In this chapter, we showed that E2F7 deficiency selectively enhanced the cytotoxic responses of KCs to UVB and doxorubicin. In contrast, E2F1 deficiency protected the KCs from UVB and doxorubicin-induced cytotoxicity. These data indicate that E2F1 and E2F7 appear to antagonise one another with respect to cytotoxic responses. Significantly, E2F8 and E2F7/8 had no effect on cytotoxic responses indicating that the role of E2F7 and E2F1 are, to an extent, isoform specific. Clearly, the overexpression of E2F7 seen in SCC patients (100 fold overexpression) (Endo-Munoz, Dahler et al. 2009) would be predicted to render them resistant to the apoptotic effects of UVB radiation, and

supports the idea that E2F7 overexpression could contribute to UV-induced malignant transformation. Moreover, these data would suggest that E2F7 overexpression may also modulate chemotherapeutic sensitivity in SCC.

Although doxorubicin and etoposide are established type II Toposiomerase blocking agents, E2F7 deficient cells only responded to the cytotoxic effects of doxorubicin. Type II Topoisomerases are ATP-dependent enzymes, and play an important role in DNA metabolism by catalysing topological changes in DNA (Dong, Yang et al. 2002). Whilst the doxorubicin-selectivity was unexpected, it is not unprecedented. For example, Bug and Dobbelstein (2011) reported that chemotherapeutic agents which are closely related, like anthracyclines, can have differing biochemical functions (Bug and Dobbelstein 2011). They ascribed these compound-specific biochemical functions to the efficiency and sequence specificity of drug intercalation with DNA. Similarly, the extent of DNA cleavage and drug-induced DNA lesions produced by these two drugs showed marked differences in non small cell lung cancer cells (Binaschi, Capranico et al. 1990).

Doxorubicin is one of the commonly employed drugs in chemotherapy for a number of cancer types (Zhang, Liu et al. 2012; Tacar, Sriamornsak et al. 2013). It is not however in use clinically for SCC treatment. To date there has been no data on the possible reasons behind this insensitivity. In this regard, our data may provide a possible explanation. The overexpression of E2F7 seen in SCC patients would have a protective effect against the cytotoxic actions of doxorubicin. Collectively, these data highlight a unique, significant and isoform-specific function for E2F7 regulating sensitivity to cytotoxic (doxorubicin) or carcinogenic (UVB) stimuli. Linked with the overexpression of E2F7 in SCCs, our data would suggest i) that E2F7 may suppress UV-induced apoptosis and hence contribute to SCC development and ii) that targeting E2F7 may sensitise SCCs to an expanded suite of chemotherapeutics. This will be examined in future chapters.

A number of transcription factors have been shown to regulate squamous differentiation (*Chapter 1* in this study). In particular, the E2F family appears to be prominent amongst them (Wang, Helin et al. 1995; Dicker, Popa et al. 2000; Wong, Barnes et al. 2003; Hazar-Rethinam, Cameron et al. 2011). E2F inhibition is required for squamous differentiation, and induces growth arrest and sensitises KCs to subsequent differentiation stimuli (Jones, Dicker et al. 1997; Dicker, Popa et al. 2000; Wong, Barnes et al. 2003; Hazar-Rethinam, Cameron et

al. 2011). Consistent with its E2F inhibitory role, we recently showed that E2F7 is able to repress the expression of the Sp1 transcription factor, a key factor involved in the induction of differentiation genes (Hazar-Rethinam, Cameron et al. 2011). These data suggest that loss of E2F7 would lead to the derepression of differentiation genes (Hazar-Rethinam, Cameron et al. 2011). Similarly, overexpression of E2F7 (as seen in SCC) would be predicted to suppress differentiation (Hazar-Rethinam, Cameron et al. 2011). However, these studies utilised an *in vitro* system of KCs in which E2F7 was manipulated using various transfection strategies. Significantly, the potential role of E2F8 has not been examined to date. Preliminary data from this chapter highlights a previously unknown and unique function for E2F8 in modulation squamous differentiation. E2F8 deficient MEKs did not show the typical differentiated KC morphology compared to E2F1, E2F7 and E2F7/8 deficient KCs in the presence of elevated levels of calcium. Moreover, loss of E2F8 inhibited the ability of these cells to undergo calcium-induced squamous differentiation *in vitro*. On the other hand, E2F1 and E2F7 deficient MEKs retained a capacity to differentiate. This data is in agreement with the qRT-PCR analysis confirming that E2F1 and E2F7 were downregulated during calcium-induced differentiation. It is important to note that earlier studies with E2F8 KO mice did not report a "skin phenotype" which may suggest that differentiation is not absolutely dependent upon E2F8 and that E2F8 may operate in concert with other differentiation factors or may only act on a subset of differentiation genes.

The present study indicates that E2F1, E2F7 and E2F8 may contribute to SCC *via* various independent mechanisms such as apoptosis or differentiation dysregulation. It is noteworthy that earlier studies have reported that E2F1 can induce E2F7 and E2F8 transcription which in turn suppresses E2F1 transcription (Di Stefano, Jensen et al. 2003; Christensen, Cloos et al. 2005; Li, Ran et al. 2008; Panagiotis Zalmas, Zhao et al. 2008; Endo-Munoz, Dahler et al. 2009). This provides for a regulatory feedback loop for E2F activity. These findings prompted us to look for a similar feedback loop in KCs. Quantitative RT-PCR results from MEKs which are deficient for E2F1, E2F7 or E2F8 confirmed the existence of a negative feed-back loop between E2F1 and atypical E2Fs. However, we also found evidence that E2F7 is able to induce E2F8 expression. To our knowledge this has not been shown before. These findings suggest that E2F7 may act as an activator contrary to its well-documented function as a transcriptional repressor whereas E2F8 retains its function as transcription inhibitor. This is not entirely unprecedented since a recent report from Weijts *et al* (2012), demonstrates that E2F7 can act as an activator through binding and activating the

transcription of HIF1α (Weijts, Bakker et al. 2012). Surprisingly, there are two other recent studies suggesting a similar role for E2F7 in the activation of TERT promoter and for E2F8 in the stimulation of cyclin D1 promoters in liver (Deng, Wang et al. 2010; Sirma, Kumar et al.). Curiously, this study highlights the existence of a complex and interdependent network between E2F1, E2F7 and E2F8 which is thought to be contributing to normal squamous differentiation and cytotoxic responses, consequently dysregulation within this network contributes to SCC formation.

In conclusion, these preliminary screens highlight isoform-specific activities of E2F7 and E2F8 in responses to UV- or chemotherapy-induced cytotoxicity and squamous differentiation, respectively. These observations provide new avenues towards improving our understanding of KC differentiation, KC neoplasia and chemotherapeutic sensitivity in squamous cell carcinoma. Therefore, understanding the molecular basis for E2F7 and E2F8 action and novel factors that regulate E2F7 and E2F8 activity may lead to a better understanding of SCCgenesis and new therapeutic strategies to treat SCC patients. In the following chapters we will explore the E2F7 dependent pathways that regulate cytotoxic responses in KCs.

CHAPTER FOUR

4 Identification of Downstream Effectors of E2F7 in the Regulation of Doxorubicin Sensitivity

4.1 Introduction

In the previous chapter, detailed analysis of E2F7 and E2F8KDs in KCs implicated the atypical E2Fs as potent biologically relevant modulators of squamous differentiation and cytotoxic responses, respectively. In particular, E2F7 could contribute to the modulation of chemoresistance in SCC. Linked with the overexpression of E2F7 in SCC, the results from the previous chapter would predict that targeting E2F7 may sensitise SCCs to the cytotoxic action of chemotherapeutics. Targeting transcription factors is a promising anticancer strategy because of the direct involvement of transcription factors in many cancer-associated events or these event indirectly modulating transcription factors. However, targeting ligand-independent transcription factors remains a considerable challenge. Therefore, an unbiased transcriptome-wide approach was taken to identify downstream effectors of E2F7-mediated suppression of doxorubicin cytotoxicity in doxorubicin sensitive and doxorubicin insensitive cell lines. Importantly, identifying genes whose expression is regulated by E2F7 may aid in understanding the mechanism by which E2F7 modulates doxorubicin sensitivity. Moreover, it would provide an opportunity to introduce doxorubicin in SCC patient treatment schedules and expand the suite of chemotherapeutics that can be offered to SCC patients. In order to identify downstream effectors of E2F7 in the regulation of doxorubicin sensitivity, a number of experimental design strategies were incorporated. Firstly, a number of SCC cell lines were screened for doxorubicin sensitivity in order to distinguish the ones which are doxorubicin sensitive and insensitive. Secondly, a correlation between expression levels of E2F7 and sensitivity to doxorubicin was made to enrich for the cell lines which can be a good candidate for transcriptomics analysis. Thirdly, E2F7 levels were manipulated with overexpression or silencing approaches in those selected cell lines in the presence or absence of doxorubicin to identify the list of differentially expressed genes. These approaches will be explained in detail in the following results section. Genes that were responsible for E2F7-mediated sensitivity to doxorubicin warrant further analysis.

4.2 Results

4.2.1 E2F7 selectively regulates cytotoxic responses to doxorubicin in KCs

In the previous chapter, we examined the dose-dependent cytotoxic profiles of uninfected control, E2F7KD, E2F8KD and E2F1KO MEKs to increasing concentrations of doxorubicin

and made the observation that E2F7 plays an important role in the regulation of sensitivity to doxorubicin and the action of E2F7 in suppressing doxorubicin sensitivity is isoform selective since E2F8 failed to modulate doxorubicin sensitivity. To confirm that the effect of E2F7 deficiency was attributable to E2F7, we reintroduced E2F7 back into E2F7 deficient MEKs, and demonstrated that reintroduction of E2F7 into E2F7 deficient MEKs was sufficient to reverse E2F7-mediated sensitivity to doxorubicin (*Figure 4.1A*). We then determined whether E2F7-mediated reduction in cell survival is due to activation of apoptotic pathways. Uninfected control MEKs isolated from E2F7 floxed mice showed a modest increase in cleaved caspase-3 levels after 48 hours treatment with 0.3 μM doxorubicin (*Figure 4.1B*). In contrast, there was a profound activation of caspase-3 when E2F7 deficient MEKs were treated with 0.3 μM doxorubicin (*Figure 4.1B*). This is consistent with previous reports that DNA damage caused by doxorubicin results in double-strand breaks that leads to apoptosis (Tacar, Sriamornsak et al. 2013). Combined, these data confirms the findings that a unique and isoform-specific function of E2F7 does exist in modulating sensitivity to doxorubicin in KCs.

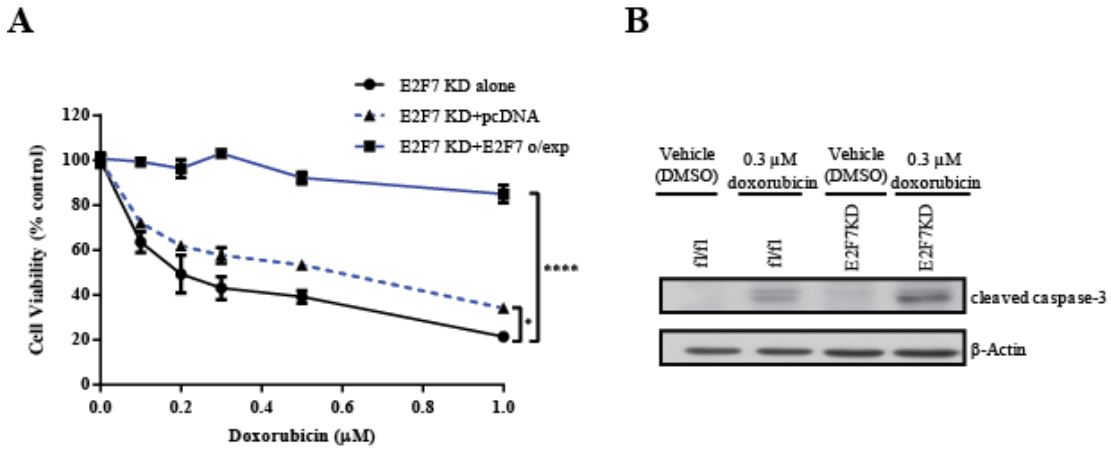

Figure 4.1 E2F7 modulates sensitivity to doxorubicin in MEKs, and it is due to activation of apoptotic pathways. Dose response curve of doxorubicin-induced cytotoxicity at 48 hour in E2F7KD MEKs which were transfected with either an E2F7b, or pcDNA3.1(+) control plasmid (A). Viability is plotted as percentage control (untreated). Quantitative data represent the mean ± SEM obtained from triplicate determinations of three independent experiments. Activation of caspase-3 was determined by immunoblotting extracts of vehicle treated and 0.3 μM doxorubicin treated E2F7 floxed and E2F7 deficient KCs (B). β-Actin is a loading control. Western blot figures are representative of three independent experiments. *, $P < 0.05$, ****, $P < 0.0001$. P value was calculated using Student's t test.

4.2.2 Dysregulation of E2F7 expression in human SCC cell lines contributes to insensitivity to the cytotoxic action of doxorubicin

It was previously shown that human SCCs overexpress E2F7 transcripts (Endo-Munoz, Dahler et al. 2009). Since we have shown that E2F7 overexpression can suppress sensitivity to doxorubicin in normal KCs, it is reasonable to speculate that the overexpression of E2F7, observed in human SCCs, may invoke insensitivity to doxorubicin. We screened a suite of 7 SCC cell lines: Cal27, Colo16, Detroit562, FaDu, KJDSV40, SCC15 and SCC25, as well as normal HEKs for their sensitivity to doxorubicin-induced cytotoxicity (*Figure 4.2A*). These studies identified variable responses of SCC cell lines to doxorubicin. In particular, KJDSV40 cell line exhibited the highest sensitivity to doxorubicin treatment with only 30% of cells remaining viable at 1 µM (*Figure 4.2A*). On the other hand, SCC25 cells displayed poor sensitivity where 80% of the cells were still viable at 1 µM (*Figure 4.2A*). Examination of E2F1 and E2F7 protein expression levels demonstrated that insensitive SCC25 cells had high levels of E2F7 to E2F1 whilst sensitive KJDSV40 cells had low levels of E2F7 relative to E2F1 (*Figure 4.2B*). Overall the insensitive SCC25 cells had 10-fold greater E2F7 expression relative to E2F1 than did sensitive KJDSV40 cells (*Figure 4.2B*). These data are consistent with our previous report on the relative mRNA expression levels in human SCC samples compared with normal human epithelium (Endo-Munoz, Dahler et al. 2009).

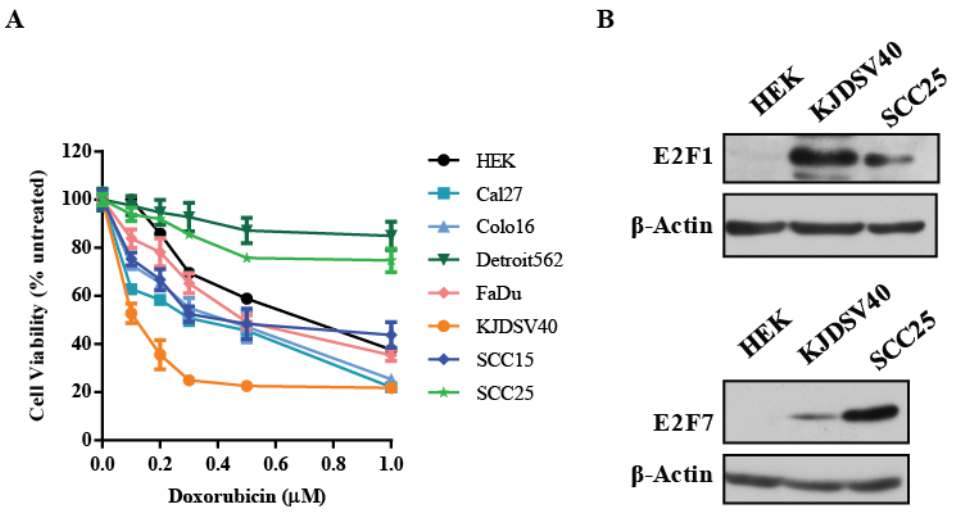

Figure 4.2 E2F7/E2F1 ratio is disrupted in SCC and contributes to doxorubicin sensitivity. HEK, Cal27, Colo16, Detroit562, FaDu, KJDSV40, SCC15 and SCC25 cells were treated with doxorubicin for 48 hours and viability plotted as percentage of untreated cells (A) Quantitative data represent the mean ± SEM obtained from triplicate determinations of three independent experiments. E2F1 and E2F7 protein expression was determined by immunoblotting extracts of HEK, KJDSV40 and SCC25 cell lines (B). β-Actin is provided as a loading control. Densitometric analysis of E2F1 and E2F7 in KJDSV40 and SCC25 cell

lines was quantified using ImageJ. Expression level was normalized against β-Actin and plotted as E2F7/E2F1 (B). Western blot figures are representative of three independent experiments.

Given that there is a close correlation between the level of E2F7 protein and sensitivity to doxorubicin in SCC cells, we sought to determine whether selective upregulation or reduction of E2F7 expression by expression plasmid or siRNA, respectively, would change the dose response profile of KJDSV40 and SCC25 cells to doxorubicin. Selective upregulation of E2F7 was achieved by transfecting KJDSV40 cells with E2F7 expression plasmid as evident by qRT-PCR and immunoblot results (*Figure 4.3A*). As a results, previously sensitive KJDSV40 cells became resistant to doxorubicin compared to vector only control cells when transfected with E2F7 expression plasmid (*Figure 4.3B*). To obtain efficient gene knockdown, we tested two different siRNAs. SCC25 cells were transfected with E2F7.siRNA1 and E2F7.siRNA2 constructs as well as control siRNA, and E2F7 transcript and protein levels were examined 48 hours post transfection. Results demonstrated that we were able to efficiently knockdown E2F7 transcript and E2F7 protein when transfected with E2F7.siRNA2 construct (*Figure 4.3C*). Results showed that silencing of E2F7 in insensitive SCC25 cells could enhance doxorubicin-induced cytotoxicity compared to control siRNA transfected SCC25 cells (*Figure 4.3D*). These data unequivocally demonstrate that resistance to doxorubicin is E2F7-dependent in SCC cells.

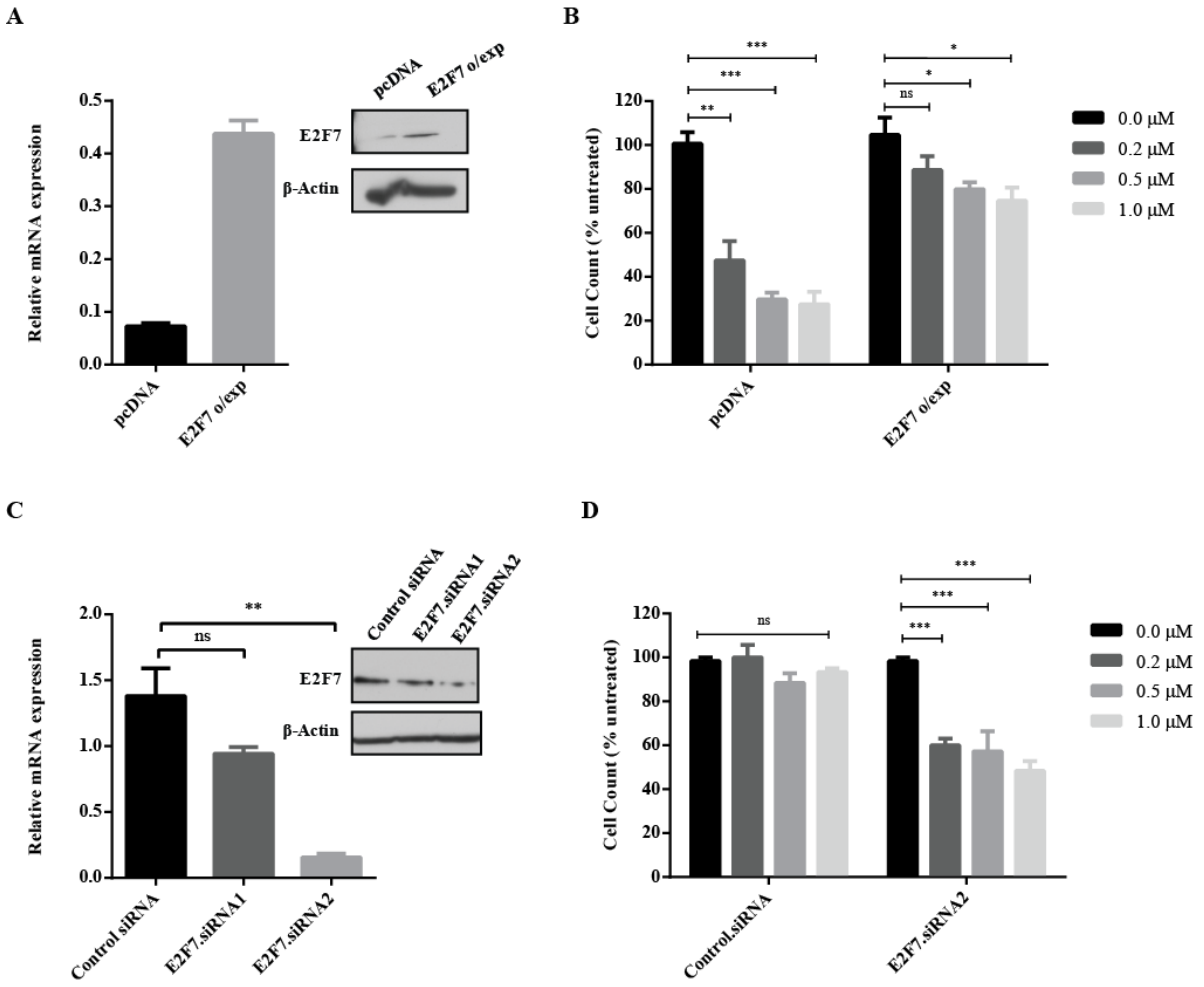

Figure 4.3 The sensitivity to doxorubicin is E2F7-dependent in SCC cells. KJDSV40 cells were transfected with E2F7b overexpression plasmid or pcDNA3.1(+) control plasmid, and E2F7 protein and transcript levels were determined by immunoblotting and qRT-PCR, respectively (A). SCC25 cells were transfected with siRNA-targeting E2F7 or a control siRNA, and E2F7 protein and transcript levels were determined by immunoblotting and qRT-PCR, respectively (C). In both instances (B and D), cells were left for 48 hours after transfection and then treated with 0, 0.2, 0.5 and 1 μM doxorubicin after which viability was estimated by trypan blue exclusion. Viability was expressed as percent viable cells and plotted as a percent untreated control. Quantitative data represent the mean ± SEM obtained from triplicate determinations of three independent experiments. Western blot figures are representative of three independent experiments for (A) and (C). β-Actin is provided as a loading control. Real time PCR data are the mean ± SEM of duplicate determinants normalized for expression of the housekeeping gene TBP; $n = 3$ for (A) and (C). *, $P \leq 0.05$, **, $P < 0.01$, ***, $P < 0.001$, ****, $P < 0.0001$. P value was calculated using Student's t test.

4.2.3 Microarray experimental design

We performed transcriptomic analyses and generated transcriptomic profiles for differentially expressed transcripts between two different SCC cell lines. This allowed us to identify genes

regulated by E2F7 that contribute to chemoresistance seen in SCC. *Table 4.1* summarises the cell lines used and their E2F7 and sensitivity status.

Table 4.1 Table of cell lines used in transcriptomics analysis.

	KJDSV40	SCC25
E2F7/E2F1 ratio	Low	High
Doxorubicin sensitivity	sensitive	insensitive

Before proceeding with the microarray experiments, we conducted time-course experiments where KJDSV40 and SCC25 cells were treated with 1 μM of doxorubicin and RNA was harvested at 4, 8, 16, 24 and 48 hours post-treatment for qRT-PCR analysis in order to optimise the time points when the transcriptional effects are fully evident. Moreover, selecting the right time point will further ensure transcriptional changes to be measured before the onset of indirect transcriptional effects through an E2F1 feedback loop. Therefore, we identified a time point at which E2F7 transcript reaches its maximum levels without yet reducing transcript levels of E2F1. As demonstrated in *Figure 4.2B*, KJDSV40 cells express high levels of E2F1 and almost no E2F7 protein. Moreover they respond to the effects of doxorubicin with a significant reduction in cell survival. Upon treatment with 1 μM doxorubicin, E2F1 transcript levels remained the same during the course of treatment (*Figure 4.4A*) in KJDSV40 cells. On the other hand, there was a time-dependent decrease in E2F7 transcript levels, where the most significant reduction observed was following 24 hours treatment with 1 μM doxorubicin. Time-course analysis of the response of SCC25 cells to doxorubicin treatment demonstrated that E2F7 reaches its maximum levels after 24 hours of treatment with 1 μM doxorubicin, whilst there is no significant change in E2F1 transcripts levels at any of the time points examined (*Figure 4.4B*). On the basis of these findings, 24 hour time point was chosen for the treatment of cells with 1 μM doxorubicin prior to RNA extraction and subsequent microarray experiments.

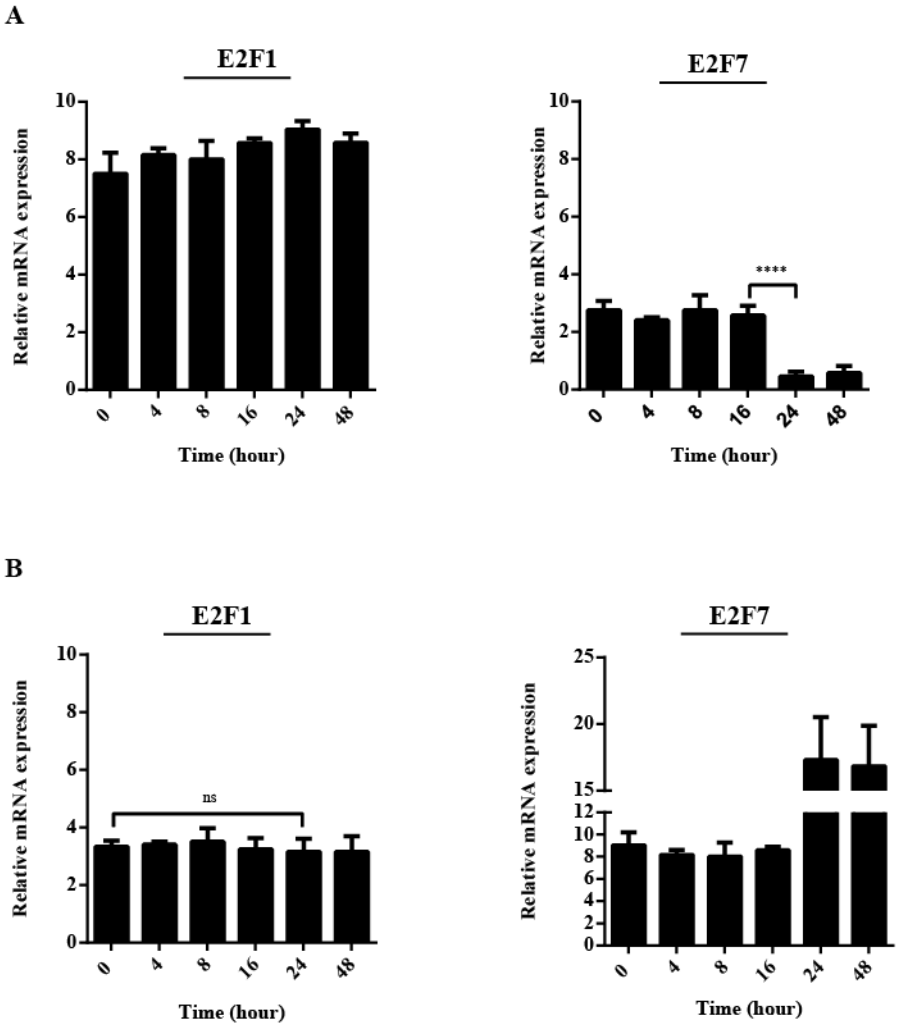

Figure 4.4 Time-course of E2F1 and E2F7 expressions. 0, 4, 8, 16, 24 and 48 hours after treatment with 1 µM doxorubicin, RNA was extracted, and E2F1 and E2F7 expressions were analysed by qRT-PCR. Shown are graphs for qRT-PCR results for E2F1 (left) and E2F7 (right) expressions in KJDSV40 cells (A), and E2F1 (left) and E2F7 (right) expression in SCC25 cells (B). mRNA expression is in arbitrary units normalised for expression of the housekeeping gene TBP; $n = 3$. ns is not significant. **** is $P < 0.0001$. P value was calculated using Student's t test.

Duplicate SCC cultures were established and RNA was harvested. RNA of biological replicates was pooled to account for the biological variations expected under standard tissue culture conditions. The RNA analysed were described in *Figure 4.5*. Briefly, where KJDSV40 cells were transfected, two different strategies were taken. KJDSV40 cells were either transfected with 3 µg of E2F7 expression plasmid for selective upregulation since these cells do not express high levels of E2F7 or with equal concentration of control plasmid (pcDNA3.1(+)). RNA was collected 48 hours post-transfection. Where KJDSV40 cells

treated with doxorubicin following transfection or not, cells were treated with doxorubicin for 24 hours and then subjected to RNA isolation.

Where SCC25 cells were transfected two different strategies were taken. SCC25 cells were either transfected with 40 nM of siRNA targeting E2F7 for selective downregulation since these cells express high levels of E2F7 or with equal concentration of control siRNA. RNA was collected 48 hours post-transfection. Where SCC25 cells treated with doxorubicin following transfection or not, cells were treated with doxorubicin for 24 hours and then subjected to RNA isolation.

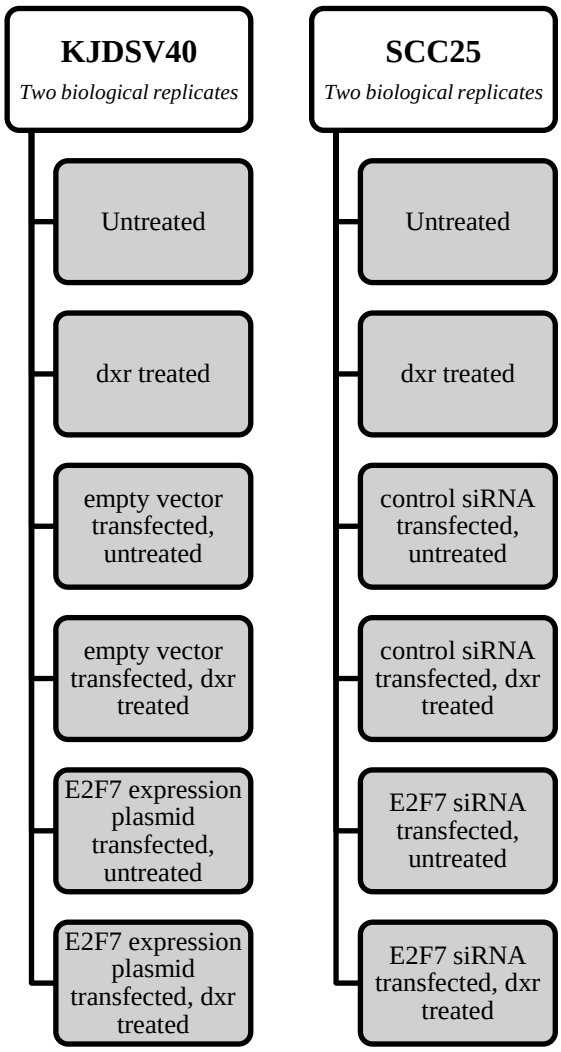

Figure 4.5 Sample preparation workflow for microarray analysis. Independent duplicate samples of RNA were isolated from cells. Subconfluent KJDSV40 cells were treated with 1 μM dxr for 48 hours. KJDSV40 cells were transfected with either 3 μg E2F7 expression plasmid or equivalent concentration of control (empty) vector. KJDSV40 cells were first transfected as described and then treated with dxr as described. Subconfluent SCC25 cells were treated with 1 μM dxr for 48 hours. SCC25 cells were transfected with either 40 nM

E2F7 siRNA or equivalent concentration of control siRNA. SCC25 cells were first transfected as described and then treated with dxr as described. dxr is doxorubicin.

Detailed methodological information including RNA preparation, RNA quality control, generation of biotinylated amplified cRNA for microarray hybridisation, microarray hybridisation and microarray analysis is available in *Section 2.8 Microarray Analysis*. Raw microarray data was normalised and analysed as pairwise comparisons to identify differentially expressed genes. Specifically, we generated transcriptomic profiles for differentially expressed transcripts between KJDSV40 and SCC25, and any genes co-regulated in these groups represented as List X (*Figure 4.6*). This strategy was taken based on previously demonstrated data in this chapter that KJDSV40 cells expressed very low levels of E2F7 and were sensitive to the effects of doxorubicin whereas SCC25 cells express greater than 10 fold more E2F7 and are insensitive to doxorubicin. Genes which were up-regulated in KJDSV40 cells and genes which were down-regulated in SCC25 cells formed this list. The second list of differentially expressed genes, representing List Y, were generated following comparisons between SCC25 cells and SCC25 cells in which E2F7 had been silenced with siRNA (*Figure 4.6*) (genes were regulated in the same direction). Any genes that were regulated in the same direction (up-regulated or down-regulated) by control siRNA and by E2F7.siRNA were excluded from List Y for further analysis. List Y genes were cross-referenced against List X to identify E2F7-modulated transcripts. This list of genes will be referred to as List A (*Figure 4.6*). E2F7 is known to regulate many genes involved in cell cycle traverse that are unlikely to be involved in chemosensitivity. Thus, it was important to design the microarray experiments in such a way that genes unlikely to be associated with doxorubicin-mediated chemoresistance could be excluded from the analysis. Therefore, in order to identify E2F7-regulated transcripts that may modulate sensitivity to doxorubicin, we generated a new list of genes (List Z) from a comparison between SCC25 cells and SCC25 cells in which E2F7 had first been silenced and then treated with 1 μM of doxorubicin (*Figure 4.6*). List Z was cross-referenced with genes generated in List Y, co-regulated genes representing List B (*Figure 4.6*). List B identified E2F7-modulated transcripts in modulating sensitivity to doxorubicin. Noticeably, all candidate genes identified in List A as differentially regulated by E2F7 were represented in List B (*Figure 4.6*), confirming the practical validity of the microarray design. Finally, combining genes generated in List A and List B allowed for the identification of genes which are downstream effectors of E2F7-dependent cytotoxic sensitivity.

It should be noted that the pairwise comparisons between KJDSV40 cells and KJDSV40 cells in which E2F7 had been overexpressed failed to detect E2F7 as one of the significantly overexpressed genes. As a consequence, data from KJDSV40 cells, except the data from untreated KJDSV40, was excluded from the resultant list for further analysis. Therefore, only the comparisons represented in *Figure 4.6* were considered in microarray analysis.

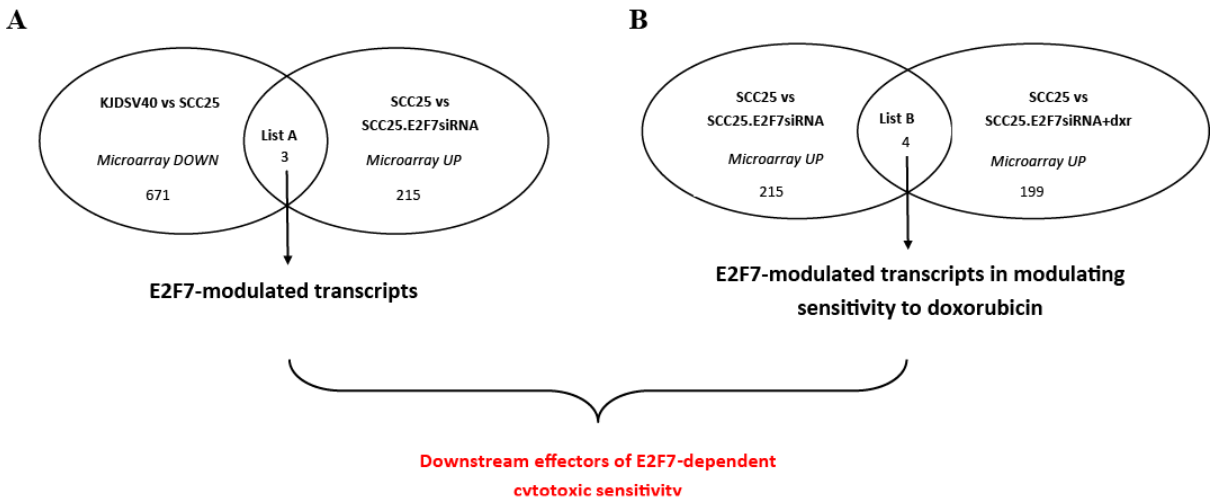

Figure 4.6 Summary of microarray analysis strategy used to enrich for differentially expressed genes. Transcriptomic profiles were generated from each comparisons presented above. Any genes that were regulated in the same direction by control siRNA in SCC25 cell line in which E2F7 was silenced by siRNA were excluded from further analysis. The lists of differentially expressed genes, List A (A) and List B (B), were combined, representing downstream effectors of E2F7-dependent cytotoxic sensitivity genes.

Table 4.2 Differentially expressed genes identified as E2F7-dependent cytotoxic sensitivity genes. Statistical cutoffs of greater than ±1-fold change and B-value greater than 3 have been applied as criteria for inclusion in this list. Negative fold change indicates a decrease in expression. B-value is a measure of statistical significance, with a B-value greater than 3 indicating 95% chance of the gene being differentially expressed. Sphk1 and RacGAP1 were selected for further analysis.

Gene name	**Entrez ID**	**Fold change** ***KJDSV40 vs SCC25***	**B-value** ***KJDSV40 vs SCC25***	**Fold change** ***SCC25 vs SCC25. E2F7si RNA***	**B-value** ***SCC25 vs SCC25. E2F7si RNA***	**Fold change** ***SCC25 vs SCC25.E2F7siRNA+ doxorubicin***	**B-value** ***SCC25 vs SCC25.E2F7siRNA+ doxorubicin***
CD44	960	-1.7	15.6	1.34	12.3	1.0	8.1
RRP8	23378	-1.16	13	1.17	13.9	1.0	11.5
Sphk1	8877	-1.22	3.2	1.16	3	1.2	3.6
RacGAP1	29127			1.3	11	1.9	17

We were able to identify 4 genes, *CD44*, *RRP8*, *SPHK1*, *RACGAP1*, following stringent analysis (*Table 4.2*). Genes had to be up- or down-regulated by at least 1-fold in both the groups compared to be reported for differential expression, with a B-value of at least 3 in both groups compared (*Table 4.2*). The B-value was calculated as a measure of the likelihood a gene is truly expressed, where a value greater than 3 corresponding to 95% likelihood of differential expression. Microarray data has been deposited to gene expression omnibus (GEO) under the reference GSE58074.

Real time PCR analysis of these four genes was undertaken to validate the results of the microarray analysis. Indeed, all of the genes found by microarray analysis to be differentially expressed could be confirmed by PCR. Moreover, induction of all four genes was confirmed in SCC25 cells compared with KJDSV40 cells (*Figure 4.7*). In addition, induction of all four genes modulated by E2F7 observed by microarray was also confirmed using real time PCR in SCC25 in which E2F7 had been depleted compared to SCC25 cells (*Figure 4.7*).

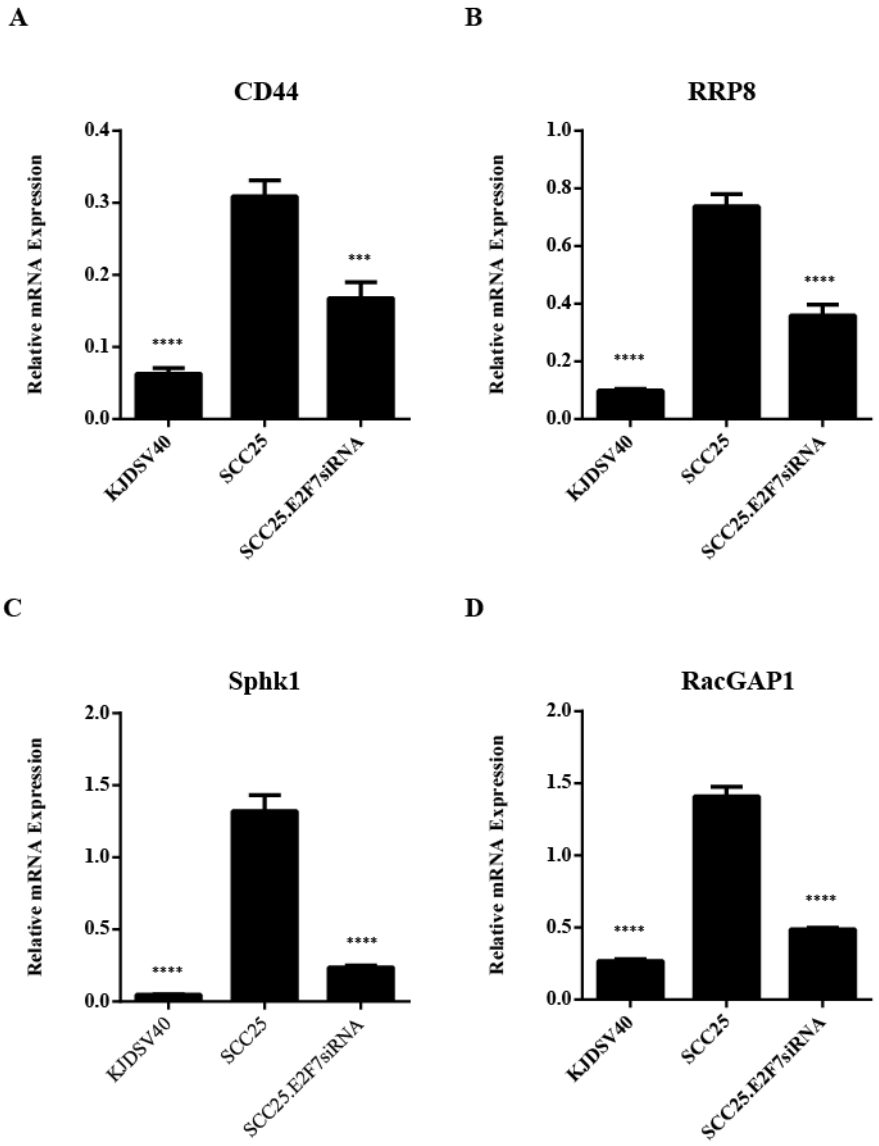

Figure 4.7 Microarray results were validated by qRT-PCR analysis. Quantitative RT-PCR was used to determine the expression of CD44 (A), RRP8 (B), Sphk1 (C) and RacGAP1 (D) transcripts using cDNA from KJDSV40 cells, SCC25 cells and SCC25 cells in which E2F7 had been depleted by siRNA. Data are the mean ± SEM of duplicate determinants normalized for expression of the housekeeping gene TBP; $n = 3$. ***, $P < 0.001$ versus SCC25, ****, $P < 0.0001$ versus SCC25. P value was calculated using Student's t test.

Some of the differentially expressed genes, CD44 and Sphk1, were known to be involved in chemotherapeutic sensitivity, whilst the association of others, RRP8 and RacGAP1, appear novel. CD44 is one of the well established cancer stem cell markers and already examined in detail in several other studies. Although RRP8 is of one of the novel transcripts identified in our microarray experiments, it was not examined further due to lack of commercially available reagents and antibodies. On the other hand, Sphk1 was selected to be investigated further for E2F7-mediated chemosensitivity, on the basis of an existing literature reporting

Sphk1 upregulation in SCC and the availability of pharmacological inhibitors. RacGAP1 identified from microarray was also selected for further analysis as a potential mediator of E2F7-dependent cytotoxic responses in SCC due to its novelty.

4.3 Discussion

In this chapter we used transcriptomic profiling to identify 4 potential downstream effectors of E2F7-dependent doxorubicin resistance. It has been shown that some apoptotic responses are regulated by E2F in an E2F isoform-specific manner (Kwong, Nguyen et al. 2003; Li, Ran et al. 2008; Endo-Munoz, Dahler et al. 2009). In this regards, the overexpression of E2F7 seen in SCC patients (100 fold overexpression) supports the idea that E2F7 overexpression could confer resistance to the apoptotic effects of chemotherapy in SCC. Significantly, the E2F7-selective action appears to be restricted to the anthracyclines which suggests that if we identify ways to manipulate the E2F7 effectors they may allow us to use anthracyclines to treat SCC. The antiapoptotic function of E2F7 is well-documented and is reported to be due to the inhibition of E2F1-induced apoptosis. To this end, our data indicates that the ratio of E2F7 relative to E2F1 protein closely correlates with sensitivity to doxorubicin in SCC cells and KCs. Recent global profiling of gene expression changes in E2F7 KO embryos identified stress responses as being regulated by E2F7. Although, dysregulation of apoptosis is common in SCC, it is incomplete and hence SCC cells retain a capacity for apoptosis under certain circumstances (Dahler, Rickwood et al. 2007; Endo-Munoz, Dahler et al. 2009). Thus, it is tempting to speculate that it is possible to target E2F7 and sensitise SCC to the cytotoxic actions of doxorubicin by targeting downstream effectors of E2F7.

In this chapter I identified *CD44, RRP8, SPHK1 and RACGAP1* as potential downstream effectors of E2F7-dependent doxorubicin sensitivity. Significantly, all 4 genes showed excellent concordance with the microarray data, evaluated by qRT-PCR. Sphk1 and RacGAP1 were deemed suitable for further study to evaluate whether they play a role in E2F7-mediated resistance to doxorubicin. I will explore the potential role of Sphk1 and RacGAP1 in *Chapters 5* and *Chapter 6*.

4.3.1 Sphingosine kinase 1 and Rac GTPase activating protein 1 in SCC

Sphingosine kinase 1 (Sphk1) is a kinase responsible for the conversion of sphingosine to sphingosine-1-phosphate (S1P) (Shida, Takabe et al. 2008; Fyrst and Saba 2010; Pyne and

Pyne 2010). Interrogation of publicly available microarray data (www.oncomine.org) shows statistically significant increases in Sphk1 expression in a number of solid tumours, including breast, colon, lung, ovary, prostate, melanoma, stomach, uterus as well as squamous cell carcinoma and it's precursor actinic keratosis. Importantly, Sphk1 has been shown to modulate proliferation, differentiation and apoptosis in KCs (Facchinetti, Gandini et al. 2010). Facchinetti and colleagues recently reported that Sphk1 is overexpressed in malignant oral epithelia compared with nonmalignant tissue, and the expression of Sphk1 was correlated with poor prognosis, shorter patient survival and loss of p21 expression in HNSCC (Facchinetti, Gandini et al. 2010). Of relevance to the present study, Bonhoure and colleagues reported that forced expression of Sphk1 led to resistance to doxorubicin- and etoposide-induced cell death in HL-60 leukemia cells (Bonhoure, Pchejetski et al. 2005), and degradation of Sphk1 resulted in induction of apoptosis in MCF7 breast cancer cells treated with doxorubicin (Sarkar, Maceyka et al. 2005). Therefore, this could, in part, explain why Sphk1 was detected in our microarray analysis as one of the differentially expressed genes is doxorubicin sensitive KJDSV40 cells. Sphk1 activity *in vitro*, in HNSCC patient samples and *in vivo* will be examined in the next chapter.

Rac GTPase activating protein (**RacGAP1**) is an evolutionarily conserved GAP protein towards Rho family GTPases. It plays a crucial role in cytokinesis and is essential for the induction and completion of cytokinesis, thus RacGAP1 depletion results in impairment of cell division *in vitro* and *in vivo* (Nishimura, Oki et al. 2013). RacGAP1 is also involved in IL6-induced macrophage differentiation, nuclear transport of STAT3/5 transcription factors and STAT3 activation by forming a complex with Rac1 and STAT3 (Kawashima, Hirose et al. 2000; Tonozuka, Minoshima et al. 2004). A positive correlation between RacGAP1 and a known proliferation marker Ki67 has been reported (Saigusa, Tanaka et al. 2014). Moreover, RacGAP1 has been shown to contribute to cancer progression through PRC1 by enhancing cell motility, proliferation and survival (Wang, Ooi et al. 2011). PI3K/AKT signalling pathway was among the most significantly altered canonical pathways following the silencing of RacGAP1 expression in hepatocellular carcinoma cells (Wang, Ooi et al. 2011). To the best of our knowledge, RacGAP1 has not been implicated in squamous cell carcinoma before. However, the clinical significance of RacGAP1 has been reported in several malignancies including meningioma, breast cancer, nonsmall-cell lung cancer and hepatocellular carcinoma (Fritz, Brachetti et al. 2002; Wang, Ooi et al. 2011; Ke, Ke et al. 2013; Kotoula, Kalogeras et al. 2013; Pliarchopoulou, Kalogeras et al. 2013). Moreover, high

RacGAP1 mRNA levels were significantly associated with tumour recurrence and poor prognosis in meningiomas (Ke, Ke et al. 2013). Therefore, upregulation of RacGAP1 in SCC25 cells could be clinically relevant and involved in doxorubicin resistance. These possibilities will be investigated using *in vitro* and *in vivo* approaches in the final results chapter of this thesis.

CHAPTER FIVE

5 Sphingosine kinase 1 is a novel downstream effector of E2F7 and regulates doxorubicin sensitivity in squamous cell carcinoma

5.1 Foreword

All of the experimental data of this chapter were presented in a manuscript which has been published in *Clinical Cancer Research* (Hazar-Rethinam, Merida de Long et al. 2014) and a PDF version of the paper is inserted in the next section of this chapter. It is then followed by supplementary figures that accompany the published version of the manuscript. Detailed materials and methods for these experiments have been included in Chapter 2.

5.2 A novel E2F/Sphingosine kinase 1 axis regulates anthracycline response in squamous cell carcinoma

A novel E2F/Sphingosine kinase 1 axis regulates anthracycline response in squamous cell carcinoma

Mehlika Hazar-Rethinam[1], Lilia Merida de Long[1], Orla M. Gannon[1], Eleni Topkas[1], Samuel Boros[2], Ana Cristina Vargas[2], Marcin Dzienis[3], Pamela Mukhopadhyay[1,*], Fiona Simpson[1], Liliana Endo-Munoz[1], and Nicholas A. Saunders[1]

Authors' Affiliations: [1]Epithelial Pathobiology Group, University of Queensland Diamantina Institute, Princess Alexandra Hospital, Translational Research Institute, Woolloongabba, Queensland, Australia, [2]Department of Pathology and [3]Department of Medical Oncology, Princess Alexandra Hospital, Woolloongabba, Queensland, Australia, *Current address: The QIMR Berghofer Medical Research Institute, Brisbane, Queensland, Australia

Running Title: A novel E2F/Sphk1 axis regulates doxorubicin sensitivity

Keywords: squamous cell carcinoma, E2F7, Sphk1, chemosensitivity

Grant Support

NS and LEM are supported by grants from the Australian NHMRC (#APP1049182) and the Cancer Council Queensland (#APP1025479). NS is supported by a Senior Research Fellowship awarded by the Cancer Council Queensland. OG is supported by a grant from the Wesley Medical Research Institute. MHR and ET are supported by an Australian Postgraduate Award.

Corresponding Author: Nicholas Saunders, Epithelial Pathobiology Group, University of Queensland Diamantina Institute, Princess Alexandra Hospital, Translational Research Institute, 37 Kent St, Woollongabba, Queensland, Australia, 4102. Phone: +61 (0)7 3443 7098; Fax: +61 (0)7 3443 6966; E-mail: nsaunders@uq.edu.au

Disclosure of Potential Conflicts of Interest

No potential conflicts of interest were disclosed.

Authors' Contributions

Conception and design: M. Hazar-Rethinam, N.A. Saunders

Development of methodology: M. Hazar-Rethinam

Acquisition of data (provided animals, acquired and managed patients, provided facilities, etc.): M. Hazar-Rethinam, S. Boros, A.C. Vargas, M. Dzienis

Analysis and interpretation of data (e.g., statistical analysis, biostatistics, computational analysis): M. Hazar-Rethinam, N.A. Saunders

Writing, review, and/or revision of the manuscript: M. Hazar-Rethinam, F. Simpson, L. Endo-Munoz, N.A. Saunders

Administrative, technical, or material support (i.e., reporting or organizing data, constructing databases): M. Hazar-Rethinam, L. Merida de Long, P. Mukhopadhyay, O.M. Gannon, E. Topkas, N.A. Saunders

Study supervision: N.A. Saunders

Abstract

Purpose: Head and neck squamous cell carcinomas (HNSCC) are frequently drug resistant and have a mortality rate of 45%. We have previously shown that E2F7 may contribute to drug resistance in SCC cells. However, the mechanism and pathways involved remain unknown.

Experimental Design: We used transcriptomic profiling to identify candidate pathways that may contribute to E2F7-dependent resistance to anthracyclines. We then manipulated the activity/expression of the candidate pathway using overexpression, knockdown and pharmacological inhibitors in *in vitro* and *in vivo* models of SCC to demonstrate causality. In addition, we examined the expression of E2F7 and a downstream effector in a tissue microarray (TMA) generated from HNSCC patient samples.

Results: E2F7-deficient keratinocytes were selectively sensitive to doxorubicin and this was reversed by overexpressing E2F7. Transcriptomic profiling identified Sphingosine kinase 1 (Sphk1) as a potential mediator of E2F7-dependent drug resistance. Knockdown and overexpression studies revealed that Sphk1 was a downstream target of E2F7. TMA studies showed that E2F7 overexpression correlated with Sphk1 overexpression in human HNSCC. Moreover, inhibition of Sphk1 by shRNA or the Sphk1 specific inhibitor, SK1-I (BML-EI411), enhanced the sensitivity of SCC cells to doxorubicin *in vitro* and *in vivo*. Furthermore, E2F7 induced doxorubicin resistance was mediated *via* Sphk1-dependent activation of AKT *in vitro* and *in vivo*.

Conclusion: We identify a novel drugable pathway in which E2F7 directly increases the transcription and activity of the Sphk1/S1P axis resulting in activation of AKT and subsequent drug resistance. Collectively, this novel combinatorial therapy can potentially be trialed in humans using existing agents.

Translational Relevance

Head and neck squamous cell carcinoma (HNSCC) is one of the most prevalent cancers diagnosed worldwide. Current chemotherapies are not considered a curative option for HNSCC. Thus, there is a need for new and selective therapies. In this regard, the E2F family of transcription factors has been shown to contribute to the development and maintenance of HNSCC. However, E2F-based therapies are currently not available. To circumvent this problem we embarked on a transcriptomics screen to identify factors that were responsible for E2F7-dependent resistance to anthracyclines in HNSCC. The present study demonstrates that E2F7 directly controls the expression of Sphk1 resulting in increases in AKT phosphorylation which drives drug resistance. Thus, we have identified a previously undescribed E2F7/Sphingosine kinase 1/Sphingosine-1-phosphate/AKT axis that contributes to anthracycline resistance in HNSCC. A significant implication of this finding is that combining an anthracycline with a Sphk1 inhibitor may provide a curative option for treating HNSCC.

Introduction

Head and neck squamous cell carcinomas (HNSCC) arise from stratified squamous epithelia of the mucosae of the upper aerodigestive tract. At present the mainstay of treatment for advanced HNSCC is surgery and/or radiation plus adjuvant chemotherapy (1). The use of adjuvant chemotherapy provides modest improvements to overall survival but are not considered curative in their own right (1). Thus, if we are to improve outcomes in patients with advanced HNSCC we need to develop systemic therapies that target novel pathways activated in HNSCC cells.

HNSCC is a complex cancer associated with a large mutational burden (2, 3) and accompanied by dysregulation of proliferation, differentiation and apoptosis. HNSCC is also accompanied by dysregulation of the main functions of the E2F transcription factor family (4, 5). E2F refers to a family of 10 gene products from 8 genes (E2Fs 1, 2, 3a, 3b, 4, 5, 6, 7a, 7b, 8) that have been broadly divided into activators (E2F1-E2F3a) and inhibitors (E2F3b and E2F4-E2F8) (6). The E2F family regulates a diverse array of functions such as proliferation, differentiation, apoptosis and stress responses (7, 8). The way in which the E2F family co-ordinate such diversity of action is through isoform specific functions of the individual E2Fs (e.g. activators *vs* inhibitors) coupled with context-specific interacting partner proteins such as pocket proteins and HDACs (7, 8). In the context of keratinocytes (KCs), it has been shown that normal human and murine KCs express all members of the E2F family with the exception of E2F6 (9, 10). It has been shown that proliferation and differentiation of KCs is regulated by the opposing actions of E2F1 and E2F7 (4, 9, 11, 12). Significantly, E2F1 and E2F7 are overexpressed in patient SCCs (10) and contribute to the development of cutaneous SCC (13, 14).

In addition, to the role of E2Fs in proliferation and differentiation, E2Fs are also key regulators of apoptosis and stress responses (7, 8). For example, E2F1 has been shown to have potent pro-apoptotic actions that regulate the numbers of thymic lymphocytes (15). Intriguingly, E2F1 mediated-apoptosis has been reported to be *via* p53-dependent and p53-independent pathways (16) suggesting that cellular context may determine the mechanism by which E2F1 induces apoptosis. More recently, E2F7 was reported to antagonise the pro-apoptotic actions of E2F1 in the context of etoposide or doxorubicin induced DNA damage (10, 17). Thus, the ratio of E2F1 to E2F7 determines apoptotic responses. However, the mechanism by which E2Fs control apoptotic responses remains unknown. In the present study, we examined downstream effectors of E2F7 that modulate resistance to chemotherapy. We now identify a previously undescribed E2F7/Sphk1/S1P/AKT axis that contributes to anthracycline resistance in SCC. In addition, we identify a novel drug combination that could represent a potentially curative option for advanced SCC.

Materials and Methods

Animal studies

All animal experiments were approved by the Institutional Animal Ethics Committee. *E2F7*$^{Flox/Flox}$, *E2F8*$^{Flox/Flox}$ and *E2f1* KO mice have been described (15, 18). FVB X C57BL/6 crosses were generated in house. *In vivo* tumour studies used female nonobese diabetic/severe combined immunodeficient (NOD/SCID).

Reagents and viability assays

The following drugs were purchased; doxorubicin (Sigma Aldrich), SK1-I (BML-EI411) (Enzo Life Sciences), S1P (Cayman Chemicals). Stocks of BGT226 were prepared as described (19). Viability was determined using trypan blue, Cell Titer 96 Aqueous One Solution Cell Proliferation Assay (Promega), or western blot for cleaved caspase 3 or PARP cleavage as described (20, 21). Sphk1 activity and S1P levels were estimated using commercially available kits (Echelon Biosciences).

Tissue culture and adenovirus infection

Murine epidermal keratinocytes (MEKs) and human epidermal keratinocytes (HEKs) were isolated and cultured as described (22, 23). SCC25 cells were obtained from the American Type Culture Collection. FaDu was a kind gift from Dr. Elizabeth Musgrove (Garvan Institute, New South Wales, Australia) and were verified by short tandem repeat genotyping (11). KJDSV40 cells were maintained as described previously (11). To generate E2F7 and E2F8 KO keratinocytes, we incubated MEKs with ready-to-use Ad-CMV-Cre as per manufacturer's recommendations (MOI of 50) (Vector Biolabs).

Gene expression studies

Total RNA was isolated, cDNA prepared and quantitative reverse transcriptase PCR (qRT-PCR) performed as described (10, 24). For microarray analysis, complementary RNA was generated with the Illumina TotalPrep RNA Amplification Kit and hybridised with Illumina HumanHT-12 v4 Expression BeadChips (Illumina) as per manufacturer's protocol. Expression data from the microarrays was analysed as previously described (25). The microarray data reported in this article have been deposited in NCBI's Gene Expression Omnibus (GEO) database under the accession number GSE58074. Chromatin immunoprecipitation (ChIP) was conducted using the SimpleChIP Enzymatic Chromatin IP Kit (Magnetic Beads) (Cell Signaling) in accordance with the manufacturer's instructions.

shRNA studies, siRNA delivery and transfections

Control and overexpression plasmids and siRNAs used for manipulating E2F7 have been described previously (10, 17). SureSilencing shRNA plasmids directed against Sphk1 were purchased from SuperArray Bioscience Corp. A Sphk1 expression (TrueORF Gold Clones) and control plasmids were purchased from OriGene Technologies.

Immunoblot

The following primary antibodies were used: E2F-1 (C-20) 1:1,000 (Santa Cruz), Anti-E2F7 1:2,000 (Abcam), cleaved caspase-3 (Asp 175) 1:1,000 (Cell Signaling), Anti-SPHK1 1:1,000 (Sigma), PARP 1:1,000 (Cell Signaling), phospho-Akt (Ser473) (D9E) XP 1:2,000 (Cell Signaling), Akt 1:2,000 (Cell Signaling), and β-actin 1:10,000 (Sigma Aldrich). Where a western blot has been quantitated, results represent relative protein levels normalised to β-actin as quantified by Image J (Wayne Rasband, National Institutes of Health, USA).

Immunohistochemistry and tissue microarrays

Immunohistochemistry was conducted as described (20, 21). The following primary antibodies were used: PCNA 1:3,000 (Sigma Aldrich), cleaved caspase-3 (Asp 175) 1:50 (Cell Signaling), phospho-Akt (Ser473) (D9E) XP 1:50 (Cell Signaling). Secondary antibody was Starr Trek Universal HRP Detection System followed by colorimetric immunohistochemical staining with Cardassian DAB Chromogen as per manufacturer's instructions (Biocare Medical). TMAs were generated using duplicate 1 mm cores of matched a) adjacent normal tissue, b) primary HNSCC lesion and c) matched metastatic lymph node from patients treated for HNSCC at the PAH. Immunohistochemistry was conducted using Dako EnVision + System-HRP (DAB) kit in accordance with the manufacturer's instructions. Sections were incubated with Anti-E2F7 1:250 (Abcam) and Anti-SPHK1 1:75 (Sigma Aldrich) antibodies. Staining intensity was evaluated by two Pathologists in a blinded fashion using a modified quickscore method as described (26).

Statistical analysis

Statistical significance was calculated by a Student's *t* test with a 95% confidence level using GraphPad Prism v5 (GraphPad software).

Results

E2F7 selectively regulates cytotoxic responses to doxorubicin in KCs

To examine the downstream pathways involved we generated primary cultures of MEKs from *E2f1* KO mice (15), or from *E2f7*$^{Flox/Flox}$ or *E2f8*$^{Flox/Flox}$ mice (18). We generated *E2f7*, and *E2f8* knock down (KD) MEKs *via* adenovirus (Ad) mediated Cre deletion of floxed sequences in primary KCs isolated from *E2f7* and *E2f8* floxed mice. *E2f1* gene expression levels in KCs isolated from conventional *E2f1*KO mice were reduced by 70% whilst *E2f7* and *E2f8* mRNA expression was reduced more than 90% following 48 hour infection of the cognate floxed KCs with Ad-CMV-Cre (Figure S1). The reduction in *E2f1* expression was less than expected but sequencing confirmed the PCR product was *E2f1*. Significantly, infection with an empty Ad viral vector did not alter cell viability, mRNA expression, differentiation-competence or cytotoxic responses to UVB, doxorubicin or cisplatin (Figure S2).

We examined the dose-dependent cytotoxic profiles of uninfected control, *E2f7* KD, *E2f8* KD and *E2f1*KO cells to increasing concentrations of doxorubicin (0-1 μM) for 48 hours. *E2f7* deficient MEKs were hypersensitive to the cytotoxic actions of doxorubicin (Figure 1A) or another anthracycline, epirubicin (Figure S3A). Significantly, *E2f7* deficiency only had minimal effect on cisplatin sensitivity (Figure S3B) and no impact on etoposide sensitivity (Figure S3C). *E2f8* had no effect on cytotoxic responses to any of the drugs (Figures 1A and S3) whilst *E2f1* deficiency resulted in modest protection against doxorubicin-induced cytotoxicity (Figure 1A). To confirm that the effect of *E2f7* deficiency was attributable to *E2f7* we reintroduced *E2f7* into *E2f7*-deficient KCs to confirm that it suppressed doxorubicin sensitivity. Reintroduction of *E2f7* into *E2f7* deficient MEKs resulted in a 2.5 fold increase in E2F7 mRNA expression determined by qRT-PCR and was sufficient to re-instate

doxorubicin resistance (Figure 1B). We then determined whether *E2f7*-mediated reduction in cell survival is due to activation of apoptotic pathways. Uninfected control MEKs isolated from floxed *E2f7* mice showed a modest increase in cleaved caspase-3 levels after 48 hours treatment with 0.3 μM doxorubicin (Figure 1C). In contrast, there was a profound activation of caspase-3 when *E2f7* deficient MEKs were treated with 0.3 μM doxorubicin (Figure 1C). Combined, these data identify a unique and isoform-specific function of *E2f7* in modulating sensitivity to anthracyclines in KCs.

Dysregulation of E2F7 expression in human SCC cell lines contributes to insensitivity to the cytotoxic action of doxorubicin

It is reasonable to speculate that the overexpression of E2F7, observed in human SCCs (10), may invoke insensitivity to doxorubicin. We screened a suite of SCC cell lines (FaDu, KJDSV40 and SCC25) as well as normal human epidermal keratinocytes (HEKs) for their sensitivity to doxorubicin-induced cytotoxicity (Figure 1D). These studies showed that KJDSV40 cell lines were the most sensitive to doxorubicin treatment with 70% reduction in cell viability at 1 μM (Figure 1D). On the other hand, SCC25 cells displayed the least sensitivity where 80% of the cells were still viable at 1 μM (Figure 1D). Examination of E2F1 and E2F7 protein expression levels demonstrated that insensitive SCC25 cells had high levels of E2F7 to E2F1 whilst sensitive KJDSV40 cells had low levels of E2F7 relative to E2F1 (Figure 1E). Overall the insensitive SCC25 cells had 10 fold greater E2F7 expression relative to E2F1 than did sensitive KJDSV40 cells. It was not possible to generate values for the HEKs due to their low levels of expression of E2F1 and E2F7.

We next sought to determine whether selective upregulation or reduction of E2F7 expression by expression plasmid or siRNA (validation of siRNA is shown in Figure S4A), respectively,

would change the dose response profile of KJDSV40 and SCC25 cells to doxorubicin. Results showed that previously sensitive KJDSV40 cells became resistant to doxorubicin compared to vector only control cells when transfected with E2F7 expression plasmid (Figure 1F). In contrast, silencing of E2F7 in insensitive SCC25 cells resulted in a 2.2 fold reduction in E2F7 mRNA expression determined by qRT-PCR and could enhance doxorubicin-induced cytotoxicity compared to control siRNA transfected SCC25 cells (Figure 1G). These data unequivocally demonstrate that resistance to doxorubicin is E2F7-dependent in SCC cells.

Sphingosine kinase 1 (Sphk1) is a downstream effector of E2F7-mediated suppression of doxorubicin-induced cytotoxicity

To identify the downstream effectors of E2F7 in SCC cells, we generated transcriptomic profiles for differentially expressed transcripts between the KJDSV40 cells (sensitive and low E2F7/E2F1 ratio) and SCC25 cells (insensitive and high E2F7/E2F1 ratio). We also generated a list of upregulated genes between SCC25 cells and SCC25 cells in which E2F7 had been silenced with siRNA. This latter list identified E2F7-modulated transcripts which were then cross-referenced against the list of genes identified as downregulated in KJDSV40 cells compared with SCC25 cells. A detailed explanation of this analysis is being prepared for publication elsewhere (Hazar-Rethinam *et al*, in preparation). By selecting for genes with a B-value greater than 3 (exceeding the 95% confidence interval) and a fold change greater than 1, we were able to identify 4 genes (Sphk1, RACGAP1, CD44, RRP8) that were differentially upregulated.

Of the transcripts identified in our screen, sphingosine kinase 1 (Sphk1) was the most significantly overexpressed. Sphk1 is a kinase responsible for the conversion of sphingosine to sphingosine-1-phosphate (S1P) (27-29). Interrogation of publicly available microarray data

indicates statistically significant increases in Sphk1 expression in breast, colon, lung, ovary, prostate, melanoma, stomach, uterus as well as squamous cell carcinoma and it's precursor actinic keratosis (28). Importantly, Sphk1 has been shown to modulate proliferation, differentiation and apoptosis in KCs (30). Facchinetti and colleagues recently reported that Sphk1 is overexpressed in malignant oral epithelia compared with nonmalignant tissue, and the expression of Sphk1 was correlated with poor prognosis, shorter patient survival and loss of p21 expression in HNSCC (30). Of relevance to the present study, Bonhoure and colleagues reported that forced expression of Sphk1 led to resistance to doxorubicin- and etoposide-induced cell death in HL-60 leukemia cells (31), and degradation of Sphk1 resulted in induction of apoptosis in MCF7 breast cancer cells treated with doxorubicin (32). Thus, there is sufficient evidence to speculate that a novel E2F7/Sphk1/S1P axis may exist in SCC cells that regulates doxorubicin sensitivity.

Quantitative RT-PCR was used to confirm that Sphk1 was more highly expressed in SCC25 cells than in KJDSV40 cells (Figure 2A). Consistent with this, we show that transfection of SCC25 cells with siRNA directed against E2F7 resulted in profound inhibition of Sphk1 expression (Figure 2A) whilst E2F1 mRNA expression was derepressed (Figure S4B). Similarly, Sphk1 activity was significantly elevated in SCC25 cells compared with KJDSV40 (Figure 2B). Moreover, we showed that knockdown of E2F7, by siRNA, in SCC25 cells reduced Sphk1 protein expression (Figure 2C) whilst transient overexpression of E2F7 in KJDSV40 cells resulted in an increase in Sphk1 protein levels (Figure 2C). These data suggested that Sphk1 may be a downstream effector of E2F7-induced resistance to doxorubicin. As shown in Figure 2D (Left and center panels), E2F7 overexpression did not protect from Sphk1 knockdown or SK1-I-enhanced cytotoxicity in KJDSV40 cells. Similarly, Sphk1 overexpression in SCC25 cells overrides doxorubicin sensitivity induced by E2F7

siRNA (Figure 2D, Right panel). These data unequivocally demonstrate that Sphk1 is the downstream effector of E2F7-dependent sensitivity of SCC cells to doxorubicin. It remains unclear whether Sphk1 is a direct or indirect target of E2F7. In this regard, ChIP assays showed that E2F7 could bind the Sphk1 and E2F1 promotersin SCC25 cells compared with low levels of binding in KJDSV40 cells indicating that the Sphk1 and E2F1 promoters are direct binding targets of E2F7 (Figure 2E).

Next, we sought to determine whether there was evidence that Sphk1 was overexpressed in primary human SCC tumours. We have generated tissue microarrays (TMAs) comprising duplicates of normal, primary tumour and matched metastasis from HNSCC patients treated at the Princess Alexandra Hospital (PAH), Queensland, Australia. The TMAs were stained for E2F7 and Sphk1 protein expression by immunohistochemistry and scored by two Pathologists. Figure 2F shows that Sphk1 and E2F7 are overexpressed in HNSCC compared to matched adjacent normal tissue. Figure 2F also shows that primary tumour and metastatic tumour do not differ significantly in the levels of E2F7 or Sphk1.

Sphk1 inhibition sensitizes SCC cells to doxorubicin-induced cytotoxicity

In order to determine whether Sphk1 contributes to doxorubicin sensitivity, we studied the effects of silencing Sphk1 in insensitive SCC25 cells. Sphk1 gene silencing was achieved *via* shRNA and caused a marked decrease in Sphk1 protein level (Figure 3A), Sphk1 enzyme activity (Figure 3B) and S1P (a product of Sphk1) measured in cell lysates (Figure 3C) and significantly enhanced sensitivity of SCC25 cells to doxorubicin (Figure 3D). Conversely, overexpression of Sphk1 in insensitive KJDSV40 cells resulted in increases in Sphk1 protein level (Figure 3E), enzyme activity (Figure 3F), S1P production (Figure 3G) and reduced sensitivity to doxorubicin compared to vector control (Figure 3H). S1P is the product of Sphk1-catalysed phosphorylation of sphingosine, and has been shown to mediate the anti-

apoptotic effects of Sphk1 (27, 29). Consistent with this, we found that treatment of KJDSV40 cells with 1 μM S1P reduced cytotoxicity by 2.6 fold (Figure 3I). Combined, these data indicate that sensitivity to doxorubicin is mediated *via* a novel E2F7/Sphk1/S1P axis in SCCs.

Knockdown of Sphk1 sensitizes resistant SCC cells to doxorubicin-induced cytotoxicity *in vivo*

Our data suggest that inhibition of Sphk1 activity, in combination with doxorubicin, may be a viable therapeutic strategy for treating SCC. To answer this question, SCC25 cells were constructed to stably express either vector control or Sphk1 shRNA and inoculated in NOD/SCID mice. When tumours were approximately 3 mm in diameter, mice were randomized into four groups and treated with vehicle dimethyl sulfoxide (DMSO) or 0.5 mg/kg doxorubicin by intraperitoneal (i.p.) injections twice per week (Figure 4A). Treatment of mice bearing vector control SCC25 tumours with/without 0.5 mg/kg doxorubicin had minimal effect on body weight (Figure 4B) or tumour growth rates (Figure 4C). Knockdown of Sphk1 in SCC25 cells did not affect tumour growth *in vivo*. In contrast, Sphk1 deficient SCC25 tumours treated with doxorubicin started to regress by day 7 post-treatment (Figure 4C) with no effect on body weight (Figure 4B). Strikingly, on day 13 post-treatment there was a complete loss of tumours in doxorubicin treated mice inoculated with SCC25/Sphk1shRNA cells (Figure 4C).

We next examined whether we could achieve similar tumour regression when tumours are larger at the commencement of therapy. Since the tumours derived from Sphk1 deficient SCC25 cells treated with vehicle (Figures 4C and 4D; blue triangle) were similar in growth rate and size to tumours in mice bearing vector control transfected SCC25 tumours that had

been treated with 0.5 mg/kg doxorubicin (Figures 4C and 4D; red square), we started to treat these mice when their tumours reached around 0.5 cm^3 with 0.5mg/kg doxorubicin (Figure 4D). As shown in Figure 4D, doxorubicin treatment dramatically reduced the tumour volume showing profound regression one week after doxorubicin was started in Sphk1 deficient group of animals as compared with those inoculated with control vector (Figure 4D). All mice were sacrificed at day 28 post-treatment when the tumour burden in the control mice reached the ethically approved maximum size. Upon autopsy, the mice inoculated with the Sphk1-deficient SCC cells (Figures 4C and 4D; green triangle) only contained a fragile cluster of cellular material that could not be harvested for histopathology.

The Sphk1 specific inhibitor, SK1-I (BML-EI411), sensitises SCC cells to doxorubicin *in vitro* and *in vivo*

SK1-I is a water-soluble sphingosine analog with a Ki value of approximately 10 μM which potently inhibits Sphk1 activity (33). Importantly, SK1-I does not significantly inhibit SPHK2, PKA, AKT1, ERK1, EGFR or CDK2 (33). We treated SCC25 cells with increasing doses of SK1-I for 48 hours and then measured Sphk1 enzyme activity. As anticipated, SK1-I significantly reduced Sphk1 activity in a dose-dependent manner, indicating inhibition of Sphk1 activity (Figure 5A). Moreover, we confirmed that the inhibition was not due to the loss of Sphk1 protein expression (Figure 5B).

Next, we investigated whether Sphk1 specific inhibition can enhance the cytotoxic effects of doxorubicin in insensitive SCC25. After 48 hours incubation with SK1-I alone, the viability of control HEK (Figure S5A) and resistant SCC25 cells did not change (Figure 5C). However, treatment of doxorubicin-resistant SCC25 cells with 1 μM doxorubicin with increasing doses of SK1-I resulted in profound and dose dependent loss of cell viability

(Figure 5C). Predictably, SK1-I did not enhance doxorubicin sensitivity in KJDSV40 cells (Figure S5B). In contrast to SCC25 cells, the addition of increasing doses of SK1-I to doxorubicin, in HEKs, did not enhance the cytotoxicity obtained with doxorubicin alone (Figure S5A). Next, we examined whether the cell death effects of SK1-I and doxorubicin were mediated *via* apoptosis. Consistent with an apoptotic reaction, we observed increases in cleaved caspase-3 and cleaved PARP1 in response to doxorubicin + SK1-I (Figure 5D).

We inoculated NOD/SCID mice with SCC25 cells and allowed tumours to establish subcutaneously. When tumours were around 4 to 5 mm in diameter, mice were randomized into six groups and treated with DMSO, 0.5 mg/kg doxorubicin, 5 mg/kg SK1-I, 10 mg/kg SK1-I, 5 mg/kg SK1-I + 0.5 mg/kg doxorubicin or 10 mg/kg SK1-I + 0.5 mg/kg doxorubicin by i.p. injection twice per week. Treatment with 5 and 10 mg/kg SK1-I was well tolerated by the NOD/SCID mice, and the body weights remained stable (Figure 5E). Tumours in animals treated with 5 and 10 mg/kg doses of SK1-I alone showed modest, yet significant, decreases in tumour growth rate (Figure 5G). Doxorubicin treatment alone did not affect the tumour size (Figures 5F and 5G). However, in sharp contrast to doxorubicin treatment alone, treatment with 10 mg/kg SK1-I + 0.5 mg/kg doxorubicin as well as 5 mg/kg SK1-I + 0.5 mg/kg doxorubicin resulted in profound regression of explanted tumours (Figures 5F and 5G). After 13 days post-treatment, animals had to be sacrificed due to the tumour burden in control mice. Tumours were excised, photographed and histologically examined (Figure 5H). The benefit of combining SK1-I with doxorubicin was not restricted to the SCC25 cell line. Specifically, we show that the FaDu cell line displays intermediate sensitivity to doxorubicin *in vitro* and *in vivo* and are completely insensitive to SK1-I *in vitro* and modestly so *in vivo* (Figure S6). However, combining doxorubicin + SK1-I *in vitro* or *in vivo* induces profound cytotoxicity (Figures S6A and S6B).

Sphk1/S1P has been shown to exert its antiapoptotic activity *via* signaling through a family of S1P receptors linked to the PI3K/AKT pathway (34, 35). Consistent with this, we found that SK1-I could reduce phospho-AKT (p-AKT) (Ser473) in a dose dependent manner (Figure 6A). Previous reports have shown that p-AKT is a downstream effector of the pro-survival effects of increased Sphk1 activity and S1P production (36). Moreover, it is established that the PI3K/AKT pathway is frequently dysregulated *via* mutations in PI3K family members, gene amplifications or pathway activation in HNSCC (37). Thus, we examined whether E2F7 induced prosurvival responses were mediated *via* increased Sphk1/S1P and subsequent AKT phosphorylation. Transient overexpression of E2F7 in KJDSV40 cells results in an increase in Sphk1 protein levels (Figure 2C, Bottom) and an increase in the p-AKT relative to total levels (Figure 6B). Conversely, siRNA-induced knockdown of E2F7 in SCC25 cells resulted in a reduction in Sphk1 expression (Figure 2C, Top) and a reduced p-AKT/total AKT ratio (Figure 6C). Furthermore, transient overexpression of Sphk1 in KJDSV40 cells or knockdown of Sphk1 with shRNA in SCC25 cells resulted in increased and decreased p-AKT respectively (Figures 6D and 6E). These data indicate that the changes in AKT activity lie downstream of Sphk1, which in turn is downstream of E2F7. These data would predict that the profound tumour regression observed as a result of a doxorubicin/SK1-I combination could be recapitulated using doxorubicin + AKT inhibitor.

We have previously shown that the mTOR/PI3K inhibitor, BGT226, is able to reduce tumour growth rates in mice transplanted with SCC cells (19). In the present study, mice were injected with SCC25 cells and when the tumours were between 4 to 5 mm in diameter we treated them with i) vehicle, ii) 0.5 mg/kg doxorubicin i.p. twice weekly, iii) 10 mg/kg BGT226 i.p. twice weekly or iv) 10 mg/kg BGT226 + 0.5 mg/kg doxorubicin i.p. twice

weekly. Tumour growth in the vehicle control (DMSO) and doxorubicin treated mice was unchanged whilst those mice treated with BGT226 alone displayed a modest reduction in tumour growth rate (Figure 6F). Mice treated with the doxorubicin/BGT226 combination displayed significant regression of the tumour mass (Figure 6F).

We next examined levels of PCNA, cleaved caspase-3 and p-AKT levels within the tumours resected from mice treated with 10 mg/kg SK1-I or 10 mg/kg BGT226, alone or in combination with 0.5 mg/kg doxorubicin. Immunohistochemical examinations showed that combination treatment inhibited intratumoral proliferation (at either dose) as measured by the levels of PCNA staining (Figure 6G). SK1-I or BGT226 treatment markedly elevated the number of apoptotic cells induced by doxorubicin treatment as shown by examination of apoptotic indices of tumours by immunohistochemical staining with antibody against cleaved caspase-3 compared with drug alone treated tumours (Figure 6G). Consistent with p-AKT lying downstream of Sphk1 we found significant inhibition of p-AKT (Ser473) in tumours treated with SK1-I or BGT226 (Figure 6G).

DISCUSSION

In the present study we provide, *in vitro*, *in vivo* and patient data that identifies a novel E2F7/Sphk1/S1P/AKT axis that regulates sensitivity to anthracyclines in SCC. Specifically, we show that (i) E2F7 selectively modulates sensitivity to doxorubicin in KCs and SCC, (ii) that E2F7-dependent doxorubicin resistance is mediated *via* induction of Sphk1 which in turn activates AKT and (iii) that pharmacological inhibition of Sphk1 or AKT sensitizes SCC cells to the cytotoxic actions of doxorubicin *in vitro* and *in vivo*. Combined, these findings highlight a novel mechanism through which SCC cells acquire resistance to anthracyclines.

Overall, current data relating to the mechanisms regulating E2F control of apoptosis are complex. For example, E2F1 is known to be induced by cytotoxic stimuli and DNA damage (7, 8). This induction can occur at the level of post-translational modification and protein stabilization and/or can occur through increased E2F1 transcription (16, 38). The main outcome of the increased E2F activity is mediated *via* ARF stimulated inhibition of MDM2 resulting in increased p53-dependent apoptosis. However, complicating this is the observation that E2F1 can recognize double strand breaks induced by UV and recruit NER machinery to the DNA break (16). In this way E2F1 has been proposed to display anti-apoptotic actions (16). This latter pathway has been demonstrated to exist in normal MEKs (39). Further complicating this is the observation that E2F7 can antagonize the pro-apoptotic activity of E2F1 in embryonic tissues as well as in normal or cancer cells (10, 17, 18, 40). Thus, in order to determine the role of E2F7 in regulating cytotoxic responses in HNSCC it is important to consider the tissue context and the nature of the cytotoxic stimulus or DNA damage.

In the present study we show that E2F7 and E2F1 suppress and induce doxorubicin sensitivity in SCC cells respectively. . We also show that cytotoxic responses to etoposide or cisplatin were not altered by E2F7. Since doxorubicin and etoposide are established type II topoisomerase blocking agents, and E2F7 did not alter etoposide sensitivity it is reasonable to suggest that the effects of E2F7 were independent of the topoisomerase inhibitory actions of doxorubicin. We also show that regulation of doxorubicin sensitivity in SCC cells is E2F isoform-specific since the other inhibitory E2F, E2F8, did not modify the sensitivity of KCs to doxorubicin or any other drug studied. In addition, we show that E2F7 suppresses doxorubicin sensitivity *via* increases in the expression of Sphk1 resulting in increased levels of S1P which in turn enhance the Ser473 p-AKT-dependent pro-survival response. The E2F-

dependence of S1P/AKT-mediated drug resistance has not been described before and has significant pathological and clinical implications in SCC.

The relevance of an E2F/Sphk1/S1P/AKT axis in SCC is highlighted by a number of independent observations. In particular E2F1 (5, 11), E2F7 (10), Sphk1 (30, 42), S1P (41), PI3K and AKT (37) are all increased in SCC. Part of these increases may be explained by activation of signaling pathways that regulate their activity/expression such as MAPK-mediated activation of AKT and/or Sphk1 (35, 37) or disrupted Rb activity mediated *via* p16 deletion or cyclin D amplification for E2F1/E2F7 (7, 8). However, PI3K/AKT is commonly mutated or amplified in SCC (2, 3, 37). Regardless of the underlying mechanism it is clear that the individual members of the E2F/Sphk1/S1P/AKT axis are all overexpressed and active in SCC. Whilst the events that initiate disruption of this axis remain unknown it is likely that dysregulation of the E2F/Rb or PI3K/AKT pathway result from mutational events early in tumour formation which could lead to overexpression of E2F7 (a direct E2F1 target) and Sphk1 (a direct E2F7 target). The mechanism by which E2F7 induces Sphk1 transcription was not established in this study. Although E2F7 is an established transcriptional repressor, it has recently been reported that an E2F7-HIF1α transcriptional complex activates the transcription of VEGFA (42). Thus, it is a formal possibility that E2F7 may be a direct activator of Sphk1 transcription. Alternatively, E2F7 could act in a dominant-negative manner by blocking the binding of other E2F repressor complexes. Regardless of the mechanism, our functional data shows that E2F7 regulates S1P levels *via* induction of Sphk1 expression.

Sphingolipid metabolites have emerged as bioactive signaling molecules that regulate cell movement, differentiation, survival, inflammation, angiogenesis, tumorigenesis and

immunity (29). In particular, ceramide and sphingosine have been shown to be profoundly pro-apoptotic whilst phosphorylated sphingosine (S1P) is profoundly anti-apoptotic (27-29). Thus, the kinase, Sphk1, responsible for catalyzing the conversion of sphingosine to S1P, is also responsible for changing the physiology of the cell from pro-apoptotic to anti-apoptotic. Many of the anti-apoptotic effects of S1P are mediated *via* a family of G protein coupled S1P receptors which in turn activate PI3K/AKT (27-29, 43). Interestingly, the use of an AKT inhibitor was able to induce modest levels of cell death and reduced tumour growth *in vivo*. Given that Sphk1 inhibitors profoundly inhibited p-AKT (Ser473), these data would suggest that some of the cytotoxic effects observed for BGT226 alone may be mediated *via* non-AKT targets. Finally, doxorubicin alone displayed no measurable anticancer activity in our xenotransplant model. These data suggest that the cytotoxicity observed with the SK1-I or BGT226 plus doxorubicin combination reflects an unidentified synthetic lethal reaction. The clinical potential for this novel combination (e.g. Sphk1 or AKT inhibitor combined with an anthracycline) is highlighted by the profound tumour regression observed in this study.

A previous report had shown that the activation of AKT in ovarian and breast cancer suppressed E2F1-induced apoptosis and was associated with a poor prognosis and chemo-resistance (44). Similarly, Reimer and colleagues reported that poor prognosis and chemoresistance of ovarian tumours was associated with a high E2F7/E2F1 ratio (45). We now provide an integrated model in which E2F7 is causally linked to the overexpression of Sphk1, the activation of the AKT pathway and doxorubicin resistance. This is definitively shown by our observation that Sphk1, S1P and p-AKT (Ser473) are all directly modulated by E2F7. Secondly, Sphk1 inhibition or overexpression directly effects the Ser473 phosphorylation of AKT. Finally, inhibition of Sphk1 or AKT sensitises SCC cells *in vivo* to the cytotoxic effects of doxorubicin. The observation that anti-apoptotic effects of S1P are

mediated *via* the PI3K/AKT pathway has been previously reported (35, 36). What is new in our study is that the dysregulation of the E2F pathway, in SCC, directly activates the Sphk1/S1P/PI3K/AKT pathway resulting in selective resistance to doxorubicin. This is an advance that can be immediately translated to a clinical trial with existing pharmacological agents.

Acknowledgments

The authors acknowledge the generous gift of *E2f7*$^{Flox/Flox}$ and *E2f8*$^{Flox/Flox}$ mice from Professor Gustavo Leone, The Ohio State University. The authors acknowledge the generous donations of tissue samples from the patients without which this project could not happen.

REFERENCES

1. Minicucci EM, da Silva GN, Salvadori DM. Relationship between head and neck cancer therapy and some genetic endpoints. World J Clin Oncol 2014;5(2):93-102.

2. Stransky N, Egloff AM, Tward AD, Kostic AD, Cibulskis K, Sivachenko A, et al. The mutational landscape of head and neck squamous cell carcinoma. Science 2011;333(6046):1157-60.

3. Agrawal N, Frederick MJ, Pickering CR, Bettegowda C, Chang K, Li RJ, et al. Exome sequencing of head and neck squamous cell carcinoma reveals inactivating mutations in NOTCH1. Science 2011;333(6046):1154-7.

4. Wong CF, Barnes LM, Dahler AL, Smith L, Popa C, Serewko-Auret MM, et al. E2F suppression and Sp1 overexpression are sufficient to induce the differentiation-specific marker, transglutaminase type 1, in a squamous cell carcinoma cell line. Oncogene 2005;24(21):3525-34.

5. Kwong RA, Nguyen TV, Bova RJ, Kench JG, Cole IE, Musgrove EA, et al. Overexpression of E2F-1 is associated with increased disease-free survival in squamous cell carcinoma of the anterior tongue. Clin Cancer Res 2003;9(10):3705-11.

6. Carvajal LA, Hamard PJ, Tonnessen C, Manfredi JJ. E2F7, a novel target, is up-regulated by p53 and mediates DNA damage-dependent transcriptional repression. Genes Dev 2012;26(14):1533-45.

7. DeGregori J, Johnson DG. Distinct and overlapping roles for E2F family members in transcription, proliferation and apoptosis. Curr Mol Med 2006;6(7):739-48.

8. Johnson DG, Degregori J. Putting the oncogenic and tumor suppressive activities of E2F into context. Curr Mol Med 2006;6(7):731-8.

9. Wong CF, Barnes LM, Dahler AL, Smith L, Serewko-Auret MM, Popa C, et al. E2F modulates keratinocyte squamous differentiation: implications for E2F inhibition in squamous cell carcinoma. J Biol Chem 2003;278(31):28516-22.

10. Endo-Munoz L, Dahler A, Teakle N, Rickwood D, Hazar-Rethinam M, Abdul-Jabbar I, et al. E2F7 can regulate proliferation, differentiation, and apoptotic responses in human keratinocytes: implications for cutaneous squamous cell carcinoma formation. Cancer Res 2009;69(5):1800-8.

11. Dicker AJ, Popa C, Dahler AL, Serewko MM, Hilditch-Maguire PA, Frazer IH, et al. E2F-1 induces proliferation-specific genes and suppresses squamous differentiation-specific genes in human epidermal keratinocytes. Oncogene 2000;19(25):2887-94.

12. Hazar-Rethinam M, Endo-Munoz L, Gannon O, Saunders N. The role of the E2F transcription factor family in UV-induced apoptosis. Int J Mol Sci 2011;12(12):8947-60.

13. Pierce AM, Fisher SM, Conti CJ, Johnson DG. Deregulated expression of E2F1 induces hyperplasia and cooperates with ras in skin tumor development. Oncogene 1998;16(10):1267-76.

14. Pierce AM, Gimenez-Conti IB, Schneider-Broussard R, Martinez LA, Conti CJ, Johnson DG. Increased E2F1 activity induces skin tumors in mice heterozygous and nullizygous for p53. Proc Natl Acad Sci U S A 1998;95(15):8858-63.

15. Field SJ, Tsai FY, Kuo F, Zubiaga AM, Kaelin WG, Jr., Livingston DM, et al. E2F-1 functions in mice to promote apoptosis and suppress proliferation. Cell 1996;85(4):549-61.

16. Knezevic D, Brash DE. Role of E2F1 in apoptosis: a case study in feedback loops. Cell Cycle 2004;3(6):729-32.

17. Panagiotis Zalmas L, Zhao X, Graham AL, Fisher R, Reilly C, Coutts AS, et al. DNA-damage response control of E2F7 and E2F8. EMBO Rep 2008;9(3):252-9.

18. Li J, Ran C, Li E, Gordon F, Comstock G, Siddiqui H, et al. Synergistic function of E2F7 and E2F8 is essential for cell survival and embryonic development. Dev Cell 2008;14(1):62-75.

19. Erlich RB, Kherrouche Z, Rickwood D, Endo-Munoz L, Cameron S, Dahler A, et al. Preclinical evaluation of dual PI3K-mTOR inhibitors and histone deacetylase inhibitors in head and neck squamous cell carcinoma. Br J Cancer 2012;106(1):107-15.

20. Erlich RB, Rickwood D, Coman WB, Saunders NA, Guminski A. Valproic acid as a therapeutic agent for head and neck squamous cell carcinomas. Cancer Chemother Pharmacol 2009;63(3):381-9.

21. Cameron SR, Dahler AL, Endo-Munoz LB, Jabbar I, Thomas GP, Leo PJ, et al. Tumor-initiating activity and tumor morphology of HNSCC is modulated by interactions between clonal variants within the tumor. Lab Invest 2010;90(11):1594-603.

22. Zhao KN, Gu W, Fang NX, Saunders NA, Frazer IH. Gene codon composition determines differentiation-dependent expression of a viral capsid gene in keratinocytes in vitro and in vivo. Mol Cell Biol 2005;25(19):8643-55.

23. Jones SJ, Dicker AJ, Dahler AL, Saunders NA. E2F as a regulator of keratinocyte proliferation: implications for skin tumor development. J Invest Dermatol 1997;109(2):187-93.

24. Endo-Munoz L, Cumming A, Sommerville S, Dickinson I, Saunders NA. Osteosarcoma is characterised by reduced expression of markers of osteoclastogenesis and antigen presentation compared with normal bone. Br J Cancer 2010;103(1):73-81.

25. Endo-Munoz L, Cumming A, Rickwood D, Wilson D, Cueva C, Ng C, et al. Loss of Osteoclasts Contributes to Development of Osteosarcoma Pulmonary Metastases. Cancer Res 2010;70(18):7063-72.

26. Detre S, Saclani Jotti G, Dowsett M. A "quickscore" method for immunohistochemical semiquantitation: validation for oestrogen receptor in breast carcinomas. J Clin Pathol 1995;48(9):876-8.

27. Pyne NJ, Pyne S. Sphingosine 1-phosphate and cancer. Nat Rev Cancer 2010;10(7):489-503.

28. Shida D, Takabe K, Kapitonov D, Milstien S, Spiegel S. Targeting SphK1 as a new strategy against cancer. Curr Drug Targets 2008;9(8):662-73.

29. Fyrst H, Saba JD. An update on sphingosine-1-phosphate and other sphingolipid mediators. Nat Chem Biol 2010;6(7):489-97.

30. Facchinetti MM, Gandini NA, Fermento ME, Sterin-Speziale NB, Ji Y, Patel V, et al. The expression of sphingosine kinase-1 in head and neck carcinoma. Cells Tissues Organs 2010;192(5):314-24.

31. Bonhoure E, Pchejetski D, Aouali N, Morjani H, Levade T, Kohama T, et al. Overcoming MDR-associated chemoresistance in HL-60 acute myeloid leukemia cells by targeting shingosine kinase-1. Leukemia 2005;20(1):95-102.

32. Sarkar S, Maceyka M, Hait NC, Paugh SW, Sankala H, Milstien S, et al. Sphingosine kinase 1 is required for migration, proliferation and survival of MCF-7 human breast cancer cells. FEBS Lett 2005;579(24):5313-7.

33. Paugh SW, Paugh BS, Rahmani M, Kapitonov D, Almenara JA, Kordula T, et al. A selective sphingosine kinase 1 inhibitor integrates multiple molecular therapeutic targets in human leukemia. Blood 2008;112(4):1382-91.

34. Song L, Xiong H, Li J, Liao W, Wang L, Wu J, et al. Sphingosine kinase-1 enhances resistance to apoptosis through activation of PI3K/Akt/NF-kappaB pathway in human non-small cell lung cancer. Clin Cancer Res 2011;17(7):1839-49.

35. Beckham TH, Cheng JC, Lu P, Shao Y, Troyer D, Lance R, et al. Acid ceramidase induces sphingosine kinase 1/S1P receptor 2-mediated activation of oncogenic Akt signaling. Oncogenesis 2013;2:e49.

36. Kapitonov D, Allegood JC, Mitchell C, Hait NC, Almenara JA, Adams JK, et al. Targeting sphingosine kinase 1 inhibits Akt signaling, induces apoptosis, and suppresses growth of human glioblastoma cells and xenografts. Cancer Res 2009;69(17):6915-23.

37. Iglesias-Bartolome R, Martin D, Gutkind JS. Exploiting the head and neck cancer oncogenome: widespread PI3K-mTOR pathway alterations and novel molecular targets. Cancer Discov 2013;3(7):722-5.

38. Real S, Espada L, Espinet C, Santidrian AF, Tauler A. Study of the in vivo phosphorylation of E2F1 on Ser403. Biochim Biophys Acta 2010;1803(8):912-8.

39. Wikonkal NM, Remenyik E, Knezevic D, Zhang W, Liu M, Zhao H, et al. Inactivating E2f1 reverts apoptosis resistance and cancer sensitivity in Trp53-deficient mice. Nat Cell Biol 2003;5(7):655-60.

40. Ouseph MM, Li J, Chen HZ, Pecot T, Wenzel P, Thompson JC, et al. Atypical E2F repressors and activators coordinate placental development. Dev Cell 2012;22(4):849-62.

41. Shirai K, Kaneshiro T, Wada M, Furuya H, Bielawski J, Hannun YA, et al. A role of sphingosine kinase 1 in head and neck carcinogenesis. Cancer Prev Res (Phila) 2011;4(3):454-62.

42. Weijts BGMW, Bakker WJ, Cornelissen PWA, Liang K-H, Schaftenaar FH, Westendorp B, et al. E2F7 and E2F8 promote angiogenesis through transcriptional activation of VEGFA in cooperation with HIF1. EMBO J 2012;31(19):3871-84.

43. Takabe K, Paugh SW, Milstien S, Spiegel S. "Inside-out" signaling of sphingosine-1-phosphate: therapeutic targets. Pharmacol Rev 2008;60(2):181-95.

44. Hallstrom TC, Mori S, Nevins JR. An E2F1-dependent gene expression program that determines the balance between proliferation and cell death. Cancer Cell 2008;13(1):11-22.

45. Reimer D, Sadr S, Wiedemair A, Stadlmann S, Concin N, Hofstetter G, et al. Clinical relevance of E2F family members in ovarian cancer--an evaluation in a training set of 77 patients. Clin Cancer Res 2007;13(1):144-51.

FIGURE LEGENDS

Figure 1. E2F7 selectively regulates sensitivity to doxorubicin in MEKs. A, dose response curve of doxorubicin-induced cytotoxicity at 48 hour in uninfected, E2F1KO, E2F7KD, E2F8KDs MEKs. B, dose response curve of doxorubicin-induced cytotoxicity at 48 hour in E2F7KD MEKs which were transfected with either an E2F7b overexpression plasmid, or pcDNA3.1(+) control plasmid. Viability is plotted as percentage control (untreated). C, activation of caspase-3 was determined by immunoblotting extracts of untreated and 0.3 μM doxorubicin treated E2F7 floxed and E2F7 deficient MEKs. β-Actin is a loading control. D, HEK, FaDu, KJDSV40 and SCC25 cells were treated with doxorubicin for 48 hours and viability plotted as percentage of untreated cells. E, E2F1 and E2F7 protein expression was determined by immunoblotting extracts of HEK, KJDSV40 and SCC25 cell lines. β-Actin is provided as a loading control. Densitometric analysis of E2F1 and E2F7 in KJDSV40 and SCC25 cell lines was quantified using ImageJ. Expression level was normalized against β-Actin and plotted as E2F7/E2F1. F, SCC25 cells were transfected with E2F7b overexpression plasmid or pcDNA3.1(+) control plasmid. G, SCC25 cells were treated with siRNA-targeting E2F7 or a control siRNA. In both instances (F and G), cells were left for 48 hours after transfection after which viability was estimated by trypan blue exclusion. Viability was expressed as percent viable cells and plotted as a percent untreated control. Western blot figures are representative of three independent experiments. Quantitative data represent the mean ± SEM obtained from triplicate determinations of three independent experiments for A, B, D, F and G. *, $P \leq 0.05$, **, $P < 0.01$, ***, $P < 0.001$.

Figure 2. Sphk1 is a downstream effector of E2F7 and is elevated in expression in SCCs. A, RNA was extracted from KJDSV40, SCC25 and SCC25 cells in which E2F7 was silenced

with siRNA. Quantitative RT-PCR was used to determine the expression of Sphk1 transcripts. Data are the mean ± SEM of duplicate determinants normalized for expression of the housekeeping gene TBP; *n* = 3. B, Sphk1 activity is shown for the KJDSV40 and SCC25 cell lines. Data represent the mean ± SEM obtained from triplicate determinations of three independent experiments. C, (Top) SCC25 cells were transfected with siRNA-targeting E2F7 or a control siRNA. (Bottom) Sphk1 protein levels are shown for KJDSV40 cells in which E2F7 was overexpressed. Immunoblot was used to determine Sphk1 levels 48 hours post-transfection. β-Actin is provided as a loading control. Western blot figure is representative of three independent experiments. D, (Left) empty vector, E2F7 expression plasmid, E2F7 expression plasmid and Sphk1 shRNA plasmids transfected KJDSV40 cells were exposed to 1 μM doxorubicin. (Center) empty vector transfected, E2F7 expression plasmid transfected, E2F7 expression plasmid transfected and 10 μM SK1-I treated KJDSV40 cells were exposed to 1 μM doxorubicin. (Right) control siRNA, E2F7 siRNA, E2F7 siRNA and Sphk1 expression plasmid transfected SCC25 cells were exposed to 1 μM doxorubicin. Viability was assessed 48 hours post-treatment and is expressed in arbitrary units. E, quantitative determinations of E2F7 binding to the E2F1 and Sphk1 promoters. ChIPs were performed using an E2F7 antibody or non-immune IgG as control in KJDSV40 and SCC25 cell lines. Each ChIP and quantitative RT-PCR were repeated, respectively, 3 and 2 times. SDs refer to the 3 independent experiments. F, quantitation of E2F7 and Sphk1 staining intensity in matched samples of primary tumour, its matched normal squamous epithelium and lymph node metastasis (*n* = 37). Tissue sections were scored using a modified quickscore method to determine the percentage of cells stained (0-100%) and the intensity of staining (1+ to 3+). Data is shown as the mean ± SEM. **, $P < 0.01$, ****, $P < 0.0001$.

Figure 3. Sphk1 contributes at a functional level to doxorubicin sensitivity. A, SCC25 cells were transfected with 4 different constructs coding for shRNAs directed against Sphk1. After 48 hours, Sphk1 protein expression was determined by immunoblotting. β-Actin is provided as a loading control. SCC25 cells were transfected with the Sphk1shRNA.2 and a scrambled shRNA constructs. After 48 hours, B, Sphk1 activity or C, S1P levels were measured. Data presented as percentage of control shRNA. D, Sphk1shRNA and control shRNA transfected SCC25 cells were treated with doxorubicin (1μM) for 48 hours and viability estimated by trypan blue exclusion. Viability was expressed as number of viable cell counts and plotted as percentage control (untreated). E, KJDSV40 cells were transfected with Sphk1 overexpression plasmid or a noncoding empty vector. After 48 hours, Sphk1 protein expression was determined by immunoblotting. β-Actin is a loading control. KJDSV40 cells were transfected with Sphk1 overexpression plasmid or a noncoding empty vector. After 48 hours, F, Sphk1 activity or G, S1P levels were estimated. Data presented as percentage of control vector. H, Sphk1 overexpression plasmid or empty vector transfected KJDSV40 cells were treated with doxorubicin (1μM) for 48 hours before viability was conducted by trypan blue exclusion. Viability was expressed as number of viable cell counts and plotted as percentage control (untreated). I, KJDSV40 cells were treated with varying doses of doxorubicin in the presence or absence of 1 μM S1P. Viability was then assessed and plotted as percentage control (untreated). Western blot figures are representative of three independent experiments. Quantification of S1P in cell lysate from same number of cells was achieved by the S1P ELISA kit. Quantification of S1P was done following the manufacturer's guidelines. All quantitative data presented as mean ± SEM obtained from triplicate determinations of three independent experiments. *, $P \leq 0.05$ versus empty vector, **, $P < 0.01$ versus control shRNA and versus empty vector. ***, $P < 0.001$ versus empty vector.

Figure 4. Sphk1 suppression enhanced sensitivity of SCC25 to the cytotoxic actions of doxorubicin *in vivo*. A, schematic representing xenograft treatment cohorts. All animals were inoculated subcutaneously with SCC25 cells expressing vector alone (scrambled shRNA) or Sphk1 shRNA and tumours allowed establishing till they reached the indicated sizes. Established tumours were then treated with vehicle or 0.5 mg /kg doxorubicin twice per week at day 1 (B, C) or day 13 (D) post-inoculation. B, animal weight was determined twice per week. C, tumour volumes were monitored twice weekly. D, dotted line indicates beginning of treatment for distinct groups. Data presented as mean ± SEM of individual measurements from six mice per group.

Figure 5. Pharmacological inhibition of Sphk1 sensitizes SCC cells to the cytotoxic actions of doxorubicin *in vitro* and *in vivo*. A, SK1-I induces a dose-dependent inhibition of Sphk1 activity in SCC25 cells that is B, independent of alterations in Sphk1 protein expression. β-Actin is provided as a loading control. C, dose response curve of SK1-I alone or in combination with doxorubicin in SCC25 cells was determined following 48 hours of treatment. Viability is plotted as percentage control (untreated). D, cleavage of PARP and activation of caspase-3 was determined by immunoblotting extracts of SK1-I and doxorubicin treated SCC25 cells. β-Actin is provided as a loading control. E, animal weight was determined twice per week. F, tumour growth curves of SCC25 xenografts treated with doxorubicin, SK1-I (5 or 10 mg/kg) or the described combinations. G, after 13 days of treatment, animals were sacrificed and tumours excised. Representative results from distinct groups are shown. H, paraffin-embedded tumour sections were stained with hematoxylin and eosin. Representative images from each group are shown (Bar = 100μm). Western blot figures are representative of three independent experiments. Data represent the mean ± SEM obtained from triplicate determinations of three independent experiments for A and C. Data

represented as mean ± SEM of individual measurements from five mice per group for E and F. *P* value was calculated using Student's *t* test.

Figure 6. Sphk1 Exerts Its Anti-Apoptotic Activity *via* the PI3K/AKT Pathway. A, p-AKT and total AKT protein levels were determined by immunblotting following treatment of SCC25 cells with varying doses of SK1-I. B, Densitometric analysis of p-AKT and total AKT was determined from immunoblots of KJDSV40 cells in which E2F7 was overexpressed. The protein levels were quantified using ImageJ, normalized for expression of total AKT and plotted as p-AKT/total AKT. C, densitometric analysis of p-AKT and total AKT was determined from immunoblots of SCC25 cells in which E2F7 was silenced. The protein levels were quantified using ImageJ, normalized for expression of total AKT and plotted as p-AKT/total AKT. D, p-AKT and total AKT levels are shown for SCC25 cells in which Sphk1 was overexpressed or E, silenced. F, tumour growth curves of SCC25 xenografts treated with doxorubicin, BGT226 or the described combinations. G, immunostaining for PCNA, cleaved caspase-3 and p-AKT. Representative images of at least three independent tumours are shown for each group (Bar = 100μm). Western blot figures are representative of three independent experiments. Data represented as mean ± SEM of individual measurements from four mice per group for F.

SUPPLEMENTARY INFORMATION

SUPPLEMENTARY FIGURE LEGENDS

Figure S1. Generation of E2F7 and E2F8 deficient murine keratinocytes and the validation of E2F1 levels in E2F1KO mice. A, level of E2F7 and B, E2F8 mRNA expression was measured by qRT-PCR in the relevant floxed keratinocytes following infection with Ad-CMV-Cre. C, quantitative RT-PCR analysis of E2F1 expression in KCs isolated from conventional E2F1KO mice. Expression is plotted as percentage uninfected control for A and B, and as percentage control murine keratinocytes for C. Data are the mean ± SEM of duplicate determinants from 3 biological replicates normalized for expression of the housekeeping gene β-actin.

Figure S2. Adenovirus infection of murine keratinocytes does not alter normal cell responses. A, cell viability 48 hours after infection of control murine keratinocytes (MEKs) with Ad-GFP was measured. B, quantitative RT-PCR was performed on MEKs isolated from control mice and MEKs which had been infected with Ad-Null. Data are the mean ± SEM of duplicate determinants or 3 biological replicates normalized for expression of the housekeeping gene β-actin. C, Uninfected and Ad-Null infected control MEKs were cultured with 1.5 mM Ca^{2+} for 48 hours to induce differentiation. Differentiation marker, involucrin, level was then detected by Western Blotting. β-actin was used as a loading control. Uninfected and Ad-Null infected control MEKs were subjected to varying doses of D, UVB, E, doxorubicin or F, cisplatin. Cell viability was assessed following 48 hours of treatment. Data represent the mean ± SEM obtained from triplicate determinations of three independent experiments for A, B, D, E and F. Western blot figures are representative of three independent experiments.

Figure S3. Cytotoxic responses to doxorubicin selectively enhanced in E2F7-deficient murine keratinocytes. Dose response curve of control, E2F1, E2F7 and E2F8 deficient murine keratinocyes to A, epirubicin, B, cisplatin and C, etoposide. Cells were exposed to drugs for 48 hours. Viability was then assessed and plotted as percentage control (untreated). Data represent the mean ± SEM obtained from triplicate determinations of three independent experiments.

Figure S4. Validation of siRNA directed against E2F7 and E2F1 mRNA expression level in SCC25 cells in which E2F7 had been silenced by siRNA. A**,** SCC25 cells were transfected with control siRNA or a siRNA for E2F7. Two different siRNAs were tested. Cells were harvested 48 hours after transfection. Knockdown was confirmed with qRT-PCR (Right) and immunoblotting (Left). B, SCC25 cells were transfected with E2F7.siRNA construct 2. Cells were harvested 48 hours after transfection. E2F1 mRNA expression was determined by qRT-PCR. Data are the mean ± SEM of duplicate determinants normalized for expression of the housekeeping gene TBP; $n = 3$. Western blot figures are representative of three independent experiments. β-actin was used as a loading control.

Figure S5. SK1-I did not enhance doxorubicin sensitivity in KJDSV40 cells *in vitro.* A, dose response curve of SK1-I alone or in combination with doxorubicin in HEK and B, KJDSV40 cells was determined following 48 hours of treatment. Viability is plotted as percentage control. Data represent the mean ± SEM obtained from triplicate determinations of three independent experiments.

Figure S6. Inhibition of Sphk1 sensitizes FaDu cells to the cytotoxic actions of doxorubicin *in vitro* and *in vivo*. A, FaDu cells were treated with vehicle, 1 μM doxorubicin, 30 μM SK1-I or 30 μM SK1-I + 1 μM doxorubicin for 48 hours after which viability was estimated and referenced against vehicle treated controls. Data represent the mean ± SEM obtained from triplicate determinations of three independent experiments. B, tumour growth curves of FaDu-derived xenografts treated with doxorubicin, SK1-I or the described combinations. Data represented as mean ± SEM of individual measurements from two mice per group.

Figure 1

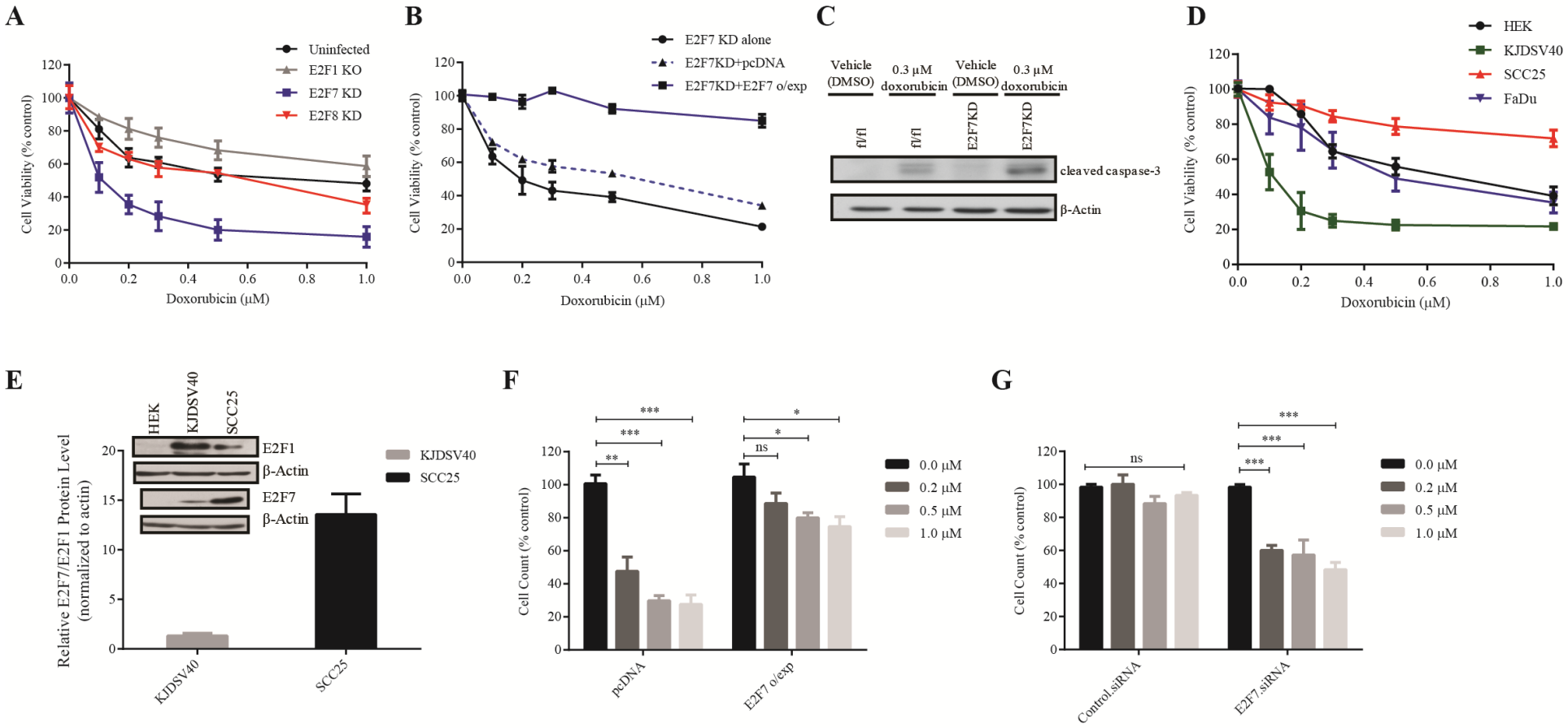

Figure 2

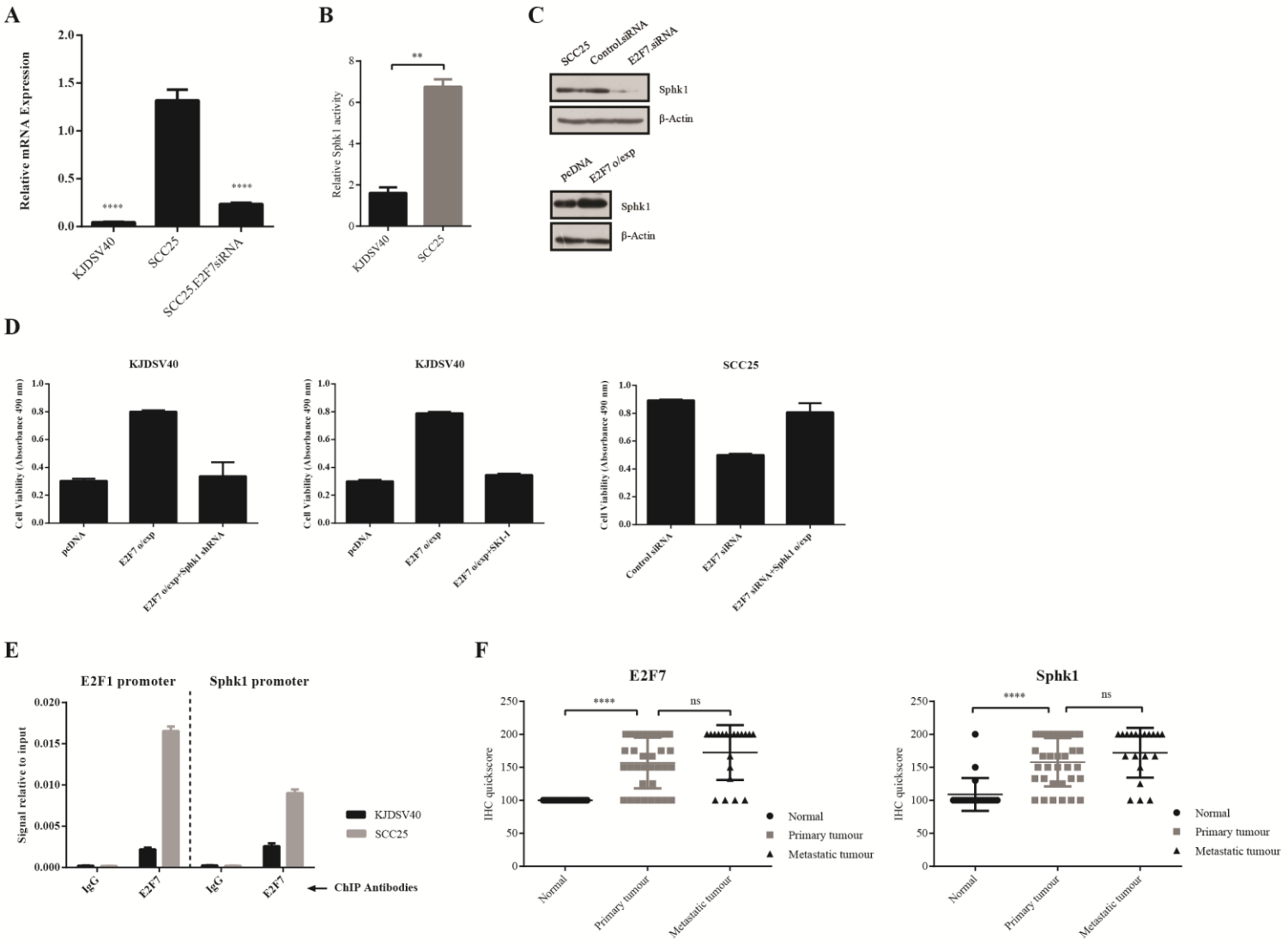

Figure 3

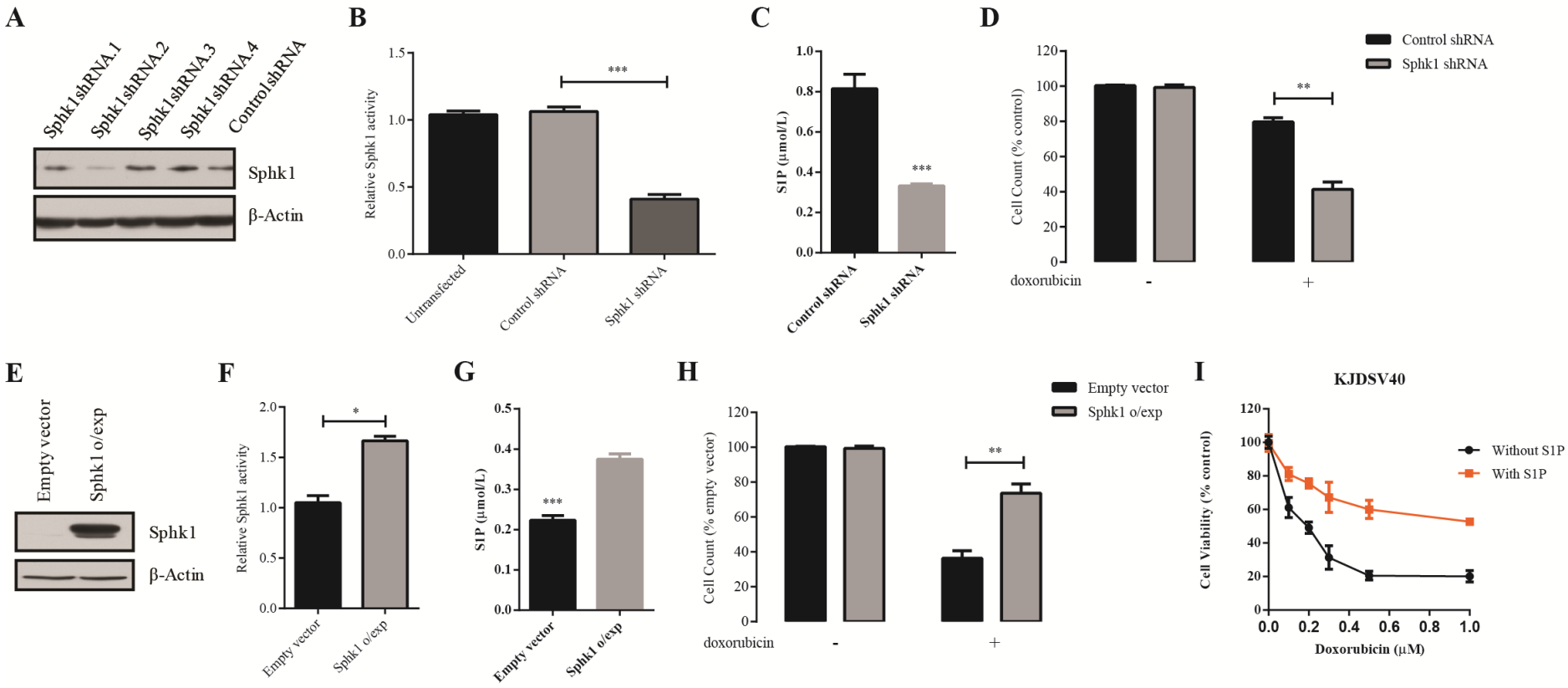

Figure 4

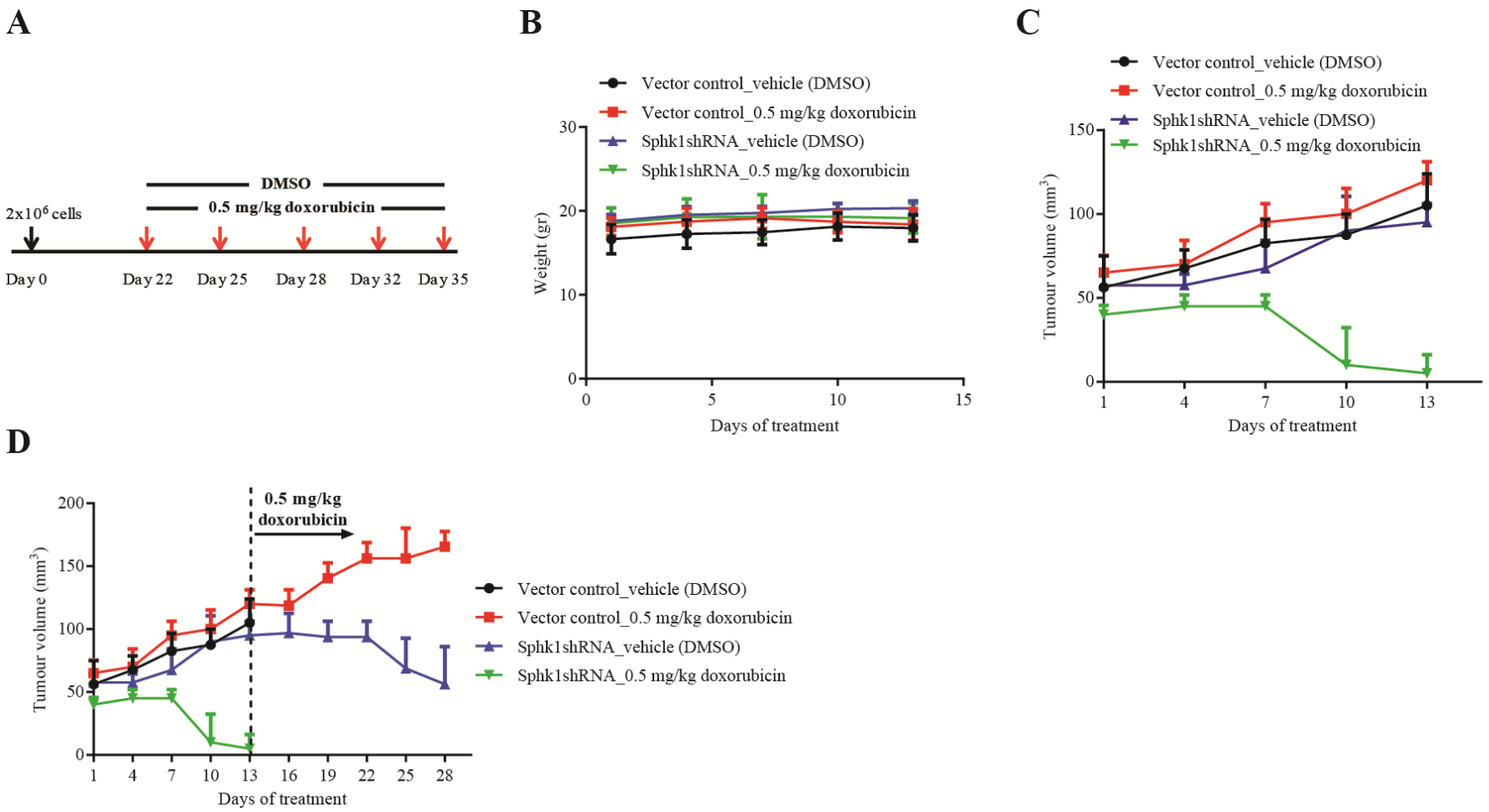

Figure 5

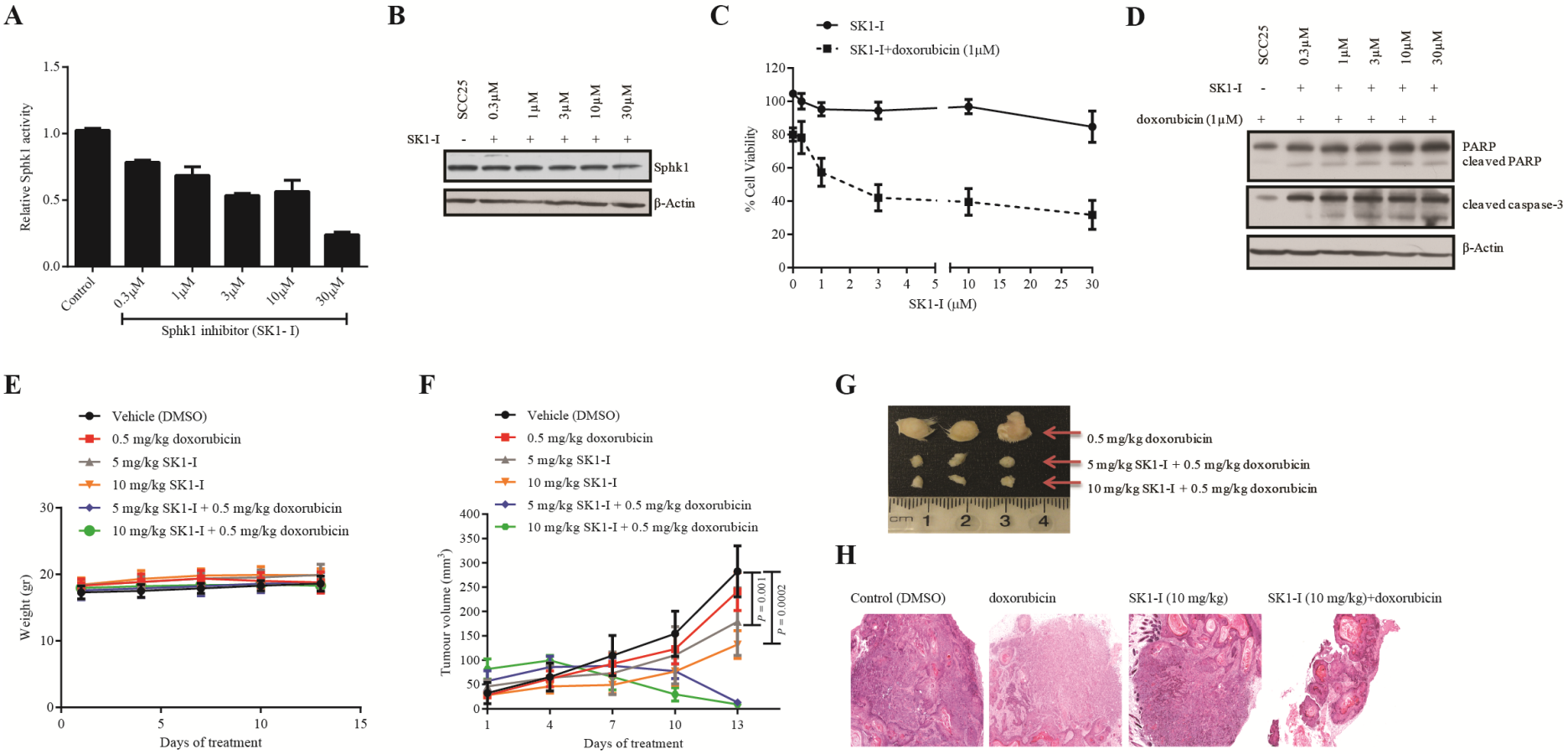

Figure 6

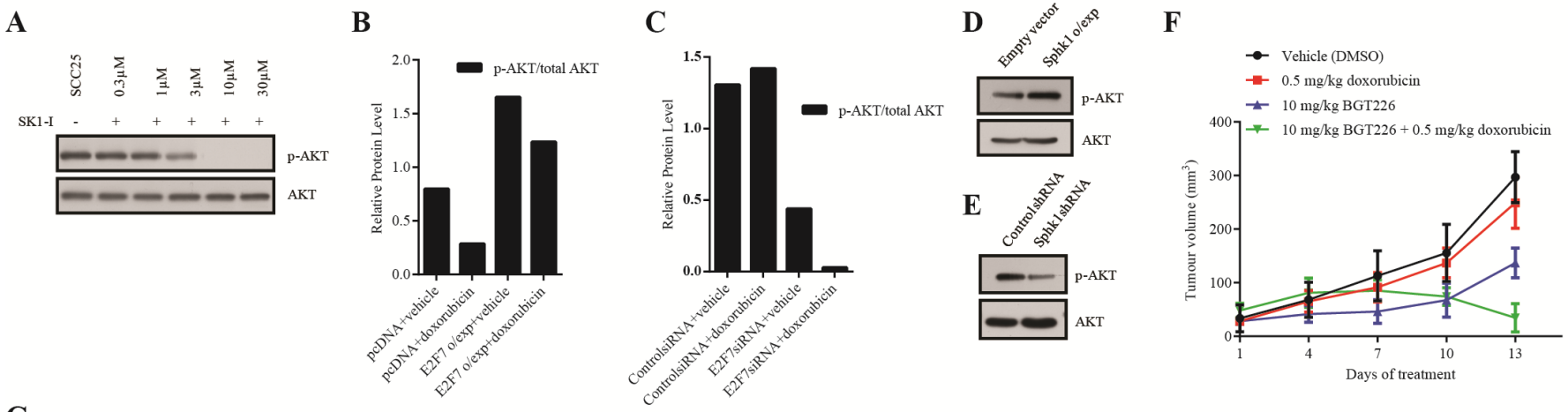

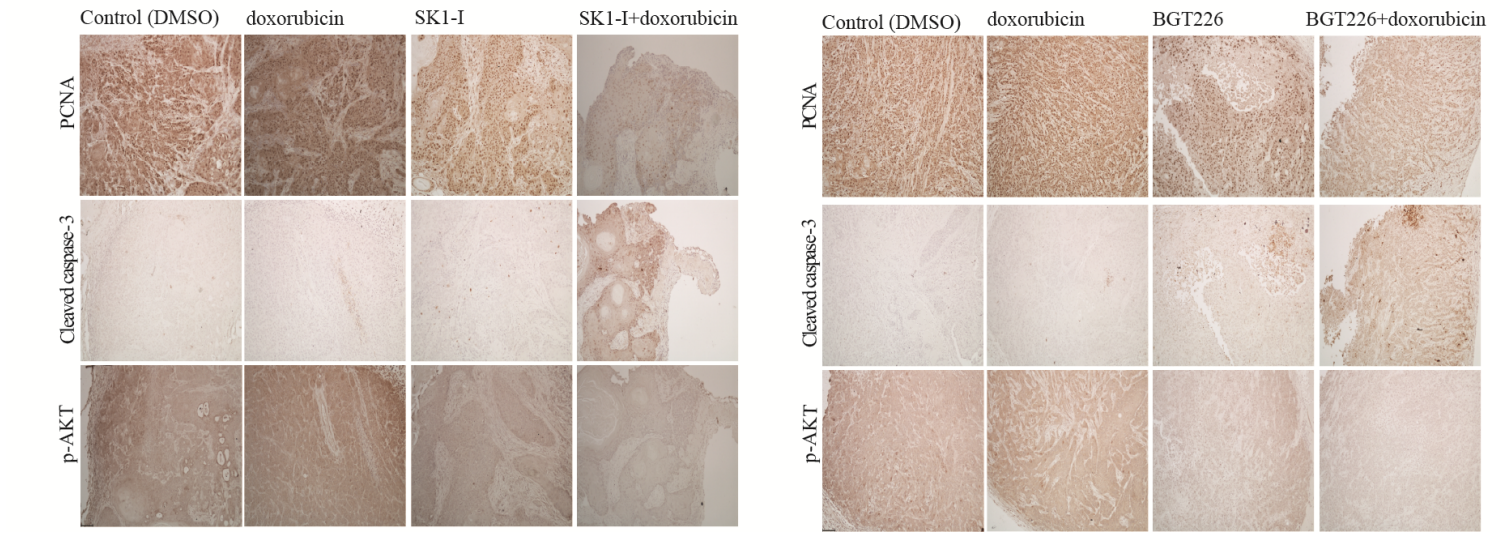

Clinical Cancer Research

A novel E2F/Sphingosine kinase 1 axis regulates anthracycline response in squamous cell carcinoma

Mehlika Hazar-Rethinam, Lilia Merida de Long, Orla Gannon, et al.

Clin Cancer Res Published OnlineFirst November 19, 2014.

5.3 Supplementary data

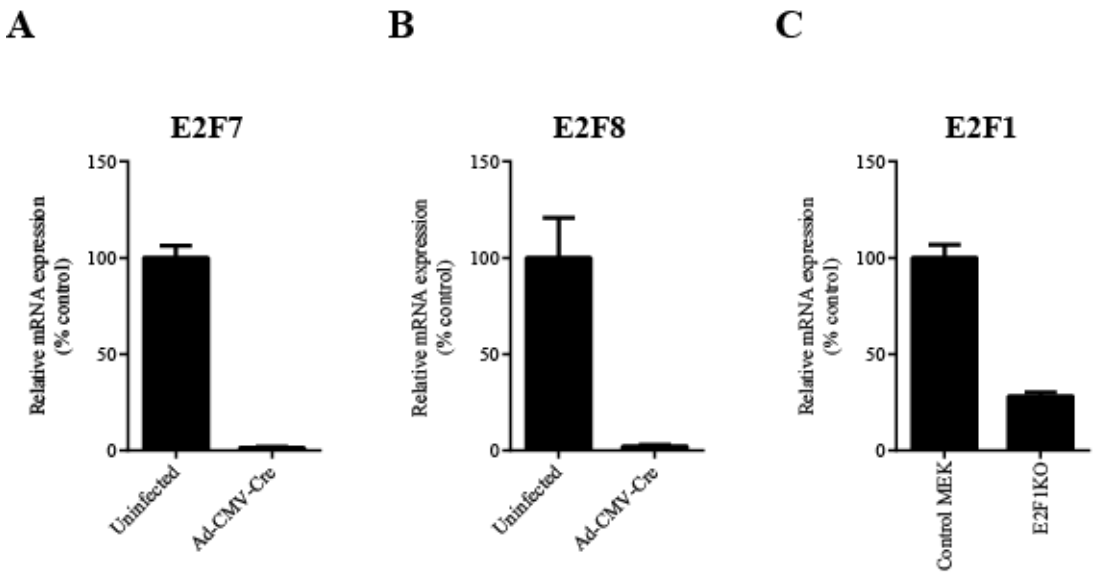

Figure 5.1 Figure S1. Generation of E2F7 and E2F8 deficient murine keratinocytes and the validation of E2F1 levels in E2F1KO mice. A, level of E2F7 and B, E2F8 mRNA expression was measured by qRT-PCR in the relevant floxed keratinocytes following infection with Ad-CMV-Cre. C, quantitative RT-PCR analysis of E2F1 expression in KCs isolated from conventional E2F1KO mice. Expression is plotted as percentage uninfected control for A and B, and as percentage control murine keratinocytes for C. Data are the mean ± SEM of duplicate determinants from 3 biological replicates normalized for expression of the housekeeping gene β-actin.

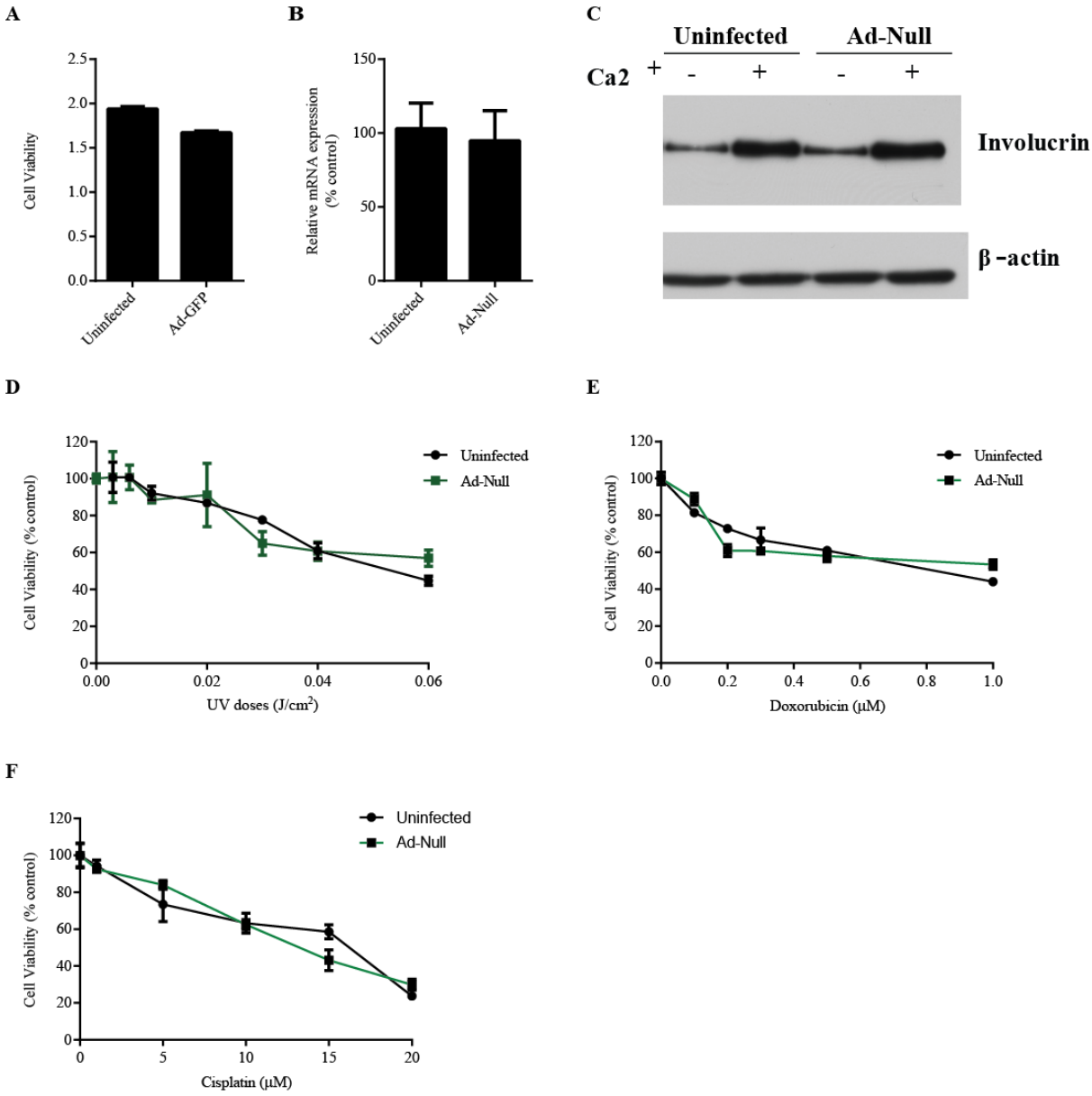

Figure 5.2 Figure S2. Adenovirus infection of murine keratinocytes does not alter normal cell responses. A, cell viability 48 hours after infection of control murine keratinocytes (MEKs) with Ad-GFP was measured. B, quantitative RT-PCR was performed on MEKs isolated from control mice and MEKs which had been infected with Ad-Null. Data are the mean ± SEM of duplicate determinants or 3 biological replicates normalized for expression of the housekeeping gene β-actin. C, Uninfected and Ad-Null infected control MEKs were cultured with 1.5 mM Ca^{2+} for 48 hours to induce differentiation. Differentiation marker, involucrin, level was then detected by Western Blotting. β-actin was used as a loading control. Uninfected and Ad-Null infected control MEKs were subjected to varying doses of D, UVB, E, doxorubicin or F, cisplatin. Cell viability was assessed following 48 hours of treatment. Data represent the mean ± SEM obtained from triplicate determinations of three independent experiments for A, B, D, E and F. Western blot figures are representative of three independent experiments.

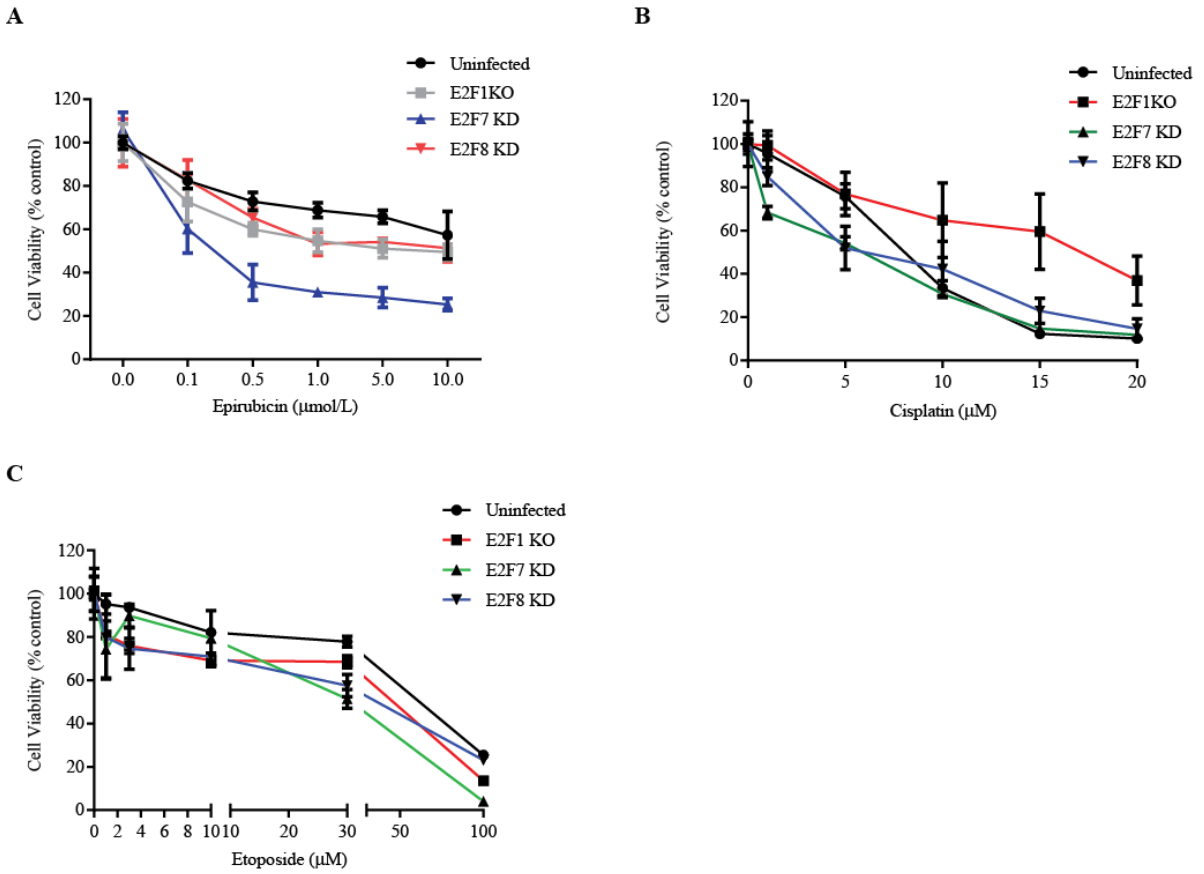

Figure 5.3 Figure S3. Cytotoxic responses to doxorubicin selectively enhanced in E2F7-deficient murine keratinocytes. Dose response curve of control, E2F1, E2F7 and E2F8 deficient murine keratinocyes to A, epirubicin, B, cisplatin and C, etoposide. Cells were exposed to drugs for 48 hours. Viability was then assessed and plotted as percentage control (untreated). Data represent the mean ± SEM obtained from triplicate determinations of three independent experiments.

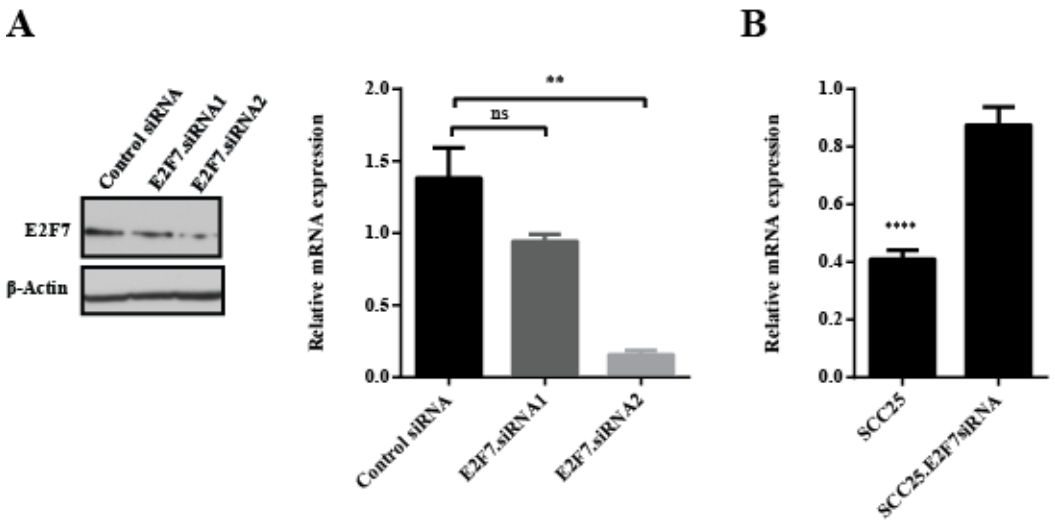

Figure 5.4 Figure S4. Validation of siRNA directed against E2F7 and E2F1 mRNA expression level in SCC25 cells in which E2F7 had been silenced by siRNA. A, SCC25 cells were transfected with control siRNA or a siRNA for E2F7. Two different siRNAs were tested. Cells were harvested 48 hours after transfection. Knockdown was confirmed with qRT-PCR (Right) and immunoblotting (Left). B, SCC25 cells were transfected with E2F7.siRNA construct 2. Cells were harvested 48 hours after transfection. E2F1 mRNA expression was determined by qRT-PCR. Data are the mean ± SEM of duplicate determinants normalized for expression of the housekeeping gene TBP; *n* = 3. Western blot figures are representative of three independent experiments. β-actin was used as a loading control.

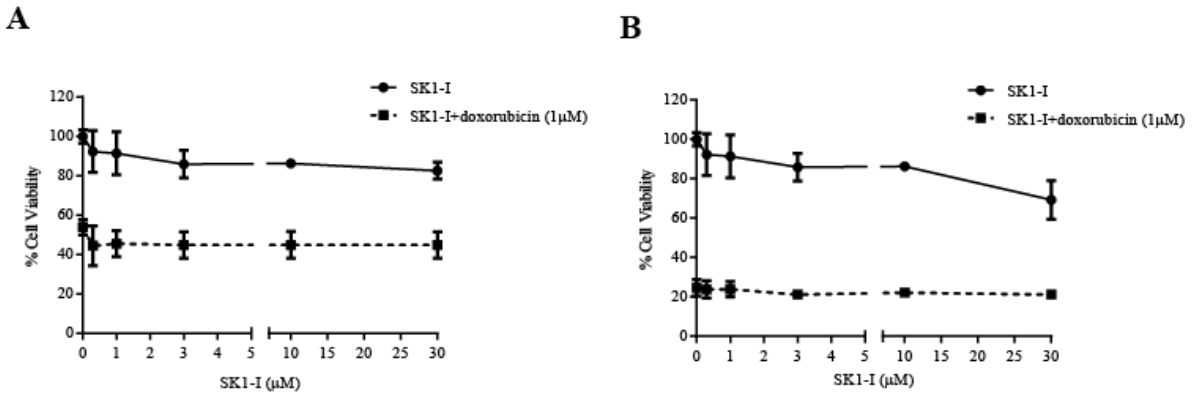

Figure 5.5 Figure S5. SK1-I did not enhance doxorubicin sensitivity in KJDSV40 cells *in vitro*. A, dose response curve of SK1-I alone or in combination with doxorubicin in HEK and B, KJDSV40 cells was determined following 48 hours of treatment. Viability is plotted as percentage control. Data represent the mean ± SEM obtained from triplicate determinations of three independent experiments.

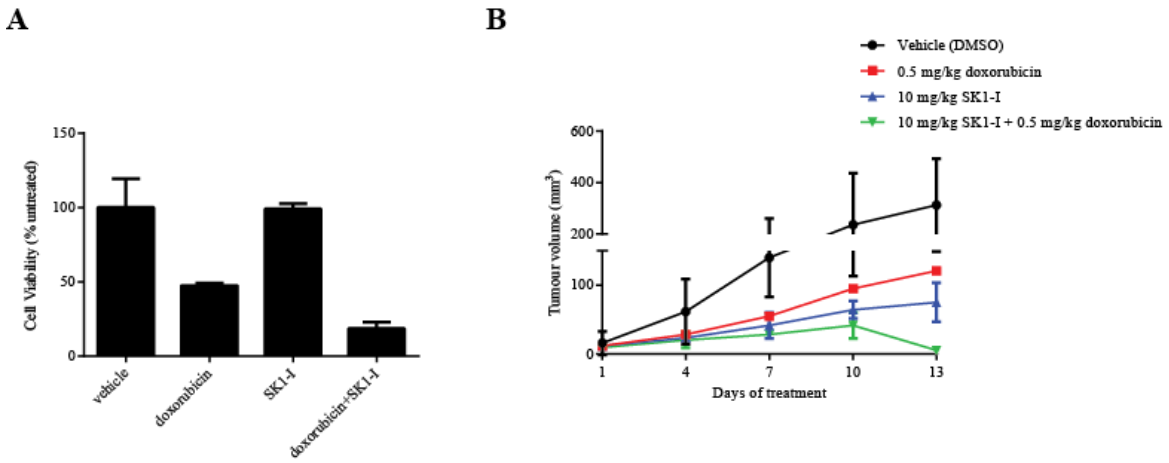

Figure 5.6 Figure S6. Inhibition of Sphk1 sensitises FaDu cells to the cytotoxic actions of doxorubicin *in vitro* and *in vivo*. A, FaDu cells were treated with vehicle, 1 µM doxorubicin, 30 µM SK1-I or 30 µM SK1-I + 1 µM doxorubicin for 48 hours after which viability was estimated and referenced against vehicle treated controls. Data represent the mean ± SEM obtained from triplicate determinations of three independent experiments. B, tumour growth curves of FaDu-derived xenografts treated with doxorubicin, SK1-I or the described combinations. Data represented as mean ± SEM of individual measurements from two mice per group.

CHAPTER SIX

6 A Novel E2F/RacGAP1 Axis Regulates Doxorubicin Response in Squamous Cell Carcinoma

6.1 Foreword

As detailed in *Chapter 3* and *Chapter 4*, E2F7 contributes to drug resistance in SCC. However, the mechanism and pathways involved remain unknown. We therefore embarked on a microarray study as described in *Chapter 4* in order to identify the downstream effectors which are responsible for E2F7-mediated resistance to doxorubicin. These studies resulted in generating a gene signature of SCC which characterized E2F7-mediated chemosensitivity. Gene signature of HNSCC *via* microarray analysis has been described in many reports which characterise HNSCC compared to normal tissue (Alevizos, Mahadevappa et al. 2001; Ginos, Page et al. 2004; Jeon, Lee et al. 2004; Jarvinen, Autio et al. 2006) and which accounts for chemoresistance (Akervall, Guo et al. 2004; van den Broek, Wildeman et al. 2009). Notably, RacGAP1 could not be found in any of these papers. Given the unique design of the experiments presented here, it is not unexpected. Moreover, it indicates the novelty of our microarray screen. Importantly, the role of RacGAP1 in SCC has not been reported before whilst accumulating evidence has demonstrated that RacGAP1 is upregulated in various tumour types (Fritz, Brachetti et al. 2002; Wang, Ooi et al. 2011; Ke, Ke et al. 2013; Kotoula, Kalogeras et al. 2013; Liang, Liu et al. 2013; Pliarchopoulou, Kalogeras et al. 2013; Saigusa, Tanaka et al. 2014). Hence, by distilling RacGAP1 expression as a prognostic marker, we can progress more rapidly towards personalized treatments for SCC. The aim of this chapter therefore is to examine the biological activities of RacGAP1 and its contribution to genetic changes which ultimately lead to the formation of SCC (SCCgenesis) and to determine whether inhibition of RacGAP1, in combination with doxorubicin, could be a viable therapeutic strategy for treating SCC *in vitro* and *in vivo* models of SCC.

We validated E2F7-dependent upregulation of RacGAP1 in doxorubicin insensitive SCC25 cells whilst demonstrating that doxorubicin sensitive KJDSV40 cells express low levels of RacGAP1. Extending this, we found that selective up-regulation of RacGAP1 made previously sensitive KJDSV40 cells resistance to doxorubicin. Similarly, stable knockdown of RacGAP1 in insensitive SCC25 cells sensitised cells to doxorubicin *in vitro*. Consistent with this, ChIP analysis of RacGAP1 promoter showed that E2F7 could bind the RacGAP1 promoter. RacGAP1 expression was validated in HNSCC patient samples utilising a custom TMA that was constructed in-house, providing first line of evidence of RacGAP1 expression

in HNSCC patient tumours. Significantly, we showed that HNSCCs that overexpress RacGAP1 are associated with a poorer overall survival following Kaplan Meier analysis. Furthermore, it was established that E2F7-induced doxorubicin resistance was mediated *via* RacGAP1-dependent activation of AKT. In addition, our results revealed the existence of an unidentified positive feedback loop between RacGAP1 and Sphk1 (*Chapter 5*) in the Ser473 p-AKT-dependent pro-survival response. We also show that SCC cells deficient in RacGAP1 grow slower *in vivo* and are sensitized to the cytotoxic actions of doxorubicin *in vivo*.

These experimental results were presented in a manuscript which has been submitted to *Oncogene*. It has been included here in a slightly amended format to fit with the style of this thesis. Detailed materials and methods for these experiments have been included in *Chapter 2*.

RacGAP1 is a novel downstream effector of E2F7-dependent resistance to doxorubicin and is prognostic for overall survival in squamous cell carcinoma

M Hazar-Rethinam[1], L Merida de Long[1], O M Gannon[1], S Boros[2], AC Vargas[2], M Dzienis[3], P Mukhopadhyay[4,*], N Saenz-Ponce[1], F Simpson[1] and N A Saunders[1]

Authors' Affiliations:

[1]Epithelial Pathobiology Group, University of Queensland Diamantina Institute, Princess Alexandra Hospital, Translational Research Institute, Woolloongabba, Queensland, Australia, [2]Department of Pathology and [3]Department of Medical Oncology, Princess Alexandra Hospital, Woolloongabba, Queensland, Australia, [4]The QIMR Berghofer Medical Research Institute, Brisbane, Queensland, Australia.

*Current address: The QIMR Berghofer Medical Research Institute, Brisbane, Queensland, Australia.

Corresponding Author: Associate Professor N A Saunders, Epithelial Pathobiology Group, University of Queensland Diamantina Institute, Princess Alexandra Hospital, Translational Research Institute, 37 Kent St, Woollongabba, Queensland, Australia, 4102. Phone: +61 (0)7 3443 7098; Fax: +61 (0)7 3443 6966; E-mail: nsaunders@uq.edu.au

Running Title: RacGAP1 is overexpressed in drug resistant SCC

Grant Support

NAS is supported by grants from the Australian NHMRC (#APP1049182) and the Cancer Council Queensland (#APP1025479). NS is supported by a Senior Research Fellowship awarded by the Cancer Council Queensland. NS is supported by a grant from the Wesley St Andrews Research Institute. MHR is supported by an Australian Postgraduate Award.

6.2 Abstract

Advanced head and neck squamous cell carcinomas (HNSCC) are frequently drug resistant and have a mortality rate of 40%. We have previously shown that overexpression of E2F7 may contribute to drug sensitivity in HNSCC cells. In the present study, we conducted a transcriptomic screen to identify downstream factors that contribute to E2F7-dependent resistance to anthracyclines in HNSCC. We provide, *in vitro*, *in vivo* and patient data that identifies a novel E2F7/RacGAP1 pathway that regulates sensitivity to anthracyclines in HNSCC. Specifically, we show that E2F7-dependent resistance to doxorubicin occurs *via* induction of RacGAP1 and is associated with reduced GTP-loading of RhoA and increased GTP-loading of Rac1. Moreover, we show that an interdependent pathway exists between E2F7, Sphk1, RacGAP1 and AKT that regulates doxorubicin sensitivity. We also show that SCC cells deficient in RacGAP1 grow slower *in vivo* and are sensitised to the cytotoxic actions of doxorubicin *in vivo.* Finally, we show that RacGAP1 is significantly overexpressed in 73 % of primary and metastatic human SCCs compared with adjacent "normal" tissue and that HNSCCs that overexpress RacGAP1 are associated with a significantly poorer overall survival. Combined, these findings identify RacGAP1 overexpression as a novel prognostic marker of survival and a potential target to sensitise SCC to anthracyclines.

Keywords: squamous cell carcinoma, E2F7, RacGAP1, chemosensitivity

6.3 Introduction

Cutaneous squamous cell carcinomas (CSCC) and head and neck SCC (HNSCC) are amongst the most common malignancies afflicting man (Li, Zang et al. 2009; Shen, Dong et al. 2011). Current treatment options for advanced SCC include adjuvant chemotherapy with platinum-based drugs such as taxanes, 5-Fluorouracil or therapeutic antibodies against EGFR (Haddad, Colevas et al. 2003; Posner and Lefebvre 2003; Sharafinski, Ferris et al. 2010; Dai, Xie et al. 2011; Hansen and Siu 2013). However, the response is generally transient and characterised by the development of drug resistance. Thus, there is a need to identify new therapeutic strategies that can bypass the emergence of a drug resistant phenotype.

The E2F transcription factor complex comprises a family of activating (E2F1, 2, 3a) or repressive/inhibitory (E2F3b, 4, 5, 6, 7 or 8) E2Fs that regulate key cellular functions such as transcription, differentiation and apoptosis. In the context of keratinocytes (KCs), the E2F transcription factor family has been shown to control i) proliferation, ii) differentiation, iii) stress responses and iv) apoptosis (Wikonkal, Remenyik et al. 2003; Berton, Mitchell et al. 2005; Johnson and Degregori 2006; Li, Ran et al. 2008; Panagiotis Zalmas, Zhao et al. 2008; Hazar-Rethinam, Endo-Munoz et al. 2011). Consistent with their roles in KCs, dysregulation of E2F is a common occurrence in SCC (Dicker, Popa et al. 2000; Wong, Barnes et al. 2003) and overexpression of E2Fs such as E2F1 and E2F7 occurs in the majority of CSCCs and HNSCCs (Dicker, Popa et al. 2000; Kwong, Nguyen et al. 2003; Endo-Munoz, Dahler et al. 2009; Hazar-Rethinam, Merida de Long et al. 2014). E2F1 and E2F7 are known to have opposing actions in the regulation of proliferation (Hazar-Rethinam, Endo-Munoz et al. 2011), differentiation (Endo-Munoz, Dahler et al. 2009) and apoptosis (Panagiotis Zalmas, Zhao et al. 2008; Endo-Munoz, Dahler et al. 2009). For example, recent reports have shown that treatment of wild-type cells with DNA damaging agents such as doxorubicin or etoposide induces E2F7 protein levels and subsequent inhibition of the E2F1-mediated DNA damage response (Li, Ran et al. 2008; Panagiotis Zalmas, Zhao et al. 2008). In the context of KCs, E2F7 was shown to causally modify responses to conventional chemotherapeutics (Hazar-Rethinam, Merida de Long et al. 2014) and UV-responses *in vitr*o (Endo-Munoz, Dahler et al. 2009). Thus, sensitivity to common cytotoxic agents and stimuli appear to be regulated by the relative ratio of E2F1 to E2F7 in the tissue. Given that both E2F1 and E2F7 are known to be overexpressed in SCC (Endo-Munoz, Dahler et al. 2009; Hazar-Rethinam, Merida de Long et al. 2014), it is reasonable to speculate that this may also contribute to drug

resistance in SCC. In this regard, we recently showed that the sphingosine kinase 1 (Sphk1) gene is a direct target of E2F7 in SCC (Hazar-Rethinam, Merida de Long et al. 2014). E2F7-dependent overexpression of Sphk1 in SCC induces increased production of the anti-apoptotic phospholipid, sphingosine-1-phosphate (S1P) which in turn invokes anthracycline-resistance *via* activation of the PI3K/AKT pathway (Hazar-Rethinam, Merida de Long et al. 2014). Thus, E2F dysregulation in SCC induced the activation of a Sphk1/S1P-dependent drug resistant phenotype (Hazar-Rethinam, Merida de Long et al. 2014). Identification of this novel pathway was noteworthy for two reasons. Firstly, anthracyclines such as doxorubicin are not in clinical use for the treatment of SCC and thus the ability to sensitise SCCs to an existing class of chemotherapeutics would be of clinical value. Secondly, the Sphk1/S1P axis is drugable and treatment of mice bearing xenotransplanted SCCs with a Sphk1 inhibitor plus an anthracycline resulted in profound tumour regression (Hazar-Rethinam, Merida de Long et al. 2014). However, the activation of the Sphk1 pathway was not the entire explanation for the anthracycline resistance observed in SCC. Thus, other pathways that control drug resistance in SCC were likely to exist.

In the present study, we used transcriptomic profiling to identify a novel drugable E2F7/RacGAP1/AKT pathway that selectively induces anthracycline resistance in SCC.

6.4 Results

6.4.1 RacGAP1 is a novel downstream effector of E2F7

We generated E2F7 knock down (KD) murine KCs *via* adenovirus mediated Cre deletion of floxed sequences in primary KCs isolated from E2F7 floxed mice (Hazar-Rethinam, Merida de Long et al. 2014). KD KCs were treated for 48 hours with increasing concentrations of doxorubicin (0-1 μM), etoposide (0-100 μM) and cisplatin (0-20 μM). *Figure 6.1A-C* shows that E2F7 deficiency sensitises KCs to doxorubicin, modestly to cisplatin but not at all to etoposide. These data suggest that E2F7-mediated doxorubicin resistance is not attributable to topoisomerase inhibition since etoposide sensitivity was not modified by E2F7. Moreover, pan-caspase inhibition significantly protected E2F7 deficient cells from doxorubicin-induced cytotoxicity (*Figure 6.1D*), indicating that apoptotic pathways are being activated.

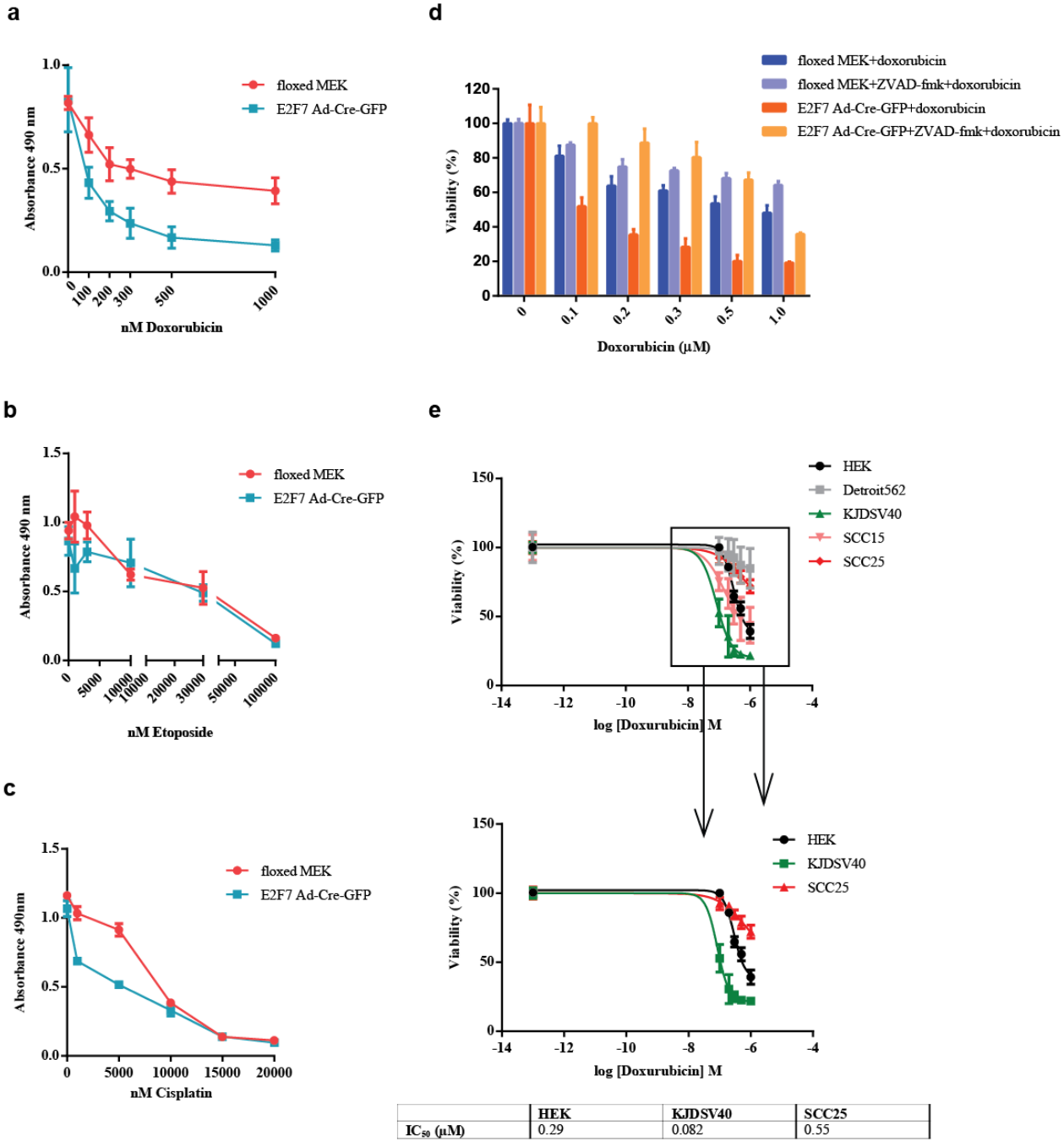

	HEK	KJDSV40	SCC25
IC_{50} (µM)	0.29	0.082	0.55

Figure 6.1 Cytotoxic responses to doxorubicin in E2F7-deficient murine KCs. E2F7-floxed keratinocytes were incubated with (squares) or without (circles) Ad-Cre-GFP for 48 hours and then incubated with varying doses of doxorubicin (A), etoposide (B) or cisplatin (C). Viability (Absorbance 490 nm) was assessed 48 hours post-treatment and is expressed as the mean ± SEM obtained from triplicate determinations of three independent experiments. Ad-Cre-GFP-uninfected E2F7 floxed or Ad-Cre-GFP-infected E2F7 deficient proliferative keratinocytes were treated with 1 µM doxorubicin in the presence or absence of ZVAD-fmk and viability determined 48 hours later (D). Viability is plotted as a percentage of doxorubicin treated uninfected E2F7 floxed MEKs and represents the mean ± SEM obtained

from triplicate determinations of three independent experiments. HEK, Detroit562, KJDSV40, SCC15 and SCC25 cells were treated with doxorubicin for 48 hours and viability plotted as percentage of untreated cells (E). The inset includes the estimated IC_{50} values for doxorubicin in HEK, KJDSV40 and SCC25 cells determined by nonlinear regression analysis.

We undertook a screen of doxorubicin sensitivity in human epidermal keratinocytes (HEK) and 4 SCC cell lines. The KJDSV40 cell line exhibited the highest sensitivity to doxorubicin (IC_{50} of 0.082 μM; *Figure 6.1E*) whilst SCC25 cells displayed the least sensitivity (IC_{50} of 0.55 μM; *Figure 6.1E*) and HEKs displayed intermediate sensitivity (IC_{50} of 0.29 μM; *Figure 6.1E*). We have previously shown that the insensitive SCC25 cell line express high levels of E2F7 whilst the sensitive KJDSV40 cell line express low levels of E2F7 (Hazar-Rethinam, Merida de Long et al. 2014). Based on these data, we selected the sensitive KJDSV40 cell line and the insensitive SCC25 cell line for transcriptomic profiling.

Specifically, we generated a list of genes which were poorly expressed in KJDSV40 cells and highly expressed in SCC25 (*Figure 6.2A*). We also generated a second list of genes that were differentially regulated in SCC25 cells in which E2F7 had been silenced with siRNA (Figure 6.2A). We then used these two lists to identify those transcripts (referred to as List A) that displayed E2F7-dependent expression between the SCC25 cell lines (*Figure 6.2A*). We also generated an additional list of transcripts for SCC25 cells or SCC25 cells in which E2F7 is silenced by siRNA that have been treated with 1 μM of doxorubicin. The transcripts that were found to be E2F7-dependent in the context of doxorubicin-treated SCC25 cells were then referred to as List B (*Figure 6.2A*). By comparing Lists A and B, we identified RacGAP1 as the most differentially overexpressed gene with a B value greater than 11.

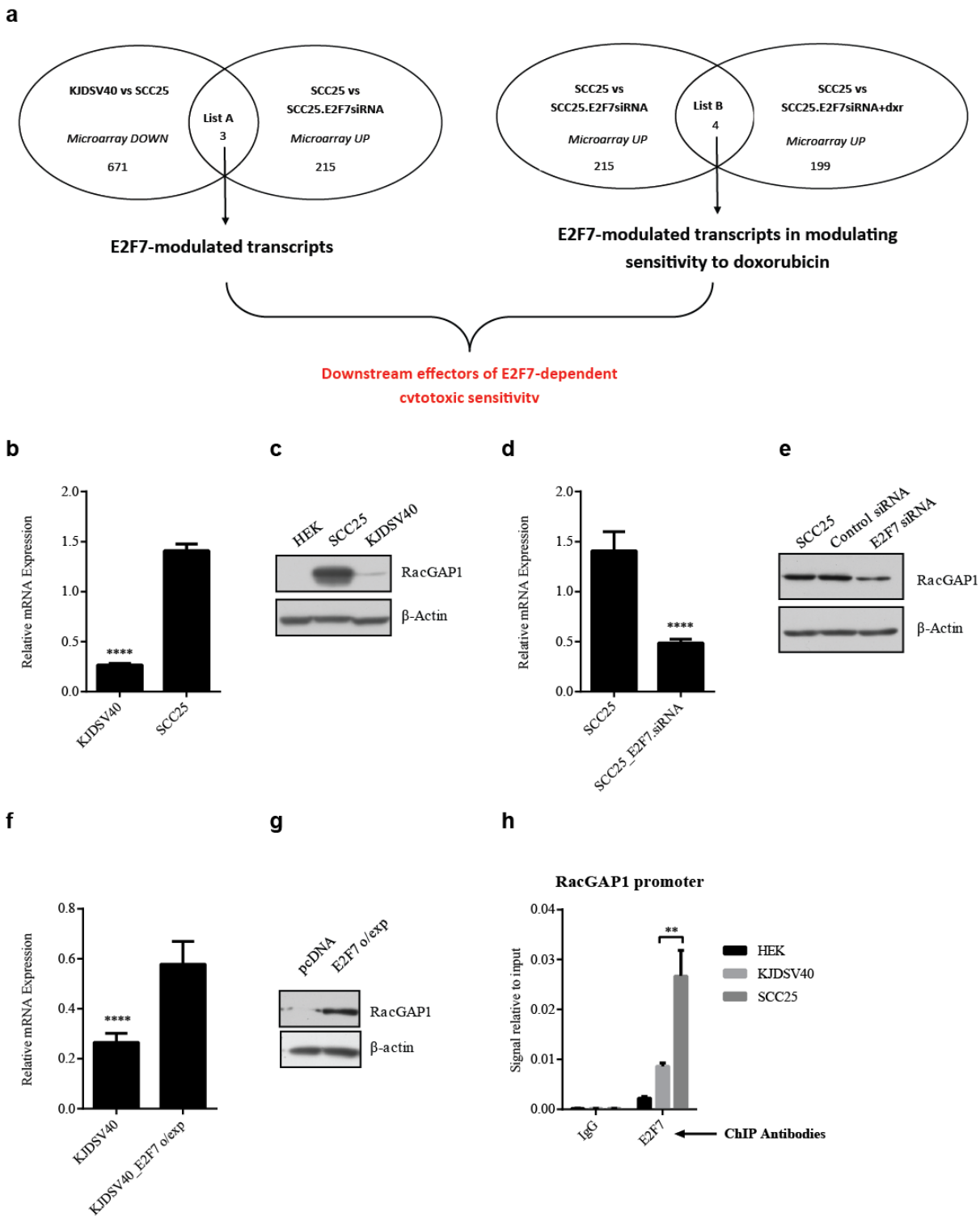

Figure 6.2 RacGAP1 is a downstream effector of E2F7. Summary of the strategy used to identify E2F7-dependent transcripts that associate with doxorubicin resistance in SCC cells (A). RacGAP1 mRNA and protein levels were determined in KJDSV40 and SCC25 cells by qRT-PCR and immunoblotting, respectively (B and C). The expression of RacGAP1 transcripts and protein were determined by qRT-PCR and immunoblotting, respectively from extracts derived from SCC25 and SCC25 cells in which E2F7 was silenced with siRNA for 48 hours (D and E). RNA was extracted from KJDSV40 and KJDSV40 cells in which E2F7

was overexpressed from an expression plasmid. The expression of RacGAP1 transcripts and protein were determined 48 hours post-transfection by qRT-PCR and immunoblotting, respectively (F and G). To quantitate E2F7 binding to the RacGAP1 promoter, ChIPs were performed using an E2F7 antibody or non-immune IgG as control in HEK, KJDSV40 and SCC25 cells (H). Each ChIP and qRT-PCR were repeated 3 or 2 times respectively. SDs refer to the 3 independent experiments. Data are the mean ± SEM of duplicate determinants normalized for expression of the housekeeping gene TBP for (B), (D), (E) and (G); $n = 3$. β-Actin is provided as a loading control for (C), (F) and (H). Western blot figure is representative of three independent experiments. ****, $P < 0.0001$.

RacGAP1 (also known as MgcRacGAP and CYK4) is an evolutionarily conserved GTPase activating protein (GAP) which displays activity towards the Rho family of GTPases. The Rho family of GTPases is a subfamily of the Ras superfamily and consists of small signalling G proteins: Rho (A, B and C isoforms), Rac (1,2,3 isoforms and RhoG) and Cdc42 (Cdc42, Tc10, TCL, Chp/Wrch-2 and Wrch-1) (Wertheimer, Gutierrez-Uzquiza et al. 2012; Pliarchopoulou, Kalogeras et al. 2013) which function as molecular switches between a GTP-loaded "ON" and a GDP-loaded "OFF" state (Pliarchopoulou, Kalogeras et al. 2013). Thus, RacGAP1 has the potential to regulate a diverse array of cellular functions through its central role as a regulator of the activation state of the Rho family of GTPases. In particular, RacGAP1 is known to play important roles in the completion of cytokinesis (Hirose, Kawashima et al. 2001; Zhao and Fang 2005), cell transformation, motility, migration and metastasis (Sahai 2005; Sanz-Moreno, Gadea et al. 2008; Vega and Ridley 2008; Yamazaki, Kurisu et al. 2009). RacGAP1 is also involved in IL6-induced macrophage differentiation (Kawashima, Hirose et al. 2000) and nuclear transport of STAT3/5 transcription factors (Tonozuka, Minoshima et al. 2004). The functions of RacGAP1 are governed by complex processes including phosphorylation, subcellular localization and control of expression (Nishimura, Oki et al. 2013). However, a role for RacGAP1 in SCC or doxorubicin sensitivity has not been shown previously.

Quantitative RT-PCR and western blotting were used to confirm that RacGAP1 was more highly expressed in SCC25 (doxorubicin insensitive) cells than in KJDSV40 (doxorubicin sensitive) cells (*Figure 6.2B and C*). Similarly, we showed that knockdown of E2F7 by siRNA in SCC25 cells caused a reduction in RacGAP1 mRNA (*Figure 6.2D*) and protein level (*Figure 6.2E*). Conversely, overexpression of E2F7 in KJDSV40 cells resulted in elevated levels of RacGAP1 transcript (*Figure 6.2F*) as well as RacGAP1 protein (*Figure 6. 2G*). These data suggest that RacGAP1 is a downstream target of E2F7 in SCC cells.

Supporting this, ChIP analysis of E2F7 binding showed that E2F7 could bind the RacGAP1 promoter suggesting that RacGAP1 is a direct transcriptional target of E2F7 (*Figure 6.2H*). This is the first report to show that RacGAP1 is a downstream effector of E2F7.

6.4.2 RacGAP1 expression is elevated in SCCs

We examined RacGAP1 expression levels by immunohistochemistry using a tissue microarray (TMA) consisting of 35 paired normal, primary tumour and matched metastasis from HNSCC patients treated at the Princess Alexandra Hospital (PAH). The TMAs were stained for E2F7 and RacGAP1 protein expression and scored blinded by two Pathologists. All matched adjacent "normal" epithelia demonstrated either negative or weak staining for RacGAP1 which was predominantly nuclear in location (*Figure 6.3A*). Conversely, moderate to high levels of RacGAP1 expression were consistently recorded for the primary tumour (*Figure 6.3B*) and its matched lymph node metastasis (*Figure 6.3C*). The tumour epithelial cells showed nuclear and cytosolic expression for RacGAP1. RacGAP1 was significantly overexpressed in 73 % of primary and metastatic human SCCs compared to matched adjacent normal tissue ($P < 0.0001$; *Figure 6.3D*). In addition, our analyses showed that E2F7 expression is significantly upregulated in HNSCC compared to matched adjacent normal tissue ($P < 0.0001$; *Figure 6.3D*). Kaplan-Meier analysis revealed an inverse relationship between RacGAP1 expression levels and progression-free survival (PFS) of HNSCC patients studied over a period of 42 months whose samples were arrayed on the TMA (*Figure 6.3E*). These data show, for the first time, that RacGAP1 is overexpressed in HNSCC and is associated with a poorer PFS.

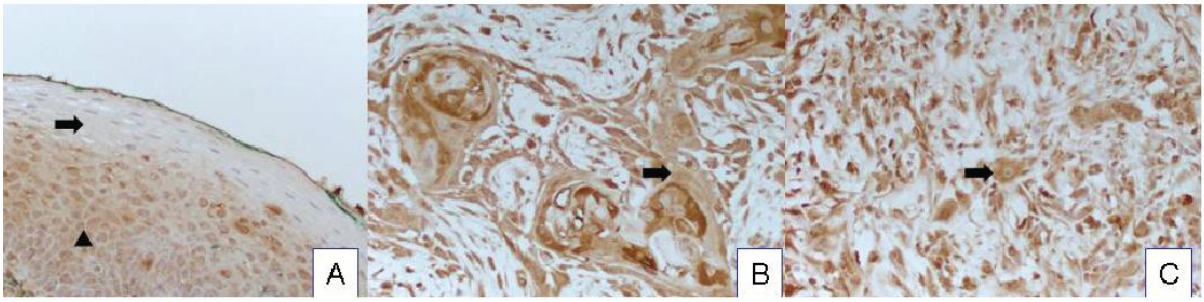

d

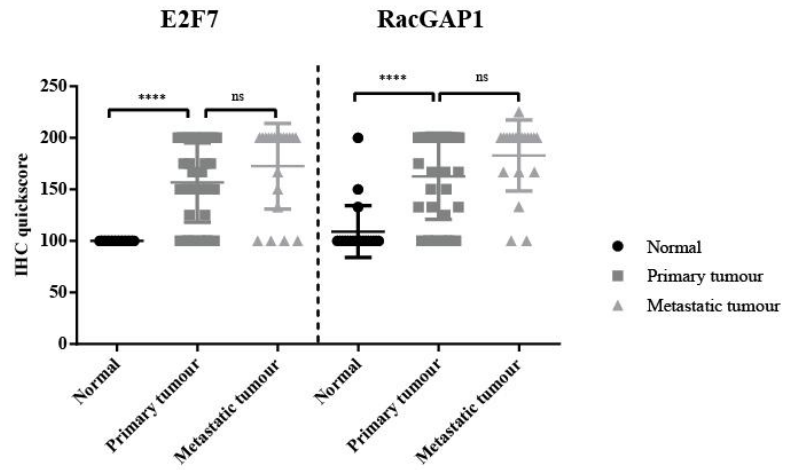

e

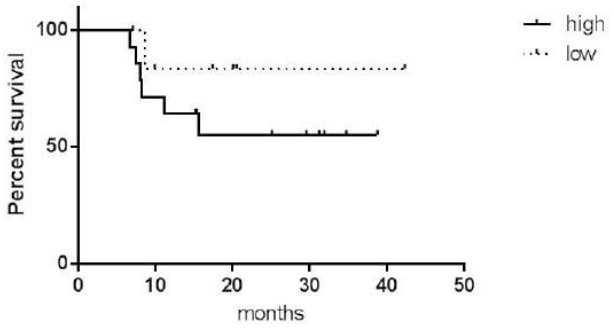

RacGAP1	Range	Median	Mean
Primary tumour	0-200	171	158

Figure 6.3 Expression of RacGAP1 in HNSCC and adjacent normal tissue and its association with progression free survival. Representative images of adjacent normal tissue (A) and HNSCC specimens stained for RacGAP1 (B and C). Quantitation of E2F7 and RacGAP1 staining intensities in matched samples of primary tumour, normal squamous epithelium and lymph node metastases (n = 35) (D). Tissue sections were scored using a modified quickscore method to determine the percentage of cells stained (0-100%) and the intensity of staining (1+ to 3+). Kaplan-Meier analysis of progression free survival stratified by RacGAP1 expression in the HNSCC patient cohort (E). ns is not significant, ****, P < 0.0001.

6.4.3 RacGAP1 expression/activity determines sensitivity to doxorubicin

We examined the effect of shRNA-mediated knockdown or RacGAP1 overexpression on sensitivity to doxorubicin. RacGAP1 gene silencing was achieved using 3 different constructs of which shRNA.3 displayed the greatest knockdown in RacGAP1 protein level (*Figure 6.4A*). For subsequent experiments, the shRNA complex shRNA.3 was employed. Consistent with previous reports (Nishimura, Oki et al. 2013), RacGAP1 shRNA transfected SCC25 cells displayed significant reductions in proliferation (*Figure 6.4B*), colony-forming efficiency *in vitro* (*Figure 6.4C*) and induced a modest increase in cleaved PARP1 (*Figure 6.4D)* compared to control vector transfected cells. Finally, silencing RacGAP1 significantly enhanced the sensitivity of SCC25 cells to doxorubicin (*Figure 6.4E*). Conversely, overexpression of RacGAP1 in insensitive KJDSV40 cells resulted in increases in RacGAP1 protein level (*Figure 6.4F*), and reduced sensitivity to doxorubicin compared to vector control (*Figure 6.4G*). Combined, these data indicate that RacGAP1 can promote proliferation and inhibit doxorubicin induced cell death in SCCs.

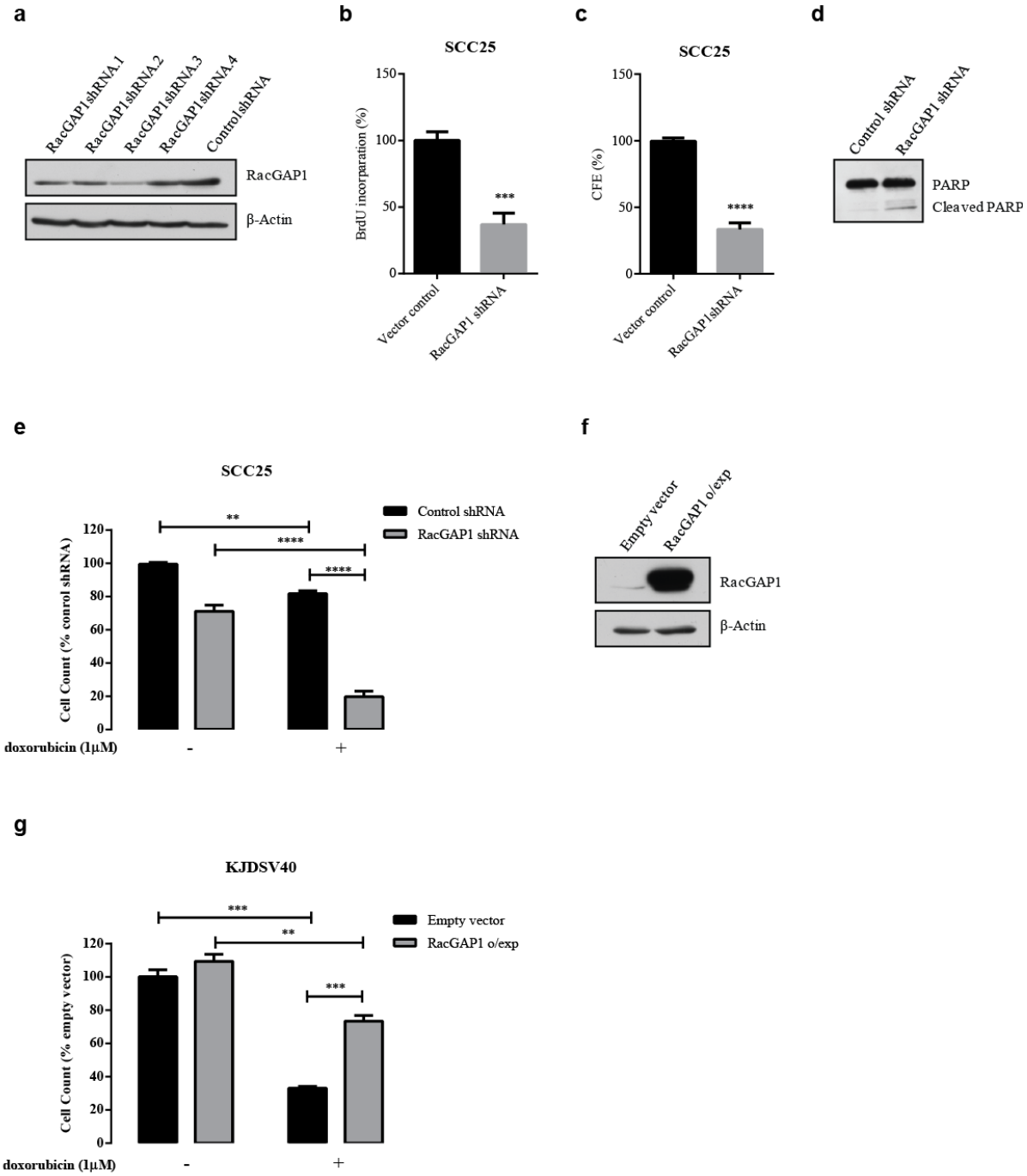

Figure 6.4 The sensitivity to doxorubicin is mediated *via* an E2F7/RacGAP1 axis in SCC. SCC25 cells were transfected with 4 different constructs coding for shRNAs directed against RacGAP1. After 48 hours, RacGAP1 protein expression was determined by immunoblotting (A). β-Actin is provided as a loading control. SCC25 cells were transfected with the RacGAP1shRNA.3 or a scrambled shRNA construct. After 48 hours, BrdU incorporation (B) and CFE (C) were determined. Data expressed as a percentage of that observed for control shRNA. Cleavage of PARP was determined by immunoblotting extracts of RacGAP1shRNA and control shRNA transfected SCC25 cells (D). β-Actin is provided as a loading control. RacGAP1shRNA and control shRNA transfected SCC25 cells were treated with doxorubicin (1μM) for 48 hours and viability estimated by trypan blue exclusion (E). Viability is plotted as percentage control (untreated). KJDSV40 cells were transfected with

RacGAP1 expression plasmid or a noncoding empty vector. After 48 hours, RacGAP1 protein expression was determined by immunoblotting (F). β-Actin is a loading control. RacGAP1 expression plasmid or empty vector transfected KJDSV40 cells were treated with doxorubicin (1μM) for 48 hours and viability estimated by trypan blue exclusion (G). Viability was expressed as percentage control (untreated). Western blot figures are representative of three independent experiments. All quantitative data presented as mean ± SEM. For viability values represent triplicate determinations of three independent experiments; for CFE, expression values represent duplicate determinations from at least three independent experiments; for BrdU values represent triplicate determinations from 4 independent experiments. **, $P < 0.01$, ***, $P < 0.001$, ****, $P < 0.0001$.

6.4.4 RacGAP1 differentially regulates the GTP-loaded state of RhoA and Rac1 in SCC cells

We examined whether the overexpression of RacGAP1 in the SCC cell lines was reflected in alterations of the GTP-loading (activation status) of the model targets RhoA and Rac1. Specifically, RhoA GTP loading was constitutively higher in KJDSV40 cells, which express very low levels of E2F7 and RacGAP1, compared to SCC25 cells which express high levels of E2F7 and RacGAP1 (*Figure 6.5A*). In contrast, GTP-loading of Rac1 was higher in SCC25 cells when compared with KJDSV40 cells (*Figure 6.5B*), and the GTP-loading of Rac1 was significantly reduced in SCC25 cells following RacGAP1 knockdown (*Figure 6.5B*). Finally, knockdown of RacGAP1 in SCC25 cells resulted in an increase in the GTP-loading of RhoA (*Figure 6.5A*). These results indicate a number of important points. Firstly, RhoA appears to be a preferred substrate for RacGAP1 in SCC25 cells. This is reflected by the high level of RhoA-GTP loading compared to Rac1-GTP loading as well as the increase in GTP-loading observed following RacGAP1 knockdown in the SCC25 cells. Secondly, whilst Rac1-GTP loading behaviour is not indicative of it being a preferred substrate of RacGAP1, it is clear that alterations in RacGAP1 activity modify Rac1-GTP loading. Finally, the preference for RhoA by RacGAP1, in SCC cells, is consistent with a previous report showing that the conventional preference for Rac1 can be switched to RhoA following phosphorylation of the Serine 387 site of RacGAP1 by Aurora B kinase (Minoshima, Kawashima et al. 2003; Doki, Kawashima et al. 2009).

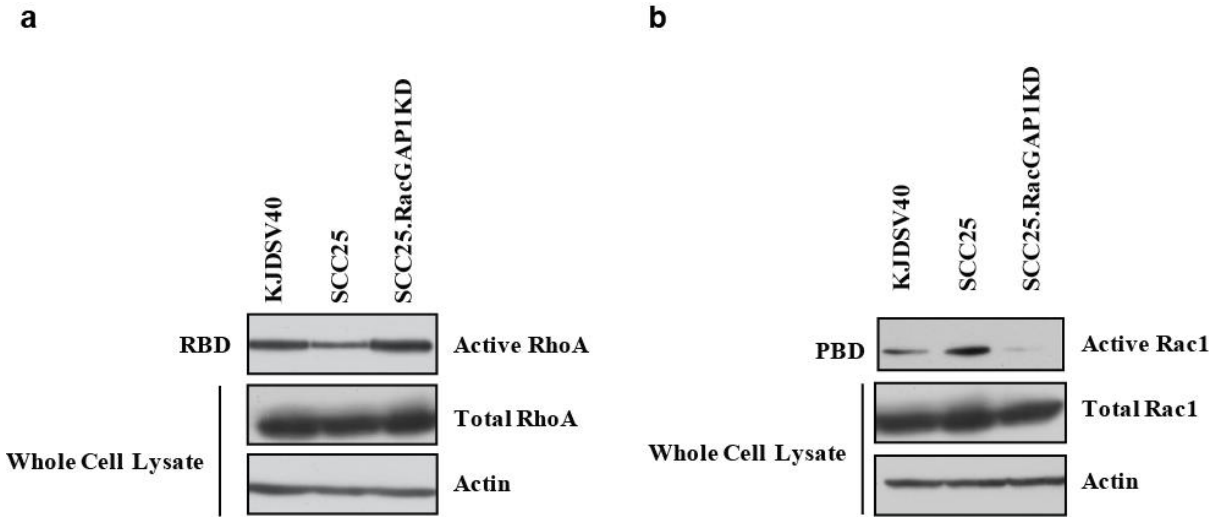

Figure 6.5 GTP-loading state of Rac1 and RhoA in SCC cells. Rhotekin-binding domain (RBD) binding and p21 activated kinase I-binding domain (PAK-PBD) assays were performed on the extracts from KJDSV40, SCC25 and SCC25 cells in which RacGAP1 had been silenced by shRNA, as indicated. The amount of activated or total RhoA and Rac1 were detected by immunoblotting the RBD and PAK-PBD samples and the whole cell lysate with RhoA or Rac1 antibodies. To confirm equal input, the membrane was re-probed with an actin antibody.

6.4.5 RacGAP1 modulates doxorubicin sensitivity *via* downstream activation of the PI3K/AKT pathway

There is an existing literature showing that the PI3K/AKT pathway is an important component of RacGAP1 signalling (Wang, Ooi et al. 2011). However, whether PI3K/AKT signalling lies upstream or downstream of the Rho family of GTPases remains less clear and appears to be context-specific (Wang, Ooi et al. 2011). Dysregulation of the PI3K/AKT pathway is a common event in HNSCC which can be attributed to multiple factors such as mutations, amplifications and signal-induced activation of the pathway (Iglesias-Bartolome, Martin et al. 2013). For example, we recently showed that E2F7 overexpression or knockdown caused an increase and decrease in p-AKT levels in SCC cells respectively (Hazar-Rethinam, Merida de Long et al. 2014). Since, RacGAP1 is a downstream effector of E2F7 in SCC cells, we examined whether RacGAP1 could modify the PI3K/AKT signalling pathway in SCC cells. In the first instance we noted that knockdown of RacGAP1 in SCC25 cells had no impact on the activation status of the ERK pathway (*Figure 6.6A*). In contrast, RacGAP1 knockdown in SCC25 cells significantly reduced the level of p-AKT (*Figure 6.6B*) whilst RacGAP1 overexpression in KJDSV40 cells increased p-AKT levels (*Figure 6.6C*). We had previously shown that the PI3K/mTOR inhibitor, BGT226, was able to ablate AKT signalling and induce apoptosis in SCC cell lines (Erlich, Kherrouche et al. 2012). We

compared the sensitivity of SCC25 cells to BGT226 in SCC25 cells or SCC25 cells in which RacGAP1 was knocked down. *Figure 6.6D* indicates that knockdown of RacGAP1 is able to reduce SCC25 cell viability to 70% that of control cells. Similarly, inhibition of PI3K activity using a dose of BGT226 known to induce maximal inhibition (Erlich, Kherrouche et al. 2012) reduced SCC25 cell viability to approximately 50% (*Figure 6.6D*). Finally, exposure of RacGAP1-deficient SCC25 cells to BGT226 resulted in a further decrease in viability to below 20% (*Figure 6.6D*). These data indicate that RacGAP1 participates in AKT-dependent and AKT-independent events.

We recently reported that E2F7 is able to directly activate the Sphk1/S1P axis in SCC cells which induces doxorubicin resistance (Hazar-Rethinam, Merida de Long et al. 2014). It is also interesting to note that both the E2F7/RacGAP1 pathway identified in this study and the E2F7/Sphk1/S1P pathway (Hazar-Rethinam, Merida de Long et al. 2014) induced doxorubicin resistance and converged on the AKT pathway. Therefore, we examined whether the Sphk1 and RacGAP1 pathways may interact with one another. *Figure 6.6E* shows that knockdown of Sphk1 can induce loss of RacGAP1 mRNA whilst knockdown of RacGAP1 induces loss of Sphk1 mRNA expression. Whilst the mechanism controlling this feedback is unknown, it is clear that targeted inhibition of either the RacGAP1 pathway or the Sphk1 pathway is likely to impact one another. To illustrate this point, knockdown of RacGAP1 or Sphk1 in SCC25 cells results in reduced p-AKT levels (*Figure 6.6F*) and increased sensitivity to doxorubicin (*Figure 6.6G*) which can be reversed by the addition of exogenous S1P (*Figure 6.6F and G*).

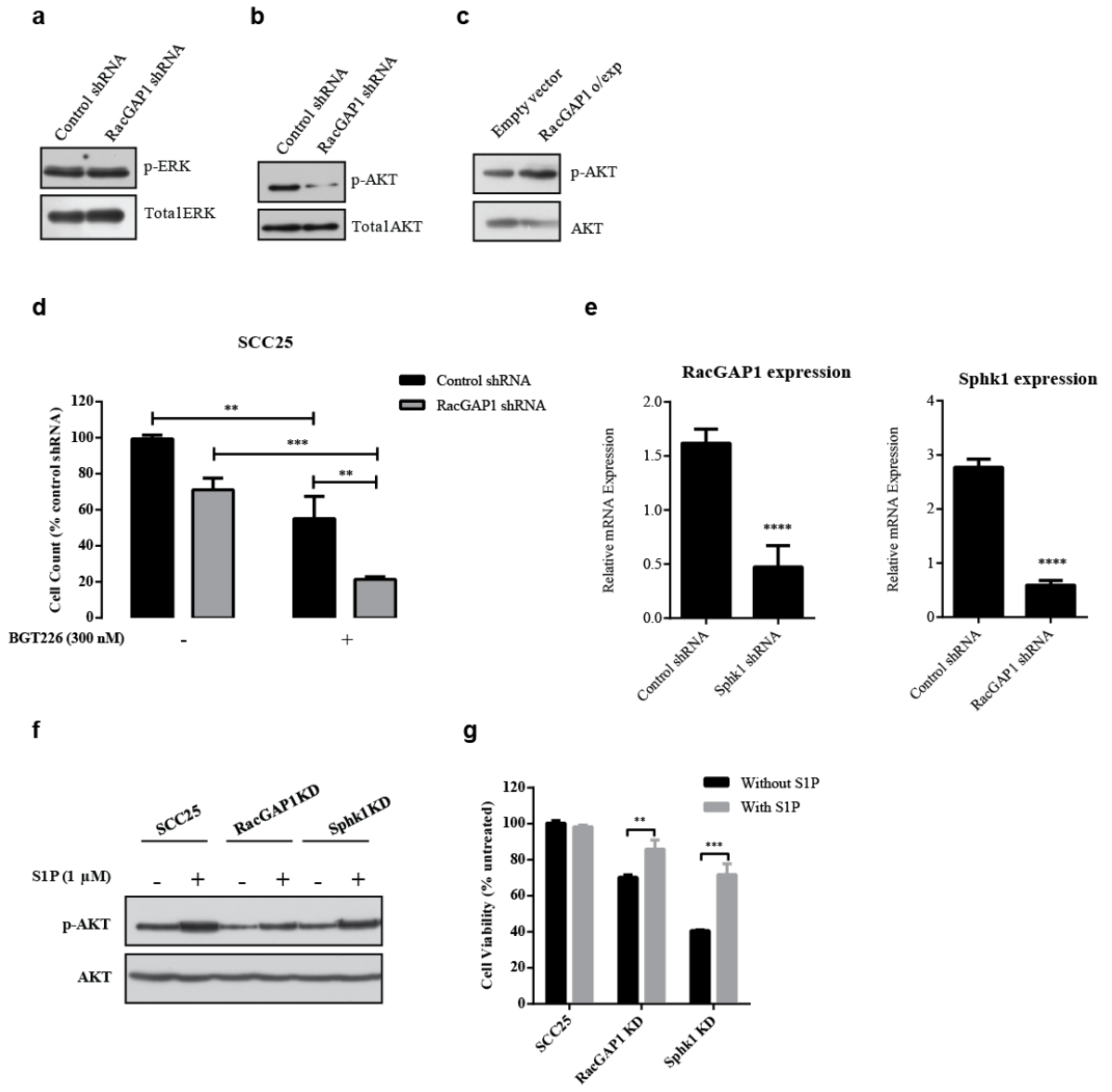

Figure 6.6 RacGAP1 lies upstream of AKT and regulates its activity. SCC25 cells were transfected with the RacGAP1shRNA or a scrambled shRNA construct. After 48 hours, p-ERK and total ERK protein levels (A) and p-AKT and total AKT protein levels (B) were determined by immunblotting. p-AKT and total AKT protein levels are shown for KJDSV40 cells in which RacGAP1 was overexpressed (C). RacGAP1shRNA and control shRNA transfected SCC25 cells were treated with doxorubicin (1μM) for 48 hours and viability estimated by trypan blue exclusion and plotted as percentage control shRNA (D). SCC25 cells were transfected with Sphk1shRNA and RacGAP1shRNA as well as control shRNA. After 48 hours, RacGAP1 (left) and Sphk1 (right) mRNA levels were determined by qRT-PCR (E). SCC25 cells were transfected with RacGAP1 or Sphk1 shRNAs. 48 hours after transfection, cells were treated with 1 μM S1P for 24 hours. p-AKT and total AKT protein levels were then determined by immunoblotting (F). SCC25, SCC25 in which RacGAP1 or Sphk1 had been silenced were treated with 1 μM doxorubicin and 1 μM S1P for 24 hours. Viability was then assessed and plotted as percentage doxorubicin only treated (G). Western blot figures are representative of three independent experiments. All quantitative data presented as mean ± SEM obtained from triplicate determinations of three independent

experiments for (D) and (G). Data are the mean ± SEM of duplicate determinants normalized for expression of the housekeeping gene TBP for (e); $n = 3$. **, $P < 0.01$, ***, $P < 0.001$, ****, $P < 0.0001$.

6.4.6 RacGAP1 suppression enhances sensitivity of SCC25 to doxorubicin *in vivo*

SCC25 cells were generated to stably express either vector control or RacGAP1 shRNA and inoculated into NOD/SCID mice. When tumours were around 4 mm in diameter, mice were randomized into four groups and treated with vehicle, dimethyl sulfoxide (DMSO), or 0.5 mg/kg doxorubicin by intraperitoneal (i.p.) injections twice per week. RacGAP1 knockdown was confirmed by western blotting immediately before the inoculation of SCC25 cells (*Figure 6.7A*). Treatment with doxorubicin was well tolerated by the NOD/SCID mice and the body weights remained stable throughout the study (*Figure 6.7A*). RacGAP1-deficient cells showed reduced tumour growth rate (*Figure 6.7B*). Treatment of mice bearing vector control SCC25 tumours with/without 0.5 mg/kg doxorubicin had minimal effect on tumour growth rates (*Figure 6.7B*). However, RacGAP1 deficient SCC25 tumours treated with doxorubicin started to regress by day 4 post-treatment which continued for a further 7 days at which time all mice were sacrificed due to the tumour burden in control mice. The subcutaneous tumours were excised, photographed and examined histologically (*Figure 6.7C*).

Immunohistochemical examination of the excised tumours showed that knockdown of RacGAP1 was maintained throughout the study (*Figure 6.7D*). Tumours from vehicle and doxorubicin treated control mice stained strongly for PCNA, indicating a higher proportion of proliferating cells in control tumours compared to RacGAP1 deficient tumours (treated or untreated; *Figure 6.7D*). In contrast, doxorubicin induced higher apoptosis indices in tumours derived from SCC25/RacGAP1shRNA than in the SCC25/vector control as estimated by immunostaining for cleaved caspase-3 (*Figure 6.7D*). Ser473 p-AKT levels in RacGAP1-deficient cells were also decreased (*Figure 6.7D*). Collectively, these results suggest that RacGAP1 contributes to the growth of HNSCC *in vivo* and that targeted inhibition of RacGAP1-overexpressing tumours may sensitise them to the cytotoxic actions of doxorubicin.

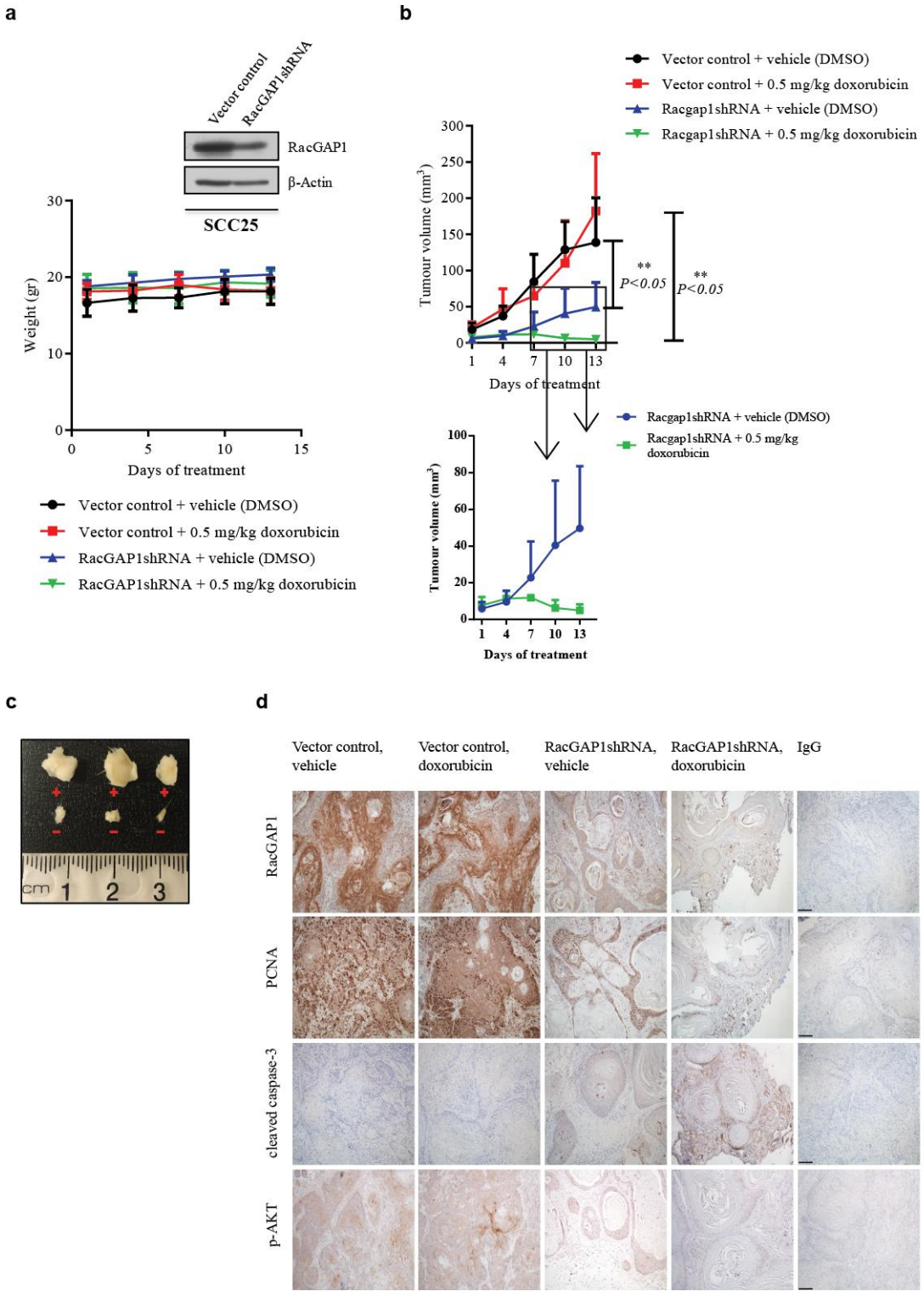

Figure 6.7 RacGAP1 suppression enhanced sensitivity of SCC25 to the cytotoxic actions of doxorubicin *in vivo*. On the day of subcutaneous injections, RacGAP1 deficiency was confirmed by immunoblotting using protein extracts from SCC25 cells in which RacGAP1 had stably silenced with shRNA (A). β-Actin is provided as a loading control. All animals were inoculated subcutaneously with $2x10^6$ SCC25 cells expressing vector alone (scrambled shRNA) or Sphk1 shRNA and tumours allowed to establish till they reached the indicated sizes. Established tumours were treated with vehicle or 0.5 mg /kg doxorubicin twice per week. Animal weight was determined twice per week (A). Tumour volumes were monitored

twice weekly (B). The inset includes vehicle or 0.5 mg /kg doxorubicin treated SCC tumours harbouring RacGAP1shRNA (B). After 13 days of treatment, animals were sacrificed and tumours excised. Representative results from distinct groups are shown (C). + indicates tumours formed from control shRNA transfected SCC25 cells; - indicates tumours formed from RacGAP1shRNA transfected SCC25 cells. Immunostaining for RacGAP1, PCNA, cleaved caspase-3 and p-AKT or normal Rabbit IgG as a negative control (D). Representative images of at least three independent tumours are shown for each group (Bar = 100μm). Data presented as mean ± SEM of individual measurements from six mice per group.

6.5 Discussion

This is the first study to identify an E2F7/RacGAP1/AKT axis through which SCC cells acquire resistance to doxorubicin. Specifically, we show that (i) RacGAP1 is a novel downstream effector of E2F7, (ii) RacGAP1 is overexpressed in patient SCC and is associated with poor progression-free survival, (iii) RacGAP1 overexpression is associated with inactivation of the RhoGTPases and activation of the RacGTPases and iv) E2F7-dependent doxorubicin resistance is mediated *via* induction of RacGAP1 and Sphk1 which in turn activates AKT-dependent and AKT-independent pathways *in vitro* and *in vivo*.

The E2F transcription factor family are involved in a diverse array of cellular functions that are controlled by the relative ratio of atypical E2F (e.g. E2F7) to activating E2F (e.g. E2F1). For example, the apoptotic actions of E2F1, in SCC cells, can be antagonised by E2F7 overexpression (Endo-Munoz, Dahler et al. 2009). Similarly, E2F7 inhibits doxorubicin-induced cytotoxicity by inducing the expression of Sphk1 resulting in increased levels of S1P which enhance the Ser473 p-AKT-dependent pro-survival response (Hazar-Rethinam, Merida de Long et al. 2014). These data are of particular relevance since we know that the majority of human SCCs express high levels of both E2F1 and E2F7. In the present study, we found that high levels of RacGAP1 in advanced SCC patients were associated with a poor progression free survival. Moreover, we demonstrated that forced overexpression of E2F7 was able to induce RacGAP1 overexpression and doxorubicin resistance whilst knockdown of E2F7 reduced RacGAP1 expression and induced sensitivity to doxorubicin *in vitro* and *in vivo*. These data indicate that RacGAP1 is a direct downstream transcriptional target of E2F7. The RacGAP1 promoter contains E2F binding sites and E2F activation has been reported to be required for the initiation of transcription at the RacGAP1 promoter in human lymphocyte cell line (Seguin, Liot et al. 2009). Consistent with this, we showed that elevated E2F7 levels in SCC are associated with increased binding of E2F7 to the RacGAP1 promoter and increased expression of RacGAP1 in SCCs. E2F7 is traditionally considered to be a transcriptional repressor, however, it has also been shown that E2F7 can function as a direct transcriptional activator of the VEGFA promoter *via* the formation of an E2F7-HIF1α transcriptional complex to regulate primary angiogenesis (Weijts, Bakker et al. 2012). Similarly, E2F7 has been shown to bind the Sphk1 promoter in SCC cells and is associated with increased Sphk1 transcription (Hazar-Rethinam, Merida de Long et al. 2014). The precise mechanism by which E2F7 regulates the transcription of RacGAP1 and Sphk1 is

currently under examination. Regardless of the mechanism, our functional data shows that E2F7 regulates doxorubicin-induced cytotoxicity *via* transcriptional induction of RacGAP1.

To our knowledge, this is the first report showing overexpression of RacGAP1 in HNSCC tumour samples. This is also the first report to show that overexpression of tumour-associated RacGAP1 is directly controlled by E2F7, which itself is known to be overexpressed in SCC and to induce drug resistance (Hazar-Rethinam, Merida de Long et al. 2014). Overexpression of RacGAP1 has been reported in high grade meningiomas, nonsmall-cell lung cancer, gastric cancer, hepatocellular carcinoma, breast cancer (Wang, Ooi et al. 2011; Ke, Ke et al. 2013; Liang, Liu et al. 2013; Pliarchopoulou, Kalogeras et al. 2013; Saigusa, Tanaka et al. 2014) as well as in the more aggressive tumour phenotypes of epithelial ovarian cancer, high-grade breast cancer and invasive cervical cancer (Ma, Salunga et al. 2003; Lu, Patterson et al. 2004; Rosty, Sheffer et al. 2005). However, it is unknown whether the overexpression of RacGAP1 in these tumours is linked to overexpression of E2F7. Whilst the overexpression of RacGAP1 is not considered to be simply a "passenger" in other cancer types, (Sahai 2005; Sanz-Moreno, Gadea et al. 2008; Vega and Ridley 2008; Yamazaki, Kurisu et al. 2009), its contribution to HNSCC is unknown. Our data shows that loss of RacGAP1 expression is able to reduce SCC growth in a xenotransplant model *via* inhibition of proliferation and increased basal apoptosis. In addition, we show that high levels of expression are associated with poor PFS of HNSCC patients. Thus, our clinical and preclinical data would suggest that E2F7-dependent overexpression of RacGAP1 is likely to be a driver of tumour growth and drug resistance in HNSCC.

The functional consequences of RacGAP1 overexpression are not reflective of a generalised loss of GTP loading of the Rho/Rac family of GTPases. Our data indicated that RacGAP1 favoured the conversion of RhoGTP to RhoGDP in HNSCC cells. However, it was clear that the GTP-loading status of Rac1 was also responsive to changes in RacGAP1 expression. For example, RacGAP1 appeared to negatively regulate the GTP-loading status of Rac1 such that knockdown of RacGAP1 resulted in a reduction in the GTP-loading state of Rac1. Whilst this seemed counterintuitive, it has been shown that phosphorylation of RacGAP1 by Aurora B kinase, on Serine 387 shifts its GAP activity from Rac to Rho, resulting in increased GTP-loading (activation) of Rac1 and reduced GTP loading of Rho (inactivation) (Doki, Kawashima et al. 2009). We were unable to determine whether the reduced proliferation, or increased doxorubicin-sensitivity, in SCC cells following RacGAP1 knockdown was due to

the reduced GTP loading state of Rac or the increased GTP-loading state of Rho members or the relative ratio of GTP-loaded Rho/GTP-loaded Rac. However, it should be noted that the antiapoptotic protein Bcl-2 has been shown to interact with Rac1, and it was suggested that this interaction could protect tumour cells from the cytotoxic actions of etoposide and daunorubicin (Velaithan, Kang et al. 2011). Moreover, it was recently suggested that Rac1 was a potential therapeutic target in chemo-radioresistant HNSCC (Skvortsov, Dudas et al. 2014). Thus, the E2F7-dependent drug resistant phenotype we observed in SCC cells is likely due to GTP-loaded Rac1.

There is an existing literature on the role of PI3K/AKT in controlling RacGAP1 activity and the GTP-loading of the Rho family of GTPases. In particular, it has been shown that AKT directly binds to and activates RacGAP1 activity *via* phosphorylation of T249 (Jacquemet, Green et al. 2013). In the present study we show that E2F7 induces RacGAP1 expression which is associated with i) an increase in activated Rac1, ii) a decrease in RhoA activity, iii) an increase in Ser473 p-AKT and iv) resistance to doxorubicin. These findings are consistent with the observation that PI3K/AKT signalling are among the most significantly altered canonical pathways following RacGAP1 silencing in HCC (Wang, Ooi et al. 2011). Our observations also suggest that the overexpression of RacGAP1 in SCC may contribute to the activation of the AKT pathway that is seen in more than 40% of all HNSCCs. However, how RacGAP1 contributes to AKT activation remains unclear. We certainly know that overexpressing or knocking down E2F7 or RacGAP1 modifies Ser473 phosphorylation of AKT. However, we also know that E2F7 directly induces Sphk1 expression and S1P levels in SCC leading to increased Ser473 phosphorylation of AKT (Hazar-Rethinam, Merida de Long et al. 2014). Finally, we now show that Sphk1 and RacGAP1 indirectly modify one another's expression. Thus, it is difficult to determine whether RacGAP1-dependent effects on AKT phosphorylation status are modified by RacGAP1 or indirectly *via* changes in Sphk1/S1P. Regardless of the mechanism, our results demonstrate the existence of a novel, complex and interdependent network between E2F7, RacGAP1 and Sphk1/S1P, and the importance of such a network in chemosensitivity.

6.6 Materials and Methods

6.6.1 Chemicals and viability assays

The following drugs were purchased: doxorubicin (Sigma Aldrich, Castle Hill, Australia), S1P (Cayman Chemicals, Sapphire Bioscience, Waterloo, Australia), ZVAD-fmk (Alexis Biochemicals, Sapphire Bioscience, Waterloo, Australia). BGT26 was provided by Novartis (Basel, Switzerland) and stocks of BGT226 were prepared as described (Erlich, Kherrouche et al. 2012). ZVAD-fmk was added 30 minutes before other treatments. Cell viability was performed by trypan blue exclusion or using Cell Titer 96 Aqueous One Solution Cell Proliferation Assay (Promega, Alexandra, Australia).

6.6.2 Tissue culture, adenovirus infection and transfection

Murine epidermal keratinocytes and human epidermal keratinocytes were isolated and cultured as described (Jones, Dicker et al. 1997; Zhao, Gu et al. 2005). E2F7 KD keratinocytes generated by ready-to-use adenovirus harbouring Cre recombinase infection of MEKs as per manufacturer's recommendations (MOI of 50) (Vector Biolabs, Philadelphia, PA, USA). Detroit562 and SCC25 cells were obtained from the American Type Culture Collection. SCC15 was a kind gift from Dr. Elizabeth Musgrove (Garvan Institute, New South Wales, Australia) and were verified by short tandem repeat genotyping (Dicker, Popa et al. 2000). KJDSV40 cells were maintained as described previously (Dicker, Popa et al. 2000). Control and overexpression plasmids used for manipulating E2F7, and the siRNA used for targeting E2F7 have been described previously (Panagiotis Zalmas, Zhao et al. 2008; Endo-Munoz, Dahler et al. 2009). SureSilencing shRNA plasmids directed against RacGAP1 or Sphk1 were purchased from SuperArray Bioscience Corp (SA Biosciences, Qiagen, Chadstone Centre, Australia). A RacGAP1 expression (TrueORF Gold Clones) and control plasmids were purchased from OriGene Technologies (Australian Biosearch, Karrinyup, Australia).

6.6.3 RNA isolation and quantitative RT-PCR

Total RNA was isolated, cDNA prepared and quantitative reverse transcriptase PCR (qRT-PCR) performed as described (Endo-Munoz, Dahler et al. 2009; Endo-Munoz, Cumming et al. 2010). Primer sequences were E2F7 Forward: GTCAGCCCTCACTAAACCTAAG, E2F7 Reverse: TGCGTTGGATGCTCTTGG; RacGAP1 Forward: GACGTTGAATAGGATGAGTCATGG, RacGAP1 Reverse:

GCTCAAACAGATTCCGCACA; Sphk1 Forward: AAGACCTCCTGACCAACTGC, Sphk1 Reverse: GGCTGAGCACAGAGAAGAGG.

6.6.4 Gene expression analysis

Each sample was analysed in duplicate. Complementary RNA was generated from samples using the Illumina TotalPrep RNA Amplification Kit and hybridised with Illumina HumanHT-12 v4 Expression BeadChips (Illumina, Scoresby, Austalia) as per manufacturer's protocol. Expression data from the microarrays was analysed as previously described (Endo-Munoz, Cumming et al. 2010). Only genes with a fold change of 1 (in either direction) or greater and a B-value of greater than 3 (exceeding the 95% probability of differential expression) were considered to be differentially expressed and further analysed. Differentially expressed probe sets were analysed as pair-wise contrasts. Microarray data has been uploaded to Gene Expression Omnibus under the reference: GSE58074.

6.6.5 Colony forming assay

Known number of SCC cells were plated and allowed to grow for 15 days. Plates were fixed and stained with Coomassie Blue and counted as previously described (Dicker, Serewko et al. 2000). Colony forming efficiency was expressed as the total number of colonies/total number of cells plated x 100.

6.6.6 DNA synthesis

DNA synthesis was measured using a colorimetric ELISA 5-bromo-2-deoxyuridine (BrdU) incorporation assay (Roche Diagnostics, Castle Hill, Australia) in accordance with the manufacturer's instructions.

6.6.7 Chromatin immunoprecipitation

Chromatin immunoprecipitation (ChIP) was performed using the SimpleChIP Enzymatic Chromatin IP Kit (Magnetic Beads) (Cell Signaling, Genesearch, Arundel, Australia) in accordance with the manufacturer's instructions. ChIP enrichment was determined by conducting qRT-PCR as described above. The primers used were as follows:

5'-GAAGTGAGTAGTGGGGGTGC-3' (RacGAP1 Forward);

5'-TCCATCTTTCACACGAACACTCT-3' (RacGAP1 Reverse).

6.6.8 Immunoblot

Immunoblotting was carried out according to previously published procedures (Erlich, Rickwood et al. 2009) using the following primary antibodies: Anti-RacGAP1 [EPR9018] 1:2,000 (Abcam, Sapphire Bioscience, Waterloo, Australia), Anti-Sphk1 1:1,000 (Sigma Aldrich), PARP 1:1,000 (Cell Signaling), phospho-Akt (Ser473) (D9E) XP 1:2,000 (Cell Signaling), Akt 1:2,000 (Cell Signaling), phospho-p44/42 MAPK (Erk1/2) (Thr202/Tyr204) (E10) 1:2 000 (Cell Signaling), ERK 1 (C-16) 1:2,000 (Santa Cruz, ThermoFisher Scientific, Scoresby, Australia) and β-actin 1:10,000 (Sigma Aldrich).

6.6.9 Immunohistochemistry

Immunohistochemistry was carried out according to previously published procedures (Erlich, Rickwood et al. 2009; Cameron, Dahler et al. 2010) using the following primary antibodies were used: Anti-PCNA 1:3,000 (Sigma Aldrich), Anti-RacGAP1 [EPR9018] 1:100 (Abcam), cleaved caspase-3 (Asp 175) 1:50 (Cell Signaling), phospho-Akt (Ser473) (D9E) XP 1:50 (Cell Signaling). Secondary antibody was Starr Trek Universal HRP Detection System (Biocare Medical, Applied medical, Stafford, Australia) followed by colorimetric immunohistochemical staining with Cardassian DAB Chromogen as per manufacturer's instructions (Biocare Medical).

6.6.10 Tissue microarrays (TMA)

Generation and composition of the patient TMAs has been previously described (Hazar-Rethinam, Merida de Long et al. 2014). Immunohistochemistry was conducted using Dako EnVision + System-HRP (DAB) Kit in accordance with the manufacturer's instructions (DAKO, Botany, Australia). Sections were incubated with Anti-E2F7 1:250 (Abcam) and Anti-RacGAP1 [EPR9018] 1:100 (Abcam) antibodies. Staining intensity was evaluated by two Pathologists in a blinded fashion using a modified quickscore method as described (Detre, Saclani Jotti et al. 1995).

6.6.11 Determination of RhoA and Rac1 activity

RhoA and Rac1 activities were measured with RhoA/Rac1/Cdc42 Activation Assay Combo Biochem Kit (Cytoskeleton, Jomar Bioscience, Kensington, Australia) in accordance with the manufacturer's instructions.

6.6.12 Animal studies

All animal experiments were approved by the Institutional Animal Ethics Committee. *In vivo* tumour studies used six-week-old female nonobese diabetic/severe combined immunodeficient mice. Mice were injected subcutaneously on the flank with 2 x 10^6 cells. Groups of 6 mice received treatments (intraperitoneal injections twice/week) when tumours were around 4 mm in diameter. Animal weight and tumour growth were monitored for a period of up to 3 weeks and animals were sacrificed when tumours reached 10 mm in diameter.

6.6.13 Statistical analysis

Statistical significance was calculated by a Student's *t* test with a 95% confidence level using GraphPad Prism v5 (GraphPad software, LA Jolla, USA).

6.7 Conflict of Interest

The authors declare no conflict of interest

6.8 Acknowledgements

The authors acknowledge the generous gift of *E2f7*$^{Flox/Flox}$ or *E2f8*$^{Flox/Flox}$ mice from Professor Gustavo Leone, The Ohio State University. The authors acknowledge the generous donations of tissue samples from the patients without which this project could not happen.

CHAPTER SEVEN

7 General discussion and conclusions

This thesis has presented data which provides new avenues towards improving our understanding of KCs differentiation, KC neoplasia and chemotherapeutic sensitivity in SCC. The key findings are discussed and summarised below. This study was undertaken to understand the molecular basis for E2F7 and E2F8 action, in the hope that novel factors that regulate E2F7 and E2F8 activity may lead to a better understanding of SCC genesis and new therapeutic strategies to treat SCC patients.

7.1 Isoform specific functions of atypical E2Fs

Evidence that has emerged over the past 2 decades is that the E2F transcription factor family are pleiotropic factors that exhibit isoform-specific and context-specific functions. Thus, it is important to consider the results of E2F studies in the specific context in which they were reported. The most obvious example of this is that E2F7 and E2F8 have both been shown to be important to the control of stress and apoptotic responses in developing embryos whereas in keratinocytes it would appear that E2F8 does not contribute to these functions.

In *Chapter 3*, we showed that E2F7 deficiency selectively enhanced the cytotoxic responses of KCs to UVB and doxorubicin (*Figure 3.8* and *Figure 3.9*). In contrast, E2F1 deficiency protected KCs from UV- and doxorubicin-induced cytotoxicity, and this is more obvious if one compares the E2F1KO dose response curve to that of the E2F7KD data (*Figure 3.8* and *Figure 3.9*). These data indicate that UV- and doxorubicin-induced cytotoxic responses may involve E2F1 and E2F7-dependent processes and that E2F1 and E2F7 appear to play opposing roles in the modulation of cytotoxic responses. Our findings are in line with previously published work in which E2F1 was shown to be a physiological target for stress-induced apoptosis, because such apoptosis could be rescued by depletion of E2F1 *in vitro* as well as *in vivo* (Li, Ran et al. 2008). In addition, our findings shed light onto some noticeable contradictions relating to the role of E2F1 in UV-induced cytotoxic responses in mouse skin. Previously, it was reported that the role of E2F1 in survival and death is context dependent (Meng and Ghosh 2014). In the context of keratinocytes, studies in which E2F1 was knocked out or overexpressed suggested that E2F1 protected against UV-induced apoptosis (Wikonkal, Remenyik et al. 2003; Knezevic and Brash 2004; Berton, Mitchell et al. 2005; Knezevic, Zhang et al. 2007). In contrast, studies from Pierce and colleagues in which E2F1 was overexpressed in the mouse epidermis resulted in increased constitutive apoptosis

(Pierce, Fisher et al. 1998; Pierce, Gimenez-Conti et al. 1998). Based on our data, we would suggest that the anti-apoptotic actions of E2F1 may be mediated via E2F1-dependent transcriptional induction of E2F7. However, high transient levels of E2F1 may induce apoptosis before E2F7 is transcribed and active.

7.2 Doxorubicin selectivity

A major finding of my thesis was the sensitivity of E2F7 deficient KCs to doxorubicin. Of particular interest, these effects are likely to be keratinocyte-specific since E2F7 expression in primary osteosarcoma is not altered compared to non-malignant bone (Endo-Munoz, Dahler et al. 2009) and osteosarcoma is sensitive to doxorubicin.

Although several possibilities might be proposed for specific interactions between a transcription regulator and a Topoisomerase II inhibitor, a transcription-independent contribution of E2F7 to these effects seems reasonable. Supporting this, La Thangue's group recently showed that E2F7 makes a contribution to DNA repair processes by physically binding to the damaged DNA and subsequently altering the local chromatin environment of the DNA lesion (Zalmas, Coutts et al. 2013). Regardless of the underlying mechanism, it seems clear that E2F7 is a multi-functional transcription factor. Furthermore, the differential effects of E2F7 knockdown on doxorubicin, etoposide and cisplatin treatments suggest that E2F7-mediated resistance to doxorubicin in SCC cells may not represent a general modulation of the survival machinery of the cells and perhaps may function outside the canonical DNA repair pathways. Therefore, we embarked on an unbiased systems-based screen in order to investigate the mechanisms that lead to enhanced resistance to doxorubicin and to identify the downstream targets of E2F7 in the modulation of doxorubicin selective sensitivity.

The physiological validity of our microarray results was confirmed by several observations. Firstly, the –omics study resulted in a very select list of candidates. Notably, one of the well known genes which is frequently dysregulated and contributes to SCCgenesis, CD44, was listed in this list. Significantly, there is literature suggesting that CD44 gene expression is regulated by the Sphk1/S1P receptor signalling pathway in colon cancer cells (Kawahara, Otsuji et al. 2013). Furthermore, Abdraboh and his colleagues reported that CD44 operates

through PI3K/AKT and E2F1 signal transduction cascade which leads to breast tumour invasion (Abdraboh, Gaur et al.).

Another important observation I made during this thesis is that E2F7 (primarily known as a transcriptional repressor) appeared to directly activate the transcription of RacGAP1 and Sphk1. This is conceptually new and intriguing and is supported by recently published papers as discussed in *Section 1.9.3 Regulation of transcription by atypical E2Fs*. It is a formal possibility that in the regulation of chemosensitivity, E2F7 could execute its role as a transcriptional regulator on non-canonical E2F7-binding sequence/sites when associated with a transcriptional activator. This is consistent with the lack of consensus E2F-binding sites within the Sphk1 promoter. Interestingly, E2F7-responsive region within the Sp1 promoter has been shown to be different than the published E2F consensus sequence (Hazar-Rethinam, Cameron et al. 2011). Alternatively, the relative ratio of E2F7 and its direct target, the transcriptional activator E2F1, may affect Sphk1 expression directly. Hence, the regulation of Sphk1 may be highly sensitive to changes in the E2F1:E2F7 ratio which in turn regulates sensitivity to doxorubicin.

In spite of not showing the precise mechanism of E2F7 action as an activator on the two novel target genes, Sphk1 and RacGAP1, our data clearly demonstrate that E2F7 regulates these genes *via* direct effects at the gene promoters. Our functional *in vitro* data confirmed that the binding of E2F7 correlates with changes in Sphk1 and RacGAP1 gene expression shortly after changes in the levels of the transcriptional regulator. Specifically, we show that i) E2F7 overexpression induces Sphk1 and RacGAP1 expressions (*Chapter 5* and *Figure 6.2*), ii) E2F7 knockdown reduces Sphk1 and RacGAP1 expressions (*Chapter 5* and *Figure 6.2*) and iii) E2F7 directly binds to the Sphk1 and RacGAP1 promoters (*Chapter 5* and *Figure 6.2*). It is an important fact to consider since the binding of a transcription factor to the promoter region of a gene does not always result in functional changes in the activity of the gene product so it remains a formal possibility that the binding of the factor contributes to minimal or even no control of the gene.

Sphk1-generated S1P has been implicated in several pathological and physiological processes, including carcinogenesis. Consistent with these roles as the major enzyme responsible for S1P synthesis, expression of Sphk1 is tightly regulated at all stages through epigenetic, transcriptional and post-transcriptional mechanisms (Fyrst and Saba 2010). Its

stable upregulation in cancer has been shown to occur at the transcriptional level by several transcriptional regulators (EGF, 17β-estradiol, PMA, histamine, prolactin) and in response to several growth factors. Notably, cancer cells are also able to maintain high levels of Sphk1 in response to HIF1α (Fyrst and Saba 2010) which is a novel binding partner of E2F7.

With respect to E2F7 and its downstream effector RacGAP1, as discussed in *Chapter 6*, the promoter of RacGAP1 contains E2F binding sites and E2F activation is absolutely required for the initiation of transcription at RacGAP1 promoter (Seguin, Liot et al. 2009). Furthermore, supporting our observation from this project is the work from Weijts *et al* (Weijts, Bakker et al. 2012) demonstrating that E2F7 directly binds and stimulates the VEGFA promoter following the formation of an E2F7-HIF1α transcriptional complex to regulate primary angiogenesis. Curiously, RacGAP1 has been shown to interact physically with HIF1α and regulates its transcriptional activity (Lyberopoulou, Venieris et al. 2007).

7.3 Novel combination of Sphk1 inhibitors/RacGAP1 inhibition and doxorubicin as a potential therapeutic for advanced SCC

An important conclusion we made in this study is that Sphk1 and RacGAP1 are downstream effectors of E2F7 and are responsible for E2F7-mediated effects on sensitivity to doxorubicin.

Two Sphk isoenzymes exist and it could be argued that the rheostat theory cannot be conclusively addressed unless both the isoforms are targeted. However, *in vivo* studies of Sphk1 or Sphk2 knockout mice suggested that these kinases may have compensatory roles as Sphk1 and Sphk2 double knockout mice die at an embryonic stage of development (Allende, Sasaki et al. 2004; Mizugishi, Yamashita et al. 2005), indicating that pan-Sphk1 inhibitors may not be ideal therapeutics and instead specific targeting of Sphk isoenzymes would be reasonable therapeutic option. SK1-I has been defined as a Sphk1 specific inhibitor: inhibits selectively Sphk1 activity, but not Sphk2. *In vitro* studies (with human histiocytic leukemia and Jurkat acute T-cell leukemia cells) and *in vivo* studies (with leukemic blasts) reported that SK1-I has significant cytotoxic and apoptotic effects as a single agent (Paugh, Paugh et al. 2008), and, moreover, SK1-I inhibits growth human glioblastoma cells in a dose dependent manner (Kapitonov, Allegood et al. 2009). Notably, we observed no cytotoxic effect after treatment of resistant SCC cells with SK1-I alone *in vitro* and no alteration in tumour growth

after treatment of SCC25 xenografts with SK1-I alone. In contrast, combination treatment of SK1-I with doxorubicin induced chemosensitivity, allowing for doses of doxorubicin that normally do not cause cell death to cause much greater cell killing, but did not potentiate the cytotoxic action of doxorubicin in normal HEKs nor in sensitive SCC cells, highlighting the selectivity of combination therapy for resistant SCC cells.

With regard to RacGAP1, in retrospect, it seems likely that its pleiotropic effects on cytokinesis have obscured their role in SCC tumourigenesis till now. There is an extensive literature indicating that RacGAP1 play key roles in important biological functions through mechanisms other than regulating Rac GTPase activity. Significantly, RacGAP1-mediated drug resistance in SCC has not been described before and has significant pathological and clinical implications in SCC.

7.4 Future directions

Future directions which may be considered with respect to isoform-specific activities of E2F8 would provide new avenues towards improving our understanding of keratinocyte differentiation and keratinocyte neoplasia. The findings from this study showed that E2F8 expression is modestly reduced during squamous differentiation and that loss of E2F8 (as observed in SCC) in murine keratinocytes inhibits the induction of differentiation. Firstly, our preliminary findings should be confirmed by growth as an organotypic culture. Other valuable information could be gained from doing organotypic culture is to be able to monitor time to reach maximal stratification as well as epithermal thickness. Transcriptomic profiling approach could next be taken to identify gene targets that are unique to E2F8 or shared with E2F1 and E2F7. The genes identified in the transcriptomic profiles could be followed up by the ChIP-Seq analysis which would also add additional information by identifying the genes modified by E2F8 that are direct targets of E2F8. Analysis of the data sets would be performed to identify potential E2F8 specific pathways associated with differentiation in normal keratinocytes and dysregulation in SCC cells. The identified specific pathway(s) would then be pursued at a functional level in our models of keratinocytes and SCC *in vitro* and *in vivo*.

As we discussed in *Chapter 4* and *Chapter 5*, our functional data clearly shows that E2F7 regulates Sphk1 and RacGAP1 expression even though we did not demonstrate the exact

mechanisms at the molecular level. There are several possible mechanisms to explain this. Firstly, it is a formal possibility that E2F7 may be a direct activator of Sphk1 and RacGAP1 transcriptions. Alternatively, E2F7 could act in a dominant-negative manner by blocking the binding of other E2F repressor complexes. One other possibility could be that the biological functions of E2F7 may be different in normal versus cancer cells. It is consistent with previously published work demonstrating that some of the E2F family of transcription factors members such as E2F4 is able to shuttle within the cells in a CRM-1 dependent manner (Gaubatz, Lees et al. 2001). Indeed, during the course of this study, it was noted that in primary SCCs and in the SCC25 cell line E2F7 was localised to the cytosol whereas in normal keratinocytes and stratified epithelium it was localised to the nucleus. So far we have demonstrated that this shift in localisation is of functional significance since ChIP analysis of the Sphk1 promoter in HEKs and SCC25 cells showed that E2F1 and E2F7 could both bind the Sphk1 promoter but there was a clear preference for E2F1 binding the Sphk1 promoter in SCC25 cells in which E2F7 is localised to the cytosol. This is ongoing work in the laboratory at present and the possibility that the functions of E2F7 described in this study could be a consequence of its cellular location will be the subject of future investigations.

As discussed in *Chapter 6*, our data demonstrated that RacGAP1 favoured the conversion of RhoGTP to RhoGDP in SCC cells. Whilst this seems counterintuitive, it has been shown that phosphorylation of RacGAP1, by Aurora B kinase, on Serine 387 shifts its GAP activity from Rac to Rho, resulting in increased GTP-loading (activation) of Rac1 and reduced GTP-loading of Rho (inactivation) (Doki, Kawashima et al. 2009). In this respect, future experiments would be first of all confirming the phosphorylation-dependent shift in RacGAP1's GAP activity using Anti-RacGAP1 phospho S387 antibody which detects endogenous levels of RacGAP1 only when phosphorylated at Serine 387. If RhoA is a preferred substrate for RacGAP1 in SCC cells due to phosphorylation on Serine 387, then one would expect to observe high levels of RacGAP1 in SCC25 when compared with KJDSV40 cells. These experiments would certainly provide unequivocal evidence that the conventional preference of RacGAP1 for Rac1 can be switched to RhoA following phosphorylation of the Serine 387 site of RacGAP1 and that the E2F7-dependent drug resistant phenotype we observed in SCC cells is likely due to GTP-loaded Rac1. It may also be considered to reiterate experiments where we were unable to show during the course of this study that the reduced proliferation or increased doxorubicin-sensitivity in SCC cells following RacGAP1 knockdown was due to the reduced GTP loading state of Rac or the

increased GTP-loading state of Rho members or the relative ratio of GTP-loaded Rho/GTP-loaded Rac.

7.5 Conclusions

My thesis addressed the following aims:

- Characterise the biological activity of E2F1, 7 and 8 in murine keratinocyte models of squamous differentiation, with particular emphasis on E2F8.
- Define the molecular basis for E2F1- and E2F7-dependent modulation of sensitivity to cytotoxic stimuli in SCC *in vitro* and *in vivo.*

In addressing these aims, I generated compelling data highlighting novel isoform-specific actions of E2F8 and E2F7 in controlling squamous differentiation and stress responses in keratinocytes, respectively, and subsequently identified the associated E2F7-dependent effectors that regulate cytotoxic responses to chemotherapy. Specifically, I identified a previously unknown and potentially significant role for E2F8 in regulating squamous differentiation which advanced our understanding of keratinocyte differentiation and keratinocyte neoplasia. Moreover, I also identified a unique and non-redundant role for E2F7 in regulating sensitivity to cytotoxic stimuli. Considering the fact that dysregulation of responses to chemotherapy–induced cytotoxicy is one of the major reasons for treatment failure in SCC, it is clear that identifying the downstream effectors that regulate E2F7-dependent sensitivity to chemotherapeutic agents may have direct clinical impact. Sphk1 and RacGAP1 were identified as mediators of E2F7-dependent cytotoxic responses in SCC, and Sphk1 or RacGAP1 inhibition unequivocally enhanced the cytotoxic activity of doxorubicin. Thus, the results of my thesis have identified a potential drug combination that is being pursued by my supervisor for translation into a human clinical trial of idarubicin + buparsilib in advanced SCC patients.

CHAPTER EIGHT

8 References

Abdraboh, M. E., R. L. Gaur, A. D. Hollenbach, D. Sandquist, M. H. Raj and A. Ouhtit (2011). "Survivin is a novel target of CD44-promoted breast tumor invasion." Am J Pathol **179**(2): 555-563.

Akervall, J., X. Guo, C. N. Qian, J. Schoumans, B. Leeser, E. Kort, A. Cole, J. Resau, C. Bradford, T. Carey, J. Wennerberg, H. Anderson, J. Tennvall and B. T. Teh (2004). "Genetic and expression profiles of squamous cell carcinoma of the head and neck correlate with cisplatin sensitivity and resistance in cell lines and patients." Clin Cancer Res **10**(24): 8204-8213.

Aksoy, O., A. Chicas, T. Zeng, Z. Zhao, M. McCurrach, X. Wang and S. W. Lowe (2012). "The atypical E2F family member E2F7 couples the p53 and RB pathways during cellular senescence." Genes & Development **26**(14): 1546-1557.

Alevizos, I., M. Mahadevappa, X. Zhang, H. Ohyama, Y. Kohno, M. Posner, G. T. Gallagher, M. Varvares, D. Cohen, D. Kim, R. Kent, R. B. Donoff, R. Todd, C. M. Yung, J. A. Warrington and D. T. Wong (2001). "Oral cancer in vivo gene expression profiling assisted by laser capture microdissection and microarray analysis." Oncogene **20**(43): 6196-6204.

Allende, M. L., T. Sasaki, H. Kawai, A. Olivera, Y. Mi, G. van Echten-Deckert, R. Hajdu, M. Rosenbach, C. A. Keohane, S. Mandala, S. Spiegel and R. L. Proia (2004). "Mice deficient in sphingosine kinase 1 are rendered lymphopenic by FTY720." J Biol Chem **279**(50): 52487-52492.

Alonso, L. and E. Fuchs (2003). "Stem cells of the skin epithelium." Proceedings of the National Academy of Sciences of the United States of America **100**(Suppl 1): 11830-11835.

Anton, M. and F. L. Graham (1995). "Site-specific recombination mediated by an adenovirus vector expressing the Cre recombinase protein: a molecular switch for control of gene expression." Journal of Virology **69**(8): 4600-4606.

Assefa, Z., M. Garmyn, R. Bouillon, W. Merlevede, J. R. Vandenheede and P. Agostinis (1997). "Differential Stimulation of ERK and JNK Activities by Ultraviolet B Irradiation and Epidermal Growth Factor in Human Keratinocytes." J Investig Dermatol **108**(6): 886-891.

Attwooll, C., E. L. Denchi and K. Helin (2004). "The E2F family: specific functions and overlapping interests." EMBO J **23**(24): 4709-4716.

Avninder, S., K. Ylaya and S. M. Hewitt (2008). "Tissue microarray: a simple technology that has revolutionized research in pathology." J Postgrad Med **54**(2): 158-162.

Baiz, D., B. Dapas, R. Farra, B. Scaggiante, G. Pozzato, F. Zanconati, N. Fiotti, L. Consoloni, S. Chiaretti and G. Grassi (2014). "Bortezomib effect on E2F and cyclin family members in human hepatocellular carcinoma cell lines." World J Gastroenterol **20**(3): 795-803.

Banks-Schlegel, S. and H. Green (1981). "Involucrin synthesis and tissue assembly by keratinocytes in natural and cultured human epithelia." The Journal of Cell Biology **90**(3): 732-737.

Bashari, D., D. Hacohen and D. Ginsberg (2011). "JNK activation is regulated by E2F and promotes E2F1-induced apoptosis." Cellular Signalling **23**(1): 65-70.

Baxter, R. M. and J. L. Brissette (2002). "Role of the Nude Gene in Epithelial Terminal Differentiation." **118**(2): 303-309.

Bell, L. A. and K. M. Ryan (2003). "Life and death decisions by E2F-1." Cell Death Differ **11**(2): 137-142.

Bernier, J. and C. Vrieling (2008). "Docetaxel in the management of patients with head and neck squamous cell carcinoma." Expert Rev Anticancer Ther **8**(7): 1023-1032.

Berton, T. R., D. L. Mitchell, R. Guo and D. G. Johnson (2005). "Regulation of epidermal apoptosis and DNA repair by E2F1 in response to ultraviolet B radiation." Oncogene **24**(15): 2449-2460.

Bielefeld, K. A., S. Amini-Nik, H. Whetstone, R. Poon, A. Youn, J. Wang and B. A. Alman (2011). "Fibronectin and β-Catenin Act in a Regulatory Loop in Dermal Fibroblasts to Modulate Cutaneous Healing." Journal of Biological Chemistry **286**(31): 27687-27697.

Binaschi, M., G. Capranico, P. De Isabella, M. Mariani, R. Supino, S. Tinelli and F. Zunino (1990). "Comparison of dna cleavage induced by etoposide and doxorubicin in two human small-cell lung cancer lines with different sensitivities to topoisomerase ii inhibitors." International Journal of Cancer **45**(2): 347-352.

Black, H. S., F. R. deGruijl, P. D. Forbes, J. E. Cleaver, H. N. Ananthaswamy, E. C. deFabo, S. E. Ullrich and R. M. Tyrrell (1997). "Photocarcinogenesis: an overview." Journal of Photochemistry and Photobiology B: Biology **40**(1): 29-47.

Blake, M. C., R. C. Jambou, A. G. Swick, J. W. Kahn and J. C. Azizkhan (1990). "Transcriptional initiation is controlled by upstream GC-box interactions in a TATAA-less promoter." Molecular and cellular biology **10**(12): 6632-6641.

Bonhoure, E., D. Pchejetski, N. Aouali, H. Morjani, T. Levade, T. Kohama and O. Cuvillier (2005). "Overcoming MDR-associated chemoresistance in HL-60 acute myeloid leukemia cells by targeting shingosine kinase-1." Leukemia **20**(1): 95-102.

Boukamp, P. (2005). "UV-induced Skin Cancer: Similarities – Variations." JDDG: Journal der Deutschen Dermatologischen Gesellschaft **3**(7): 493-503.

Bug, M. and M. Dobbelstein (2011). "Anthracyclines induce the accumulation of mutant p53 through E2F1-dependent and -independent mechanisms." Oncogene **30**(33): 3612-3624.

Byrne, C., M. Tainsky and E. Fuchs (1994). "Programming gene expression in developing epidermis." Development **120**(9): 2369-2383.

Cam, H. and B. D. Dynlacht (2003). "Emerging roles for E2F: Beyond the G1/S transition and DNA replication." Cancer Cell **3**(4): 311-316.

Cameron, S. R., A. L. Dahler, L. B. Endo-Munoz, I. Jabbar, G. P. Thomas, P. J. Leo, K. Poth, D. Rickwood, A. Guminski and N. A. Saunders (2010). "Tumor-initiating activity and tumor morphology of HNSCC is modulated by interactions between clonal variants within the tumor." Lab Invest **90**(11): 1594-1603.

Carcagno, A. L., M. F. Ogara, S. V. Sonzogni, M. C. Marazita, P. F. Sirkin, J. M. Ceruti and E. T. Cánepa (2009). "E2F1 transcription is induced by genotoxic stress through ATM/ATR activation." IUBMB Life **61**(5): 537-543.

Carvajal, L. A., P. J. Hamard, C. Tonnessen and J. J. Manfredi (2012). "E2F7, a novel target, is up-regulated by p53 and mediates DNA damage-dependent transcriptional repression." Genes Dev **26**(14): 1533-1545.

Chaturvedi, V., J.-Z. Qin, M. F. Denning, D. Choubey, M. O. Diaz and B. J. Nickoloff (1999). "Apoptosis in Proliferating, Senescent, and Immortalized Keratinocytes." Journal of Biological Chemistry **274**(33): 23358-23367.

Chaussepied, M. and D. Ginsberg (2005). "E2F and Signal Transduction Pathways." Cell Cycle **4**(3): 392-396.

Chen, H.-Z., M. M. Ouseph, J. Li, T. Pécot, V. Chokshi, L. Kent, S. Bae, M. Byrne, C. Duran, G. Comstock, P. Trikha, M. Mair, S. Senapati, C. K. Martin, S. Gandhi, N. Wilson, B. Liu, Y.-W. Huang, J. C. Thompson, S. Raman, S. Singh, M. Leone, R. Machiraju, K. Huang, X. Mo, S. Fernandez, I. Kalaszczynska, D. J. Wolgemuth, P. Sicinski, T. Huang, V. Jin and G. Leone (2012). "Canonical and atypical E2Fs regulate the mammalian endocycle." Nat Cell Biol **14**(11): 1192-1202.

Chen, H. Z., S. Y. Tsai and G. Leone (2009). "Emerging roles of E2Fs in cancer: an exit from cell cycle control." Nat Rev Cancer **9**(11): 785-797.

Chin, D., G. M. Boyle, S. Porceddu, D. R. Theile, P. G. Parsons and W. B. Coman (2006). "Head and neck cancer: past, present and future." Expert Rev Anticancer Ther **6**(7): 1111-1118.

Chong, J.-L., P. L. Wenzel, M. T. Saenz-Robles, V. Nair, A. Ferrey, J. P. Hagan, Y. M. Gomez, N. Sharma, H.-Z. Chen, M. Ouseph, S.-H. Wang, P. Trikha, B. Culp, L. Mezache, D. J. Winton, O. J. Sansom, D. Chen, R. Bremner, P. G. Cantalupo, M. L. Robinson, J. M. Pipas and G. Leone (2009). "E2f1-3 switch from activators in progenitor cells to repressors in differentiating cells." Nature **462**(7275): 930-934.

Christensen, J., P. Cloos, U. Toftegaard, D. Klinkenberg, A. P. Bracken, E. Trinh, M. Heeran, L. Di Stefano and K. Helin (2005). "Characterization of E2F8, a novel E2F-like cell-cycle regulated repressor of E2F-activated transcription." Nucleic Acids Research **33**(17): 5458-5470.

Clayman, G. L., J. J. Lee, F. C. Holsinger, X. Zhou, M. Duvic, A. K. El-Naggar, V. G. Prieto, E. Altamirano, S. L. Tucker, S. S. Strom, M. L. Kripke and S. M. Lippman (2005). "Mortality Risk From Squamous Cell Skin Cancer." Journal of Clinical Oncology **23**(4): 759-765.

Conney, A. H., P. Kramata, Y.-R. Lou and Y.-P. Lu (2008). "Effect of Caffeine on UVB-induced Carcinogenesis, Apoptosis, and the Elimination of UVB-induced Patches of p53 Mutant Epidermal Cells in SKH-1 Mice." Photochemistry and Photobiology **84**(2): 330-338.

Cooper, S. J. and G. T. Bowden (2007). "Ultraviolet B regulation of transcription factor families: roles of nuclear factor-kappa B (NF-kappaB) and activator protein-1 (AP-1) in UVB-induced skin carcinogenesis." Current cancer drug targets **7**(4): 325-334.

Copper, M. P., A. Jovanovic, J. J. Nauta, B. J. Braakhuis, N. de Vries, I. van der Waal and G. B. Snow (1995). "Role of genetic factors in the etiology of squamous cell carcinoma of the head and neck." Arch Otolaryngol Head Neck Surg **121**(2): 157-160.

Cranmer, L. D., C. Engelhardt and S. S. Morgan (2010). "Treatment of Unresectable and Metastatic Cutaneous Squamous Cell Carcinoma." The Oncologist **15**(12): 1320-1328.

D'Souza, S. J. A., A. Pajak, K. Balazsi and L. Dagnino (2001). "Ca2+ and BMP-6 Signaling Regulate E2F during Epidermal Keratinocyte Differentiation." Journal of Biological Chemistry **276**(26): 23531-23538.

Dahler, A. L., S. J. Jones, A. J. Dicker and N. A. Saunders (1998). "Keratinocyte growth arrest is associated with activation of a transcriptional repressor element in the human cdk1 promoter." Journal of Cellular Physiology **177**(3): 474-482.

Dahler, A. L., D. Rickwood, A. Guminski, N. Teakle and N. A. Saunders (2007). "Indole-3-carbinol - induced growth inhibition can be converted to a cytotoxic response in the presence of TPA+Ca(2+) in squamous cell carcinoma cell lines." FEBS Lett **581**(20): 3839-3847.

Dai, Y., C. H. Xie, J. P. Neis, C. Y. Fan, E. Vural and P. M. Spring (2011). "MicroRNA expression profiles of head and neck squamous cell carcinoma with docetaxel-induced multidrug resistance." Head Neck **33**(6): 786-791.

de Bruin, A., B. Maiti, L. Jakoi, C. Timmers, R. Buerki and G. Leone (2003). "Identification and Characterization of E2F7, a Novel Mammalian E2F Family Member Capable of Blocking Cellular Proliferation." Journal of Biological Chemistry **278**(43): 42041-42049.

de Gruijl, F. R., H. J. van Kranen and L. H. F. Mullenders (2001). "UV-induced DNA damage, repair, mutations and oncogenic pathways in skin cancer." Journal of Photochemistry and Photobiology B: Biology **63**(1-3): 19-27.

DeGregori, J. and D. G. Johnson (2006). "Distinct and overlapping roles for E2F family members in transcription, proliferation and apoptosis." Curr Mol Med **6**(7): 739-748.

Deng, Q., Q. Wang, W.-Y. Zong, D.-L. Zheng, Y.-X. Wen, K.-S. Wang, X.-M. Teng, X. Zhang, J. Huang and Z.-G. Han (2010). "E2F8 Contributes to Human Hepatocellular Carcinoma via Regulating Cell Proliferation." Cancer Research **70**(2): 782-791.

Detre, S., G. Saclani Jotti and M. Dowsett (1995). "A "quickscore" method for immunohistochemical semiquantitation: validation for oestrogen receptor in breast carcinomas." J Clin Pathol **48**(9): 876-878.

Deyrieux, A. F., G. Rosas-Acosta, M. A. Ozbun and V. G. Wilson (2007). "Sumoylation dynamics during keratinocyte differentiation." Journal of Cell Science **120**(1): 125-136.

Di Stefano, L., M. R. Jensen and K. Helin (2003). "E2F7, a novel E2F featuring DP-independent repression of a subset of E2F-regulated genes." EMBO J **22**(23): 6289-6298.

Dicker, A. J., C. Popa, A. L. Dahler, M. M. Serewko, P. A. Hilditch-Maguire, I. H. Frazer and N. A. Saunders (2000). "E2F-1 induces proliferation-specific genes and suppresses squamous differentiation-specific genes in human epidermal keratinocytes." Oncogene **19**(25): 2887-2894.

Dicker, A. J., M. M. Serewko, A. L. Dahler, K. K. Khanna, P. Kaur, A. Li, G. M. Strutton and N. A. Saunders (2000). "Functional characterization of cultured cells derived from an intraepidermal carcinoma of the skin (IEC-1)." Exp Cell Res **258**(2): 352-360.

Diepgen, T. L. and V. Mahler (2002). "The epidemiology of skin cancer." British Journal of Dermatology **146**: 1-6.

Dimova, D. K. and N. J. Dyson (2005). "The E2F transcriptional network: old acquaintances with new faces." Oncogene **24**(17): 2810-2826.

Dlugosz, A. A. and S. H. Yuspa (1993). "Coordinate changes in gene expression which mark the spinous to granular cell transition in epidermis are regulated by protein kinase C." The Journal of Cell Biology **120**(1): 217-225.

Doki, N., T. Kawashima, Y. Nomura, A. Tsuchiya, C. Oneyama, T. Akagi, Y. Nojima and T. Kitamura (2009). "Constitutive phosphorylation of a Rac GAP MgcRacGAP is implicated in v-Src-induced transformation of NIH3T3 cells." Cancer Science **100**(9): 1675-1679.

Dong, Y. B., H. L. Yang, M. J. Elliott and K. M. McMasters (2002). "Adenovirus-mediated E2F-1 Gene Transfer Sensitizes Melanoma Cells to Apoptosis Induced by Topoisomerase II Inhibitors." Cancer Research **62**(6): 1776-1783.

Du, P., W. A. Kibbe and S. M. Lin (2008). "lumi: a pipeline for processing Illumina microarray." Bioinformatics **24**(13): 1547-1548.

Eckel-Passow, J. E., C. M. Lohse, Y. Sheinin, P. L. Crispen, C. J. Krco and E. D. Kwon (2010). "Tissue microarrays: one size does not fit all." Diagn Pathol **5**: 48.

Eckert, R., J. Crish, E. Banks and J. Welter (1997). "The epidermis: Genes On-Genes Off." Journal of Investigative Dermatology **109**: 501-509.

Eckert, R. L. (1989). "Structure, function, and differentiation of the keratinocyte." Physiological Reviews **69**(4): 1316-1346.

Eckert, R. L., M. T. Sturniolo, A.-M. Broome, M. Ruse and E. A. Rorke (2005). "Transglutaminase Function in Epidermis." J Investig Dermatol **124**(3): 481-492.

Edge, S. B. and C. C. Compton (2010). "The American Joint Committee on Cancer: the 7th edition of the AJCC cancer staging manual and the future of TNM." Ann Surg Oncol **17**(6): 1471-1474.

Eichner, R., T.-T. Sun and U. Aebi (1986). "The Role of Keratin Subfamilies and Keratin Pairs in the Formation of Human Epidermal Intermediate Filaments." The Journal of Cell Biology **102**(5): 1767-1777.

Endo-Munoz, L., A. Cumming, D. Rickwood, D. Wilson, C. Cueva, C. Ng, G. Strutton, A. I. Cassady, A. Evdokiou, S. Sommerville, I. Dickinson, A. Guminski and N. A. Saunders (2010). "Loss of Osteoclasts Contributes to Development of Osteosarcoma Pulmonary Metastases." Cancer Research **70**(18): 7063-7072.

Endo-Munoz, L., A. Cumming, S. Sommerville, I. Dickinson and N. A. Saunders (2010). "Osteosarcoma is characterised by reduced expression of markers of osteoclastogenesis and antigen presentation compared with normal bone." Br J Cancer **103**(1): 73-81.

Endo-Munoz, L., A. Dahler, N. Teakle, D. Rickwood, M. Hazar-Rethinam, I. Abdul-Jabbar, S. Sommerville, I. Dickinson, P. Kaur, S. Paquet-Fifield and N. Saunders (2009). "E2F7 can

regulate proliferation, differentiation, and apoptotic responses in human keratinocytes: implications for cutaneous squamous cell carcinoma formation." Cancer Res **69**(5): 1800-1808.

Erb, P., J. Ji, M. Wernli, E. Kump, A. Glaser and S. A. Büchner (2005). "Role of apoptosis in basal cell and squamous cell carcinoma formation." Immunology Letters **100**(1): 68-72.

Erlich, R. B., Z. Kherrouche, D. Rickwood, L. Endo-Munoz, S. Cameron, A. Dahler, M. Hazar-Rethinam, L. M. de Long, K. Wooley, A. Guminski and N. A. Saunders (2012). "Preclinical evaluation of dual PI3K-mTOR inhibitors and histone deacetylase inhibitors in head and neck squamous cell carcinoma." Br J Cancer **106**(1): 107-115.

Erlich, R. B., D. Rickwood, W. B. Coman, N. A. Saunders and A. Guminski (2009). "Valproic acid as a therapeutic agent for head and neck squamous cell carcinomas." Cancer Chemother Pharmacol **63**(3): 381-389.

Facchinetti, M. M., N. A. Gandini, M. E. Fermento, N. B. Sterin-Speziale, Y. Ji, V. Patel, J. S. Gutkind, M. G. Rivadulla and A. C. Curino (2010). "The expression of sphingosine kinase-1 in head and neck carcinoma." Cells Tissues Organs **192**(5): 314-324.

Field, S. J., F. Y. Tsai, F. Kuo, A. M. Zubiaga, W. G. Kaelin, Jr., D. M. Livingston, S. H. Orkin and M. E. Greenberg (1996). "E2F-1 functions in mice to promote apoptosis and suppress proliferation." Cell **85**(4): 549-561.

Fleckman, P., B. A. Dale and K. A. Holbrook (1985). "Profilaggrin, a High-Molecular-Weight Precursor of Filaggrin in Human Epidermis and Cultured Keratinocytes." J Investig Dermatol **85**(6): 507-512.

Fritz, G., C. Brachetti, F. Bahlmann, M. Schmidt and B. Kaina (2002). "Rho GTPases in human breast tumours: expression and mutation analyses and correlation with clinical parameters." Br J Cancer **87**(6): 635-644.

Fuchs, E. (1990). "Epidermal differentiation: the bare essentials." The Journal of Cell Biology **111**(6): 2807-2814.

Fuchs, E. and S. Raghavan (2002). "Getting under the skin of epidermal morphogenesis." Nat Rev Genet **3**(3): 199-209.

Fyrst, H. and J. D. Saba (2010). "An update on sphingosine-1-phosphate and other sphingolipid mediators." Nat Chem Biol **6**(7): 489-497.

Gambardella, L. and Y. Barrandon (2003). "The multifaceted adult epidermal stem cell." Current Opinion in Cell Biology **15**(6): 771-777.

Gasparoni, A., L. Fonzi, G. B. Schneider, P. W. Wertz, G. K. Johnson and C. A. Squier (2004). "Comparison of differentiation markers between normal and two squamous cell carcinoma cell lines in culture." Archives of oral biology **49**(8): 653-664.

Gaubatz, S., J. A. Lees, G. J. Lindeman and D. M. Livingston (2001). "E2F4 Is Exported from the Nucleus in a CRM1-Dependent Manner." Molecular and cellular biology **21**(4): 1384-1392.

Ghazaryan, S., C. Sy, T. Hu, X. An, N. Mohandas, H. Fu, M. I. Aladjem, V. T. Chang, R. Opavsky and L. Wu (2014). "Inactivation of Rb and E2f8 synergizes to trigger stressed DNA replication during erythroid terminal differentiation." Mol Cell Biol **34**(15): 2833-2847.

Giangrande, P. H., W. Zhu, S. Schlisio, X. Sun, S. Mori, S. Gaubatz and J. R. Nevins (2004). "A role for E2F6 in distinguishing G1/S- and G2/M-specific transcription." Genes Dev **18**(23): 2941-2951.

Ginos, M. A., G. P. Page, B. S. Michalowicz, K. J. Patel, S. E. Volker, S. E. Pambuccian, F. G. Ondrey, G. L. Adams and P. M. Gaffney (2004). "Identification of a gene expression signature associated with recurrent disease in squamous cell carcinoma of the head and neck." Cancer Res **64**(1): 55-63.

Gordon, J. A. and V. H. Gattone (1986). "Mitochondrial alterations in cisplatin-induced acute renal failure." American Journal of Physiology - Renal Physiology **250**(6): F991-F998.

Haddad, R., A. D. Colevas, R. Tishler, P. Busse, L. Goguen, C. Sullivan, C. M. Norris, B. Lake-Willcutt, M. A. Case, R. Costello and M. Posner (2003). "Docetaxel, cisplatin, and 5-fluorouracil-based induction chemotherapy in patients with locally advanced squamous cell carcinoma of the head and neck: the Dana Farber Cancer Institute experience." Cancer **97**(2): 412-418.

Hallstrom, T. C., S. Mori and J. R. Nevins (2008). "An E2F1-dependent gene expression program that determines the balance between proliferation and cell death." Cancer Cell **13**(1): 11-22.

Han, S., K. Park, B.-N. Bae, K. H. Kim, H.-J. Kim, Y.-D. Kim and H.-Y. Kim (2003). "E2F1 Expression is Related with the Poor Survival of Lymph Node-positive Breast Cancer Patients Treated with Fluorouracil, Doxorubicin and Cyclophosphamide." Breast Cancer Research and Treatment **82**(1): 11-16.

Hanahan, D. and R. A. Weinberg (2000). "The Hallmarks of Cancer." Cell **100**(1): 57-70.

Hansen, A. R. and L. L. Siu (2013). "Epidermal Growth Factor Receptor Targeting in Head and Neck Cancer: Have We Been Just Skimming the Surface?" Journal of Clinical Oncology **31**(11): 1381-1383.

Harvat, B. L., A. Wang, P. Seth and A. M. Jetten (1998). "Up-regulation of p27Kip1, p21WAF1/Cip1 and p16Ink4a is associated with, but not sufficient for, induction of squamous differentiation." Journal of Cell Science **111**(9): 1185-1196.

Harwood, C. A., T. Surentheran, J. M. McGregor, P. J. Spink, I. M. Leigh, J. Breuer and C. M. Proby (2000). "Human papillomavirus infection and non-melanoma skin cancer in immunosuppressed and immunocompetent individuals." J Med Virol **61**(3): 289-297.

Hazar-Rethinam, M., S. R. Cameron, A. L. Dahler, L. B. Endo-Munoz, L. Smith, D. Rickwood and N. A. Saunders (2011). "Loss of E2F7 Expression Is an Early Event in Squamous Differentiation and Causes Derepression of the Key Differentiation Activator Sp1." J Invest Dermatol **131**(5): 1077-1084.

Hazar-Rethinam, M., L. Endo-Munoz, O. Gannon and N. Saunders (2011). "The role of the E2F transcription factor family in UV-induced apoptosis." Int J Mol Sci **12**(12): 8947-8960.

Hazar-Rethinam, M., L. Merida de Long, O. Gannon, E. Topkas, S. Boros, A. C. Vargas, M. Dzienis, P. Mukhopadhyay, F. Simpson, L. B. Endo-Munoz and N. A. Saunders (2014). "A novel E2F/Sphingosine kinase 1 axis regulates anthracycline response in squamous cell carcinoma." Clin Cancer Res.

Helin, K., J. A. Lees, M. Vidal, N. Dyson, E. Harlow and A. Fattaey (1992). "A cDNA encoding a pRB-binding protein with properties of the transcription factor E2F." Cell **70**(2): 337-350.

Hirose, K., T. Kawashima, I. Iwamoto, T. Nosaka and T. Kitamura (2001). "MgcRacGAP is involved in cytokinesis through associating with mitotic spindle and midbody." J Biol Chem **276**(8): 5821-5828.

Holmberg, C., K. Helin, M. Sehested and O. Karlström (1998). "E2F-1 induced p53-independent apoptosis apoptosis in transgenic mice." Oncogene **17**: 143-155.

Huff, C. A., S. H. Yuspa and D. Rosenthal (1993). "Identification of control elements 3' to the human keratin 1 gene that regulate cell type and differentiation-specific expression." Journal of Biological Chemistry **268**(1): 377-384.

Hunt, K. K., J. Deng, T.-J. Liu, M. Wilson-Heiner, S. G. Swisher, G. Clayman and M.-C. Hung (1997). "Adenovirus-Mediated Overexpression of the Transcription Factor E2F-1 Induces Apoptosis in Human Breast and Ovarian Carcinoma Cell Lines and Does Not Require p53." Cancer Research **57**(21): 4722-4726.

Hwang, J., R. Kita, H.-S. Kwon, E. H. Choi, S. H. Lee, M. C. Udey and M. I. Morasso (2011). "Epidermal ablation of Dlx3 is linked to IL-17–associated skin inflammation." Proceedings of the National Academy of Sciences.

Ianari, A., R. Gallo, M. Palma, E. Alesse and A. Gulino (2004). "Specific Role for p300/CREB-binding Protein-associated Factor Activity in E2F1 Stabilization in Response to DNA Damage." Journal of Biological Chemistry **279**(29): 30830-30835.

Iaquinta, P. J. and J. A. Lees (2007). "Life and death decisions by the E2F transcription factors." Current Opinion in Cell Biology **19**(6): 649-657.

Ichihashi, M., M. Ueda, A. Budiyanto, T. Bito, M. Oka, M. Fukunaga, K. Tsuru and T. Horikawa (2003). "UV-induced skin damage." Toxicology **189**(1-2): 21-39.

Iglesias-Bartolome, R., D. Martin and J. S. Gutkind (2013). "Exploiting the head and neck cancer oncogenome: widespread PI3K-mTOR pathway alterations and novel molecular targets." Cancer Discov **3**(7): 722-725.

Ito, T., N. Udaka, T. Yazawa, K. Okudela, H. Hayashi, T. Sudo, F. Guillemot, R. Kageyama and H. Kitamura (2000). "Basic helix-loop-helix transcription factors regulate the neuroendocrine differentiation of fetal mouse pulmonary epithelium." Development **127**(18): 3913-3921.

Jacquemet, G., D. M. Green, R. E. Bridgewater, A. von Kriegsheim, M. J. Humphries, J. C. Norman and P. T. Caswell (2013). "RCP-driven α5β1 recycling suppresses Rac and promotes RhoA activity via the RacGAP1–IQGAP1 complex." The Journal of Cell Biology **202**(6): 917-935.

Jamshidi-Parsian, A., Y. Dong, X. Zheng, H. S. Zhou, W. Zacharias and K. M. McMasters (2005). "Gene expression profiling of E2F-1-induced apoptosis." Gene **344**(0): 67-77.

Jang, S.-I. and P. M. Steinert (2002). "Loricrin Expression in Cultured Human Keratinocytes Is Controlled by a Complex Interplay between Transcription Factors of the Sp1, CREB, AP1, and AP2 Families." Journal of Biological Chemistry **277**(44): 42268-42279.

Jang, S.-I., P. M. Steinert and N. G. Markova (1996). "Activator Protein 1 Activity Is Involved in the Regulation of the Cell Type-specific Expression from the Proximal Promoter of the Human Profilaggrin Gene." Journal of Biological Chemistry **271**(39): 24105-24114.

Jarvinen, A. K., R. Autio, S. Haapa-Paananen, M. Wolf, M. Saarela, R. Grenman, I. Leivo, O. Kallioniemi, A. A. Makitie and O. Monni (2006). "Identification of target genes in laryngeal squamous cell carcinoma by high-resolution copy number and gene expression microarray analyses." Oncogene **25**(52): 6997-7008.

Jeon, G. A., J. S. Lee, V. Patel, J. S. Gutkind, S. S. Thorgeirsson, E. C. Kim, I. S. Chu, P. Amornphimoltham and M. H. Park (2004). "Global gene expression profiles of human head and neck squamous carcinoma cell lines." Int J Cancer **112**(2): 249-258.

Johnson, D. G. and J. Degregori (2006). "Putting the oncogenic and tumor suppressive activities of E2F into context." Curr Mol Med **6**(7): 731-738.

Johnson, D. G., K. Ohtani and J. R. Nevins (1994). "Autoregulatory control of E2F1 expression in response to positive and negative regulators of cell cycle progression." Genes & Development **8**(13): 1514-1525.

Jones, S. J., A. J. Dicker, A. L. Dahler and N. A. Saunders (1997). "E2F as a regulator of keratinocyte proliferation: implications for skin tumor development." J Investig Dermatol **109**(2): 187-193.

Kadonaga, J. T., K. R. Carner, F. R. Masiarz and R. Tjian (1987). "Isolation of cDNA encoding transcription factor Sp1 and functional analysis of the DNA binding domain." Cell **51**(6): 1079-1090.

Kaelin, W. G., Jr., W. Krek, W. R. Sellers, J. A. DeCaprio, F. Ajchenbaum, C. S. Fuchs, T. Chittenden, Y. Li, P. J. Farnham, M. A. Blanar and et al. (1992). "Expression cloning of a cDNA encoding a retinoblastoma-binding protein with E2F-like properties." Cell **70**(2): 351-364.

Kalyankrishna, S. and J. R. Grandis (2006). "Epidermal growth factor receptor biology in head and neck cancer." J Clin Oncol **24**(17): 2666-2672.

Kapitonov, D., J. C. Allegood, C. Mitchell, N. C. Hait, J. A. Almenara, J. K. Adams, R. E. Zipkin, P. Dent, T. Kordula, S. Milstien and S. Spiegel (2009). "Targeting sphingosine kinase 1 inhibits Akt signaling, induces apoptosis, and suppresses growth of human glioblastoma cells and xenografts." Cancer Res **69**(17): 6915-6923.

Karin, M. (1995). "The Regulation of AP-1 Activity by Mitogen-activated Protein Kinases." Journal of Biological Chemistry **270**(28): 16483-16486.

Kawahara, S., Y. Otsuji, M. Nakamura, M. Murakami, T. Murate, T. Matsunaga, H. Kanoh, M. Seishima, Y. Banno and A. Hara (2013). "Sphingosine kinase 1 plays a role in the upregulation of CD44 expression through extracellular signal-regulated kinase signaling in human colon cancer cells." Anti-Cancer Drugs **24**(5): 473-483 410.1097/CAD.1090b1013e32835f32705f.

Kawashima, T., K. Hirose, T. Satoh, A. Kaneko, Y. Ikeda, Y. Kaziro, T. Nosaka and T. Kitamura (2000). "MgcRacGAP is involved in the control of growth and differentiation of hematopoietic cells." Blood **96**(6): 2116-2124.

Ke, H.-L., R.-H. Ke, S.-T. Li, B. Li, H.-T. Lu and X.-Q. Wang (2013). "Expression of RACGAP1 in high grade meningiomas: a potential role in cancer progression." Journal of Neuro-Oncology **113**(2): 327-332.

Knezevic, D. and D. E. Brash (2004). "Role of E2F1 in apoptosis: a case study in feedback loops." Cell Cycle **3**(6): 729-732.

Knezevic, D., W. Zhang, P. J. Rochette and D. E. Brash (2007). "Bcl-2 is the target of a UV-inducible apoptosis switch and a node for UV signaling." Proc Natl Acad Sci U S A **104**(27): 11286-11291.

Kornberg, R. (1999). "Eukaryotic transcriptional control." Trends in Cell Biology **9**(12): M46-M49.

Kosugi, S. and Y. Ohashi (2002). "E2Ls, E2F-like Repressors of Arabidopsis That Bind to E2F Sites in a Monomeric Form." Journal of Biological Chemistry **277**(19): 16553-16558.

Kotoula, V., K. T. Kalogeras, G. Kouvatseas, D. Televantou, R. Kronenwett, R. M. Wirtz and G. Fountzilas (2013). "Sample parameters affecting the clinical relevance of RNA biomarkers in translational breast cancer research." Virchows Arch **462**(2): 141-154.

Kwong, R. A., T. V. Nguyen, R. J. Bova, J. G. Kench, I. E. Cole, E. A. Musgrove, S. M. Henshall and R. L. Sutherland (2003). "Overexpression of E2F-1 is associated with increased disease-free survival in squamous cell carcinoma of the anterior tongue." Clin Cancer Res **9**(10): 3705-3711.

Laethem, A. V., S. Claerhout, M. Garmyn and P. Agostinis (2005). "The sunburn cell: Regulation of death and survival of the keratinocyte." The International Journal of Biochemistry & Cell Biology **37**(8): 1547-1553.

Lammens, T., J. Li, G. Leone and L. De Veylder (2009). "Atypical E2Fs: new players in the E2F transcription factor family." Trends in Cell Biology **19**(3): 111-118.

Lazzerini Denchi, E. and K. Helin (2005). "E2F1 is crucial for E2F-dependent apoptosis." EMBO Rep **6**(7): 661-668.

Le, Q.-T. and A. J. Giaccia (2003). "Therapeutic Exploitation of the Physiological and Molecular Genetic Alterations in Head and Neck Cancer." Clinical Cancer Research **9**(12): 4287-4295.

Lee, J.-H., S.-I. Jang, J.-M. Yang, N. G. Markova and P. M. Steinert (1996). "The Proximal Promoter of the Human Transglutaminase 3 Gene." Journal of Biological Chemistry **271**(8): 4561-4568.

Leone, G., J. DeGregori, Z. Yan, L. Jakoi, S. Ishida, R. S. Williams and J. R. Nevins (1998). "E2F3 activity is regulated during the cell cycle and is required for the induction of S phase." Genes & Development **12**(14): 2120-2130.

Li, A., P. J. Simmons and P. Kaur (1998). "Identification and isolation of candidate human keratinocyte stem cells based on cell surface phenotype." Proceedings of the National Academy of Sciences **95**(7): 3902-3907.

Li, D., T. G. Turi, A. Schuck, I. M. Freedberg, G. Khitrov and M. Blumenberg (2001). "Rays and arrays: the transcriptional program in the response of human epidermal keratinocytes to UVB illumination." FASEB J **15**(13): 2533-2535.

Li, J., C. Ran, E. Li, F. Gordon, G. Comstock, H. Siddiqui, W. Cleghorn, H. Z. Chen, K. Kornacker, C. G. Liu, S. K. Pandit, M. Khanizadeh, M. Weinstein, G. Leone and A. de Bruin (2008). "Synergistic function of E2F7 and E2F8 is essential for cell survival and embryonic development." Dev Cell **14**(1): 62-75.

Li, R., Y. Zang, C. Li, N. S. Patel, J. R. Grandis and D. E. Johnson (2009). "ABT-737 synergizes with chemotherapy to kill head and neck squamous cell carcinoma cells via a Noxa-mediated pathway." Mol Pharmacol **75**(5): 1231-1239.

Liang, Y., M. Liu, P. Wang, X. Ding and Y. Cao (2013). "Analysis of 20 genes at chromosome band 12q13: RACGAP1 and MCRS1 overexpression in nonsmall-cell lung cancer." Genes, Chromosomes and Cancer **52**(3): 305-315.

Lippens, S., G. Denecker, P. Ovaere, P. Vandenabeele and W. Declercq (2005). "Death penalty for keratinocytes: apoptosis versus cornification." Cell Death Differ **12 Suppl 2**: 1497-1508.

Liu, B., I. Shats, S. P. Angus, M. L. Gatza and J. R. Nevins (2013). "Interaction of E2F7 transcription factor with E2F1 and C-terminal-binding protein (CtBP) provides a mechanism for E2F7-dependent transcription repression." J Biol Chem **288**(34): 24581-24589.

Liu, H. and R. Baliga (2005). "Endoplasmic Reticulum Stress–Associated Caspase 12 Mediates Cisplatin-Induced LLC-PK1 Cell Apoptosis." Journal of the American Society of Nephrology **16**(7): 1985-1992.

Liu, K., F.-T. Lin, J. M. Ruppert and W.-C. Lin (2003). "Regulation of E2F1 by BRCT Domain-Containing Protein TopBP1." Mol. Cell. Biol. **23**(9): 3287-3304.

Logan, N., L. Delavaine, A. Graham, C. Reilly, J. Wilson, T. R. Brummelkamp, E. M. Hijmans, R. Bernards and N. B. La Thangue (2004). "E2F-7: a distinctive E2F family member with an unusual organization of DNA-binding domains." Oncogene **23**(30): 5138-5150.

Logan, N., A. Graham, X. Zhao, R. Fisher, B. Maiti, G. Leone and N. B. L. Thangue (2005). "E2F-8: an E2F family member with a similar organization of DNA-binding domains to E2F-7." Oncogene **24**(31): 5000-5004.

López-Camarillo, C., E. Aréchaga Ocampo, M. López Casamichana, C. Pérez-Plasencia, E. Álvarez-Sánchez and L. A. Marchat (2011). "Protein Kinases and Transcription Factors Activation in Response to UV-Radiation of Skin: Implications for Carcinogenesis." International Journal of Molecular Sciences **13**(1): 142-172.

Lu, K. H., A. P. Patterson, L. Wang, R. T. Marquez, E. N. Atkinson, K. A. Baggerly, L. R. Ramoth, D. G. Rosen, J. Liu, I. Hellstrom, D. Smith, L. Hartmann, D. Fishman, A. Berchuck, R. Schmandt, R. Whitaker, D. M. Gershenson, G. B. Mills and R. C. Bast (2004). "Selection of Potential Markers for Epithelial Ovarian Cancer with Gene Expression Arrays and Recursive Descent Partition Analysis." Clinical Cancer Research **10**(10): 3291-3300.

Lyberopoulou, A., E. Venieris, I. Mylonis, G. Chachami, I. Pappas, G. Simos, S. Bonanou and E. Georgatsou (2007). "MgcRacGAP Interacts with HIF-1α and Regulates its Transcriptional Activity." Cellular Physiology and Biochemistry **20**(6): 995-1006.

Ma, X. J., R. Salunga, J. T. Tuggle, J. Gaudet, E. Enright, P. McQuary, T. Payette, M. Pistone, K. Stecker, B. M. Zhang, Y. X. Zhou, H. Varnholt, B. Smith, M. Gadd, E. Chatfield, J. Kessler, T. M. Baer, M. G. Erlander and D. C. Sgroi (2003). "Gene expression profiles of human breast cancer progression." Proc Natl Acad Sci U S A **100**(10): 5974-5979.

Magnaldo, T., L. Pommes, D. Asselineau and M. Darmon (1990). "Isolation of a GC-rich cDNA identifying mRNA present in human epidermis and modulated by calcium and retinoic acid in cultured keratinocytes. Homology with murine loricrin mRNA." Molecular Biology Reports **14**(4): 237-246.

Maiti, B., J. Li, A. de Bruin, F. Gordon, C. Timmers, R. Opavsky, K. Patil, J. Tuttle, W. Cleghorn and G. Leone (2005). "Cloning and Characterization of Mouse E2F8, a Novel Mammalian E2F Family Member Capable of Blocking Cellular Proliferation." Journal of Biological Chemistry **280**(18): 18211-18220.

Mariconti, L., B. Pellegrini, R. Cantoni, R. Stevens, C. Bergounioux, R. Cella and D. Albani (2002). "The E2F Family of Transcription Factors from Arabidopsis thaliana." Journal of Biological Chemistry **277**(12): 9911-9919.

Martinez, E. (2002). "Multi-protein complexes in eukaryotic gene transcription." Plant Molecular Biology **50**(6): 925-947.

Marur, S. and A. A. Forastiere (2008). "Head and Neck Cancer: Changing Epidemiology, Diagnosis, and Treatment." Mayo Clinic Proceedings **83**(4): 489-501.

Marvin, K. W., M. D. George, W. Fujimoto, N. A. Saunders, S. H. Bernacki and A. M. Jetten (1992). "Cornifin, a cross-linked envelope precursor in keratinocytes that is down-regulated by retinoids." Proceedings of the National Academy of Sciences **89**(22): 11026-11030.

Maverakis, E., Y. Miyamura, M. P. Bowen, G. Correa, Y. Ono and H. Goodarzi (2010). "Light, including ultraviolet." Journal of Autoimmunity **34**(3): J247-J257.

Maytin, E. V., J. C. Lin, R. Krishnamurthy, N. Batchvarova, D. Ron, P. J. Mitchell and J. F. Habener (1999). "Keratin 10 Gene Expression during Differentiation of Mouse Epidermis Requires Transcription Factors C/EBP and AP-2." Developmental Biology **216**(1): 164-181.

Meng, P. and R. Ghosh (2014). "Transcription addiction: can we garner the Yin and Yang functions of E2F1 for cancer therapy[quest]." Cell Death Dis **5**: e1360.

Minoshima, Y., T. Kawashima, K. Hirose, Y. Tonozuka, A. Kawajiri, Y. C. Bao, X. Deng, M. Tatsuka, S. Narumiya, W. S. May Jr, T. Nosaka, K. Semba, T. Inoue, T. Satoh, M. Inagaki and T. Kitamura (2003). "Phosphorylation by Aurora B Converts MgcRacGAP to a RhoGAP during Cytokinesis." Developmental Cell **4**(4): 549-560.

Mizugishi, K., T. Yamashita, A. Olivera, G. F. Miller, S. Spiegel and R. L. Proia (2005). "Essential role for sphingosine kinases in neural and vascular development." Mol Cell Biol **25**(24): 11113-11121.

Moon, N.-S. and N. Dyson (2008). "E2F7 and E2F8 Keep the E2F Family in Balance." Developmental cell **14**(1): 1-3.

Morris, E. J. and N. J. Dyson (2001). Retinoblastoma protein partners. Advances in Cancer Research, Academic Press. **Volume 82:** 1-54.

Muthusamy, V. and T. Piva (2010). "The UV response of the skin: a review of the MAPK, NFκB and TNFα signal transduction pathways." Archives of Dermatological Research **302**(1): 5-17.

Nevins, J. (1998). "Toward an understanding of the functional complexity of the E2F and retinoblastoma families." Cell Growth Differ **9**(8): 585-593.

Nickoloff, B. J., J.-Z. Qin, V. Chaturvedi, P. Bacon, J. Panella and M. F. Denning (2002). "Life and Death Signaling Pathways Contributing to Skin Cancer." J Investig Dermatol Symp Proc **7**(1): 27-35.

Nijwening, J. H., E. J. Geutjes, R. Bernards and R. L. Beijersbergen (2011). "The histone demethylase Jarid1b (Kdm5b) is a novel component of the Rb pathway and associates with E2f-target genes in MEFs during senescence." PLoS One **6**(9): e25235.

Nindl, I., M. Gottschling and E. Stockfleth (2007). "Human papillomaviruses and non-melanoma skin cancer: basic virology and clinical manifestations." Dis Markers **23**(4): 247-259.

Nishigori, C. (2006). "Cellular aspects of photocarcinogenesis." Photochemical & Photobiological Sciences **5**(2): 208-214.

Nishimura, K., T. Oki, J. Kitaura, S. Kuninaka, H. Saya, A. Sakaue-Sawano, A. Miyawaki and T. Kitamura (2013). "APC(CDH1) targets MgcRacGAP for destruction in the late M phase." PLoS One **8**(5): e63001.

Ogawa, H., K.-i. Ishiguro, S. Gaubatz, D. M. Livingston and Y. Nakatani (2002). "A Complex with Chromatin Modifiers That Occupies E2F- and Myc-Responsive Genes in G0 Cells." Science **296**(5570): 1132-1136.

Ohba, M., K. Ishino, M. Kashiwagi, S. Kawabe, K. Chida, N.-H. Huh and T. Kuroki (1998). "Induction of Differentiation in Normal Human Keratinocytes by Adenovirus-Mediated Introduction of the eta and delta Isoforms of Protein Kinase C." Mol. Cell. Biol. **18**(9): 5199-5207.

Ohtsuki, M., M. Tomic-Canic, I. M. Freedberg and M. Blumenberg (1992). "Nuclear Proteins Involved in Transcription of the Human K5 Keratin Gene." J Investig Dermatol **99**(2): 206-215.

Ouseph, M. M., J. Li, H. Z. Chen, T. Pecot, P. Wenzel, J. C. Thompson, G. Comstock, V. Chokshi, M. Byrne, B. Forde, J. L. Chong, K. Huang, R. Machiraju, A. de Bruin and G. Leone (2012). "Atypical E2F repressors and activators coordinate placental development." Dev Cell **22**(4): 849-862.

Panagiotis Zalmas, L., X. Zhao, A. L. Graham, R. Fisher, C. Reilly, A. S. Coutts and N. B. La Thangue (2008). "DNA-damage response control of E2F7 and E2F8." EMBO Rep **9**(3): 252-259.

Pandit, S. K., B. Westendorp, S. Nantasanti, E. van Liere, P. C. Tooten, P. W. Cornelissen, M. J. Toussaint, W. H. Lamers and A. de Bruin (2012). "E2F8 is essential for polyploidization in mammalian cells." Nat Cell Biol **14**(11): 1181-1191.

Panikkar, R. P., I. Astsaturov and C. J. Langer (2008). "The emerging role of cetuximab in head and neck cancer: a 2007 perspective." Cancer Invest **26**(1): 96-103.

Paramio, J. M. and M. Blumenberg (2006). Transcriptional Regulation of Keratin Gene Expression Intermediate Filaments, Springer US: 93-109.

Paugh, S. W., B. S. Paugh, M. Rahmani, D. Kapitonov, J. A. Almenara, T. Kordula, S. Milstien, J. K. Adams, R. E. Zipkin, S. Grant and S. Spiegel (2008). "A selective sphingosine kinase 1 inhibitor integrates multiple molecular therapeutic targets in human leukemia." Blood **112**(4): 1382-1391.

Perez-Ordoñez, B., M. Beauchemin and R. C. K. Jordan (2006). "Molecular biology of squamous cell carcinoma of the head and neck." Journal of Clinical Pathology **59**(5): 445-453.

Pierce, A. M., S. M. Fisher, C. J. Conti and D. G. Johnson (1998). "Deregulated expression of E2F1 induces hyperplasia and cooperates with ras in skin tumor development." Oncogene **16**(10): 1267-1276.

Pierce, A. M., I. B. Gimenez-Conti, R. Schneider-Broussard, L. A. Martinez, C. J. Conti and D. G. Johnson (1998). "Increased E2F1 activity induces skin tumors in mice heterozygous and nullizygous for p53." Proc Natl Acad Sci U S A **95**(15): 8858-8863.

Pierce, A. M., R. Schneider-Broussard, I. B. Gimenez-Conti, J. L. Russell, C. J. Conti and D. G. Johnson (1999). "E2F1 Has Both Oncogenic and Tumor-Suppressive Properties in a Transgenic Model." Mol. Cell. Biol. **19**(9): 6408-6414.

Pliarchopoulou, K., K. T. Kalogeras, R. Kronenwett, R. M. Wirtz, A. G. Eleftheraki, A. Batistatou, M. Bobos, N. Soupos, G. Polychronidou, H. Gogas, E. Samantas, C. Christodoulou, T. Makatsoris, N. Pavlidis, D. Pectasides and G. Fountzilas (2013). "Prognostic significance of RACGAP1 mRNA expression in high-risk early breast cancer: a study in primary tumors of breast cancer patients participating in a randomized Hellenic Cooperative Oncology Group trial." Cancer Chemotherapy and Pharmacology **71**(1): 245-255.

Polager, S., M. Ofir and D. Ginsberg (2008). "E2F1 regulates autophagy and the transcription of autophagy genes." Oncogene **27**(35): 4860-4864.

Posner, M. R. (2005). "Paradigm shift in the treatment of head and neck cancer: the role of neoadjuvant chemotherapy." Oncologist **10 Suppl 3**: 11-19.

Posner, M. R. and J. L. Lefebvre (2003). "Docetaxel induction therapy in locally advanced squamous cell carcinoma of the head and neck." Br J Cancer **88**(1): 11-17.

Poumay, Y. and M. R. Pittelkow (1995). "Cell Density and Culture Factors Regulate Keratinocyte Commitment to Differentiation and Expression of Suprabasal K1/K10 Keratins." J Investig Dermatol **104**(2): 271-276.

Prost, S., S. Sheahan, D. Rannie and D. J. Harrison (2001). "Adenovirus-mediated Cre deletion of floxed sequences in primary mouse cells is an efficient alternative for studies of gene deletion." Nucleic Acids Research **29**(16): e80.

Pyne, N. J. and S. Pyne (2010). "Sphingosine 1-phosphate and cancer." Nat Rev Cancer **10**(7): 489-503.

Qin, J.-Z., V. Chaturvedi, M. F. Denning, P. Bacon, J. Panella, D. Choubey and B. J. Nickoloff (2002). "Regulation of apoptosis by p53 in UV-irradiated human epidermis, psoriatic plaques and senescent keratinocytes." Oncogene **21**: 2991-3002.

Raj, D., D. E. Brash and D. Grossman (2006). "Keratinocyte Apoptosis in Epidermal Development and Disease." J Invest Dermatol **126**(2): 243-257.

Ramesh, G. and W. B. Reeves (2003). "TNFR2-mediated apoptosis and necrosis in cisplatin-induced acute renal failure." American Journal of Physiology - Renal Physiology **285**(4): F610-F618.

Ramsay, H. M., P. N. Harden, S. Reece, A. G. Smith, P. W. Jones, R. C. Strange and A. A. Fryer (2001). "Polymorphisms in glutathione S-transferases are associated with altered risk of nonmelanoma skin cancer in renal transplant recipients: a preliminary analysis." J Invest Dermatol **117**(2): 251-255.

Rangarajan, A., C. Talora, R. Okuyama, M. Nicolas, C. Mammucari, H. Oh, J. C. Aster, S. Krishna, D. Metzger, P. Chambon, L. Miele, M. Aguet, F. Radtke and G. P. Dotto (2001). "Notch signaling is a direct determinant of keratinocyte growth arrest and entry into differentiation." EMBO J **20**(13): 3427-3436.

Ratushny, V., M. D. Gober, R. Hick, T. W. Ridky and J. T. Seykora (2012). "From keratinocyte to cancer: the pathogenesis and modeling of cutaneous squamous cell carcinoma." The Journal of Clinical Investigation **122**(2): 464-472.

Rijnkels, M. and J. M. Rosen (2001). "Adenovirus-Cre-mediated recombination in mammary epithelial early progenitor cells." Journal of Cell Science **114**(17): 3147-3153.

Rodust, P. M., E. Stockfleth, C. Ulrich, M. Leverkus and J. Eberle (2009). "UV-induced squamous cell carcinoma – a role for antiapoptotic signalling pathways." British Journal of Dermatology **161**: 107-115.

Rossi, A., S. I. Jang, R. Ceci, P. M. Steinert and N. G. Markova (1998). "Effect of AP1 transcription factors on the regulation of transcription in normal human epidermal keratinocytes." J Invest Dermatol **110**(1): 34-40.

Rosty, C., M. Sheffer, D. Tsafrir, N. Stransky, I. Tsafrir, M. Peter, P. de Cremoux, A. de La Rochefordiere, R. Salmon, T. Dorval, J. P. Thiery, J. Couturier, F. Radvanyi, E. Domany and X. Sastre-Garau (2005). "Identification of a proliferation gene cluster associated with HPV E6/E7 expression level and viral DNA load in invasive cervical carcinoma." Oncogene **24**(47): 7094-7104.

Rowland, B. D. and R. Bernards (2006). "Re-Evaluating Cell-Cycle Regulation by E2Fs." Cell **127**(5): 871-874.

Sahai, E. (2005). "Mechanisms of cancer cell invasion." Curr Opin Genet Dev **15**(1): 87-96.

Saigusa, S., K. Tanaka, Y. Mohri, M. Ohi, T. Shimura, T. Kitajima, S. Kondo, Y. Okugawa, Y. Toiyama, Y. Inoue and M. Kusunoki (2014). "Clinical significance of RacGAP1 expression at the invasive front of gastric cancer." Gastric Cancer: 1-9.

Salvatori, B., I. Iosue, A. Mangiavacchi, G. Loddo, F. Padula, S. Chiaretti, N. Peragine, I. Bozzoni, F. Fazi and A. Fatica (2012). "The microRNA-26a target E2F7 sustains cell proliferation and inhibits monocytic differentiation of acute myeloid leukemia cells." Cell Death Dis **3**: e413.

Sankaranarayanan, R., E. Masuyer, R. Swaminathan, J. Ferlay and S. Whelan (1998). "Head and neck cancer: a global perspective on epidemiology and prognosis." Anticancer Res **18**(6B): 4779-4786.

Sanz-Moreno, V., G. Gadea, J. Ahn, H. Paterson, P. Marra, S. Pinner, E. Sahai and C. J. Marshall (2008). "Rac activation and inactivation control plasticity of tumor cell movement." Cell **135**(3): 510-523.

Sark, M. W. J., D. F. Fischer, E. de Meijer, P. van de Putte and C. Backendorf (1998). "AP-1 and Ets Transcription Factors Regulate the Expression of the Human SPRR1A Keratinocyte Terminal Differentiation Marker." Journal of Biological Chemistry **273**(38): 24683-24692.

Sarkar, S., M. Maceyka, N. C. Hait, S. W. Paugh, H. Sankala, S. Milstien and S. Spiegel (2005). "Sphingosine kinase 1 is required for migration, proliferation and survival of MCF-7 human breast cancer cells." FEBS Lett **579**(24): 5313-5317.

Saunders, N. A., S. H. Bernacki, T. M. Vollberg and A. M. Jetten (1993). "Regulation of transglutaminase type I expression in squamous differentiating rabbit tracheal epithelial cells and human epidermal keratinocytes: effects of retinoic acid and phorbol esters." Molecular Endocrinology **7**(3): 387-398.

Schaal, C., S. Pillai and S. P. Chellappan (2014). Chapter Four - The Rb–E2F Transcriptional Regulatory Pathway in Tumor Angiogenesis and Metastasis. Advances in Cancer Research. D. T. Kenneth and B. F. Paul, Academic Press. **Volume 121:** 147-182.

Seguin, L., C. Liot, R. Mzali, R. Harada, A. Siret, A. Nepveu and J. Bertoglio (2009). "CUX1 and E2F1 Regulate Coordinated Expression of the Mitotic Complex Genes Ect2, MgcRacGAP, and MKLP1 in S Phase." Molecular and Cellular Biology **29**(2): 570-581.

Senoo, M., F. Pinto, C. P. Crum and F. McKeon (2007). "p63 Is Essential for the Proliferative Potential of Stem Cells in Stratified Epithelia." Cell **129**(3): 523-536.

Serewko, M. M., C. Popa, A. L. Dahler, L. Smith, G. M. Strutton, W. Coman, A. J. Dicker and N. A. Saunders (2002). "Alterations in gene expression and activity during squamous cell carcinoma development." Cancer Res **62**(13): 3759-3765.

Shan, B., X. Zhu, P. L. Chen, T. Durfee, Y. Yang, D. Sharp and W. H. Lee (1992). "Molecular cloning of cellular genes encoding retinoblastoma-associated proteins: identification of a gene with properties of the transcription factor E2F." Mol Cell Biol **12**(12): 5620-5631.

Sharafinski, M. E., R. L. Ferris, S. Ferrone and J. R. Grandis (2010). "Epidermal growth factor receptor targeted therapy of squamous cell carcinoma of the head and neck." Head Neck **32**(10): 1412-1421.

Shen, B., P. Dong, D. Li and S. Gao (2011). "Expression and function of ABCG2 in head and neck squamous cell carcinoma and cell lines." Exp Ther Med **2**(6): 1151-1157.

Sherr, C. J. and F. McCormick (2002). "The RB and p53 pathways in cancer." Cancer Cell **2**(2): 103-112.

Shida, D., K. Takabe, D. Kapitonov, S. Milstien and S. Spiegel (2008). "Targeting SphK1 as a new strategy against cancer." Curr Drug Targets **9**(8): 662-673.

Shintani, S., M. Mihara, Y. Nakahara, A. Kiyota, Y. Ueyama, T. Matsumura and D. T. W. Wong (2002). "Expression of cell cycle control proteins in normal epithelium, premalignant and malignant lesions of oral cavity." Oral Oncology **38**(3): 235-243.

Simon, M. and H. Green (1984). "Participation of membrane-associated proteins in the formation of the cross-linked envelope of the keratinocyte." Cell **36**(4): 827-834.

Sinha, S., L. Degenstein, C. Copenhaver and E. Fuchs (2000). "Defining the Regulatory Factors Required for Epidermal Gene Expression." Molecular and cellular biology **20**(7): 2543-2555.

Sirma, H., M. Kumar, J. K. Meena, B. Witt, J. M. Weise, A. Lechel, S. Ande, V. Sakk, C. Guguen-Guillouzo, L. Zender, K. L. Rudolph and C. Gunes (2011). "The promoter of human telomerase reverse transcriptase is activated during liver regeneration and hepatocyte proliferation." Gastroenterology **141**(1): 326-337, 337 e321-323.

Skvortsov, S., J. Dudas, P. Eichberger, M. Witsch-Baumgartner, J. Loeffler-Ragg, C. Pritz, V. H. Schartinger, H. Maier, J. Hall, P. Debbage, H. Riechelmann, P. Lukas, I. Skvortsova and E. P. Group (2014). "Rac1 as a potential therapeutic target for chemo-radioresistant head and neck squamous cell carcinomas (HNSCC)." Br J Cancer **110**(11): 2677-2687.

Smyth, G. K. (2005). limma: Linear Models for Microarray Data. Bioinformatics and Computational Biology Solutions Using R and Bioconductor. R. Gentleman, V. Carey, W. Huber, R. Irizarry and S. Dudoit, Springer New York: 397-420.

Specenier, P. M. and J. B. Vermorken (2009). "Current concepts for the management of head and neck cancer: chemotherapy." Oral Oncol **45**(4-5): 409-415.

Stanelle, J. and B. M. Pützer (2006). "E2F1-induced apoptosis: turning killers into therapeutics." Trends in Molecular Medicine **12**(4): 177-185.

Staples, M., M. Elwood, R. Burton, J. Williams, R. Marks and G. GG (2006). "Non-melanoma skin cancer in Australia: the 2002 national survey and trends since 1985." the Medical Journal of Australia **184**(6-10).

Stevens, C. and N. B. La Thangue (2003). "E2F and cell cycle control: a double-edged sword." Archives of Biochemistry and Biophysics **412**(2): 157-169.

Stevens, C. and N. B. La Thangue (2004). "The emerging role of E2F-1 in the DNA damage response and checkpoint control." DNA Repair **3**(8-9): 1071-1079.

Sugihara, T. M., E. I. Kudryavtseva, V. Kumar, J. J. Horridge and B. Andersen (2001). "The POU Domain Factor Skin-1a Represses the Keratin 14 Promoter Independent of DNA Binding." Journal of Biological Chemistry **276**(35): 33036-33044.

Sugiyama, M., P. M. Speight, S. S. Prime and F. M. Watt (1993). "Comparison of integrin expression and terminal differentiation capacity in cell lines derived from oral squamous cell carcinomas." Carcinogenesis **14**(10): 2171-2176.

Tacar, O., P. Sriamornsak and C. R. Dass (2013). "Doxorubicin: an update on anticancer molecular action, toxicity and novel drug delivery systems." J Pharm Pharmacol **65**(2): 157-170.

Takahashi, Y., J. B. Rayman and B. D. Dynlacht (2000). "Analysis of promoter binding by the E2F and pRB families in vivo: distinct E2F proteins mediate activation and repression." Genes & Development **14**(7): 804-816.

Tonozuka, Y., Y. Minoshima, Y. C. Bao, Y. Moon, Y. Tsubono, T. Hatori, H. Nakajima, T. Nosaka, T. Kawashima and T. Kitamura (2004). "A GTPase-activating protein binds STAT3 and is required for IL-6-induced STAT3 activation and for differentiation of a leukemic cell line." Blood **104**(12): 3550-3557.

Trakatelli, M., U. C, d. M. V, S. Euvrard, E. Stockfleth and D. Abeni (2007). "Epidemiology of non-melanoma skin cancer (NMSC) in Europe: accurate and comparable data are needed for effective public monitoring and interventions." British Journal of Dermatology **156**: 1-7.

Trimarchi, J. M. and J. A. Lees (2002). "Sibling rivalry in the E2F family." Nat Rev Mol Cell Biol **3**(1): 11-20.

Truong, A. B., M. Kretz, T. W. Ridky, R. Kimmel and P. A. Khavari (2006). "p63 regulates proliferation and differentiation of developmentally mature keratinocytes." Genes & Development **20**(22): 3185-3197.

Ulrich, C., J. S. Jürgensen, A. Degen, M. Hackethal, M. Ulrich, M. J. Patel, J. Eberle, D. Terhorst, W. Sterry and E. Stockfleth (2009). "Prevention of non-melanoma skin cancer in organ transplant patients by regular use of a sunscreen: a 24 months, prospective, case–control study." British Journal of Dermatology **161**: 78-84.

van den Broek, G. B., M. Wildeman, C. R. Rasch, N. Armstrong, E. Schuuring, A. C. Begg, L. H. Looijenga, R. Scheper, J. E. van der Wal, L. Menkema, P. J. van Diest, A. J. Balm, M. L. van Velthuysen and M. W. van den Brekel (2009). "Molecular markers predict outcome in squamous cell carcinoma of the head and neck after concomitant cisplatin-based chemoradiation." Int J Cancer **124**(11): 2643-2650.

Vega, F. M. and A. J. Ridley (2008). "Rho GTPases in cancer cell biology." FEBS Lett **582**(14): 2093-2101.

Velaithan, R., J. Kang, J. L. Hirpara, T. Loh, B. C. Goh, M. Le Bras, C. Brenner, M. V. Clement and S. Pervaiz (2011). "The small GTPase Rac1 is a novel binding partner of Bcl-2 and stabilizes its antiapoptotic activity." Blood **117**(23): 6214-6226.

Veness, M. J., S. Porceddu, C. E. Palme and G. J. Morgan (2007). "Cutaneous head and neck squamous cell carcinoma metastatic to parotid and cervical lymph nodes." Head & Neck **29**(7): 621-631.

Walshe, J., M. M. Serewko-Auret, N. Teakle, S. Cameron, K. Minto, L. Smith, P. C. Burcham, T. Russell, G. Strutton, A. Griffin, F.-F. Chu, S. Esworthy, V. Reeve and N. A. Saunders (2007). "Inactivation of Glutathione Peroxidase Activity Contributes to UV-Induced Squamous Cell Carcinoma Formation." Cancer Research **67**(10): 4751-4758.

Wang, D., J. L. Russell and D. G. Johnson (2000). "E2F4 and E2F1 Have Similar Proliferative Properties but Different Apoptotic and Oncogenic Properties In Vivo." Mol. Cell. Biol. **20**(10): 3417-3424.

Wang, J., K. Helin, P. Jin and B. Nadal-Ginard (1995). "Inhibition of in vitro myogenic differentiation by cellular transcription factor E2F1." Cell Growth Differ **6**(10): 1299-1306.

Wang, S. M., L. L. P. J. Ooi and K. M. Hui (2011). "Upregulation of Rac GTPase-Activating Protein 1 Is Significantly Associated with the Early Recurrence of Human Hepatocellular Carcinoma." Clinical Cancer Research **17**(18): 6040-6051.

Wang, Y., L. A. Krushel and G. M. Edelman (1996). "Targeted DNA recombination in vivo using an adenovirus carrying the cre recombinase gene." Proceedings of the National Academy of Sciences **93**(9): 3932-3936.

Watanabe, S., E. Ichikawa, H. Takahashi and F. Otsuka (1995). "Changes of cytokeratin and involucrin expression in squamous cell carcinomas of the skin during progression to malignancy." British Journal of Dermatology **132**(5): 730-739.

Watt, F. M. and H. Green (1982). "Stratification and terminal differentiation of cultured epidermal cells." Nature **295**(5848): 434-436.

Watt, S. A., C. Pourreyron, K. Purdie, C. Hogan, C. L. Cole, N. Foster, N. Pratt, J. C. Bourdon, V. Appleyard, K. Murray, A. M. Thompson, X. Mao, C. Mein, L. Bruckner-Tuderman, A. Evans, J. A. McGrath, C. M. Proby, J. Foerster, I. M. Leigh and A. P. South (2011). "Integrative mRNA profiling comparing cultured primary cells with clinical samples reveals PLK1 and C20orf20 as therapeutic targets in cutaneous squamous cell carcinoma." Oncogene **30**(46): 4666-4677.

Weijts, B. G. M. W., W. J. Bakker, P. W. A. Cornelissen, K.-H. Liang, F. H. Schaftenaar, B. Westendorp, C. A. C. M. T. de Wolf, M. Paciejewska, C. L. G. J. Scheele, L. Kent, G. Leone, S. Schulte-Merker and A. de Bruin (2012). "E2F7 and E2F8 promote angiogenesis through transcriptional activation of VEGFA in cooperation with HIF1." EMBO J **31**(19): 3871-3884.

Weijts, B. G. M. W., A. van Impel, S. Schulte-Merker and A. de Bruin (2013). "Atypical E2fs Control Lymphangiogenesis through Transcriptional Regulation of Ccbe1 and Flt4." PLoS ONE **8**(9): e73693.

Welter, J. F., J. F. Crish, C. Agarwal and R. L. Eckert (1995). "Fos-related Antigen (Fra-1), junB, and junD Activate Human Involucrin Promoter Transcription by Binding to Proximal and Distal AP1 Sites to Mediate Phorbol Ester Effects on Promoter Activity." Journal of Biological Chemistry **270**(21): 12614-12622.

Welter, J. F., H. Gali, J. F. Crish and R. L. Eckert (1996). "Regulation of Human Involucrin Promoter Activity by POU Domain Proteins." Journal of Biological Chemistry **271**(25): 14727-14733.

Wenzel, P. L., J. L. Chong, M. T. Saenz-Robles, A. Ferrey, J. P. Hagan, Y. M. Gomez, R. Rajmohan, N. Sharma, H. Z. Chen, J. M. Pipas, M. L. Robinson and G. Leone (2011). "Cell proliferation in the absence of E2F1-3." Dev Biol **351**(1): 35-45.

Wertheimer, E., A. Gutierrez-Uzquiza, C. Rosemblit, C. Lopez-Haber, M. S. Sosa and M. G. Kazanietz (2012). "Rac signaling in breast cancer: A tale of GEFs and GAPs." Cellular Signalling **24**(2): 353-362.

Westendorp, B., M. Mokry, M. J. A. Groot Koerkamp, F. C. P. Holstege, E. Cuppen and A. de Bruin (2011). "E2F7 represses a network of oscillating cell cycle genes to control S-phase progression." Nucleic Acids Research.

Wikonkal, N. M., E. Remenyik, D. Knezevic, W. Zhang, M. Liu, H. Zhao, T. R. Berton, D. G. Johnson and D. E. Brash (2003). "Inactivating E2f1 reverts apoptosis resistance and cancer sensitivity in Trp53-deficient mice." Nat Cell Biol **5**(7): 655-660.

Wolff-Schreiner, E. C. (1977). "Ultrastructural cytochemistry of the epidermis." Int J Dermatol **16**(2): 77-102.

Won, J., J. Yim and T. K. Kim (2002). "Sp1 and Sp3 Recruit Histone Deacetylase to Repress Transcription of Human Telomerase Reverse Transcriptase (hTERT) Promoter in Normal Human Somatic Cells." Journal of Biological Chemistry **277**(41): 38230-38238.

Wong, C. F., L. M. Barnes, A. L. Dahler, L. Smith, M. M. Serewko-Auret, C. Popa, I. Abdul-Jabbar and N. A. Saunders (2003). "E2F modulates keratinocyte squamous differentiation: implications for E2F inhibition in squamous cell carcinoma." J Biol Chem **278**(31): 28516-28522.

Wong, C. F., L. M. Barnes, L. Smith, C. Popa, M. M. Serewko-Auret and N. A. Saunders (2004). "E2F6: a member of the E2F family that does not modulate squamous differentiation." Biochemical and Biophysical Research Communications **324**(2): 497-503.

Wrone-Smith, T., J. Bergstrom, M. E. Quevedo, V. Reddy, C. Gutierrez-Steil and B. J. Nickoloff (1999). "Differential expression of cell survival and cell cycle regulatory proteins in cutaneous squamoproliferative lesions." Journal of dermatological science **19**(1): 53-67.

Wu, L., C. Timmers, B. Maiti, H. I. Saavedra, L. Sang, G. T. Chong, F. Nuckolls, P. Giangrande, F. A. Wright, S. J. Field, M. E. Greenberg, S. Orkin, J. R. Nevins, M. L. Robinson and G. Leone (2001). "The E2F1-3 transcription factors are essential for cellular proliferation." Nature **414**(6862): 457-462.

Wu, Z., S. Zheng and Q. Yu (2009). "The E2F family and the role of E2F1 in apoptosis." The International Journal of Biochemistry & Cell Biology **41**(12): 2389-2397.

Yamazaki, D., S. Kurisu and T. Takenawa (2009). "Involvement of Rac and Rho signaling in cancer cell motility in 3D substrates." Oncogene **28**(13): 1570-1583.

Ye, H., T. Yu, S. Temam, B. Ziober, J. Wang, J. Schwartz, L. Mao, D. Wong and X. Zhou (2008). "Transcriptomic dissection of tongue squamous cell carcinoma." BMC Genomics **9**(1): 69.

Young, C. (2009). "Solar ultraviolet radiation and skin cancer." Occupational Medicine **59**(2): 82-88.

Yu, F., J. Megyesi and P. M. Price (2008). "Cytoplasmic initiation of cisplatin cytotoxicity." American Journal of Physiology - Renal Physiology **295**(1): F44-F52.

Yu, F., J. Megyesi, R. L. Safirstein and P. M. Price (2007). "Involvement of the CDK2-E2F1 pathway in cisplatin cytotoxicity in vitro and in vivo." American Journal of Physiology - Renal Physiology **293**(1): F52-F59.

Zalmas, L. P., A. S. Coutts, T. Helleday and N. B. La Thangue (2013). "E2F-7 couples DNA damage-dependent transcription with the DNA repair process." Cell Cycle **12**(18): 3037-3051.

Zenz, R. and E. F. Wagner (2006). "Jun signalling in the epidermis: From developmental defects to psoriasis and skin tumors." The International Journal of Biochemistry & Cell Biology **38**(7): 1043-1049.

Zhan, L., C. Huang, X. M. Meng, Y. Song, X. Q. Wu, C. G. Miu, X. S. Zhan and J. Li (2014). "Promising roles of mammalian E2Fs in hepatocellular carcinoma." Cell Signal **26**(5): 1075-1081.

Zhang, S., X. Liu, T. Bawa-Khalfe, L.-S. Lu, Y. L. Lyu, L. F. Liu and E. T. H. Yeh (2012). "Identification of the molecular basis of doxorubicin-induced cardiotoxicity." Nat Med **18**(11): 1639-1642.

Zhao, K. N., W. Gu, N. X. Fang, N. A. Saunders and I. H. Frazer (2005). "Gene codon composition determines differentiation-dependent expression of a viral capsid gene in keratinocytes in vitro and in vivo." Mol Cell Biol **25**(19): 8643-8655.

Zhao, L. J., T. Subramanian, S. Vijayalingam and G. Chinnadurai (2014). "CtBP2 proteome: Role of CtBP in E2F7-mediated repression and cell proliferation." Genes Cancer **5**(1-2): 31-40.

Zhao, W. M. and G. Fang (2005). "MgcRacGAP controls the assembly of the contractile ring and the initiation of cytokinesis." Proc Natl Acad Sci U S A **102**(37): 13158-13163.

Zhu, S., H.-S. Oh, M. Shim, E. Sterneck, P. F. Johnson and R. C. Smart (1999). "C/EBPβ Modulates the Early Events of Keratinocyte Differentiation Involving Growth Arrest and Keratin 1 and Keratin 10 Expression." Molecular and cellular biology **19**(10): 7181-7190.

CHAPTER 9

9 Appendix

9.1 Appendix I General buffers and media

9.1.1 Phosphate-buffered saline (PBS)

136.9 mM NaCI

2.7 mM KCI

1.5 mM KH_2PO_4

2.5 mM Na_2HPO_4.2H2O

pH 7.4

9.1.2 1x Tris-Borate EDTA buffer

45 mM Tris

45 mM boric acid

1 mM EDTA

9.1.3 SCC media (for SCC cells)

1:1 volume:volume of DMEM:Ham's F12 nutrient mix pH 7.1

5% FBS

0.43 µg/mL hydrocortisone

1% v/v penicillin/streptomycin/glutamine

10 µg/mL gentamycin

9.1.4 RIPA buffer

50 mM Tris-HCI pH 7.4

150 mM NaCI

1% v/v NP-40

0.5% w/v sodium deoxycholate

0.1% SDS

9.1.5 1x Sample buffer

10% glycerol

2% SDS

50 mM Tris-HCI pH 6.8

100 mM DTT

0.005% w/v bromophenol blue

9.1.6 4x sample buffer

40% glycerol

8% SDS

200 mM Tris-HCI pH 6.8

400 mM DTT

0.02% bromophenol blue

9.1.7 Electrophoresis running buffer

25 mM Tris

191 mM Glycine

0.1% v/v SDS

9.1.8 Transfer buffer

25 mM Tris

191 mM Glycine

20% v/v methanol

9.1.9 TBS-T

20 mM Tris pH 7.6

137 mM NaCI

0.1% v/v Tween 20

9.1.10 Acrylamide gels for SDS-PAGE

Resolving layer		
Gel	**Components**	**per 10 mL final volume**
10%	H_2O	5.3 mL
	30% acrylamide mix	3.3 mL
	1.5 M Tris pH 8.8	2.5 mL
	10% SDS	0.1 mL
	10% ammonium persulfate	0.1 mL
	TEMED	0.004 mL
12%	H_2O	3.3 mL
	30% acrylamide mix	4.0 mL
	1.5 M Tris pH 8.8	2.5 mL
	10% SDS	0.1 mL
	10% ammonium persulfate	0.1 mL
	TEMED	0.004 mL

Stacking layer	
Components	**per 10 mL final volume**
H_2O	6.8 mL
30% acrylamide mix	1.7 mL
1.0 M Tris pH 6.8	1.25 mL
10% SDS	0.1 mL
10% ammonium persulfate	0.1 mL
TEMED	0.01 mL

9.2 Appendix II Publication (review paper)

Int. J. Mol. Sci. **2011**, *12*, 8947-8960; doi:10.3390/ijms12128947

OPEN ACCESS

International Journal of
Molecular Sciences
ISSN 1422-0067
www.mdpi.com/journal/ijms

Review

The Role of the E2F Transcription Factor Family in UV-Induced Apoptosis

Mehlika Hazar-Rethinam [1], Liliana Endo-Munoz [1], Orla Gannon [1] and Nicholas Saunders [1,2,*]

[1] Epithelial Pathobiology Group, University of Queensland Diamantina Institute, Princess Alexandra Hospital, Queensland 4102, Australia; E-Mails: m.rethinam@uq.edu.au (M.H.-R.); l.munoz@uq.edu.au (L.E.-M.); o.gannon@uq.edu.au (O.G.)

[2] School of Biomedical Sciences, University of Queensland, Queensland 4072, Australia

* Author to whom correspondence should be addressed; E-Mail: nsaunders@uq.edu.au; Tel.: +61-7-3176-5894; Fax: +61-7-3176-5946.

Received: 11 October 2011; in revised form: 15 November 2011 / Accepted: 30 November 2011 / Published: 6 December 2011

Abstract: The E2F transcription factor family is traditionally associated with cell cycle control. However, recent data has shown that activating E2Fs (E2F1-3a) are potent activators of apoptosis. In contrast, the recently cloned inhibitory E2Fs (E2F7 and 8) appear to antagonize E2F-induced cell death. In this review we will discuss (i) the potential role of E2Fs in UV-induced cell death and (ii) the implications of this to the development of UV-induced cutaneous malignancies.

Keywords: UV; sunburn cells; E2F; apoptosis

1. What is UV?

Life on earth is dependent upon UV radiation as an energy source. Ironically, whilst humans are dependent upon UV radiation for their existence, UV radiation is a common and potent carcinogen for people of Caucasian descent [1].

Ultraviolet (beyond violet) refers to wavelengths shorter than visible violet light and longer than X-rays [2]. The UV radiation spectrum is grouped into three categories based on wavelength. UVC (200–280 nm) is the most potent carcinogenic band of UV but poses little threat to terrestrial organisms since it is almost completely absorbed by the earth's atmosphere. Only 10% of incident UVB (280–320 nm) radiation penetrates the atmosphere. The vast majority of incident UV (greater

than 90%) radiation comes from UVA (320–400 nm). Although UVA radiation predominates at sea level, UVB has the highest energy and is 1,000 times more erythematogenic than UVA [2]. Thus, the carcinogenic potential of the UV spectrum reaching the earth's surface is a composite of a small amount of high energy UVB and a large amount of low energy UVA. Combined, UVA and UVB radiation damage DNA, disrupt pro-apoptotic signaling pathways and suppress immune responses ultimately contributing to the carcinogenic action of sunlight [3]. Despite the more potent carcinogenic activity of UVB it is only capable of penetrating the more superficial epidermal layers whereas UVA can penetrate deeper into the dermis [2].

2. Mutagenic Effects of UV Radiation

UV light is a physical mutagen and can ionize molecules resulting in the conversion of absorbed light energy into biochemical reactions. DNA is one of the major molecules capable of absorbing UV radiation. Absorbed UV radiation causes DNA damage via the formation of DNA lesions often referred to as photolesions [4]. DNA damage caused by UVA and UVB can be direct or indirect. Direct absorption of UVB by DNA results in the formation of photolesions such as cyclo-butane-pyrimidine dimers (CPDs) and pyrimidine (6–4) pyrimidone dimers [5] (Table 1). If these pyrimidine dimers are not repaired by DNA repair mechanisms, it may result in heritable base transitions. Formation of these, C→T single or CC→TT double, transitions at dipyrimidine sites is mutagenic and the nature and the presence of these lesions are frequently referred to as the UVB signature [6]. On the other hand, UVA is not absorbed by DNA and causes DNA damage via an indirect mechanism involving the generation of reactive oxygen species (ROS) generated by UVA-mediated activation of photosensitizers (e.g., riboflavin, porphyrins, quinines) resulting in the accumulation of CPDs [7]. UVB may also cause the accumulation of ROS and hence can also facilitate indirect DNA damage, albeit to a lesser extent than observed with UVA [8] (Table 1).

Table 1. Summary of mutagenic effects of UVA and UVB.

	UVA	**UVB**
Wavelength (nm)	320–400	280–320
Chromophores	Photosensitizers	DNA
Site of damage	ROS	Pyrimidine dimers (CDP) 6–4 photoproducts
Mechanism	Indirect	Direct

3. Sunburn Cells (UV-Induced Cell Death)

Following UV exposure keratinocytes will follow one of two fates. If the damage to DNA is perceived to be reparable, the keratinocytes will undergo a reversible growth arrest accompanied by the mobilisation and activation of the nucleotide excision repair system (NER). This leads to the repair of damaged DNA (mutations/DNA lesions) and is facilitated by secreted cytokines, IL12 and IL18, which can restore immune responses and prevent from UV-induced immunosuppression [9–11]. Alternatively, if the DNA damage is perceived to be too great and the cells lack the capacity to repair the damage then the cells will be induced to apoptose [12,13]. Apoptosis, or programmed cell death, is a mechanism that prevents cells from passing on mutated DNA to their progeny. Thus, the apoptotic

machinery provides a means by which mutated, potentially premalignant cells are able to be eliminated [14]. UV-induced apoptosis results in the formation of so-called "sunburn cells" or apoptotic keratinocytes. Sunburn cells are easily identified by the presence of photo lesions, pyknotic nuclei and cytoplasmic shrinkage characteristic of apoptotic cells [15]. UV-induced apoptotic responses are mediated via extrinsic/death receptor signaling and intrinsic/mitochondrial death pathways [11,16]. The extrinsic death pathway is initiated by the binding of membrane death receptors TNF-R1, CD95, TRAIL-R1 and TRAIL-R2 to their cognate ligands, TNF-α, CD95L/FASL or TRAIL (TNF-related apoptosis-inducing ligand). UV can also activate CD95 death receptor signaling pathways independent of its natural ligand CD95L [17]. The subsequent formation of a death-inducing signaling complex (DISC) is characteristic of death receptor-mediated apoptosis in response to UV radiation [18,19]. Activation of death receptor signaling ultimately activates the initiator pro-caspases-8/-10 leading to the eventual activation of downstream effector procaspases-3,-6,-7 [12]. Activation of the intrinsic apoptotic pathway is stimulated by the release of cytochrome c from outer mitochondrial membrane [20]. Activation of the intrinsic apoptotic pathway is controlled by the balance between pro-apoptotic (Bax, Bak, Bad, Bid, Bim) and anti-apoptotic (Bcl-2, Bcl-Xl, Mcl-Xl) Bcl-2 family proteins. When pro-apoptotic stimuli predominate, it leads to the permeabilisation of the mitochondrial outer membrane potential leading to cytochrome C release and eventual procaspase-9 activation [21,22] (Figure 1).

Figure 1. UV-mediated keratinocyte apoptosis can be initiated by extrinsic or intrinsic pathways. Extrinsic pathways include death receptor activation via death ligand binding, DISC formation, activation of pro-caspases and activation of effector caspase-3 leading to apoptosis. Activation of intrinsic pathways induces cytochrome c release from mitochondria and activation of pro-apoptotic Bcl-2 proteins and inhibition of anti-apoptotic Bcl-2 proteins, activation of pro-caspase-9 and activation of effector caspase-3 leading to apoptosis.

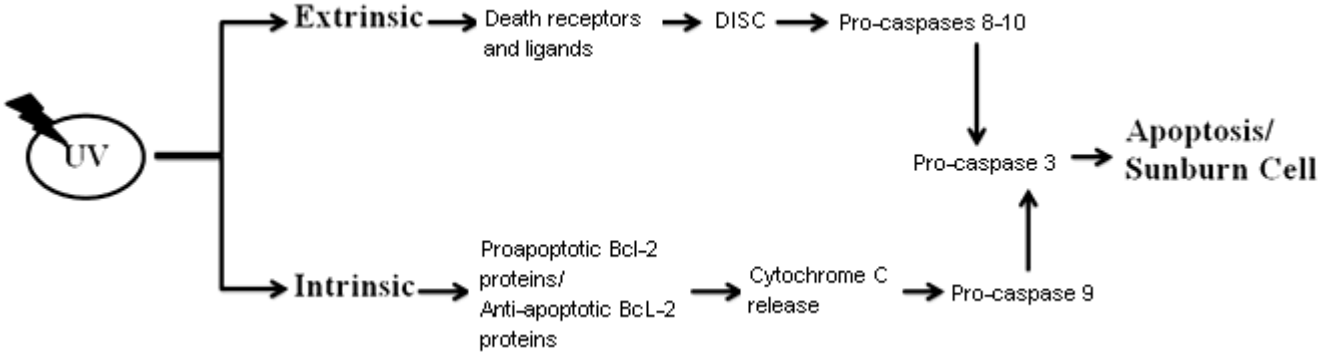

4. Role of UV in Skin Carcinogenesis

Skin cancers are frequently divided into melanoma and non-melanoma skin cancers (NMSC). Regardless of classification, the main contributory factor in the development of cutaneous malignancies, in humans, is UV exposure [23]. Melanoma is a common and aggressive tumour type derived from melanocytes. The major forms of non-melanoma skin cancer are basal cell carcinoma (BCC) and squamous cell carcinoma (SCC) [24]. In a recent study, Trakatelli *et al.* [25] showed that NMSC had

significantly increased in incidence in Caucasians in the last decade. NMSC skin cancers are the most common malignancy in Caucasians and their incidence reflects the potent carcinogenic activity of UV radiation [26]. There are a number of reviews on the molecular mechanisms associated with UV-induced skin cancer and in particular we refer the reader to other articles within this issue of the journal. Of relevance to the current review are reports that UV-induced SCC formation is associated with dysregulation of the control of proliferation, differentiation and apoptosis [27–31]. Amongst these known changes it is notable that disruption of the Rb/E2F axis is over-represented. In particular, there is considerable data relating to the expression, activity and role of dysregulated E2F1 in SCC formation [26,32–35]. For example, disruption of the Rb/E2F axis is common in almost all human cancers including SCC [36]. Loss of function mutations of p53, Rb, or upstream regulators of the Rb/E2F axis such as INK4A (p16) are frequently associated with SCC and may result from mutation, deletion or promoter hypermethylation [37–39]. Moreover, SCCs are frequently associated with amplification/activation of mitogenic pathways controlled by cyclin D1, cdk4 or EGFR [31,40]. All these events are known to contribute to the dysregulation of proliferation and differentiation [31,40,41]. In addition, dysregulation of enzymes regulating oxidative stress such as GPX2 have also been shown to contribute casually to UV-induced SCC formation [25]. Dysregulation of antioxidant enzymes is known to disturb the apoptotic axis. Indeed, apoptotic regulators related to sensitivity and response to UV-induced damage are invariably targeted during keratinocyte transformation [13]. Consequently, the major safeguard that keratinocytes use to protect themselves against UV-induced mutations, namely sunburn cell formation, is compromised in keratinocytes following exposure to carcinogenic doses of UV [41]. However, the exact mechanisms by which UV-induced mutational damage contributes to the biological events controlling keratinocyte transformation and SCC progression remain unclear.

5. The E2F Family

The squamous differentiation program of the epidermis involves co-ordinate regulation of proliferation, differentiation and apoptosis. The barrier functions of the epidermis depend upon the integrity of this program and its ability to respond to environmental insults such as UV radiation [7,42]. The process of squamous differentiation is a tightly regulated process in which transcription factors control the differentiation program and its barrier functions [36]. Thus, it is not surprising that disruption to transcriptional control is a frequent target in oncogenesis [43]. Many transcription factors have been implicated in the control of squamous differentiation and carcinogenesis. However, the E2F family of transcription factors have emerged as pleiotropic regulators, directly controlling (i) cell proliferation, (ii) apoptosis, (iii) differentiation, (iv) DNA-damage response and DNA repair, (v) development, (vi) senescence and (vii) autophagy [28,29,44–49]. Moreover, E2Fs are also indirectly involved in modulating the activity of important cellular signaling pathways such as MAPK, p38 and PI3-K/AKT through transcriptional regulation of upstream pathway components [50,51].

E2F was first discovered as a cellular factor required for the activation of the E2 viral promoter [29,52]. This factor was later cloned and named E2F1 [43]. However, it was quickly recognised that E2F1 was just one member of, what is now, a family of 8 members, E2Fs 1–8, coding for 10 different E2F forms [53]. The role of the E2Fs is complex. Individual E2F family members can be involved in multiple cellular activities. For example, E2F1 is directly involved in the G1/S transition

of the cell cycle [54], stimulating apoptosis [44,55], suppressing differentiation [35,36,56] and acting as a transducer of the DNA damage response in keratinocytes [57]. In addition, multiple E2F family members can play a role in the same cellular functions and frequently share the same E2F binding sites in gene promoters (consensus E2F binding site is TTTCGCGC). For example E2Fs 1, 2 and 3a are all involved in the transition through the G1/S phase of the cell cycle [58]. Finally, there is emerging evidence to indicate that E2F isoform specific-sites and functions may also exist. For example, in keratinocytes we recently showed that E2F7 could selectively suppress differentiation through the repression of Sp1 transcription mediated via a selective and novel E2F7-specific response element (5'-CTCCTTTCCCCCTCCCTCAT-3') [59]. Thus, the E2F transcription factor family is involved in complex and varied roles in cellular physiology.

The E2F family can be broadly classified as typical E2Fs (E2F1-6) and atypical E2Fs (E2F7-E2F8). All typical E2Fs carry one N-terminally located, evolutionary conserved, DNA-binding domain (DBD) (Figure 2). The DBD is followed by a dimerization partner binding domain [60]. There are two members of DP family proteins, DP1 and DP2 that interact with E2F isoforms through the conserved Dimerization Partner-binding domain [28]. In mammalian cells, most E2F DNA-binding takes place once E2F-DP heterodimers form [61]. In contrast, the DBD is duplicated in atypical E2Fs and they bind target gene promoters in a DP-independent fashion [28,62–66] due to the lack of a DP-binding domain. In addition, atypical E2Fs also lack a recognisable *trans*activation domain or pocket protein binding domain compared to typical E2Fs [55] (Figure 2).

Figure 2. Domain organization of activating, repressive or inhibitory E2Fs. Number of amino acid is indicated on the right. Same colour boxes indicate homologues regions. There are two known E2F7 isoforms; E2F7a and E2F7b which differ only in their C termini. Both isoforms of E2F7 are expressed in all cell lines analysed.

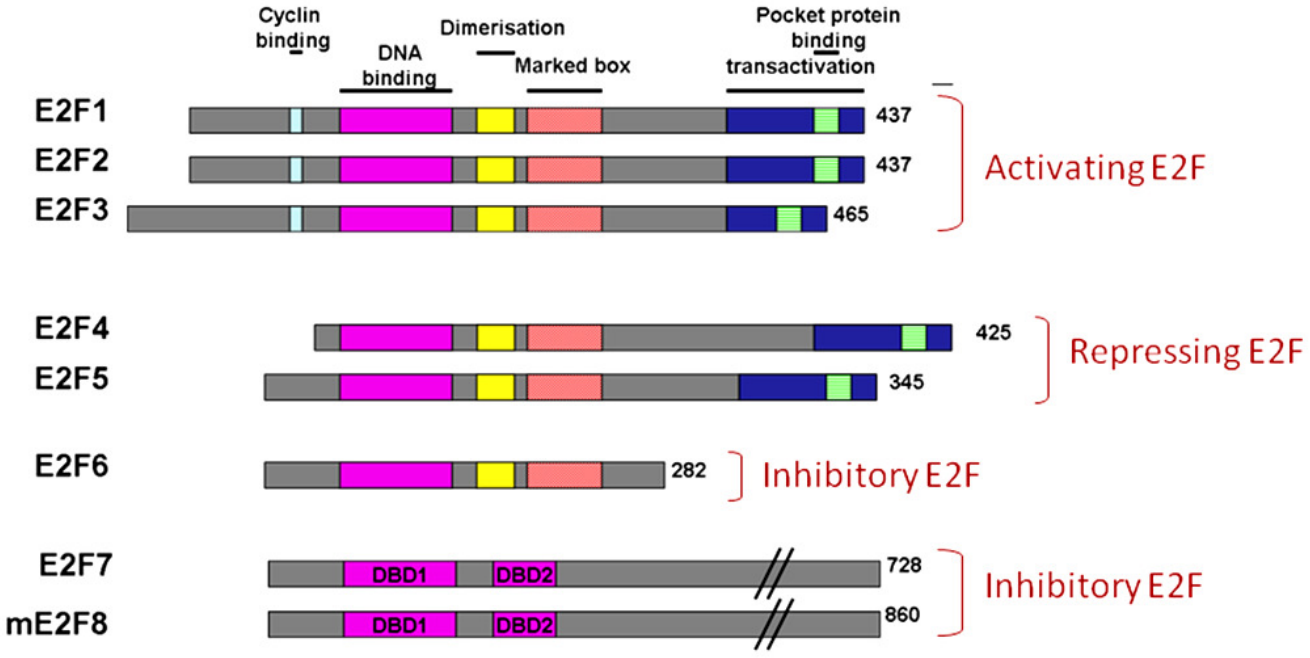

E2Fs are most frequently classified based on their transcriptional activity. For example, the E2F family is generally divided into three subclasses: activator E2Fs (E2F1-E2F3a), repressor E2Fs

(E2F3b-5) and inhibitory E2Fs (E2F6-E2F8). The expression of activator E2Fs varies during the cell cycle reaching a peak of activity, bound to target gene promoters via E2F response elements, during late G1/S phase. In this context, they control the expression of genes and activities required for DNA synthesis [53,67,68]. The expression and activity of the repressor E2Fs (E2F3b, E2F4, E2F5, E2F6) remain relatively constant throughout the cell cycle [53]. They bind target gene promoters during G_0 with E2F inhibitory pocket proteins coupled with repressive histone deacetylases [39,69] and prevent promiscuous transcription of proliferation genes [53,57,70]. The so-called repressor E2Fs get their name due to their ability to actively recruit transcriptional inhibitors such as histone deacetylase 1 (e.g., E2F4 and 5) or PRC2 (E2F6) to the E2F sites resulting in transcriptional repression [57,58]. In contrast, inhibitory E2Fs (E2F 7 and 8) compete for binding sites with other E2Fs and mediate their inhibition by excluding active or repressive E2Fs from binding [55]. The expression of E2F7 and E2F8 is cell-cycle regulated. Transcription of E2F7 and E2F8 increases towards G_1-to-S transition reaching its peak during S-to-G_2 transition [28,57,59,60,71]. Thus, the role of E2F7/8 in cell cycle control appears to tie in with the direct inhibition of the E2F1 activities related to cell cycle traverse [42,63]. In contrast, the role of the inhibitory E2Fs in the control of differentiation appears to be isoform-specific and is mediated via isoform-specific DNA response elements [26,54]. Finally, the anti-apoptotic action of the inhibitory E2Fs appears to be mediated via direct inhibition of E2F1-mediated apoptosis [42,63]. The interplay between E2F1-stimulated apoptosis and E2F7/8-mediated inhibition of apoptosis is critical to understanding the role of E2Fs in UV-induced skin cancer formation and their potential as drugable targets for treating squamous cell carcinomas or enhancing chemotherapeutic responses.

6. E2F-Induced Apoptosis and Skin Cancer Formation

The ability of the different E2Fs to contribute to apoptosis especially to UV-mediated apoptosis is contentious. Much of this controversy arises from some seemingly paradoxical data relating to the action of E2F1. Earlier studies with E2F1 reported that overexpression of E2F1 in tissue culture cells and in transgenic mice caused a stimulation of apoptosis and an enhancement of tumour formation [33,34,72,73]. In particular, overexpression of E2F1 in the epidermis of transgenic mice caused elevated apoptotic indices in keratinocytes of the basal layer and an increase in skin tumour formation in mice that overexpressed E2F1 and cyclin D1 [34]. In contrast, mice transgenic for E2F4 expression in skin did not have increased apoptotic indices [74]. Similarly, mice deficient for E2F1 were predisposed to thymomas due to their inability to delete t cells via E2F1-mediated apoptosis [75,76]. These earlier studies clearly supported the concept that the pro-proliferative actions of E2F1 were oncogenic whilst the pro-apoptotic actions of E2F1 were tumour suppressive [77]. E2F1-stimulated apoptosis can be mediated by p53-dependent and p53-independent pathways. The p53-dependent pathway involves the stabilization of p53 via p14/p19^{ARF} [78] whilst activation of APAF1 and p73 or CHK2 is required for p53-independent apoptosis [79–81]. In response to UV, E2F1 transcript and protein levels increase in an ATM/ATR dependent manner and leads to accumulation of events required for apoptosis [82]. This suggested that UV-induced E2F1 mediated apoptosis in skin may have tumour suppressive effects. However, studies by Dimova and Dyson reported that the ectopic expression of E2F1 may result in the expression of survival genes suggesting that E2F1 may be anti-apoptotic under certain conditions [48]. This suggests that the role of E2F1 in regulating apoptosis

may be context-specific. Consistent with this, it has been reported that E2F1 is anti-apoptotic in keratinocytes in the context of UVB irradiation [52,83]. Specifically, E2F1 deficient mice and mice transgenic for E2F1 in skin displayed increased and reduced apoptotic indices in response to UVB irradiation respectively [52,78]. Wikonkal *et al.* [52] also showed that the pro-survival effect of E2F1, in response to UVB, was p53-independent. Finally, it was shown that the pro-survival effect of E2F1, in response to UVB irradiation of keratinocytes/epidermis could be attributed to the ability of E2F1 to sense DNA damage and co-ordinate the DNA damage repair [52]. In this regard, E2F1 has been reported to function directly at sites of DNA repair to eliminate DNA photoproducts [84,85] or indirectly by controlling the transcription of genes required for DNA repair machinery [86,87].

Whilst these data appear to definitively show that E2F1 is oncogenic in skin due to its anti-apoptotic effects, there still remain some unresolved issues. For example, studies have shown that E2F1-mediated responses to UVB irradiation may be dose-dependent such that low doses of UVB activate DNA repair mechanisms whilst high doses induce apoptosis in cells in which the cellular DNA repair machinery is unable to repair the damage [88]. Moreover, another important consideration is the level of E2F1. For example, it is easy to see the benefit of a pro-survival signal being generated in response to the relatively low levels of E2F1 that may be experienced during cell cycle traverse. It is also easy to see biological justification that elevation of E2F1, in response to stressors such as UVB, could invoke apoptotic responses [89,90]. Earlier studies by Yang and his colleagues have shown that E2F6 is able to repress UV-induced apoptosis in human embryonic kidney cells via direct interaction with BRCA1 [91]. Intriguingly, the expression of E2F6 is influenced by E2F1 [92]. However, it is noteworthy that keratinocytes do not appear to express detectable levels of E2F6 [51] suggesting this situation may not apply in skin. The same cannot be said for recent studies with E2F7 and E2F8. E2F7 and 8 are inhibitory E2Fs that bind to, and repress, E2F1 transcription and E2F1-induced apoptosis [63]. Both E2F7 and E2F8 are expressed in skin [57,61] and are able to influence the cellular DNA damage response [41]. Zalmas *et al.* [41] demonstrated that DNA damage induced by etoposide treatment induced E2F7 and E2F8 expression. Moreover, they demonstrated that DNA damage invoked an increase in E2F7 and E2F8 binding to E2F-responsive genes such as E2F1 resulting in an inhibition of E2F1-mediated apoptosis [41]. In fact, microarray analysis of cells subjected to DNA damage revealed that E2F7 and E2F8 could be considered *bona fide* DNA damage response genes [58,63] (Figure 3). These studies seem to be relevant to skin UV responses since we recently reported that E2F7 plays a role in regulating proliferation, differentiation and UV-induced cytotoxicity in human keratinocytes *in vitro* [26]. Moreover, we reported that E2F1 and E2F7 were overexpressed in human squamous cell carcinomas approximately 50 fold and 200 fold respectively [26]. Such elevations in E2F1 and E2F7 are clearly pathologic and the consequences on UV-induced tumour development and progression remain unknown. However, given that E2F1 and E2F7 are said to autoregulate the expression of one another and given that E2F7 antagonises E2F1-induced apoptosis and UV-induced apoptosis in human keratinocytes [26], it would seem reasonable to speculate that E2F7 may also play a role in UV responses in human epidermis (Figure 4). Thus, apoptotic responses of keratinocytes, to UV, or chemotherapeutics, are likely to be dictated by the relative levels of E2F1 and E2F7.

Figure 3. Regulatory network on E2F1 and E2F7/8 activity representing upstream events (growth-dependant and/or DNA damage mediated activation) and downstream targets.

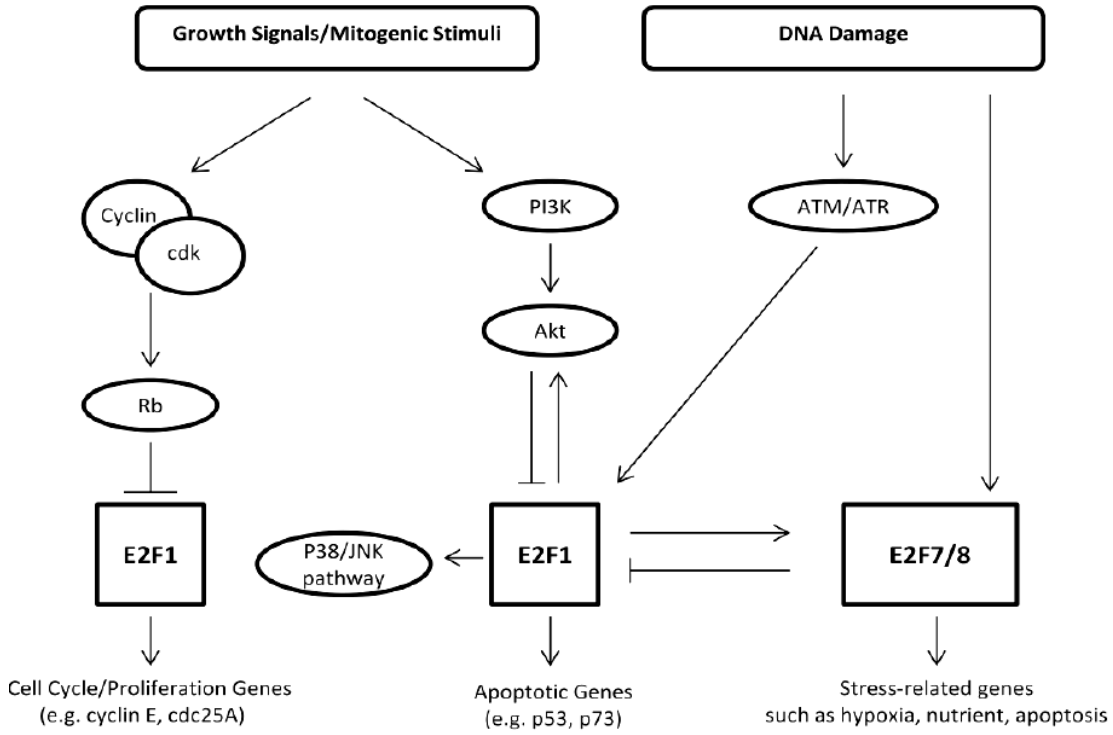

Figure 4. Schematic showing how E2F1 and E2F7 contribute to formation of cutaneous malignancies due to dysregulated apoptotic control.

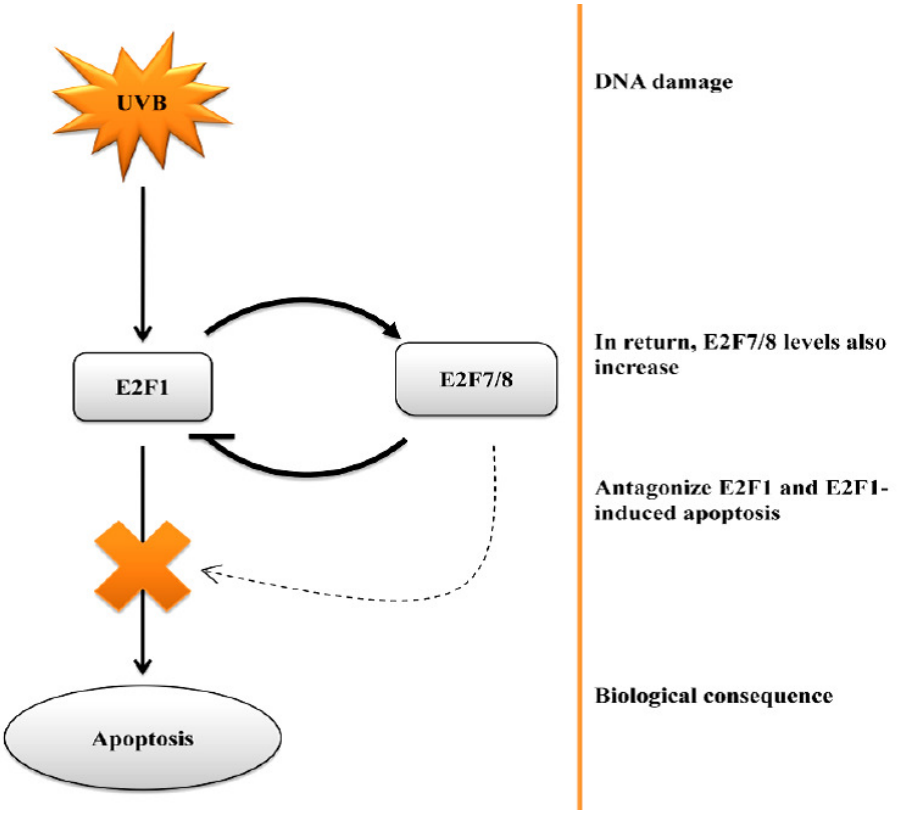

In conclusion, the carcinogenic components of sunlight, relevant to humans, are UVA and UVB. UV radiation induces either a cell cycle arrest or an apoptotic response in human keratinocytes. Both the cell cycle arrest and the apoptotic response appear to be mediated by E2F1. More recently, an antagonistic form of E2F, E2F7, has been reported that antagonizes the pro-proliferative and apoptotic effects of E2F1. Both E2F1 and E2F7 are significantly overexpressed in transformed keratinocytes and there is evidence that the dysregulation of expression of the E2F1 and E2F7 isoforms may contribute to skin cancer formation.

Conflict of Interest

The authors declare no conflict of interest.

Acknowledgments

MHR is supported by a postgraduate scholarship from the University of Queensland. O.G is supported by a scholarship from the Australian National Health and Medical Research Council. This work was supported by grants to NS from the Australian National Health and Medical Research Council (#569689) and the Cancer Council Queensland (#631479).

References

1. Urbach, F. Ultraviolet radiation and skin cancer of humans. *J. Photochem. Photobiol. B* **1997**, *40*, 3–7.
2. Maverakis, E.; Miyamura, Y.; Bowen, M.P.; Correa, G.; Ono, Y.; Goodarzi, H. Light, including ultraviolet. *J. Autoimmun.* **2010**, *34*, J247–J257.
3. Nickoloff, B.J.; Qin, J.-Z.; Chaturvedi, V.; Bacon, P.; Panella, J.; Denning, M.F. Life and death signaling pathways contributing to skin cancer. *J. Investig. Dermatol. Symp. Proc.* **2002**, *7*, 27–35.
4. Hellweg, C.; Baumstark-Khan, C. Detection of UV-induced activation of nf-κb in a recombinant human cell line by means of enhanced green fluorescent protein (egfp). *Radiat. Environ. Biophys.* **2007**, *46*, 269–279.
5. Matsunaga, T.; Hieda, K.; Nikaido, O. Wavelength dependent formation of thymine dimers and (6–4) photoproducts in DNA by monochromatic ultraviolet light ranging from 150 to 365 nm. *Photochem. Photobiol.* **1991**, *54*, 403–410.
6. Nishigori, C. Cellular aspects of photocarcinogenesis. *Photochem. Photobiol. Sci.* **2006**, *5*, 208–214.
7. Lippens, S.; Hoste, E.; Vandenabeele, P.; Agostinis, P.; Declercq, W. Cell death in the skin. *Apoptosis* **2009**, *14*, 549–569.
8. Marchese, C.; Maresca, V.; Cardinali, G.; Belleudi, F.; Ceccarelli, S.; Bellocci, M.; Frati, L.; Torrisi, M.R.; Picardo, M. UVB-induced activation and internalization of keratinocyte growth factor receptor. *Oncogene* **2003**, *22*, 2422–2431.
9. Schwarz, T.; Schwarz, A. DNA repair and cytokine responses. *J. Investig. Dermatol. Symp. Proc.* **2009**, *14*, 63–66.

10. Schwarz, A.; Maeda, A.; Ständer, S.; van Steeg, H.; Schwarz, T. Il-18 reduces ultraviolet radiation-induced DNA damage and thereby affects photoimmunosuppression. *J. Immunol.* **2006**, *176*, 2896–2901.
11. Schwarz, A.; Maeda, A.; Kernebeck, K.; van Steeg, H.; Beissert, S.; Schwarz, T. Prevention of UV radiation–induced immunosuppression by il-12 is dependent on DNA repair. *J. Exp. Med.* **2005**, *201*, 173–179.
12. Chaturvedi, V.; Qin, J.-Z.; Denning, M.F.; Choubey, D.; Diaz, M.O.; Nickoloff, B.J. Apoptosis in proliferating, senescent, and immortalized keratinocytes. *J. Biol. Chem.* **1999**, *274*, 23358–23367.
13. Qin, J.-Z.; Chaturvedi, V.; Denning, M.F.; Bacon, P.; Panella, J.; Choubey, D.; Nickoloff, B.J. Regulation of apoptosis by p53 in UV-irradiated human epidermis, psoriatic plaques and senescent keratinocytes. *Oncogene* **2002**, *21*, 2991–3002.
14. Rodust, P.M.; Stockfleth, E.; Ulrich, C.; Leverkus, M.; Eberle, J. UV-induced squamous cell carcinoma—A role for antiapoptotic signalling pathways. *Br. J. Dermatol.* **2009**, *161*, 107–115.
15. Laethem, A.V.; Claerhout, S.; Garmyn, M.; Agostinis, P. The sunburn cell: Regulation of death and survival of the keratinocyte. *Int. J. Biochem. Cell Biol.* **2005**, *37*, 1547–1553.
16. Kulms, D.; Schwarz, T. Molecular mechanisms involved in UV-induced apoptotic cell death. *Skin Pharmacol. Appl. Skin Physiol.* **2002**, *15*, 342–347.
17. Aragane, Y.; Kulms, D.; Metze, D.; Wilkes, G.; Pöppelmann, B.; Luger, T.A.; Schwarz, T. Ultraviolet light induces apoptosis via direct activation of cd95 (fas/apo-1) independently of its ligand cd95l. *J. Cell Biol.* **1998**, *140*, 171–182.
18. Eberle, J.; Fecker, L.F.; Forschner, T.; Ulrich, C.; Röwert-Huber, J.; Stockfleth, E. Apoptosis pathways as promising targets for skin cancer therapy. *Br. J. Dermatol.* **2007**, *156*, 18–24.
19. Conney, A.H.; Kramata, P.; Lou, Y.-R.; Lu, Y.-P. Effect of caffeine on uvb-induced carcinogenesis, apoptosis, and the elimination of UVB-induced patches of p53 mutant epidermal cells in skh-1 mice. *Photochem. Photobiol.* **2008**, *84*, 330–338.
20. Danial, N.N.; Korsmeyer, S.J. Cell death: Critical control points. *Cell* **2004**, *116*, 205–219.
21. Roos, W.P.; Kaina, B. DNA damage-induced cell death by apoptosis. *Trends Mol. Med.* **2006**, *12*, 440–450.
22. Schafer, Z.T.; Kornbluth, S. The apoptosome: Physiological, developmental, and pathological modes of regulation. *Dev. Cell* **2006**, *10*, 549–561.
23. Black, H.S.; deGruijl, F.R.; Forbes, P.D.; Cleaver, J.E.; Ananthaswamy, H.N.; deFabo, E.C.; Ullrich, S.E.; Tyrrell, R.M. Photocarcinogenesis: An overview. *J. Photochem. Photobiol. B* **1997**, *40*, 29–47.
24. Sander, C.S.; Hamm, F.; Elsner, P.; Thiele, J.J. Oxidative stress in malignant melanoma and non-melanoma skin cancer. *Br. J. Dermatol.* **2003**, *148*, 913–922.
25. Trakatelli, M.; Ulrich, C.; del Marmol, V.; Euvrard, S.; Stockfleth, E.; Abeni, D. Epidemiology of non-melanoma skin cancer (nmsc) in europe: Accurate and comparable data are needed for effective public monitoring and interventions. *Br. J. Dermatol.* **2007**, *156*, 1–7.
26. Clayman, G.L.; Lee, J.J.; Holsinger, F.C.; Zhou, X.; Duvic, M.; El-Naggar, A.K.; Prieto, V.G.; Altamirano, E.; Tucker, S.L.; Strom, S.S.; *et al.* Mortality risk from squamous cell skin cancer. *J. Clin. Oncol.* **2005**, *23*, 759–765.

27. De Gruijl, F.R.; van Kranen, H.J.; Mullenders, L.H.F. UV-induced DNA damage, repair, mutations and oncogenic pathways in skin cancer. *J. Photochem. Photobiol. B* **2001**, *63*, 19–27.
28. Ichihashi, M.; Ueda, M.; Budiyanto, A.; Bito, T.; Oka, M.; Fukunaga, M.; Tsuru, K.; Horikawa, T. UV-induced skin damage. *Toxicology* **2003**, *189*, 21–39.
29. Erb, P.; Ji, J.; Wernli, M.; Kump, E.; Glaser, A.; Büchner, S.A. Role of apoptosis in basal cell and squamous cell carcinoma formation. *Immunol. Lett.* **2005**, *100*, 68–72.
30. Walshe, J.; Serewko-Auret, M.M.; Teakle, N.; Cameron, S.; Minto, K.; Smith, L.; Burcham, P.C.; Russell, T.; Strutton, G.; Griffin, A.; *et al.* Inactivation of glutathione peroxidase activity contributes to UV-induced squamous cell carcinoma formation. *Cancer Res.* **2007**, *67*, 4751–4758.
31. Endo-Munoz, L.; Dahler, A.; Teakle, N.; Rickwood, D.; Hazar-Rethinam, M.; Abdul-Jabbar, I.; Sommerville, S.; Dickinson, I.; Kaur, P.; Paquet-Fifield, S.; *et al.* E2F7 can regulate proliferation, differentiation, and apoptotic responses in human keratinocytes: Implications for cutaneous squamous cell carcinoma formation. *Cancer Res.* **2009**, *69*, 1800–1808.
32. Pierce, A.M.; Gimenez-Conti, I.B.; Schneider-Broussard, R.; Martinez, L.A.; Conti, C.J.; Johnson, D.G. Increased E2F1 activity induces skin tumors in mice heterozygous and nullizygous for p53. *Proc. Natl. Acad. Sci. USA* **1998**, *95*, 8858–8863.
33. Pierce, A.M.; Schneider-Broussard, R.; Gimenez-Conti, I.B.; Russell, J.L.; Conti, C.J.; Johnson, D.G. E2F1 has both oncogenic and tumor-suppressive properties in a transgenic model. *Mol. Cell. Biol.* **1999**, *19*, 6408–6414.
34. Dicker, A.J.; Popa, C.; Dahler, A.L.; Serewko, M.M.; Hilditch-Maguire, P.A.; Frazer, I.H.; Saunders, N.A. E2F-1 induces proliferation-specific genes and suppresses squamous differentiation-specific genes in human epidermal keratinocytes. *Oncogene* **2000**, *19*, 2887–2894.
35. Wong, C.F.; Barnes, L.M.; Dahler, A.L.; Smith, L.; Serewko-Auret, M.M.; Popa, C.; Abdul-Jabbar, I.; Saunders, N.A. E2F modulates keratinocyte squamous differentiation. *J. Biol. Chem.* **2003**, *278*, 28516–28522.
36. DeGregori, J.; Johnson, D.G. Distinct and overlapping roles for E2F family members in transcription, proliferation and apoptosis. *Curr. Mol. Med.* **2006**, *6*, 739–748.
37. Dyson, N. The regulation of E2F by prb-family proteins. *Genes Dev.* **1998**, *12*, 2245–2262.
38. Einspahr, J.G.; Alberts, D.S.; Wameke, J.A.; Bozzo, P.; Basye, J.; Grogan, T.M.; Nelson, M.A.; Bowden, G.T. Relationship of p53 mutations to epidermal cell proliferation and apoptosis in human uv-induced skin carcinogenesis. *Neoplasia* **1999**, *1*, 468–475.
39. Sherr, C.J.; McCormick, F. The rb and p53 pathways in cancer. *Cancer Cell* **2002**, *2*, 103–112.
40. Martínez-Carpio, P.A.; Trelles, M.A. Cutaneous epidermal growth factor receptor system following ultraviolet irradiation: Exploring the role of molecular mechanisms. *Photodermatol. Photoimmunol. Photomed.* **2010**, *26*, 250–256.
41. Wrone-Smith, T.; Bergstrom, J.; Quevedo, M.E.; Reddy, V.; Gutierrez-Steil, C.; Nickoloff, B.J. Differential expression of cell survival and cell cycle regulatory proteins in cutaneous squamoproliferative lesions. *J. Dermatol. Sci.* **1999**, *19*, 53–67.
42. Raj, D.; Brash, D.E.; Grossman, D. Keratinocyte apoptosis in epidermal development and disease. *J. Invest. Dermatol.* **2006**, *126*, 243–257.

43. Serewko, M.M.; Popa, C.; Dahler, A.L.; Smith, L.; Strutton, G.M.; Coman, W.; Dicker, A.J.; Saunders, N.A. Alterations in gene expression and activity during squamous cell carcinoma development. *Cancer Res.* **2002**, *62*, 3759–3765.
44. Trimarchi, J.M.; Lees, J.A. Sibling rivalry in the E2F family. *Nat. Rev. Mol. Cell Biol.* **2002**, *3*, 11–20.
45. Stevens, C.; La Thangue, N.B. The emerging role of E2F-1 in the DNA damage response and checkpoint control. *DNA Repair* **2004**, *3*, 1071–1079.
46. Panagiotis Zalmas, L.; Zhao, X.; Graham, A.L.; Fisher, R.; Reilly, C.; Coutts, A.S.; La Thangue, N.B. DNA-damage response control of E2F7 and E2F8. *EMBO Rep.* **2008**, *9*, 252–259.
47. Moon, N.-S.; Dyson, N. E2F7 and E2F8 keep the E2F family in balance. *Dev. Cell* **2008**, *14*, 1–3.
48. Helin, K.; Lees, J.A.; Vidal, M.; Dyson, N.; Harlow, E.; Fattaey, A. A cdna encoding a prb-binding protein with properties of the transcription factor E2F. *Cell* **1992**, *70*, 337–350.
49. Polager, S.; Ofir, M.; Ginsberg, D. E2F1 regulates autophagy and the transcription of autophagy genes. *Oncogene* **2008**, *27*, 4860–4864.
50. Bashari, D.; Hacohen, D.; Ginsberg, D. Jnk activation is regulated by E2F and promotes E2F1-induced apoptosis. *Cell. Signal.* **2011**, *23*, 65–70.
51. Chaussepied, M.; Ginsberg, D. E2F and signal transduction pathways. *Cell Cycle* **2005**, *4*, 392–396.
52. Nevins, J. Toward an understanding of the functional complexity of the E2F and retinoblastoma families. *Cell Growth Differ.* **1998**, *9*, 585–593.
53. Dimova, D.K.; Dyson, N.J. The E2F transcriptional network: Old acquaintances with new faces. *Oncogene* **2005**, *24*, 2810–2826.
54. Johnson, D.G.; Ohtani, K.; Nevins, J.R. Autoregulatory control of E2F1 expression in response to positive and negative regulators of cell cycle progression. *Genes Dev.* **1994**, *8*, 1514–1525.
55. Iaquinta, P.J.; Lees, J.A. Life and death decisions by the E2F transcription factors. *Curr. Opin. Cell Biol.* **2007**, *19*, 649–657.
56. Wong, C.F.; Barnes, L.M.; Smith, L.; Popa, C.; Serewko-Auret, M.M.; Saunders, N.A. E2F6: A member of the E2F family that does not modulate squamous differentiation. *Biochem. Biophys. Res. Commun.* **2004**, *324*, 497–503.
57. Berton, T.R.; Mitchell, D.L.; Guo, R.; Johnson, D.G. Regulation of epidermal apoptosis and DNA repair by E2F1 in response to ultraviolet b radiation. *Oncogene* **2005**, *24*, 2449–2460.
58. Leone, G.; DeGregori, J.; Yan, Z.; Jakoi, L.; Ishida, S.; Williams, R.S.; Nevins, J.R. E2F3 activity is regulated during the cell cycle and is required for the induction of S phase. *Genes Dev.* **1998**, *12*, 2120–2130.
59. Hazar-Rethinam, M.; Cameron, S.R.; Dahler, A.L.; Endo-Munoz, L.B.; Smith, L.; Rickwood, D.; Saunders, N.A. Loss of E2F7 expression is an early event in squamous differentiation and causes derepression of the key differentiation activator sp1. *J. Invest. Dermatol.* **2011**, *131*, 1077–1084.
60. Lammens, T.; Li, J.; Leone, G.; de Veylder, L. Atypical E2Fs: New players in the E2F transcription factor family. *Trends Cell Biol.* **2009**, *19*, 111–118.
61. Stevens, C.; la Thangue, N.B. E2F and cell cycle control: A double-edged sword. *Arch. Biochem. Biophys.* **2003**, *412*, 157–169.

62. De Bruin, A.; Maiti, B.; Jakoi, L.; Timmers, C.; Buerki, R.; Leone, G. Identification and characterization of E2F7, a novel mammalian E2F family member capable of blocking cellular proliferation. *J. Biol. Chem.* **2003**, *278*, 42041–42049.
63. Di Stefano, L.; Jensen, M.R.; Helin, K. E2F7, a novel E2F featuring dp-independent repression of a subset of E2F-regulated genes. *EMBO J.* **2003**, *22*, 6289–6298.
64. Logan, N.; Delavaine, L.; Graham, A.; Reilly, C.; Wilson, J.; Brummelkamp, T.R.; Hijmans, E.M.; Bernards, R.; La Thangue, N.B. E2F-7: A distinctive E2F family member with an unusual organization of DNA-binding domains. *Oncogene* **2004**, *23*, 5138–5150.
65. Logan, N.; Graham, A.; Zhao, X.; Fisher, R.; Maiti, B.; Leone, G.; Thangue, N.B.L. E2F-8: An E2F family member with a similar organization of DNA-binding domains to E2F-7. *Oncogene* **2005**, *24*, 5000–5004.
66. Maiti, B.; Li, J.; de Bruin, A.; Gordon, F.; Timmers, C.; Opavsky, R.; Patil, K.; Tuttle, J.; Cleghorn, W.; Leone, G. Cloning and characterization of mouse E2F8, a novel mammalian E2F family member capable of blocking cellular proliferation. *J. Biol. Chem.* **2005**, *280*, 18211–18220.
67. Cam, H.; Dynlacht, B.D. Emerging roles for E2F: Beyond the g1/s transition and DNA replication. *Cancer Cell* **2003**, *3*, 311–316.
68. Li, J.; Ran, C.; Li, E.; Gordon, F.; Comstock, G.; Siddiqui, H.; Cleghorn, W.; Chen, H.-Z.; Kornacker, K.; Liu, C.-G.; *et al.* Synergistic function of E2F7 and E2F8 is essential for cell survival and embryonic development. *Dev. Cell* **2008**, *14*, 62–75.
69. Takahashi, Y.; Rayman, J.B.; Dynlacht, B.D. Analysis of promoter binding by the E2F and prb families *in vivo*: Distinct E2F proteins mediate activation and repression. *Genes Dev.* **2000**, *14*, 804–816.
70. Attwooll, C.; Denchi, E.L.; Helin, K. The E2F family: Specific functions and overlapping interests. *EMBO J.* **2004**, *23*, 4709–4716.
71. Christensen, J.; Cloos, P.; Toftegaard, U.; Klinkenberg, D.; Bracken, A.P.; Trinh, E.; Heeran, M.; di Stefano, L.; Helin, K. Characterization of E2F8, a novel E2F-like cell-cycle regulated repressor of E2F-activated transcription. *Nucleic Acids Res.* **2005**, *33*, 5458–5470.
72. Qin, X.Q.; Livingston, D.M.; Kaelin, W.G.; Adams, P.D. Deregulated transcription factor E2F-1 expression leads to s-phase entry and p53-mediated apoptosis. *Proc. Natl. Acad. Sci. USA* **1994**, *91*, 10918–10922.
73. Holmberg, C.; Helin, K.; Sehested, M.; Karlström, O. E2F-1 induced p53-independent apoptosis apoptosis in transgenic mice. *Oncogene* **1998**, *17*, 143–155.
74. Wang, D.; Russell, J.L.; Johnson, D.G. E2F4 and E2F1 have similar proliferative properties but different apoptotic and oncogenic properties *in vivo*. *Mol. Cell. Biol.* **2000**, *20*, 3417–3424.
75. Field, S.J.; Tsai, F.-Y.; Kuo, F.; Zubiaga, A.M.; Kaelin, W.G.; Livingston, D.M.; Orkin, S.H.; Greenberg, M.E. E2F-1 functions in mice to promote apoptosis and suppress proliferation. *Cell* **1996**, *85*, 549–561.
76. Yamasaki, L.; Jacks, T.; Bronson, R.; Goillot, E.; Harlow, E.; Dyson, N.J. Tumor induction and tissue atrophy in mice lacking E2F-1. *Cell* **1996**, *85*, 537–548.
77. Hanahan, D.; Weinberg, R.A. The hallmarks of cancer. *Cell* **2000**, *100*, 57–70.

78. Pediconi, N.; Ianari, A.; Costanzo, A.; Belloni, L.; Gallo, R.; Cimino, L.; Porcellini, A.; Screpanti, I.; Balsano, C.; Alesse, E.; *et al.* Differential regulation of E2F1 apoptotic target genes in response to DNA damage. *Nat. Cell Biol.* **2003**, *5*, 552–558.
79. Irwin, M.; Marin, M.C.; Phillips, A.C.; Seelan, R.S.; Smith, D.I.; Liu, W.; Flores, E.R.; Tsai, K.Y.; Jacks, T.; Vousden, K.H.; *et al.* Role for the p53 homologue p73 in E2F-1-induced apoptosis. *Nature* **2000**, *407*, 645–648.
80. Moroni, M.C.; Hickman, E.S.; Denchi, E.L.; Caprara, G.; Colli, E.; Cecconi, F.; Muller, H.; Helin, K. Apaf-1 is a transcriptional target for E2F and p53. *Nat. Cell Biol.* **2001**, *3*, 552–558.
81. Rogoff, H.A.; Pickering, M.T.; Frame, F.M.; Debatis, M.E.; Sanchez, Y.; Jones, S.; Kowalik, T.F. Apoptosis associated with deregulated E2F activity is dependent on E2F1 and atm/nbs1/chk2. *Mol. Cell. Biol.* **2004**, *24*, 2968–2977.
82. Carcagno, A.L.; Ogara, M.F.; Sonzogni, S.V.; Marazita, M.C.; Sirkin, P.F.; Ceruti, J.M.; Cánepa, E.T. E2F1 transcription is induced by genotoxic stress through atm/atr activation. *IUBMB Life* **2009**, *61*, 537–543.
83. Wikonkal, N.M.; Remenyik, E.; Knezevic, D.; Zhang, W.; Liu, M.; Zhao, H.; Berton, T.R.; Johnson, D.G.; Brash, D.E. Inactivating E2F1 reverts apoptosis resistance and cancer sensitivity in trp53-deficient mice. *Nat. Cell Biol.* **2003**, *5*, 655–660.
84. Maser, R.S.; Mirzoeva, O.K.; Wells, J.; Olivares, H.; Williams, B.R.; Zinkel, R.A.; Farnham, P.J.; Petrini, J.H.J. Mre11 complex and DNA replication: Linkage to E2F and sites of DNA synthesis. *Mol. Cell. Biol.* **2001**, *21*, 6006–6016.
85. Liu, K.; Lin, F.-T.; Ruppert, J.M.; Lin, W.-C. Regulation of E2F1 by brct domain-containing protein topbp1. *Mol. Cell. Biol.* **2003**, *23*, 3287–3304.
86. Polager, S.; Kalma, Y.; Berkovich, E.; Ginsberg, D. E2Fs up-regulate expression of genes involved in DNA replication, DNA repair and mitosis. *Oncogene* **2002**, *21*, 437–446.
87. Ren, B.; Cam, H.; Takahashi, Y.; Volkert, T.; Terragni, J.; Young, R.A.; Dynlacht, B.D. E2F integrates cell cycle progression with DNA repair, replication, and g2/m checkpoints. *Genes Dev.* **2002**, *16*, 245–256.
88. Abu-Yousif, A.O.; Smith, K.A.; Getsios, S.; Green, K.J.; van Dross, R.T.; Pelling, J.C. Enhancement of uvb-induced apoptosis by apigenin in human keratinocytes and organotypic keratinocyte cultures. *Cancer Res.* **2008**, *68*, 3057–3065.
89. Lin, W.-C.; Lin, F.-T.; Nevins, J.R. Selective induction of E2F1 in response to DNA damage, mediated by atm-dependent phosphorylation. *Genes Dev.* **2001**, *15*, 1833–1844.
90. Stevens, C.; Smith, L.; la Thangue, N.B. Chk2 activates E2F-1 in response to DNA damage. *Nat. Cell Biol.* **2003**, *5*, 401–409.
91. Yang, W.W.; Wang, Z.H.; Zhu, Y.; Yang, H.T. E2F6 negatively regulates ultraviolet-induced apoptosis via modulation of brca1. *Cell Death Differ.* **2006**, *14*, 807–817.
92. Lyons, T.E.; Salih, M.; Tuana, B.S. Activating E2Fs mediate transcriptional regulation of human E2F6 repressor. *Am. J. Physiol.* **2006**, *290*, C189–C199.